UNIVERSITÀ
DEGLI STUDI
DI PADOVA

DIPARTIMENTO
DI INGEGNERIA
DELL'INFORMAZIONE

DIPARTIMENTO DI INGEGNERIA DELL'INFORMAZIONE

CORSO DI LAUREA IN BIOINGEGNERIA

"Biomechanical evaluation of a novel fiberglass reinforced polyamide custom ankle-foot orthosis: gait analysis and energy assessment in a population of mild foot-drop patients"

Relatore: **Zimi Sawacha, PhD**

Laureando: **Luca Zamagni**

Correlatori: **Paolo Caravaggi, PhD, Giulia Rogati, MEng, Alberto Leardini, DPhil**

ANNO ACCADEMICO 2022 – 2023
Data di laurea 06/03/2023

Ringrazio Paolo, Giulia e Alberto per avermi accolto nel loro progetto e saputo aiutare e consigliare al meglio nella stesura di questa tesi.

Ringrazio la mia famiglia, per avermi permesso di proseguire gli studi di ciò che mi appassiona, non senza fare sacrifici e superare difficoltà.

Ringrazio Giulia, per essere la donna che sei, saggia consigliera e premurosa certezza al mio fianco, fonte di ispirazione e modello di vita.

Ringrazio tutti coloro che ho conosciuto in questi anni di università, che siete diventati fidati amici e compagni di serate da ricordare, e i vecchi amici di sempre, solide certezze.

A voi tutti, GRAZIE.

Abstract

Ankle foot orthoses (AFOs) are medical devices used to stabilise the ankle following traumatic injuries, or lesion to the central or peripheral nervous systems leading to foot-drop. This represents the inability to lift the foot during the swing phase of walking, due to neuro-muscular impairments of the ankle dorsiflexor muscles. Mild foot-drop patients may need a comfortable AFO that provides support to the ankle and that can bend seamlessly with the physiological ankle motion in common daily motor tasks. While off-the-shelf AFOs are cost-effective solutions, they may not fully comply with the foot and leg shape and the patient-specific functional requirements. Over the last 20 years, advancements in additive manufacturing technologies have allowed to manufacture custom orthotic devices that better fit the affected anatomical segment.

This thesis aimed at evaluating the functional and biomechanical outcome of a novel fibreglass-reinforced polyamide passive-dynamic custom AFO, manufactured via Selective Laser Sintering, in a population of foot-drop patients (n = 10; age = 64.9 ± 11.4 years, BMI = 26.2 ± 2.1 kg/m^2). The energy absorbed and released by the custom AFO during the stance phase of walking has been estimated from its experimentally-measured stiffness and motion tracked via a 8-camera motion analysis system. The functional evaluation was assessed via gait analysis in the three conditions: shod (no-AFO), wearing an off-the-shelf AFO (a Codivilla spring) and wearing the custom AFO. Kinematics and kinetics of the hip, knee and ankle joints were estimated via skin-markers attached to relevant bony landmarks according to the IOR-gait kinematic protocol.

Both AFOs resulted in decreased sagittal-plane range of motion of the ankle in the swing phase of gait, as well as in reduced plantarflexion angle. Spatiotemporal parameters analysis showed a significant increased stance time (63.7 ± 1.5 vs 63.7 ± 2.1 vs 61.0 ± 2.7 [% stride time]), normalised speed of walking (52.3 ± 12.9 vs 51.8 ± 14.1 vs 49.3 ± 13.9 [% height/s]) and normalised stride length (64.7 ± 11.0 vs 64.2 ± 11.6 vs 63.3 ± 11.3 [% height]) for the custom AFO with respect to the off-the-shelf one and to the shod condition. The energetic evaluation highlighted that the custom AFO releases part of the stored energy at foot-off thus contributing to the propulsive phase. Moreover, patients perceived the custom AFO more comfortable than the Codivilla spring (VAS score: 8.6 ± 1.2 vs 5.3 ± 1.3).

This study provides evidence for the beneficial functional outcomes of AFO personalization, especially for mild foot-drop patients not satisfied with standard orthotics.

Contents

1. Introduction

1.1 IRCCS Rizzoli Orthopaedic Institute

The IRCCS Rizzoli Orthopaedic Institute (IOR) is an inpatient and nursing institution of scientific nature located in Bologna, Emilia-Romagna, Italy. It is a centre of excellence for orthopaedics and traumatology, as well as being a world-renowned scientific research centre. It was founded in 1896 by Francesco Rizzoli, a well-known surgeon from Bologna. The Institute is divided into the Rizzoli Hospital and the Codivilla-Putti Research Centre (Figure 1). The latter is home to numerous laboratories: among them the Movement Analysis Laboratory, which hosted me from April to December 2022 permitting to work on this thesis project. The laboratory was founded in 1989 and has the purpose of performing quantitative instrumental analyses of human movement, particularly of the musculoskeletal system. The laboratory, always in close collaboration with the Orthopaedic and Traumatology Clinic and other care and research units at Rizzoli, specialises in gait analysis of normal and pathological subjects. In particular, patients are frequently analysed before or after orthopaedic surgery and following rehabilitation programs of the musculoskeletal system.

Figure 1: The Codivilla-Putti Research Center at IRCCS Rizzoli.

1.2 Background

Foot-drop is a debilitating pathology that alters the ability to lift the front part of the foot, causing dragging during the swing phase of the gait cycle. It manifests itself in weakness or paralysis of the muscles responsible for the ankle dorsiflexion, such as tibialis anterior, as a result of neuromuscular pathologies. The principal causes of foot drop may be various, and generally they are associated with a damage or alterations of the central or peripheral nervous system, such as peroneal nerve injury, or brain and spinal cord disorders. This problem generally affects only one leg, but there are also bilateral cases. Foot-drop affects men and women at any age, causing difficulty in performing everyday activities due to mobility dysfunctions. It may imply paraesthesia, pain and could be a temporary or permanent condition. In order to compensate for the functional limitations due to the foot-drop condition, it can be useful to wear an Ankle-Foot Orthosis (AFO). Orthoses are medical devices applied externally to the body, aiming at modifying the structural and functional characteristics of the neuromuscular and skeletal systems. On the market there are several standard prefabricated AFOs, made with single and composite materials such as carbon fibre, metals or polymers, and produced with different technologies. The choice of the perfect material for the AFO's production is linked to the functional demands that must satisfy, in terms of flexibility, durability, resistance, comfort, weight and aesthetic acceptability. Standard orthoses' design was traditionally based on the experience of professional technicians. Now, the application of modern technologies for the design and production of custom devices, like additive manufacturing, is becoming increasingly widespread. The aim of custom orthoses is to cover the functional needs of individual patients, unlike the standard ones that are manufactured to meet a set of general functional requirements, adjustable to fit the majority of patients but not tailored to a particular subject. On the contrary, custom orthoses can address specific medical requirements and patient's foot and leg morphology. Moreover, these can be considered as a valid alternative to generic orthoses which do not fully satisfy patients in terms of functional outcome, comfort, and/or aesthetic pleasure.

1.3 Anatomy and biomechanics of the lower limb

1.3.1 Anatomical planes

Before talking about the anatomy of the lower limb, it is correct to explain how we refer to the spatial orientation of the body and every segment of it. Anatomical planes are imaginary planes that ideally divide the body into sections, they are used to describe every section's anatomical position. There are three anatomical planes (Figure 2):

- the **sagittal** plane, also known as the **anterior-posterior** plane, divides vertically the body into a left segment and the right one. So, it is a symmetry plane, and it's perpendicular to the ground.
- the **coronal** plane, also known as the **frontal** or **lateral** plane, divides the body into an anterior and a posterior segment. It is perpendicular to the sagittal plane and passes through the body's centre of mass.
- the **transverse** plane, also known as the **axial** or **horizontal** plane, divides the body horizontally into an upper and a lower segment. It's orthogonal to the previous planes and parallel to the ground.

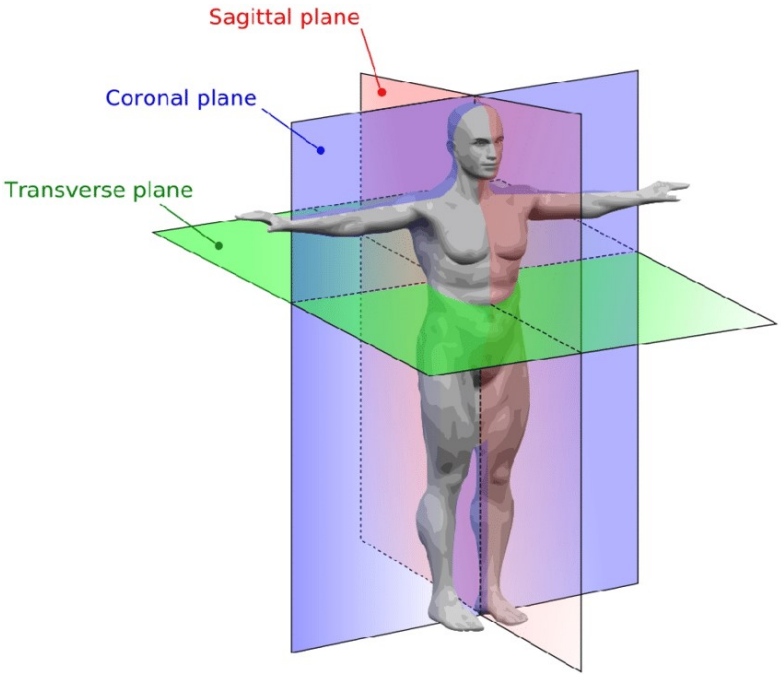

Figure 2: Anatomical planes.

Then there are also the axes around which each body segment can rotate. They are shown in Figure 3, and more in detail, they are:

- **longitudinal** axis, also known as **polar** axis, which goes from the top of the head, vertically down to the middle of the heels. Around this axis segments can rotate on the transverse plane.
- **transverse** axis, also known as **horizontal** axis, which crosses the body from the right to the left part, it's parallel to the ground. Around it, segments can flex or extend on the sagittal plane.
- **sagittal** axis, also known as **anterior-posterior** axis, is the imaginary line, parallel to the ground and orthogonal to the previous axes, that goes from front to back. Around it, body segments can abduct or adduct on the coronal plane.

To explain how each joint of the lower limb works, that is the interesting compartment of this study, the lecture is organised into paragraphs – hip, knee and ankle – and each of these is divided into a part about the anatomy and a part about the biomechanics.

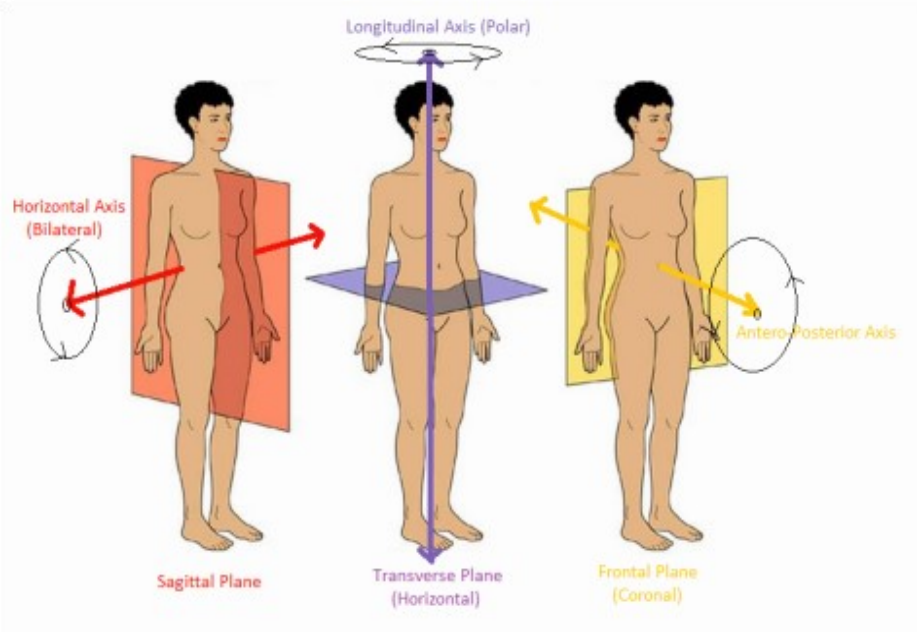

Figure 3: Anatomical axes.

1.3.2 Hip joint

1.3.2.1 Anatomy

The hip joint is the anatomical district that connects the lower limb to the trunk, especially it joins the head of the femur with the acetabulum of the pelvis [1]. It is a diarthrosis and is composed by the femur bone and the pelvis bone: the head of the femur is located into the acetabulum, which has a concave shape, and the complex is stable thanks to the ligaments that surround it (Figure 4). These ligaments provide stability and permit the joint to move around the three anatomical axes without generating dislocations: the iliofemoral ligament lies anteriorly and prevents hyperextension, the pubofemoral lies anteroinferiorly and prevents excessive abduction and extension, the ischiofemoral ligament, that lies posteriorly and is the weakest of the three, prevents extension too. Usually, ligaments are relaxed during hip flexion, while they are tight during extension.

The principal function of the hip is to **support the body weight** and **transmit loads** to the ground: it can support the body weight in static and dynamic activities, so it must be constantly lubricated to permit movements. Lubrication is possible thanks to the continuous production of synovial fluid by the acetabular labrum. Beyond that, the labrum also has the function of containment of the femoral head, and this permits a wider area of force distribution on the neck of the femur.

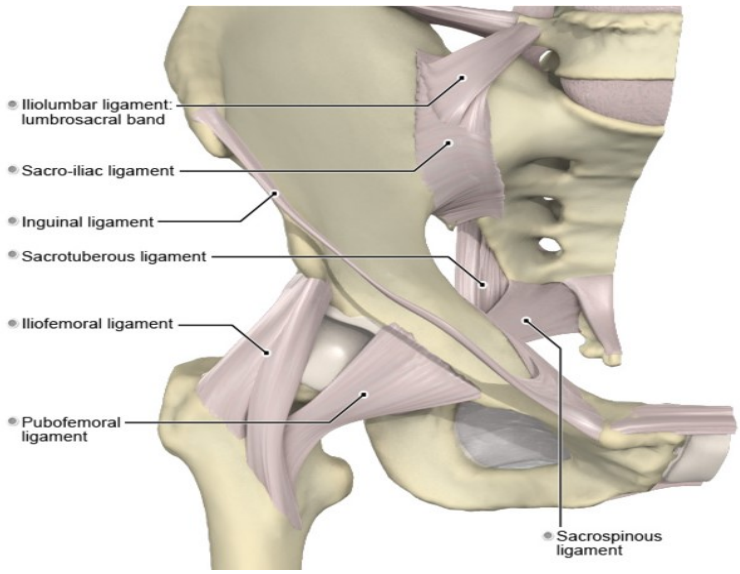

Figure 4: Anatomy of the hip joint.

Hip joint is highly dense in muscles (Figure 5): the major muscles for hip movements are psoas major, psoas minor, iliacus and rectus femoris for flexion, biceps femoris and gluteus maximus for extension, then there are the adductors and the gracilis for adduction, gluteus medius for abduction, gluteus minimus for internal rotation, and gemellus, obturators and piriformis for external rotation. **Rectus femoris** runs straight down the thigh, and its contraction is the cause of knee extension beyond hip flexion. It originates from the anterior inferior iliac spine and inserts at the patella and tibial tuberosity[2].

Biceps femoris lies in the posterior compartment of the thigh, originating in the ischial tuberosity and inserting in the lateral aspect of fibula head. Beyond hip extension, it is responsible for knee flexion and lateral rotation of thigh and lower leg when hip is extended, and knee flexed [3].

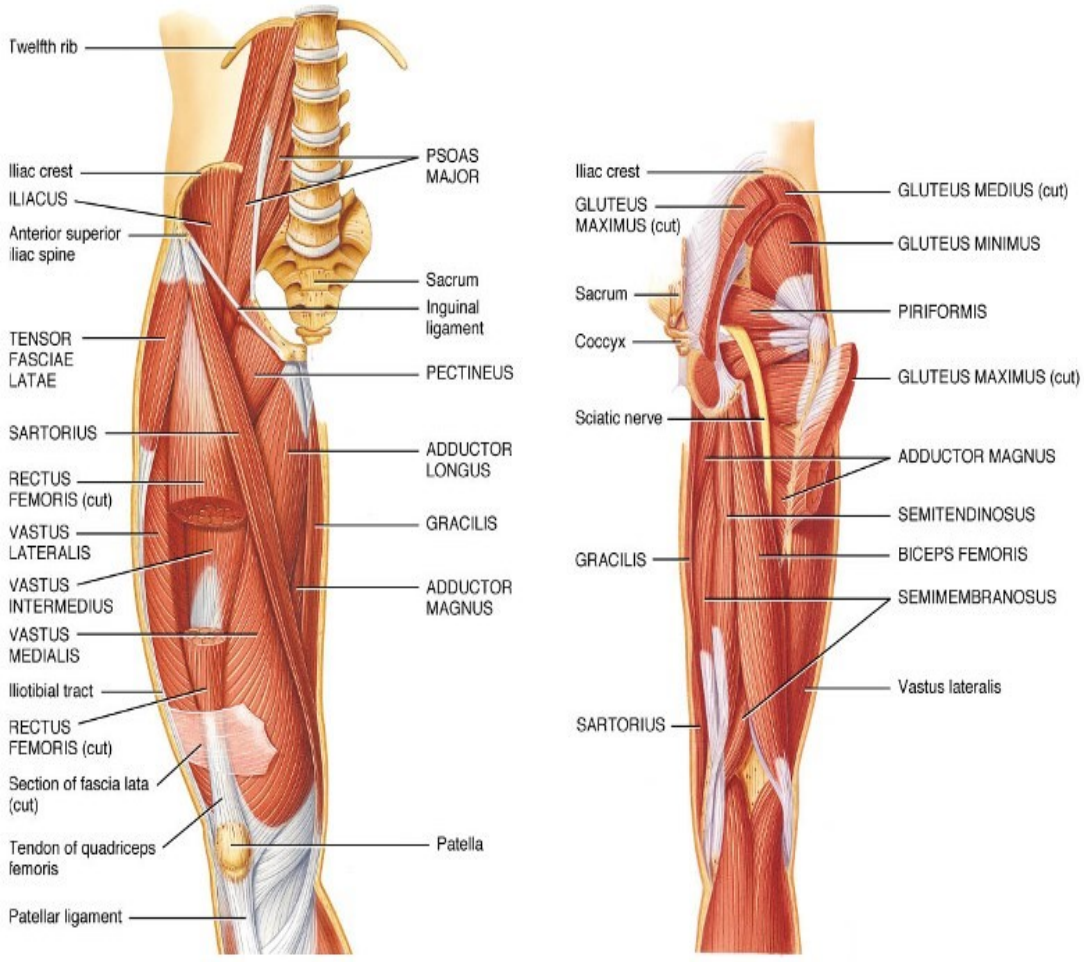

Figure 5: Muscles of the hip joint: anterior (on the left) and posterior (on the right) superficial view.

1.3.2.2 Biomechanics

Hip joint is a ball & socket joint, in fact it has three degrees of freedom that permit the movement of the lower limb around the three anatomical planes. On the sagittal plane, hip can flex or extent: flexion is the movement that brings the leg toward the trunk and can go up to 90 deg with knee extended, or up to 120 deg with knee flexed; on the other side, extension is the movement that takes the lower limb posteriorly to the frontal plane, and it can go up to 20 deg or up to 10 deg, respectively with knee extended or flexed. On the frontal plane, hip can abduct or adduct moving around the sagittal axis: abduction is the movement that brings the femur externally, away from the symmetry plane, and can go up to 50 deg, while adduction brings femur closer to it. Obviously, to adduct the hip requires a little flexion or extension too, because of the presence of the other leg. The last movement possible is the rotation around the longitudinal axis on the transverse plane: internal rotation brings the tip of the foot towards the symmetry plane and can arrive to 40 deg, external rotation takes the tip of the foot away from the symmetry plane and can arrive to 60 deg (Figure 6).

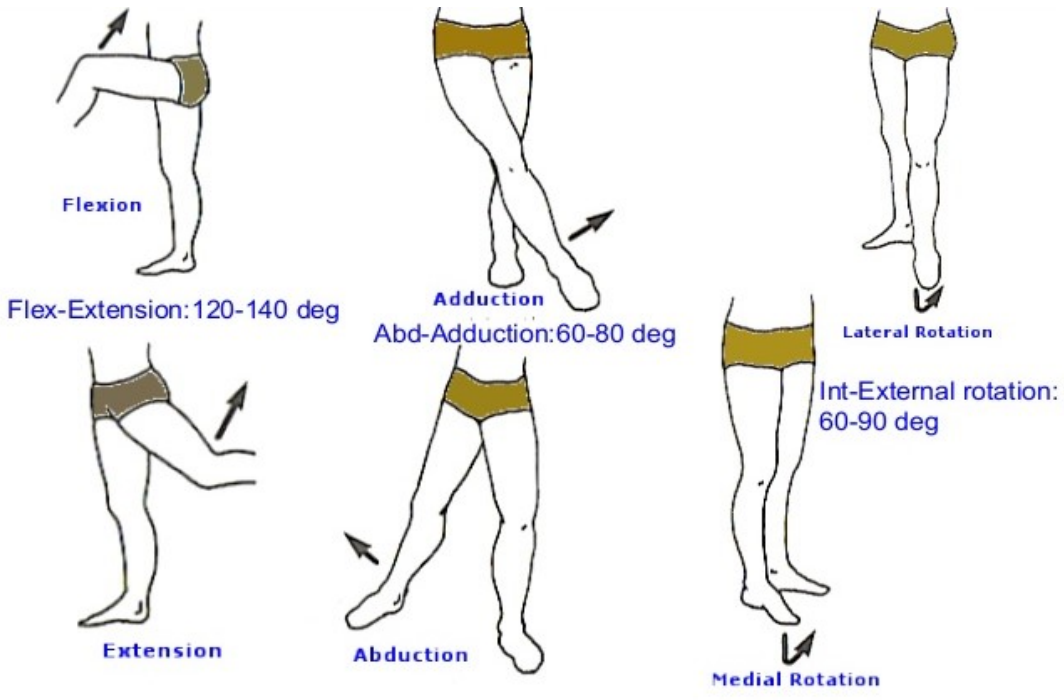

Figure 6: Hip movements.

1.3.3 Knee joint

1.3.3.1 Anatomy

The knee joint is a diarthrosis that connects the lower leg to the upper leg, especially the proximal part of the tibia with the distal part of the femur. It is the most complex and largest joint of the body and is composed of two joints: the tibiofemoral joint, and the patellofemoral joint between the patella and the femur (Figure 7). The tibiofemoral is a hinge joint, so the movement allowed is mostly around an axis, the horizontal, even if in minimum part it can rotate around the other two axes too. The patella is essential for knee extension: it is a plate bone that transmits force from the quadriceps femoris to the tibia and permits the vertical action of traction on it [4].

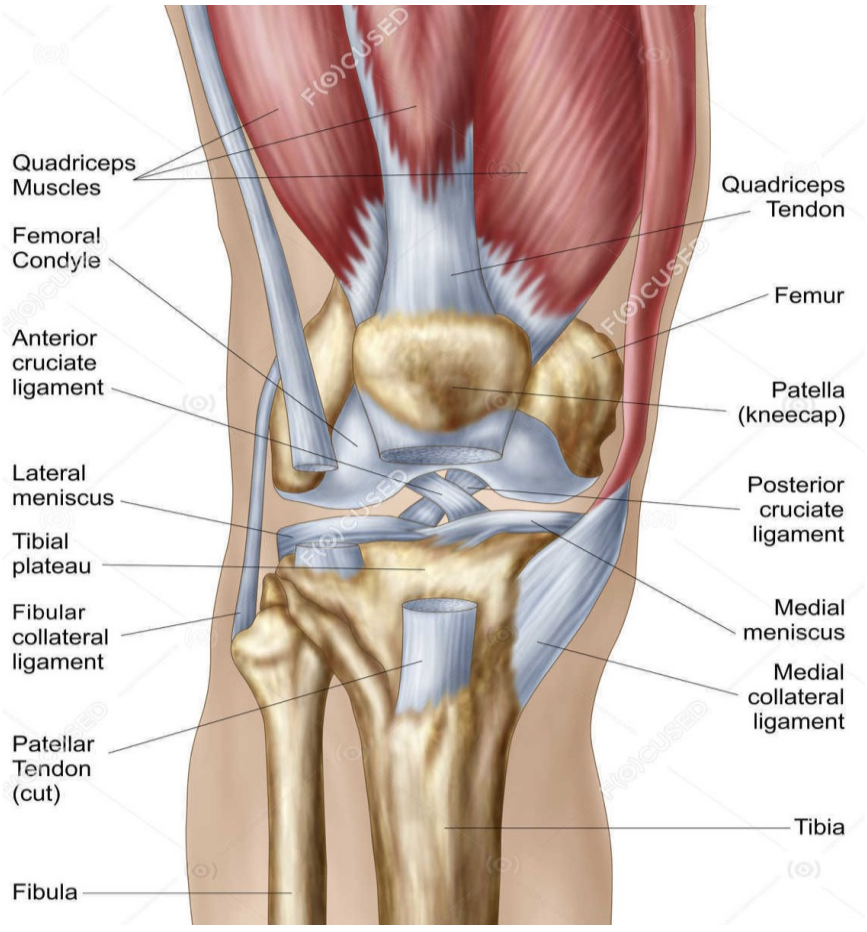

Figure 7: Knee anatomy.

The articular surfaces of the knee are covered by cartilage, a connective tissue that protects against wear and reduces internal frictions. The articular capsule is the structure that contains patella, menisci, ligaments and the bursae of the knee. There are two articular discs, the menisci, that help in dispersing the body weight and the friction in the knee joint. They are made of fibrocartilaginous tissue, have a semilunar shape and a triangular section. The menisci are divided into a lateral meniscus and a medial meniscus, positioned respectively between the lateral and the medial condyle of the femur, and the upper plate of the tibia. Stability to the articulation is also given by a set of ligaments that surround it: two are intracapsular – the anterior cruciate ligament (ACL) and the posterior cruciate ligament (PCL) – and six are extracapsular. The ACL stretches from the lateral femoral condyle to the anterior intercondylar area while the PCL stretches from the medial femoral condyle to the posterior intercondylar area, and they prevent respectively the anterior and the posterior rolling of the tibia with respect to the femur. The two most important extracapsular ligaments are the medial collateral ligament (MCL) and the lateral collateral ligament (LCL): the first stretches from the medial femoral epicondyle to the medial tibial condyle and prevents against valgus deformity caused by medial forces, the second is attached proximally to the lateral femoral epicondyle and distally to the head of the fibula and prevents varus knee deformities caused by lateral forces.

The knee is subjected to a set of muscles that, contracting, permit its movements. In the anterior thigh compartment there are, generally, extensor muscles, such as rectus femoris, quadriceps femoris, and the vastus lateralis, intermedius, medialis. All of them help in extending the knee in the sagittal plane, stabilising it, and the first two of them permit the hip flexion too. On the other side, the knee flexor muscles are positioned in the posterior thigh compartment – except for the gracilis, which is in the medial thigh compartment – and are represented by sartorius, biceps femoris, semitendinosus, semimembranosus and, in the shank, by gastrocnemius, plantaris and popliteus. The gastrocnemius and the plantaris also contribute to plantarflexion at the ankle joint, while biceps femoris participates in hip extension too (Figure 8).

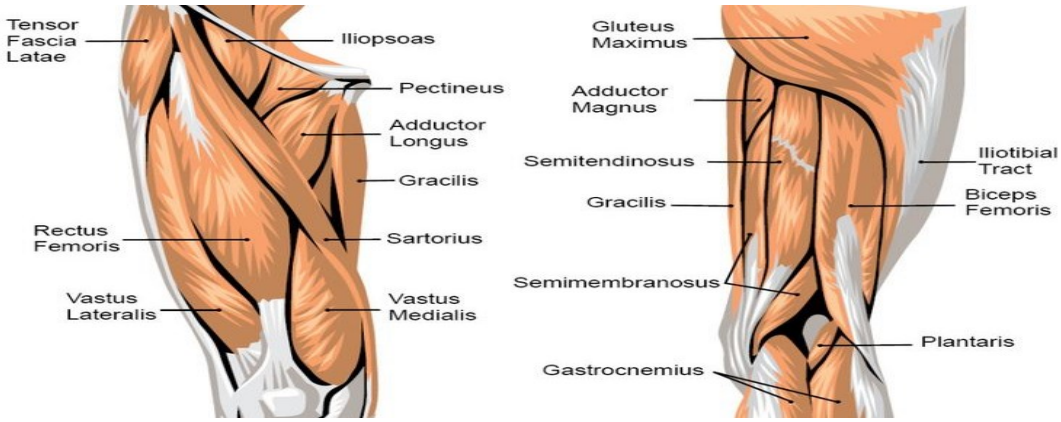

Figure 8: Knee principal muscles.

1.3.3.2 Biomechanics

As seen in the previous paragraph, the knee is a hinge joint, so the prevalent movement that is permitted is flexion/extension on the sagittal plane around the transverse axis, thanks to the "rolling and gliding" movement of the femur over menisci. Flexion is the movement that brings posteriorly the shank toward the thigh and can go up to 120/150 deg – normally the limiting factor is the thigh/calf contact [5] – , while extension brings anteriorly the lower leg with respect to the coronal plane and can go up to 10 deg. Moreover, thanking to flexor muscles such as biceps femoris, popliteus, sartorius, the knee can rotate around the longitudinal axis in the transverse plane: internal (or medial) rotation, which can go up to 10 deg, is the movement that rotates the lower leg towards the symmetry axis, external (or lateral) rotation, on the opposite rotates the shank far away from the symmetry axis and can go up to 40 deg (Figure 9). At last, movements of abduction and adduction on the coronal plane are possible, in minimum part, only with the knee flexed, but they can go up to 5 deg only.

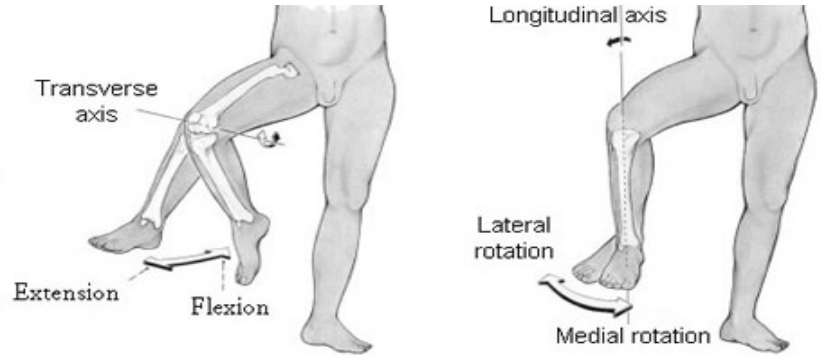

Figure 9: Knee movements.

1.3.4 Ankle and foot complex

The ankle is the interested joint of this study, so we will focus more on it. It is a diarthrosis, hinged synovial joint, formed by the articulation of the tibia, the fibula and the talus, that connects the lower leg, the shank, with the foot [6].

1.3.4.1 Anatomy

The ankle joint is the articulation formed by three bones: the tibia and the fibula from the lower leg, and the talus from the foot. Especially, the bony prominence of the fibula represents the lateral border of the joint, the medial malleolus of the tibia is the medial border, while the superior margin of the talus represents the inferior border (Figure 10).

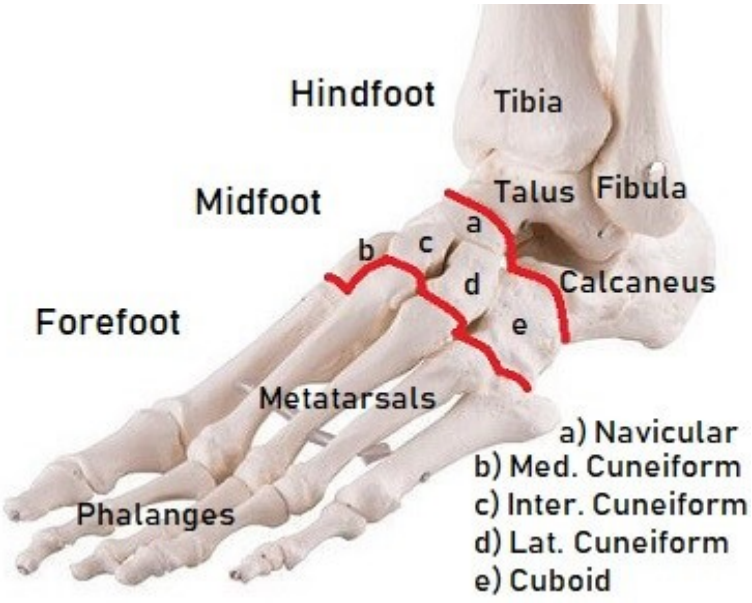

Figure 10: Ankle and foot bones.

Tibia and fibula are distally stabilised by a set of ligaments – the anterior and the posterior tibiofibular ligaments – and by an interosseous membrane. Tibia has a groove in the posterior medial surface, in which the tendon of the tibialis posterior muscle inserts, while fibula has a posterior groove in which inserts the fibularis longus muscle's tendon. The talus bone articulates above with tibia and fibula, below with the calcaneus bone, which is also known as the heel foot, and anteriorly with the navicular bone of the foot. Talus has a shape in which we can see an anterior head, a neck and a posterior body: the head is wide, so during the

dorsiflexion movement – in which the foot goes toward the lower leg – it gets wedged between the two malleoli, making the joint stable. The superior surface of the talus, which articulates with the inferior surface of the tibia and has a cylindrical shape, is also called trochlear surface.

There is a set of **ligaments** that stabilise the ankle: laterally there are three ligaments, two of them connect the fibula to the talus – one anteriorly and the other posteriorly – while the last binds the fibula to the calcaneus (Figure 11); medially there is a complex of four ligaments, called deltoid, which connect the tibia to the talus (anterior and posterior tibiotalar ligaments), to the navicular anteriorly (tibionavicular ligament) and to the calcaneus inferiorly (tibiocalcaneal ligament). This complex formed by the medial ligaments of the ankle is called deltoid because it remembers a triangular shape.

All these ligaments have the function to stabilise the joint during gait and static posture, especially the lateral ligaments prevent fractures from inversion and internal rotation forces, while deltoid ligaments reinforce the joint and control plantarflexion and dorsiflexion.

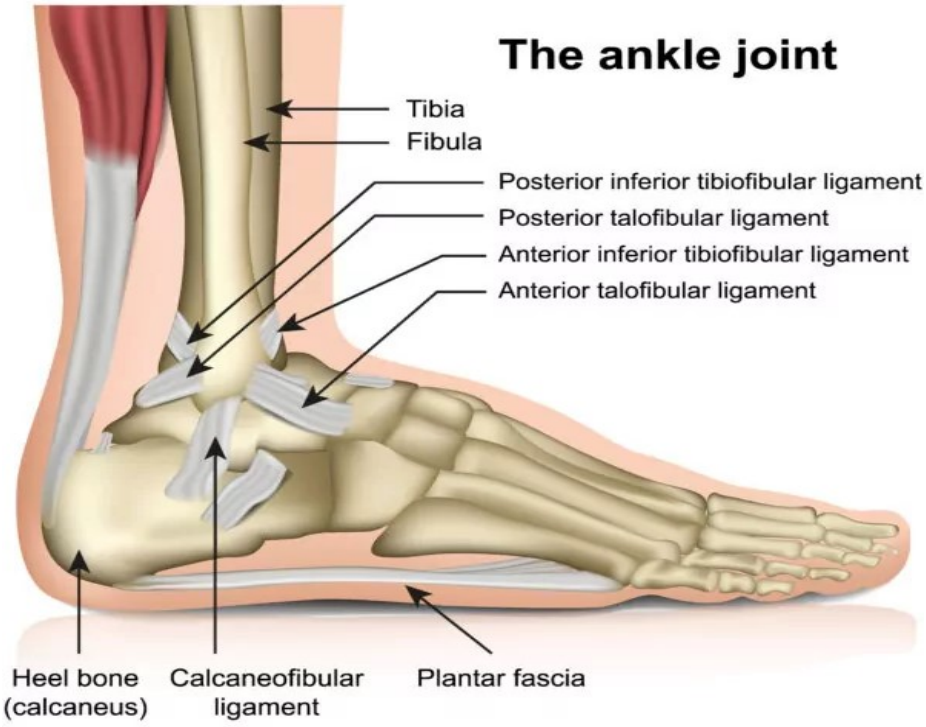

Figure 11: Lateral view of the ankle and ligaments involved.

The **foot** is the most distal anatomical district of the body and is in constant contact with the ground. It is composed of 26 small bones (or 28 if we consider the two sesamoid bones of the first metatarsophalangeal joint) that can be divided into three groups: tarsals, metatarsals, and phalanges [7]. These bones are designed for weight bearing and force distribution The reader can see them at Figure 10.

- There are 7 **tarsal** bones that make up the rearfoot: from the ankle there is the talus, which joins with the navicular and the calcaneus, then there are the cuboid and the three cuneiforms – medial, lateral and intermediate – which join anteriorly with metatarsals.
- **Metatarsals** are 5 bones, one for each toe, classified from the medial (the first, or big toe) to the lateral (the fifth, or little toe). The first joins with the medial cuneiform, the second with the intermediate, the third with the lateral, while the fourth and the fifth metatarsals join posteriorly with the cuboid.
- **Phalanges** are 14 small bones that join posteriorly with the metatarsals. They are three for each toe – proximal, middle and distal phalanx – except for the big toe which has only two phalanges – proximal and distal –.

All these small bones join each other and articulate thanking to the presence of ligaments: every metatarsophalangeal joint has three ligaments – plantar, lateral collateral and medial collateral – that support the joint capsule, except for the big toe that has another ligament which joins the medial sesamoid with the lateral one.

Again, for every toe there are three interphalangeal ligaments – plantar, lateral collateral and medial collateral – that support the interphalangeal articulations, connecting the proximal phalanx to the distal one.

As seen in Figure 11, under the foot bones there is a structure, the plantar fascia – also known as **plantar aponeurosis** – that is a thick connective tissue of triangular shape which supports and protects the vital elements of the foot, such as nerves and vessels [8]. It inserts in the calcaneus and finishes, with five processes, into the five metatarsals. It is also important for the maintenance of the longitudinal

arch foot, in preventing excessive dorsiflexion, in the attachment of muscular foot structures, and in distributing the plantar loading (Figure 12).

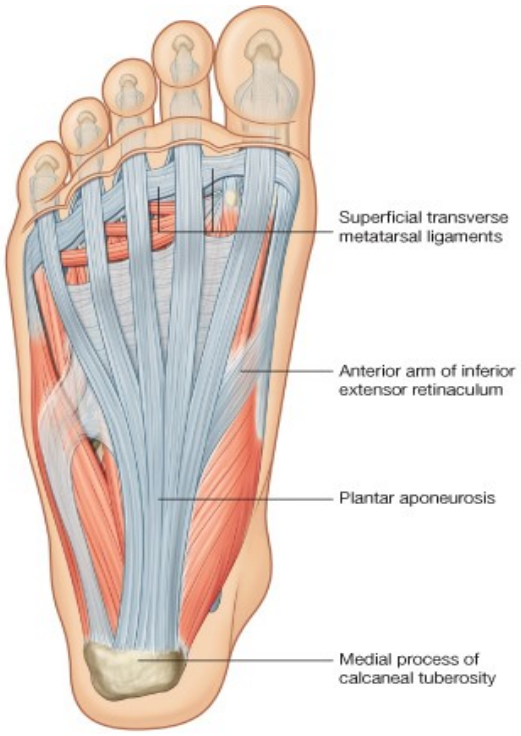

Figure 12: Plantar aponeurosis.

Talking about the **muscles** that involve the ankle and foot complex, they can be treated first by showing the leg muscles, which are considered as the extrinsic muscles (Figure 13), and then seeing the foot ones, that are known as intrinsic muscles. The extrinsic ones can be divided into the three leg compartments in which they are positioned: posterior, anterior and lateral [6].

- In the posterior compartment, the main function of the muscles is the plantarflexion of the foot at the ankle joint. There are superficial muscles, such as gastrocnemius, soleus and plantaris, and there is a deeper layer of muscles such as tibialis posterior, flexor hallucis longus, flexor digitorum longus and popliteus. **Gastrocnemius** has two heads – one medial and the other lateral – that origin from the medial and lateral femur condyles respectively and come together into a single muscle belly that narrows into the Achilles tendon, and then inserts in the posterior surface of the calcaneus [9]. Its main

function, in conjunction with soleus and triceps surae muscle, is the plantarflexion of the foot at the ankle joint. Secondly, it contributes to knee flexion.

- In the anterior compartment the principal function of the muscles is the dorsiflexion of the ankle: they are represented by tibialis anterior, extensor digitorum longus, fibularis tertius, extensor hallucis longus. **Tibialis anterior** is the most important of them: as suggested by the name, it is located anteriorly to the tibia, and originates from the lateral tibial condyle inserting in the medial cuneiform bone of the foot. It's innervated by the common fibular nerve, and its principal function is the dorsiflexion of the foot at the ankle, so the reader must know that most of the patients suffering from foot-drop have deficit in muscle activation of tibialis anterior, with the consequence of being unable to lift the foot during the swing phase of the gait cycle.
- In the lateral compartment there are two muscles – the fibularis (or peroneus) longus and the fibularis (or peroneus) brevis – that mainly contribute to eversion and plantarflexion of the foot. They arise from the fibula and insert in the foot bones.

The intrinsic muscles are the ones that involve the fine movements of the foot, such as flexion and extension of each toe. They are organised in a dorsal layer and a plantar one. The former are represented only by extensor digitorum brevis and extensor hallucis brevis, that permit the extension of the five toes, while the latter can be divided in four depth levels: these muscles are responsible for the movements of the digits such as flexion, abduction and adduction [10].

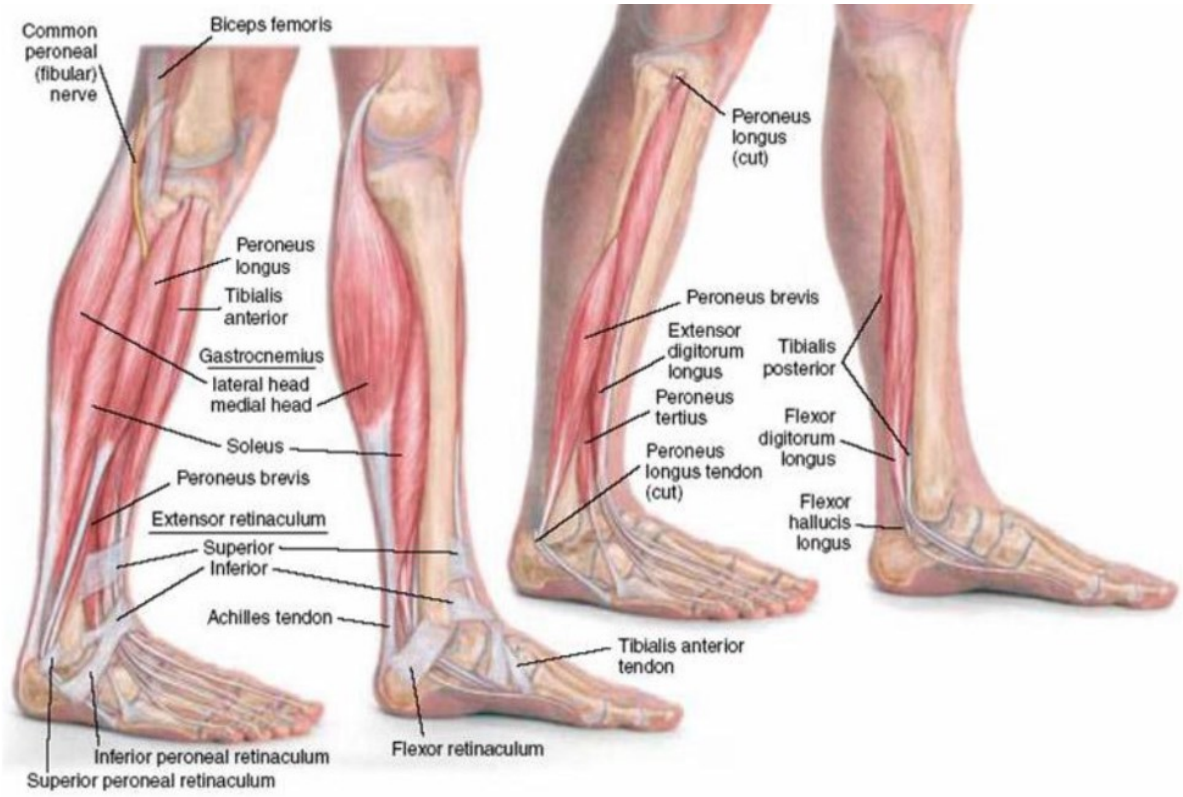

Figure 13: Ankle extrinsic muscles.

1.3.4.2 Biomechanics

The ankle joint is important because it permits to transmit the body weight to the foot, which can correctly distribute it to the ground. Thanking to this articulation, the foot can move along three spatial directions, executing dorsiflexion and plantarflexion in the sagittal plane, inversion and eversion in the coronal plane and abduction and adduction in the transverse plane (Figure 14).

Dorsiflexion and plantarflexion are the most important movements, because they help the individual in walking. Dorsiflexion is the action in which the foot flexes up towards the lower leg, and it can go up to 20 deg. It is important in the swing phase of gait, in which the subject must dorsiflex the foot in order to avoid dropping it to the ground. On the opposite, plantarflexion is the movement in which the foot moves away from the lower leg, and it can go up to 50 deg. It is a stronger action than dorsiflexion due to the greater number of muscles that allow it, such as gastrocnemius, soleus, plantaris and all the intrinsic muscles of the plantar foot. Plantarflexion is important in the foot-off phase of the gait cycle to prepare the foot

to the consequent swing phase. The range of motion (ROM) of the ankle in the sagittal plane has been shown to vary between individuals as a consequence of geographical and cultural differences [11], but it generally goes from 65 deg to 75 deg.

Inversion and eversion are the movements that respectively rotate the medial and lateral compartment of the foot upward with respect to the anterior-posterior axis that passes through the malleoli of the ankle. They can go up to 25 deg and 15 deg respectively, so the ankle ROM in the frontal plane can reach 40 deg.

At last, abduction and adduction are the movements that respectively rotate the tip toes externally and internally with respect to the simmetrical axis of the lower limb that goes from the hip to the ankle. They can go up to 10 deg and 20 deg respectively, producing an ankle transverse' ROM of about 30 deg.

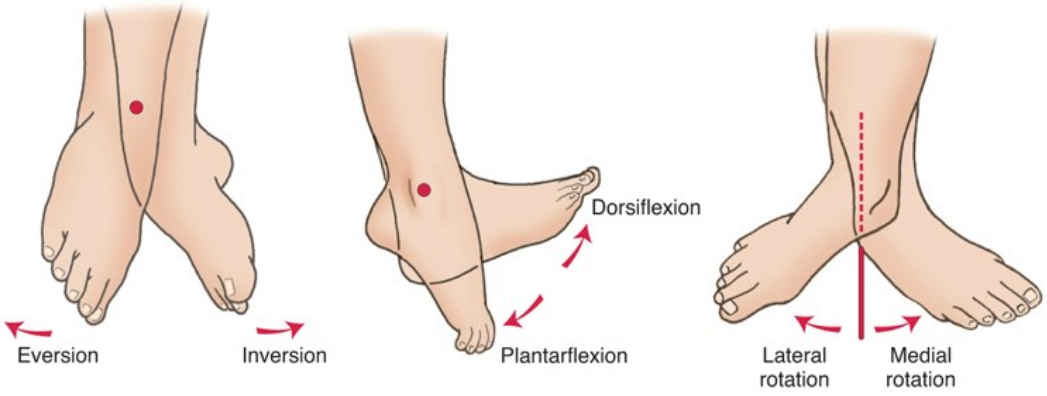

Figure 14: Ankle movements.

1.4 Foot-drop

Foot-drop is a pathology that involves the foot and ankle compartment: it consists of an inability in lifting the forefoot due to the weakness of the dorsiflexor muscles (Figure 15). As a result of this, the subject affected by foot-drop may develop a compensation gait technique in the other joints interested – hip and knee – aimed at maintaining the clearance and avoiding possible consequent falls [12]. The causes of this disorder can be various, they are briefly treated in the following paragraph.

Figure 15: Foot-drop pathology: it involves the ankle compartment and consists in the inability to dorsiflex it. It is often the consequence of peroneal nerve compression due to traumatic injuries or spinal surgery.

1.4.1 Aetiology

Nerve compression

One of the principal causes of dorsiflexor muscles weakness, and consequently of foot-drop, is the compression of the nerves linked to them. As seen in the previous paragraph, the principal muscle for dorsiflexion is the tibialis anterior, innervated by the common fibular nerve. This nerve is the lateral branch of the sciatic nerve, which runs in the posterior thigh originating from L4 and L5 lumbar nerves. Because it is superficial near the head of the fibula, it's vulnerable to pressure palsies. Some factors that can contribute to fibular nerve compression are weight loss, prolonged bedridden

status and bone metastasis at the fibular head. Fibular neuropathy has an incidence of 19 per 100000 and is more common in males than in females.

Moreover, a study demonstrated that about 10% of patients who protract bed rest in Intensive Care Units for more than four weeks are expected to develop paresis of the fibular nerve [13].

Other nerve compression disorders can be associated to disc herniation – about 1% of European population is affected by this condition, and about 23% of disc herniation patients show foot-drop [14] –, lumbar L5 radiculopathy, extraforaminal compression of the L5 nerve, spondylolysis at the lumbosacral vertebrae, and sciatic nerve compression between the two heads of the piriformis muscle. Beyond that, it has been seen that patients with diabetes are more subjected to these compression neuropathies.

Traumatic injuries

Traumatic injuries are often considered as foot-drop causes, or as nerves compressor's causes. They are associated with orthopaedic injuries such as knee dislocations, tibia or fibula fractures, blunt trauma, musculoskeletal injuries. Sciatic nerve compression, which is usually associated with foot-drop, is the consequence of surgery or hip traumatic injury.

Lumbosacral plexopathies, which can be consequences of abdominal or pelvic surgeries, complication of neoplasm or radiation therapy, or to traumatic injuries, are also common causes of foot-drop.

Neurologic disorders

There are several pathologies that affect the central or peripheral nervous system, that can result in foot-drop or more generally in locomotor disorders. The amyotrophic lateral sclerosis (ALS), also known as Lou Gehrig disease, is a neurodegenerative disorder that consists of muscle weakness, difficulty in speaking and in swallowing, due to the death of motor neurons in the anterior horn of the spinal cord. It can have, among other symptoms, initial foot-drop, and has an yearly incidence of 1.54 per 100000 [12].

Another neural pathology that must be considered is cerebrovascular disease (CVA), which can present hemiplegia, increased muscle tone, hyperreflexia, aphasia, circumduction of the lower arm during ambulation.

Multiplex mononeuritis affects one or more sensory and peripheral motor nerves and can damage the axons of the sciatic nerve leading to dorsiflexor muscles weakness.

Charcot-Marie Tooth (CMT) is a congenital inherited demyelinating peripheral neuropathy, which affects both motor and sensory neurons, has an incidence of 1 over 25000, and has foot-drop as main consequence.

At last, acute inflammatory demyelinating polyneuropathy (AIDP) must be considered: it consists in segment demyelination, resulting in slowing the nerve conduction velocity, progressive motor weakness, sensory loss and areflexia. AIDP has an incidence from 1.0 to 1.2 per 100000 and has been reported that men are 1.5 times more affected than women.

Excluded by the previous categories, it has been reported that about 20% of patients affected by stroke (incidence about 0.1% of EU population [14]) suffers from foot-drop.

1.4.2 Symptoms

The most common symptom that a patient affected by foot-drop manifests is the inability in lifting the foot during the swing phase of the gait cycle. There are some signals that can lead to a foot-drop diagnosis: firstly, patients can feel weakness in the muscles of the foot and toes, but other important symptoms are the loss of balance with consequent stumbles and falls, the reduction of the time of stance during walking due to the instability in placing the foot on the ground, the difficulty in climbing stairs, the reduced walking speed and the consequent reduction of the stride length. Beyond that, an important symptom is numbness and loss of sensitivity on the front and upper side of the lower leg and along the upper part of the foot [15].

The evaluation of foot-drop weakness degree can be assessed by qualitative or quantitative estimates: the method most used by clinicians to classify the degree of

muscular deficit involves the use of the Medical Research Council (MRC) Scale. This is a subjective assessment of muscle strength which ranks the residual muscle force on a scale of 0 to 5 in relation to the maximum expected for that muscle. Strength is graded by manually applying a resistance against the patient's foot plantarflexion/dorsiflexion movements with the patient lying supine. In particular, the score 0 indicates no contraction of the dorsiflexor muscles, while score of 5 indicates normal muscle contraction, which allows foot movements against gravity even if external resistance is applied.

Quantitative estimation includes MRI investigation of the lumbar spine, knee and ankle compartments, with the objective to find eventual compressive neuropathies. Other evaluations can be assessed studying the nerves conduction in the lower legs, providing information about the viability of myelin, and introducing electromyography needles into muscles supplied by sciatic or fibular nerve, due to identify the location and severity of the lesion and estimate the prognosis for recovery [12].

1.4.3 Treatments

The approach to treat a foot-drop patient depends on the nature of the compressive lesion and is based on the evaluation and diagnostic findings. Depending on the treatment reserved to the patient, foot-drop may reduce its gravity or even disappear.

Conservative approaches

Less severe patients might improve their impairment degree with an initial conservative treatment, practising physical exercises and physiotherapy in order to strengthen leg muscles and help maintain knee and ankle ROM. A helpful rehabilitative treatment could be walking barefoot on sand, which provides a soft ground to the foot and deforms depending on the pressure exerted.

Moreover, functional electrical stimulation of the motor neurons that innervate the weak dorsiflexor muscles could be a right approach. This technique consists in using electrical stimulators, which can be intern, percutaneous or implanted, aiming at activating and contracting a group of desired muscles. It is possible to modulate the electricity intensity and to place the stimulators on different muscle groups. A limit of

this approach is the difficulty in stimulating the deep muscles that contribute to fine movements, so this technique only allows for the execution of coarser movements.

The last conservative method to treat foot-drop patients is the application of external devices to the ankle and foot compartment (AFOs). They are not implanted in the body but allow to modify the functional and structural characteristics of the lower leg, in order to help patients to walk correctly without dragging or stumbling on the ground. AFOs will be deeply discussed in the following paragraph.

Surgical approach

For more severe patients with food-drop caused by trauma injuries, the correct treatment may be the surgical intervention. For a complete action, nerve decompression, nerve transection and nerve reconstruction should take place within 72 hours from the injury. Usually, the repair of the fibular nerve is performed using autologous nerve grafts. Return to function has been reported in about 97% of patients treated with this technique [16]. The risks of surgical intervention are due to the expertise of the surgeon and may lead to temporary or permanent weakness of the muscles innervated by the reconstructed nerve.

1.5 Ankle-Foot Orthosis (AFO)

An orthosis is a medical device worn or applied externally to the body with the aim of modifying the functional and structural characteristics of the compartment in which it is located. Orthoses can be applied to most limb joints, and usually their function is to provide partial or total immobilisation of a joint affected by trauma, arthrosis, ligament sprains, or which underwent surgery. Another use of orthoses is in conjunction with rehabilitation or functional re-education. Moreover, they can be used to reduce the load on a joint and decrease its pain, and for preventive purposes in cases of osteoporosis or bone failure.

Summarising, the most important functions that an orthosis may satisfy are: the management and correction of a deformity, limiting the ROM of a joint, the management of abnormal muscular functions.

1.5.1 Classification

This study focused on passive dynamic ankle foot orthoses (PD-AFOs), involving the lower limb in the tibio-tarsal articulation and in the foot, usually fixed to the lower leg via a strap that wraps the calf at the upper part of the tibia. The main function of PD-AFOs is to provide stability to the ankle and prevent the foot from dropping during the swing phase of the gait cycle [17]. Depending on the presence or not of electric actuators, AFOs can be classified as follows:

- **Passive AFOs**, which are the ones without any electric actuator or other active device. These interact with the subject without the need of external forces or moments, and rely on passive mechanical elements such as springs, dampers or flexible struts to improve the patient's walking ability [18].
- **Active AFOs**, which provide a tunable assistive torque about the ankle joint due to electric actuators. These facilitate great ROM, active damping upon heel strike, and powered push-off, but are often heavier and bulkier than passive designs and need external power and electronics [19]. Thanks to their activation, active AFOs can be helpful in saving patient's walking energy and are used as clinical tools for rehabilitation.

In this study we will consider only passive AFOs. These ones, in turn, can be classified as follows:

- **Rigid AFOs**, also known as solid or static, are the orthoses that more immobilise the ankle, controlling its movements in the three anatomical planes. They are usually indicated for more severe patients who don't feel stable during walking and have a low degree of residual force of the ankle dorsiflexor muscles. Structurally, rigid AFOs totally cover the back of the lower leg, from just below the fibular head to the heel, and fully support the sole of the foot to the toes. These AFOs are rigid, so they cannot bend following the natural flexion of the ankle during the midstance phase of gait, but they provide both a rigid control to the articulation and walking stability (Figure 16).

Figure 16: A rigid AFO.

- **Hinged AFOs**, are orthoses with a posterior calf shell separated from the foot-plate, connected to each other by metallic or polymeric hinges. Thanks to these elements, hinged AFOs can follow the plantar- and dorsiflexion movements of the ankle during the gait cycle, especially controlling the plantarflexion during the swing phase, but it has been seen that these allow excessive dorsiflexion during midstance. Moreover, due to the presence of hinges, these devices do not fit in most types of footwears, becoming uncomfortable (Figure 17).

Figure 17: A hinged AFO.

- **Dynamic AFOs**, are orthoses that can bend around their transverse rotation axis, which ideally corresponds to the horizontal axis of the ankle that goes from the fibular malleolus to the tibial malleolus. Dynamic AFOs can be considered like a spring due to their mechanical/dynamic behaviour: by flexing, these can store energy during the midstance phase of gait which can be released in the pre-swing phase, being helpful in the pushing phase and in preserving the energy cost of the patient. These AFOs are produced in less rigid materials, such as polymers and metal-polymer composites. Due to their lower stiffness, dynamic AFOs are not recommended for severe foot-drop patients who need a great amount of stability at the ankle joint during walking. Despite this, they can support the foot and have a minimal control of ankle inversion and eversion. Generally, their structure is less invasive than the other type of AFOs, leaving the heel "free to move" (Figure 18).

Figure 18: A dynamic AFO.

A key aspect to consider is that, although standard off-the-shelf orthoses can be found on the market available in different sizes, AFOs can also be customised following the individual morphology and needs, starting from the morphological measures and scans of the patient's compartment of interest.

1.5.2 Materials

AFOs can be made of various materials. The choice of the material is associated with a list of desired mechanical characteristics for the orthosis, such as stiffness, elasticity, durability, weight, fatigue, and corrosion resistance. The material used for PD-AFOs production must be elastic enough to follow the ankle movements, but also have a high yield strength allowing large deformations without reaching the plastic regime. Based on this knowledge, the most used materials for AFOs fabrication are:

- **Thermoplastic polymers** – such as polyethylene and polypropylene – are light polymers with an elastic behaviour in a little deformations regime. For high stress deformation they reach the plastic regime, without returning at the exact starting shape, but showing a permanent deformation. This phenomenon is known as "plastic memory" and is an important property, because within some stress limits the material is capable of returning to its initial configuration. When heated they become softer and malleable, when cooled they harden and crystallise.
- **Thermosetting polymers** – such as polyamides (nylon) and polyurethanes – are materials with the characteristic of becoming rigid, insoluble, and infusible once they work above their glass transition temperature. They behave as thermoplastics below this temperature limit.
- **Metals** – such as titanium alloys, cobalt chrome alloys, stainless steel – are materials with high mechanical properties. They are easy to work with due to their malleability, compactness, highly strength, and generally they have a high yield stress and fracture tensile.
- **Composites** – such as carbon fibre or fibreglass composites – are usually the combination of a matrix and fibres immersed in it. Generally, they combine the best characteristics of the materials they are composed of. Carbon fibre is

a composite formed by a resin matrix and carbon fibres and it is an excellent material due to its great properties such as stiffness, strength, chemical and temperature resistance, low thermal expansion, low density, and lightness. On the contrary, as each fibre composite, carbon fibre is a highly anisotropic material, so it has a preferred working direction along the fibres. Composites best fit for custom-made AFOs fabrication, due to their ease of being 3D printed.

Usually, an AFO can be produced with a materials combination from the categories listed above, to obtain an orthosis with the desired features from the best properties of each material.

1.5.3 Manufacturing

An optimum AFO should respect a list of requirements due to be functional to the foot-drop patient. Firstly, it must support the affected foot and give stability during gait, but it's important that it must be easy to use and not irritate or injure the skin too. Moreover, it would be preferable for the AFO to be light, durable, and aesthetically pleasing. Beyond that, the orthosis should be impact-resistant, fatigue-resistant, and flexible. Lastly, it would be favourable for the AFO to be cheap and manufactured in a short time.

Considering all these requirements, it is clear that creating the optimum AFO is really challenging. By the first prototypes, AFOs' fabrication technology has evolved from the conventional manufacturing – such as thermoformed polymer sheets – to 3D printing additive manufacturing – like stereolithography and selective laser sintering – that increase the possibility to produce complex shapes and decrease production's cost and time.

Conventional manufacturing: standard AFOs

The majority of standard AFOs available on the market in different sizes are produced via conventional subtractive technologies. Usually the process starts creating a plaster caster of the leg and foot, to produce a positive mould on which the AFO will be modelled. A thermoformed polymer sheet is applied around the positive mould via vacuum moulding in order to obtain the orthosis [20]. Beyond being used to produce

different sizes for standard off-the-shelf orthoses, this fabrication process is used to produce customised AFOs too, starting from the creation of a plaster cast of the subject's foot and leg. However, generally this is a long process that requires high human skills.

Additive manufacturing: custom-made AFOs

To date, modern 3D printing technologies allow us to obtain customised objects with excellent results in terms of cost and time of the entire production process. The most commonly used 3D printing techniques for AFOs manufacturing are described below.

- **Selective laser sintering (SLS)**: it consists in a high-power laser beam used to sinter powder particles, usually polymer-based or composite, in order to produce three-dimensional objects. The process starts from the input of a 3D file generated by CAD software, representing the model of the desired artefact. The powder is initially deposited in a platform to form a thin compact layer (from 10 to 200 μm thickness); the particles sinter when hit by the laser beam. The platform moves below, and layers are built one at a time, until the object is finished. To prevent oxidation, SLS is usually performed into a nitrogen-filled chamber. The not melted powder is used as support for the object during printing, then the final object is removed from the built chamber and cleaned from excess powder [17]. This process allows to obtain complex objects with high resolution, little costs and short-time fabrication; the absence of a support structure also helps to increase productivity. On the contrary, due to surface roughness of the printed object, it is not rare to require secondary processes, such as application of protective coatings.
- **Fused deposition modelling (FDM)**: this technique works on an "additive" principle by releasing material on layers. Like SLS, it is based on the input of a CAD file representing the model of the desired object. A thermoplastic filament is unwound from a spool, which delivers the material to an extrusion nozzle, with which the flow can be managed. The nozzle is heated in order to melt the material and can be guided in

both horizontal and vertical directions by a numerically controlled mechanism, that is, by following a path traced by slicing software, sent to the machine in the form of G-code. To promote the adhesion of certain materials to the printing surface, heated platens, or additives, are often used to counteract compression due to the cooling of the material. The minimum thickness of the printed layers depends on a list of factors such as the type of material, the nozzle's diameter, or the kinematic of the numeric control mechanism: it will result in a high anisotropy behaviour of the printed object. Another disadvantage of FDM is the need of a support structure for the printing of parts with an undercut, or otherwise geometries with an angle to the printing plane greater than 45 deg [21]. Moreover, FDM has a lower resolution than SLS.

- **Stereolithography (SLA)**: as the above technologies, SLA prints a three-dimensional object starting from a CAD file. This technique consists in a UV source capable of solidifying photosensitive polymer resins. The source may be a laser beam, DLP projectors (digital light processing) or LCD screens backlit by UV source. When exposed to UV, the resin polymerizes: the process is done layer by layer, slightly moving up or down the plate that contains the resin. After printing, the finished part is removed from the resin bath and heated in a UV hoven. A disadvantage of this technique is the need for manual support whether the printed object has parts not constrained to the base, as well as the long times requested for the full process realisation [22].

As mentioned above, all these 3D-printing additive manufacturing technologies require a file generated by CAD software, representing the model of the desired object. Therefore, to obtain a CAD model of a custom AFO, a 3D scan of the patient's foot and leg morphology is required. In the following section, methods about the design and manufacture of patient-specific AFOs will be briefly discussed.

1.6 Aims and thesis outline

"Custom-AFO" is a study performed by the Movement Analysis Laboratory of the Rizzoli Orthopaedic Institute (IOR) in Bologna. Using the selective laser sintering 3D printing additive manufacturing (SLS-3D technology), the study aims to produce a PD-AFO with a novel composite material, a fibreglass-reinforced polyamide (Windform® GT, CRP Technology, Modena), customised for each subject from a controlled group of foot-drop patients.

In agreement with the project, this thesis has two main objectives: the first is to analyse the kinematic and spatiotemporal data collected for the functional evaluation of a group of patients walking in three conditions - shod, wearing a standard off-the-shelf AFO (the Codivilla spring AFO), wearing the custom-made AFO – comparing them with each other and with kinematic data of a control group of healthy subjects: the main hypothesis is that the custom AFO should give support to the foot during the swing phase of the gait cycle and, at the same time, be more comfortable than a standard off-the-shelf one. Moreover, it is desirable for orthosis to better respond to the functional outcomes required by a subject by improving spatiotemporal functionalities such as walking speed and stride length. The second objective of this study is to declare an innovative procedure to correctly calculate the energy and the power absorbed by the custom AFO during the stance phase of walking and released during the foot-off phase, evaluating the hypothesis whether it is an effective amount of energy helping the patient in walking, or not.

Having declared in Section 1 "Introduction" the state of the art of the foot-drop pathology and of the orthoses and treatments used to supplant it, this thesis is organised as follows. In Section 2 "Materials and methods" the procedures and instruments used to carry on the study are described by paying attention to the custom AFO production process and to the measurements for its mechanical properties. Section 3 "Results" shows the relevant graphs obtained by the gait analysis, divided into the kinematic data, the spatiotemporal ones, the electromyographic data and the energy and power ones. At last, Section 4 "Discussion" gives an objective analysis of the results obtained considering the initial hypothesis of the study, evaluating the success or not and the limits and future developments.

2. Materials and methods

This section is organised in order to describe the principal steps to produce custom-made PD-AFOs with a novel fibreglass reinforced polyamide (Windform® GT, CRP Technology, Modena), starting from the scanning method of patient's leg and foot, following with the design of the AFO model, concluding with the fabrication of the orthosis and the firsts mechanical tests of the device. Functional evaluation methods via gait analysis will be discussed with the description of laboratory instrumentations and data processing methods.

2.1 Foot-drop patients

Patient ID	Age [years]	Height [cm]	Weight [kg]	BMI [kg/m^2]	Shoe size	Affected leg
2	68.2	180	83	25.6	44	left
3	77.5	195	96	25.2	45	right
4	50.3	184	95	28.1	45	left
6	49.5	183	97	29.0	45	left
8	57.3	183	85	25.4	45	left
9	63.0	178	94	29.7	43	left
10	69.9	175	76	24.5	40	left
11	73.6	172	80	27.0	44	right
13	56.9	178	77	24.3	41	left
14	82.9	159	59	23.3	39	left
Average ± std	**64.9 ± 11.4**	**178.7 ± 9.3**	**84.2 ± 12.0**	**26.2 ± 2.1**	**43.1 ± 2.3**	/

Table 1: The patients of the project study.

The study was approved by the Ethical Committee of the hosting institution (No. 0016384, 23 December 2019), and patients have provided informed consent to participate in the study. Patients were selected according to the following inclusion criteria: foot-drop due to nerve compression at the lumbosacral region of the spine; insufficiency of the ankle dorsiflexion muscles (power ≤ 3, according to the Medical Research Council (MRC) Scale

for power [23]), and agreement to wear the custom AFO for at least 6 months. Disorders of the central nervous system, severe degenerative diseases, and/or BMI > 30 kg/m^2 were considered exclusion criteria [17]. This study considered a group of 10 unilateral subjects suffering from foot-drop, reported in Table 1.

2.1.1 Clinical evaluation

Before the gait session and the treatment wearing the custom-made AFO, each patient was clinically evaluated being asked to fill out a questionnaire on its ankle or foot discomfort and overall inability status. The followed model was the Manchester Oxford Foot Questionnaire (MOxFQ), which is a 16-question validated patient-recorded outcome measure (PROM) for surgery of the foot and ankle. Each answer is scored from 0 to 4, with 4 denoting the 'most severe' status. Scores for each item are summed to form three separate subscales representing underlying domains: walking/standing problems (seven items), foot pain (five items), and issues related to social interaction (four items). Raw scale scores are then each converted to a metric from 0 to 100, where 100 denotes the most severe. At last, scores of the 16-items are summed up and converted to a metric from 0 to 100 to describe the overall disease status of the patient, with 0 denoting no severity and 100 the most severe status [24].

2.2 Codivilla spring AFO

Beyond wearing the customised composite AFO, during the functional evaluation in the motion analysis laboratory each patient is asked to walk on the pathway wearing a Codivilla spring AFO. This one is a standard off-the-shelf orthosis used to correct foot-drop or other foot and leg pathologies such as valgus foot or clubfoot. It's available on the market in four different sizes: Small for shoe size between 34 and 36, Medium from 37 to 40, Large from 41 to 44 and Extra-Large over 44 shoe sizes. It is a passive dynamic AFO, capable of bending during the stance phase of the gait cycle, and usually it is produced in thermoplastic materials such as polyethylene or polypropylene; the latter is the type used in this study (Ottobock). As being capable to flex, Codivilla spring's stiffness of the four sizes has been assessed through a novel apparatus in ranging from 0.154 to 0.378 $\frac{\mathrm{N\cdot m}}{\mathrm{deg}}$ in

dorsiflexion and from 0.231 to 0.419 $\frac{\mathrm{N \cdot m}}{\mathrm{deg}}$ in plantarflexion, with a direct proportionality between stiffness and size [25].

As each standard AFO, Codivilla spring is not tailored to a particular subject, but it is produced with the purpose to meet a set of more general functional requirements. Despite having a low cost, the orthosis can be uncomfortable in fit, as well as causing skin irritation from rubbing and being unsightly (Figure 19).

Figure 19: The Codivilla spring AFO.

2.3 Custom-AFO production

As stated in Paragraph 1.5.3, to produce a custom AFO, modern additive manufacturing technologies require a three-dimensional model of the orthosis, obtained by the scanning of the foot and leg of the subject. The main design criteria are based on the need for a comfortable and light object, capable of supporting the foot during the swing phase of walking, which is also easy to wear with most shoes. The custom AFO is characterised by a posterior hole to allow easy donning and comfort for the calcaneus. In addition, the footplate can be modified to address possible foot postural alterations such as excessive foot pronation or supination; in case of severe foot pronation, the footplate can be shaped to apply some inversion to the midfoot- and rearfoot. An important aspect to consider is that AFOs must resist ankle joint plantarflexion moments due to the weight and the inertial forces acting on the foot and footwear, especially during the swing phase (Figure 20). The definitive design of the custom AFO presents a curved calf shell aiming at providing enough rigidity and ensuring a rigid rotation around an axis aligned and close

to that of the ankle joint. Moreover, the calf shell cross-section is dimensioned to provide enough stiffness to prevent the foot from dropping during the swing phase of gait, while keeping the maximum stress of the regions subjected to the largest deformations below the material yield strength [17].

Considering these design principles, the main steps for the production of the fibreglass reinforced polyamide custom AFO are described in the following paragraphs.

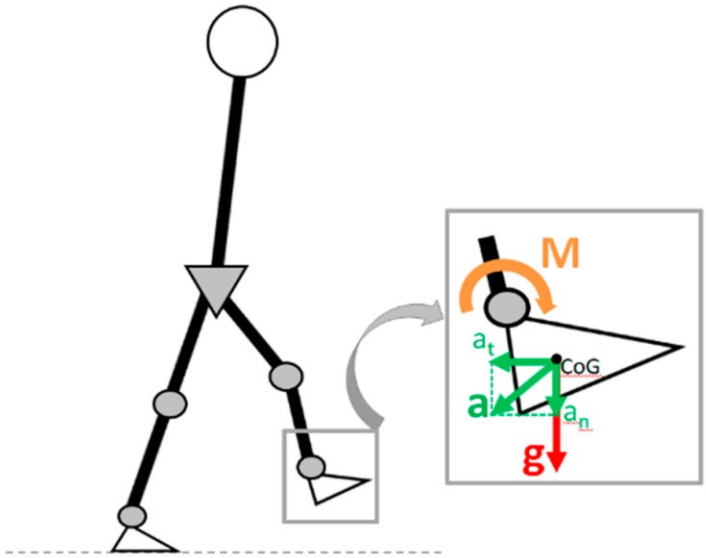

Figure 20: Schematic representation of sagittal-plane forces at the ankle joint. a and g represent acceleration and gravity vectors acting on the foot, respectively. The forces related to these accelerations cause a plantarflexion moment M at the ankle that must be counteracted by the action of the dorsiflexor muscles.

2.3.1 Scanning of foot and lower limb

The first step of the custom AFO's fabrication process is the scan of the patient's affected foot and leg morphology. To scan the foot with the patient in weight-bearing, a novel Kinect-based (Microsoft, Remond, WA, USA) 3D plantar foot scanner is used [26]. The patient stands on a 15 mm thick glass positioned 0.55 m above the Kinect depth-sensor which is set on a rotating plate (Figure 21). The Kinect sensor (Figure 22) is a depth camera which can capture depth and colours data of the surrounding environment: it consists of an infrared and RGB laser emitter which permits to obtain a 300000-point cloud 3D image of the scanned object through a triangulation process at a maximum 30 fps frequency.

Figure 21: The Kinect-based 3D foot scanner.

Figure 22: The Kinect depth-camera.

The sensor is manually rotated by 360 deg to obtain a 3D image of the foot plantar surface. In addition, a scan of the leg is performed by moving the Kinect sensor for 360 deg around the patient. To process the raw 3D data a commercial software is used (Skanect software, version 1.8, Occipital, Inc., San Francisco, USA). Then the STL files are imported in Geomagic Control (version 12, 3D Systems, Rock Hill, SC, USA) to edit and remove possible noise. At last, the scan of foot plantar surface and the scan of the leg are merged to create a complete three-dimensional representation of the lower limb of the subject (Figure 23), which will be useful to design the custom AFO.

Figure 23: A complete lower limb representation obtained by merging the foot and leg 3D scans.

2.3.2 3D design

The 3D model of the lower limb of the patient is imported in Blender (Blender Foundation, Amsterdam, Europe), an open-source 3D modelling software. It is used to anatomically adapt the AFO to the lower limb of the subject, with a manual and real-time control of freeform geometries, allowing a correct design tailored on the patient's geometry (Figure 24).

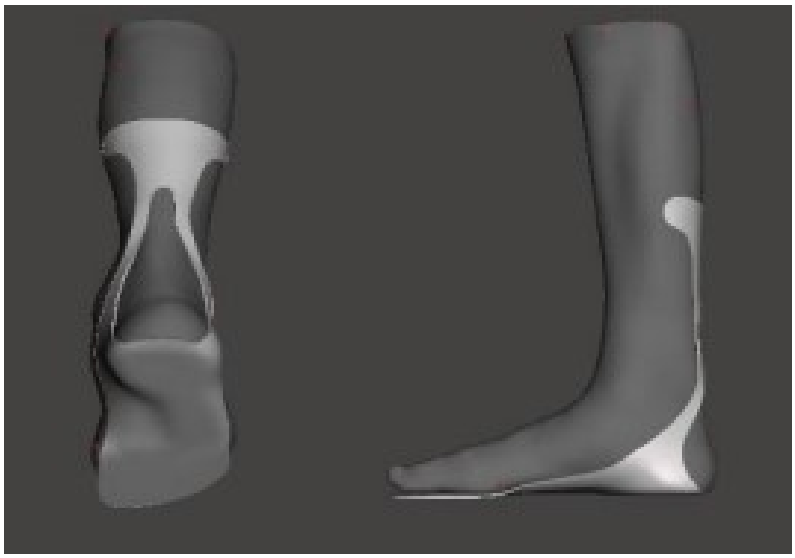

Figure 24: Posterior (left) and medial (right) views of a custom AFO 3D model.

Proper attention is taken into the congruence of the AFO both to the foot plantar surface and to the calf, to ensure a comfortable fixation of the orthosis to the leg and to avoid irritation from contact rubbing as much as possible. The optimal AFO thickness is parametrically calculated starting from the patient's foot length and body weight [17]. The final result of Blender editing is an STL file representing the 3D model of the patient-specific AFO, which will be the starting point for the additive manufacturing process.

2.3.3 Manufacturing

After checked that all the dimensions – such as plantar and calf shell lengths, thicknesses and bending stiffness – of the model correspond to those established in the design phase, the STL file of the custom AFO is sent to CRP Technology, a company

that produces high-performance components and devices via additive manufacturing. In about one day's time, the AFO is produced via SLS technology, following the process described in Paragraph 1.5.3. The material used is the Windform® GT, a fibreglass-reinforced-polyamide-based powder: it is highly elastic and flexible and is presented with an intense black coloration. Furthermore, it has excellent characteristics such as ductility, impact resistance, waterproofness, electrical non-conductance, and has obtained the safety certification for contact with the skin. All these qualities, in addition to the excellent technical parameters seen in Figure 26 – such as tensile yield strength = 56 MPa; tensile modulus = 3.3 GPa; elongation at break = 14.8%; bending strength = 88 MPa; bending modulus 3.2 GPa; density = 1.19 g/cm^3 – contributed to consider Windform® GT a suitable choice for custom dynamic AFOs. The resultant AFO is aesthetically pleasing to the eye, with a smooth finish to the touch (Figure 25).

Figure 25: Frontal (left) and lateral (right) views of a custom PD-AFO made of Windform® GT.

WINDFORM® GT

WINDFORM® GT	Test Method	SI Unity	Windform® GT
General Properties			
Density (20° C)		g/cc	1,19
Colour			BLACK
Thermal Properties			
Melting point	ISO 11357-2	°C	193,0
HDT, 1.82 Mpa	ASTM D 648 TYPE B	°C	169,4
Vicat 10N	ASTM D1525-09	°C	188,9
Mechanical Properties			
Tensile Strength	UNI EN ISO 527-1	Mpa	56,21
Tensile Modulus	UNI EN ISO 527-1	Mpa	3289,80
Elongation at break	UNI EN ISO 527-1	%	14,82
Flexural Strength	UNI EN ISO 14125	Mpa	87,90
Flexural Modulus	UNI EN ISO 14125	Mpa	3227
Impact Strength Unnotched (Charpy 23°C)	UNI EN ISO 179-1	KJ/m^2	54,28
Impact Strength Notched (Charpy 23°C)	UNI EN ISO 179-1	KJ/m^2	8,69
Electrical Properties			
Resistivity, Volume	ASTM D257	ohm*cm	2,62 x 10^15
Resistivity, Surface	ASTM D257	ohm	1,02 x 10^16
Surface Finish			
After SLS Process		Ra µm	6,20
After manual finishing		Ra µm	1,45
After CNC machining		Ra µm	1,15
Properties per Density Unit			
UTS per density unit		Mpa/(g/cc)	47,24
Tensile Modulus per density unit		Mpa/(g/cc)	2764,54
Flexural Strength per density unit		Mpa/(g/cc)	73,87
Flexural Modulus per density unit		Mpa/(g/cc)	2711,76

Figure 26: Windform® GT technical data sheet.

2.4 Custom-AFO mechanical properties

Before being used in patient's gait analysis functional evaluation, the custom AFO is mechanically evaluated at the Medical Technology Laboratory of IOR in order to control if its actual bending stiffness matches the stiffness analytically estimated prior to its fabrication.

Laboratory stiffness evaluation

To assess the AFO stiffness, a setup consisting of an axial-torsional testing machine (Biaxial 858 Mini-Bionix, MTS System Corp., Eden Prairie, MN, USA) is used, by simulating the midstance phase of walking. The footplate of the AFO is fixed to a rigid wall, thus the actuator is aligned with the ideal ankle joint axis parametrically measured according to anatomical proportions: vertical distance from the footplate is assumed to be 21% of foot length, horizontal distance from the calf shell plane – orthogonal to the footplate and passing through the posterior foot tip – is assumed to be 25% of foot length [27]. The actuator is composed by an aluminum rod replicating the leg, and by a plastic cylinder free to translate along and to rotate around the rod. The AFO calf strap constrains the upper border of the calf shell to the cylinder, with the subsequent flexion of the AFO at its posterior support when the actuator rod rotates under angular displacement simulating ankle dorsiflexion (DF) and plantarflexion (PF). The actuator is connected to a torque cell, which measures the AFO-resisting moment (Figure 27).

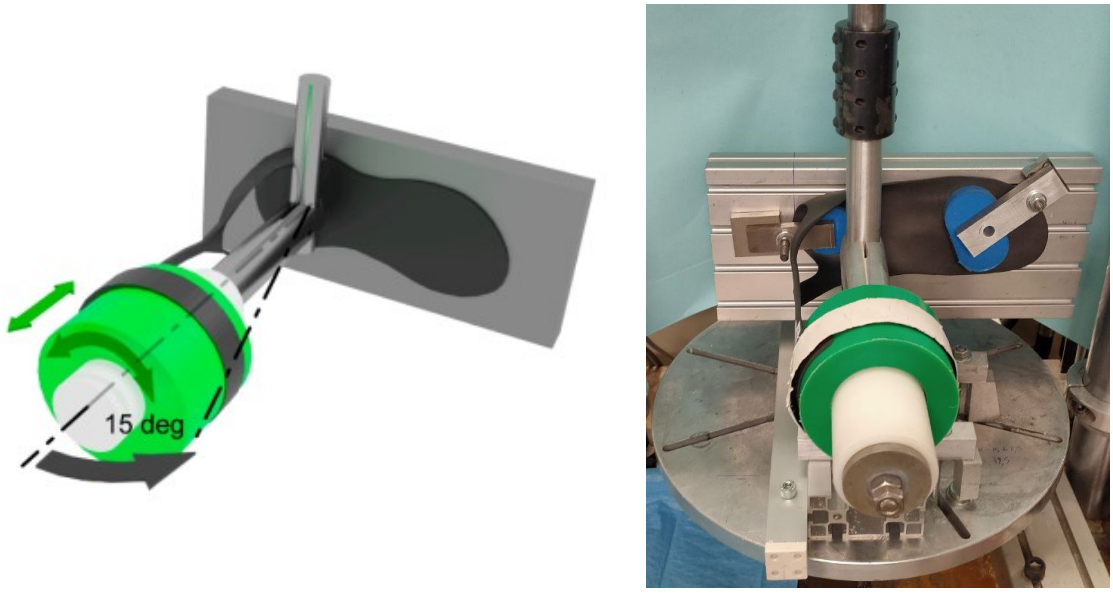

Figure 27: The experimental setup of the custom-AFO stiffness mechanical test.

According to the physiological ROM of the ankle during walking, 15 deg rotation in DF and PF are applied to the AFO at 15 deg/s speed [28]. The average slope of the torque/angle curve across five test repetitions is used to determine the AFO stiffness $[\frac{\mathrm{N \cdot m}}{\mathrm{deg}}]$ both in DF and in PF [25].

Analytical stiffness evaluation

At the same time the AFO calf shell stiffness can be analytically measured, approximating the posterior leaf to a rigid beam fixed to an end (Figure 28).

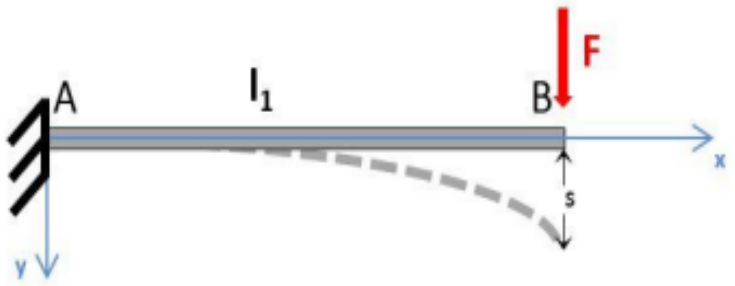

Figure 28: Analytical model of the AFO calf shell behaviour during midstance phase – l_1 is the length of the posterior leaf from the malleoli (A) to the calf strap (B). F is the force the AFO is subjected to during midstance dorsiflexion. s is the horizontal displacement of the posterior leaf due to the flexion.

Using trigonometric relations and considering the maximum dorsiflexion angle during midstance as $\alpha = 15$ deg, the horizontal displacement can be calculated as Equation 1 (Figure 29).

$$s = l_1 \cdot sin(\alpha) \qquad (1)$$

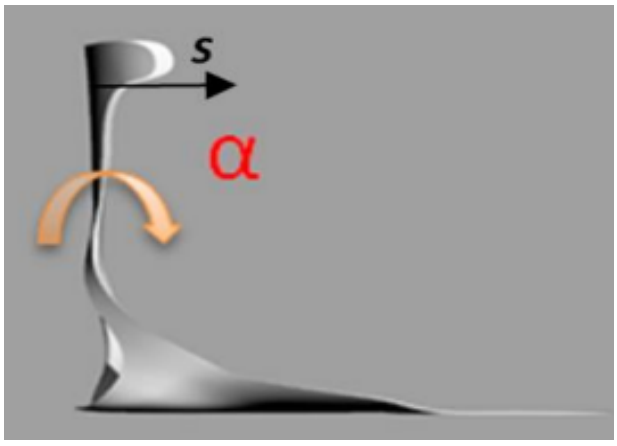

Figure 29: Angular deformation and displacement of AFO calf shell.

Horizontal displacement can also be measured as in Equation 2, where *E* is the Young modulus of the material (E = 3.3 GPa for Windform® GT), *I* is the area moment of inertia. In case of rectangular cross section with dimensions b and h: $I = \frac{b \cdot h^3}{12}$. *F* is the force impressed to the AFO calf strap and l_1 is the calf shell length.

$$s = \frac{F \cdot l_1^3}{3 \cdot E \cdot I} \tag{2}$$

The maximum bending moment *M* of a fixed beam of length l_1 and subjected to a concentrated load *F* is equal to $M = F \cdot l_1$. By expressing *F* from Equation 2, it is as follows:

$$M = \frac{3 \cdot E \cdot I \cdot s}{{l_1}^2} \tag{3}$$

The beam stiffness can be expressed as $K = \frac{M_{max}}{\varphi_{max}}$, where M_{max} is the maximum bending moment as *M* in Equation 3, and φ_{max} is the bending angle expressed in radians as follows, by substituting $M = F \cdot l_1$:

$$\varphi_{max} = \frac{F \cdot l_1^2}{2 \cdot E \cdot I} = \frac{M \cdot l_1}{2 \cdot E \cdot I} \tag{4}$$

By converting Equation 4 in deg from radians ($1 \text{ rad} \cong 57.3\ deg$) and substituting it in the moment equation, stiffness of a beam of length l_1 with a *b*h* rectangular section, and with a Young modulus *E*, becomes:

$$K = \frac{E \cdot b \cdot h^3}{57.3\ deg \cdot 6 \cdot l_1} \tag{5}$$

Equation 5 represents the approximate analytical calculation of the stiffness $[\frac{\text{N} \cdot \text{m}}{\text{deg}}]$ of a custom AFO with a posterior leaf calf shell of length l_1, subjected to a bending moment due to dorsiflexion during midstance phase of walking. *b* and *h* represent respectively the longitudinal length and the thickness of the AFO posterior support, while *E* is Windform® GT' Young modulus.

2.5 Functional evaluation via gait analysis

Once the AFO is fabricated and its mechanical properties are tested, the next step for the correct evaluation of its functional outcome is the gait analysis session. For the purpose of analysing spatiotemporal data and kinematic angles recorded, as well as the perceived comfort, each patient is asked to walk at comfortable speed along a 10 m pathway in three conditions: wearing his/her footwear (without AFO), wearing a Codivilla spring, and wearing the patient-specific custom-AFO. In the following paragraphs the procedures and the instrumentation needed for the AFO functional evaluation will be discussed.

2.5.1 Laboratory instrumentation

IOR's Movement Analysis Laboratory is fitted with a Vicon 612 stereophotogrammetric system (Vicon Motion Capture, Oxford, UK) consisting of eight M2 optoelectronic cameras sampling at 100 Hz (Figure 30). The system allows to track the position in 3D space of reflective markers applied in anatomical landmarks according to the IOR gait kinematic protocol [29]. A workstation is used to process and analyse the markers' trajectories and calculate the 3D position of each reflective marker. Rotations in the three anatomical planes are calculated at each joint in the lower limb throughout the gait cycle.

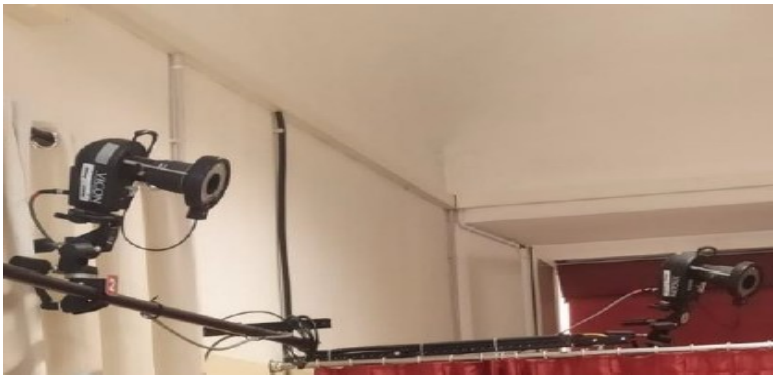

Figure 30: Two Vicon 612 cameras of the IOR's Movement Analysis Laboratory.

The eight Vicon cameras are positioned all around the gait pathway so that each marker on the subject can be seen simultaneously by at least two cameras at each instant of the session (Figure 31). The reflective markers are applied to the body of the subject

in accordance with IOR gait kinematic protocol (Figure 32). These measurements are affected by the accuracy in the markers positioning (operator dependent) on the subject's anatomical landmarks, as well as by soft tissue artefacts, resulting in kinematic data that are not always accurate.

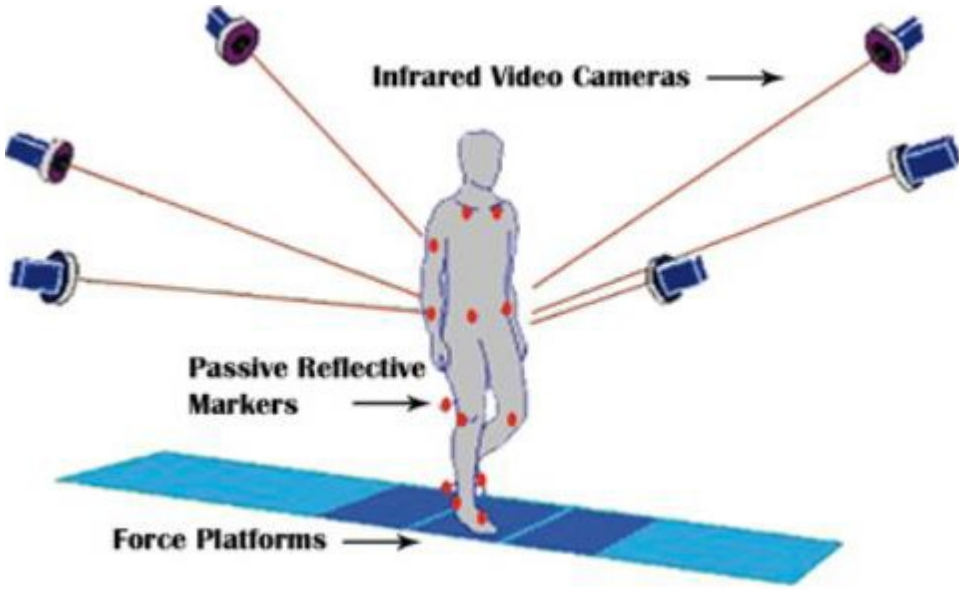

Figure 31: The gait analysis session setup - Red points are reflective markers positioned on the anatomical landmarks of the patient.

As seen in Figure 31, on the walking pathway there are two force platforms (Kistler Instruments, Einterthur, Switzerland), model 9281, based on piezoelectric sensors that measure the ground reaction forces sampling at 2000 Hz. These provide the three components of the force (vertical, medio-lateral and antero-posterior), the moments and the coordinates of the pressure centre. The platforms are "hidden" under the laboratory floor and arranged in sequence to be stepped over by the right foot and the left foot during a gait cycle.

In order to quantify muscular activation during walking, a set of wireless electromyographic sensors (Zerowire, Cometa, Milan, Italy) is applied on each patient (Figure 33). These sensors record the myoelectric activity of the underlying muscles, sampling at 2000 Hz. Four surface-electromyographic (sEMG) sensors are applied on both lower limbs: one on the tibialis anterior, one on the gastrocnemius, one on the rectus femoris, and one on the biceps femoris.

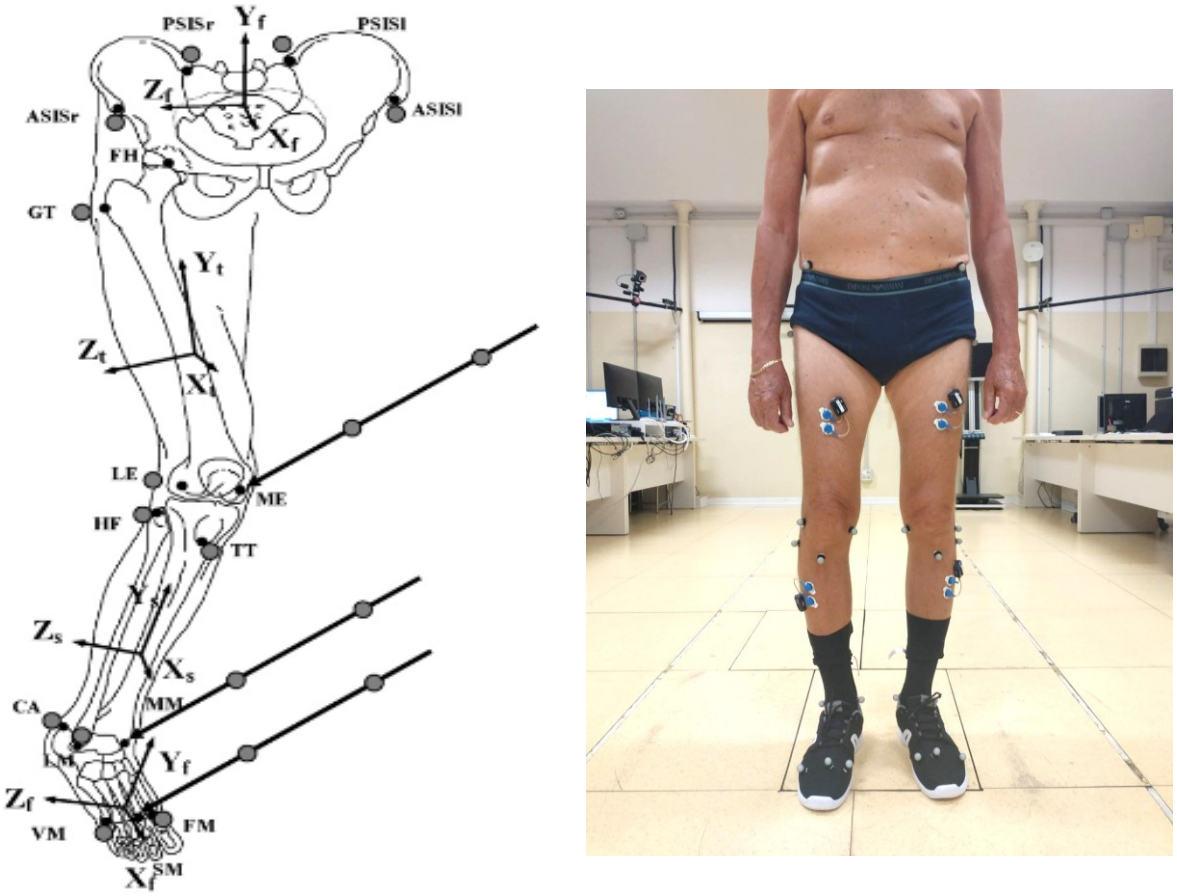

Figure 32: The body markers' positions according to the IOR gait kinematic protocol: on the foot they are positioned on the first (FM), second (SM) and fifth (VM) metatarsal head and on the calcaneus (CA), while LM and MM track the position of the lateral and medial malleolus of the ankle respectively.

Figure 33: A Zerowire electromyographic sensor.

2.5.2 Experimental data collection

Patients are clinically evaluated using the MRC Scale [30]: a clinician evaluates the plantarflexion and dorsiflexion residual force of the muscles of each leg manually applying respectively a dorsiflexion and plantarflexion force to the foot of the patient and asking him/her to contract the muscles in order to resist the external force. The muscular residual force is classified from 0 – no contraction – to 5 – normal muscle contraction. Patients undergoing this study must have a dorsiflexion muscular force in the affected leg ≤ 3, according to the inclusion criteria.

After the clinical evaluation, the clinician evaluates the plantar foot shape and morphology by positioning the patient in weight-bearing on a podoscope (Figure 34), which highlights the footprint and consequently helps evaluating the shape of the plantar arch to classify the foot as cavus, normal or flat. This analysis is necessary to consider a possible correction of the rearfoot during the scanning procedure, which would result in a insole-shaped AFO plantar surface, especially in case of iper-prone or supinated-foot, aiming to better distribute the body weight on the AFO/footwear.

Figure 34: A podoscope showing a normal footprint.

The patient is then asked to walk along the gait pathway in three different conditions – shod, wearing a Codivilla spring, wearing the custom AFO (Figure 36). Five good walking trials are recorded for each condition. Each patient is asked to familiarise with the AFOs several minutes before the recording session. The patient then is asked to fill a visual analog scale (VAS) questionnaire (Figure 35), indicating

the perceived comfort at the plantar foot-plate, at the calf shell, the overall comfort and the perceived support to the pushing phase, when wearing the two AFOs.

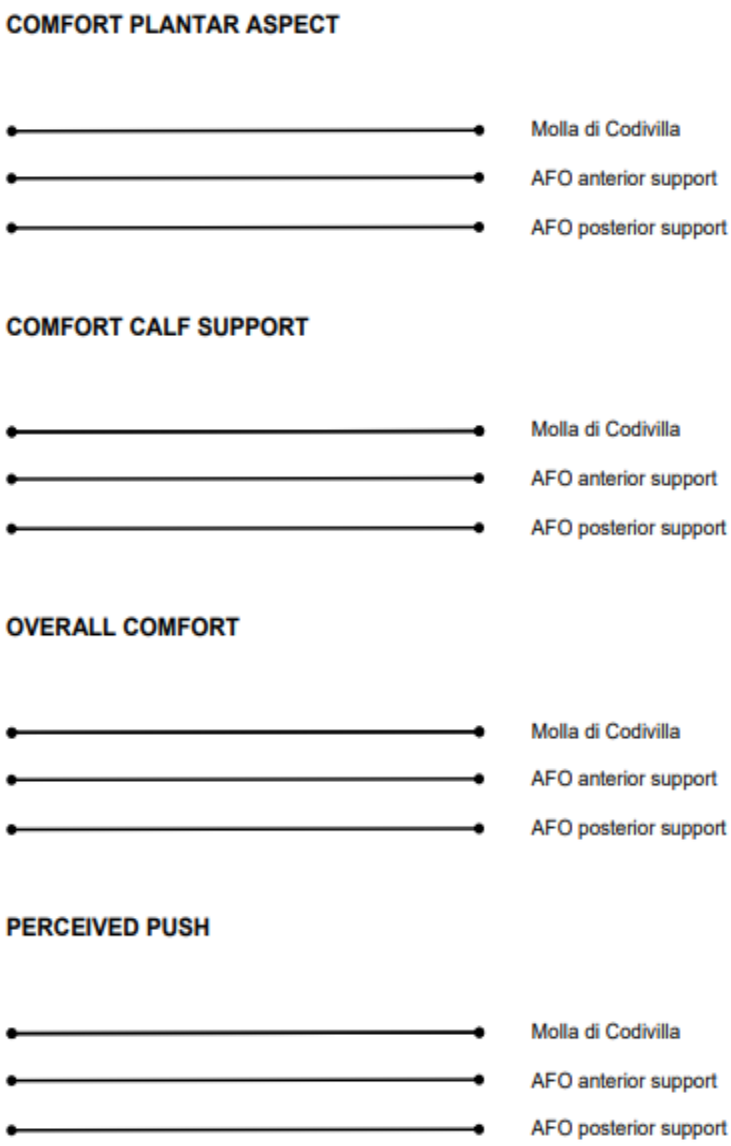

Figure 35: The VAS questionnaire asked to fill out by the patient after every gait session.

Before starting each walking session, the patient is asked to stand still in an upright position for a few seconds in order to record the static position of the markers, which will be used to calculate the neutral angles at all joints. In this calibration procedure, the markers positioned on the second metatarsal heads, on the medial malleolus, on the medial epicondyles and on the seventh cervical vertebrae are removed.

Figure 36: Gait analysis walking trials by a patient wearing a Codivilla spring (left) and the custom AFO (right) on the left foot. On the floor the two "hidden" Kistler force platforms are visible.

In order to calculate the energy absorbed and released by the custom PD-AFO due to its bending, three reflective markers are positioned on the posterior support of the AFO, as seen in Figure 37: two are placed medially and laterally on the lower part above the calcaneal donning hole, ideally along the ankle bending axis, while the third is positioned at the center of the upper extremity of the posterior calf shell.

Figure 37: A custom AFO (on the right leg) with the three markers placed on the posterior calf shell (one on the upper extremity, the other two on the lower one along the ankle bending axis passing through the malleoli).

2.5.3 Data processing

Once the gait analysis data are acquired, they are grouped in a .csv file for each walking trial in the three walking conditions. Each file contains the trajectories of the markers along the three spatial directions, the spatiotemporal data, the electromyographic muscular activation values and the ground reaction forces. In this study I mostly used the Matlab software to process the data, starting from the .csv file import. In the following paragraphs the data processing methods will be described.

2.5.3.1 Kinematics and kinetics

For each walking trial, all kinematic and kinetic data are time-normalised over the gait cycle duration – stance phase and swing phase of the gait cycle. Average and standard deviation of the angles recorded in the five trials of each condition are calculated, both for the affected and the unaffected leg. Kinematic angles of each lower limb joint around the three anatomical axes are plotted considering the different curves that the shod condition produces rather than those

produced by wearing the different AFOs. A population of 10 healthy subjects (mean age = 28.2 ± 10.0 years, mean height = 1.64 ± 0.04 m, mean weight = 55.1 ± 3.7 kg, mean BMI = 20.4 ± 1.2 kg/m^2) recorded with the IOR gait kinematic protocol is used as control for the ankle, knee and hip kinematic data.

2.5.3.2 Spatiotemporal data

In order to evaluate whether the AFOs result in better spatiotemporal parameters than the shod walking condition, data are processed to extrapolate the following parameters:

- **Stance time [% stride time]**, measured as the percentage of a gait cycle. It represents the time between the first contact of the foot to the ground, known as heel strike, and the moment in which the same foot leaves the ground, known as heel off. It is approximately around 60% of gait cycle.
- **Swing time [% stride time]**, measured as a percentage of the gait cycle, is complementary to stance time and is approximately around 40%. It starts when the foot leaves the ground and finishes when the same foot touches the ground again with the heel strike.
- **Stride length [% height]**, measured in metres as the distance between two consecutive heel strikes of the same foot. Healthy subjects are supposed to have the same stride length for both feet. It differs from the step length, which represents the distance between the consecutive heel strikes of the two different feet. To get more uniform data, stride length of each walking trial condition has been normalised on the height of the patient.
- **Walking speed [% height/s]**, calculated as the multiplication product of the step length and the cadence of a subject, which is the number of strides in the time unit. A healthy subject normally has a walking speed of about 1.4 m/s [31] To get more uniform data, walking speed of each walking trial condition has been normalised on the height of the patient.

For each patient, the parameters above are calculated for both legs as the average of the parameters recorded for each of the five-walking trials. This procedure is performed in each of the three walking conditions.

2.5.3.3 Electromyography

In order to objectively measure the degree of impairment in the foot-drop patient, the activation of the tibialis anterior m. in the affected leg has been recorded during each of the five walking trials in the three conditions, as well as the muscular activation of the gastrocnemius, the rectus femoris and the biceps femoris. For each muscle, the envelope of the sEMG, combination of rectification and low pass filtering of the signal, was considered. This allows to visualise the activation (μV) of each muscle at any frame of the gait cycle. The average of the five walking trials of each AFO condition is calculated and compared to the shod condition.

Thereafter, each average EMG envelope is normalised on the maximum contraction value recorded during the gait session, considering both affected and healthy leg in the three walking conditions. EMG data from 25 healthy subjects (mean age = 53.1 ± 8.7 years) were used as control for the tibialis anterior and the gastrocnemius muscles. These control data represent the envelope of the EMG signals recorded during a gait analysis session normalised on the maximum voluntary contraction value of the tibialis anterior and gastrocnemius of the healthy subjects.

2.5.3.4 Energy contribution

The following section reports the methods used to estimate the energy contribution of the custom AFO to the patient during the stance phase of the gait cycle. Some energy is absorbed and released in the calf shell and in the foot plate due to the bending mainly in the sagittal plane. The 3D coordinates of the reflective markers placed on the posterior aspect of the calf shell (Figure 37) are used to establish the axes of the calf shell local reference system, while the coordinates of the markers positioned on the calcaneus and on the first, the second and the fifth

metatarsal heads are used to establish the reference system of the foot plate (which is assumed to move rigidly with the footwear).

- The direction of the mediolateral versor of the **calf shell reference system** (Figure 38, on the left) is defined by the vector passing through the two markers placed on the lower posterior aspect of the calf shell just above the calcaneal donning hole. Its positive direction is from left to right (Az in the Figure). The longitudinal (vertical) versor lies on the vector orthogonal to the mediolateral one and passes through the marker placed on the superior part of the AFO calf shell, and its positive direction is upwards (Ax). Lastly, the antero-posterior versor is the cross product of the two previously calculated versors and its positive direction is forward (Ay, towards the foot toes).
- The **foot plate reference system** has the origin located at the calcaneus landmark (CA). As seen on the right in Figure 38, the antero-posterior versor – By in the Figure – is directed on the vector that is the intersection between the plane defined by CA, the first (FM) and the fifth (VM) metatarsal heads, and the plane – orthogonal to the previous one – that passes through CA and the second metatarsal head (SM). Its positive direction is proximal (backward). The mediolateral versor – Bz in the Figure – lies on the same plane that contains y and is orthogonal to it, with a positive direction from left to right. Lastly, the longitudinal versor – Bx in the Figure – is the cross product of the two previously calculated versors and its positive direction is dorsal [32].

The location and orientation of the two reference systems are calculated both during gait and in the static posture. Thereafter, the rotations between calf shell and foot plate are calculated according to the convention established by Grood & Suntay in 1983 [33].

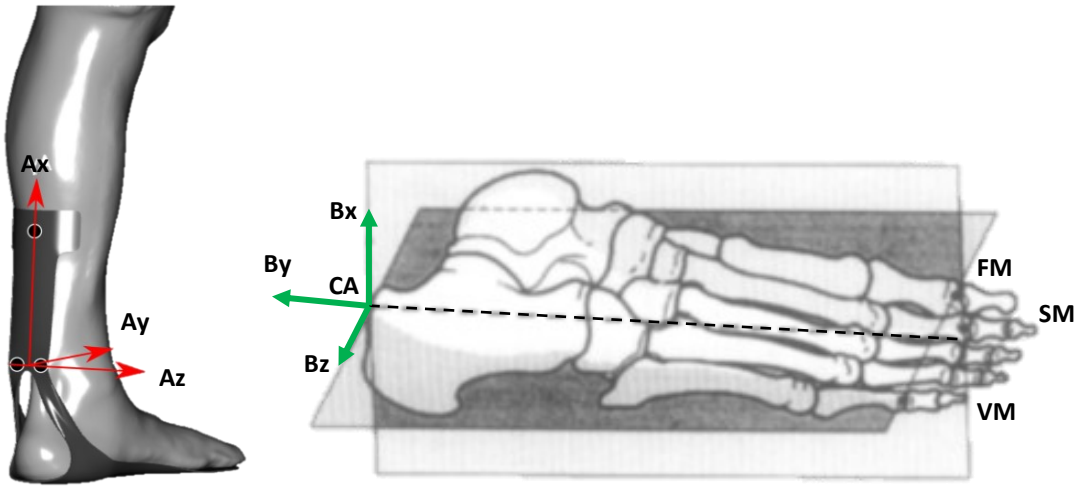

Figure 38: The calf shell (left) and foot plate (right) reference systems useful to measure the custom AFO flexion in the sagittal plane.

In order to visualise and report the actual deformation of the calf shell with respect to its neutral (0 deg deformation) position, the static posture neutral angles between calf shell and foot plate are subtracted from the angles recorded during the dynamic movements. Lastly, the calf shell rotation angles recorded are averaged for each patient across the five walking trials. The resisting torque in the calf shell is then estimated from the angle/torque relationship measured during the laboratory mechanical tests (see Paragraph 2.4), using both the flexion and extension regression data. According to this procedure, the resisting torque (y) is linearly correlated to the flexion/extension rotation angle (x) as in the following relationship:

$y = m*x + q$, where m is the actual stiffness of the AFO.

We have determined that a linear relationship has a lower root mean square error (RMSE) than a second degree relationship (Figure 39).

Subsequently, the work [J] produced by the AFO is obtained as the product between the resisting torque [N*m] and the flexion/extension rotation angle [deg]. The work is assumed to be negative, as energy absorbed by the AFO, when the torque and the first derivative of the angles have the same sign. The work is assumed to be positive, thus energy released by the AFO to the patient, when the torque and the slope of the angle curve have opposite signs. At last, each AFO's work is normalised on each patient's body weight [J/kg].

Furthermore, the power exerted and absorbed by the calf shell, known as the energy produced in the time unit $[\frac{J}{Kg\ s}]$, is calculated as the first derivative of the work.

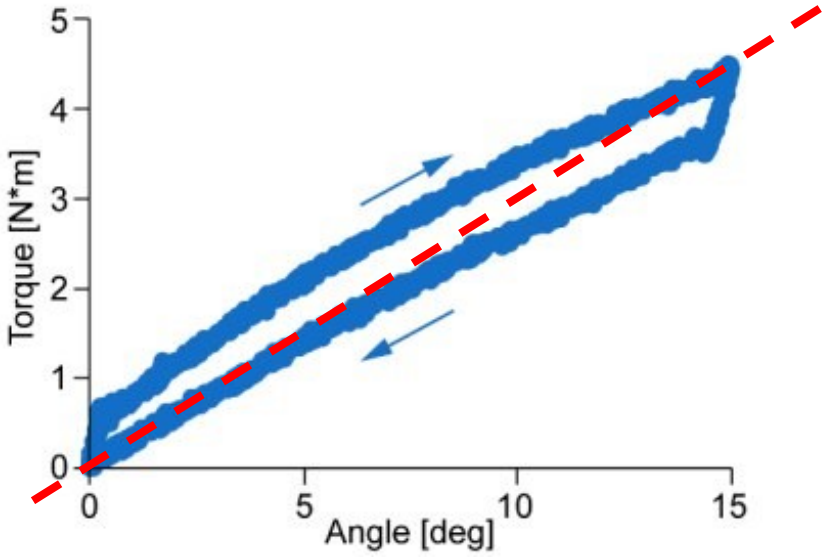

Figure 39: The linear relationship between the calf shell resisting moment and the AFO flexion angle.

2.5.4 Statistical analysis

The statistical analysis has been carried out through the non-parametric Friedman test [34] evaluating the kinematics data processed – as the ROM, the highest and the lowest angle recorded by each patient's joints in the three anatomical planes during stance, swing and full gait – and the spatiotemporal parameters as described in paragraph 2.5.3.2. For each parameter considered, the test ranks the mean values of each patient's walking condition in three groups – 1, 2 and 3 – from the lowest to the highest. Considering the shod condition as the pathologic baseline group, and the conditions wearing the Codivilla spring and the custom AFO as the treatments, Friedman test reports whether each treatment is significantly different from the pathologic condition, thus the p-value is lower than 5%.

3. Results

This section reports the main outcomes of the study divided into paragraphs in the following order: clinical evaluation; spatio-temporal parameters; lower limb kinematics and kinetics; sEMG data; custom AFO energy contribution, and comfort evaluation.

3.1 Clinical evaluation

Table 2 is reporting the outcome of the clinical evaluation according on the MOxFQ – on a metric from 0 to 100 – for each foot-drop patient in the following domains: walking/standing problems, foot pain, issues related to social interaction, overall status of disease. Grade 0 denotes no issues, while grade 100 denotes the most severe/painful condition.

Manchester Oxford Foot Questionnaire (MOxFQ)				
Patient ID	**Walking/standing problems**	**Foot pain**	**Issues related to social interaction**	**Overall disability status**
3	0.0/100	40.0/100	0.0/100	**12.5**/100
4	17.9/100	45.0/100	43.8/100	**32.8**/100
8	71.4/100	95.0/100	62.5/100	**76.6**/100
10	0.0/100	20.0/100	0.0/100	**6.3**/100
11	14.3/100	40.0/100	0.0/100	**18.8**/100
13	14.3/100	40.0/100	0.0/100	**18.8**/100
14	64.3/100	40.0/100	43.8/100	**51.6**/100
Average ± std	**26.0 ± 27.3**	**45.7 ± 21.5**	**21.4 ± 25.4**	**31.1 ± 23.2**

Table 2: The clinical evaluation of the patients of the study according to the MOxFQ validated PROM for surgery of the foot and ankle. For each patient a grade from 0 to 100 denotes the disability severity for the domains indicated in the column headers, and for the overall disability status. 0 is the less severe case, 100 is the most one.

3.2 Spatiotemporal parameters

Spatiotemporal parameters are important factors to consider to evaluate whether the AFO improves the quality of gait of foot-drop patients. Figures 40, 41, 42 and 43 show the mean values and the standard deviations of stance time, swing time, walking speed (normalised to height) and stride length (normalised to height) in each of the three walking conditions, across the 10 patients of the study, and the corresponding values in the control group.

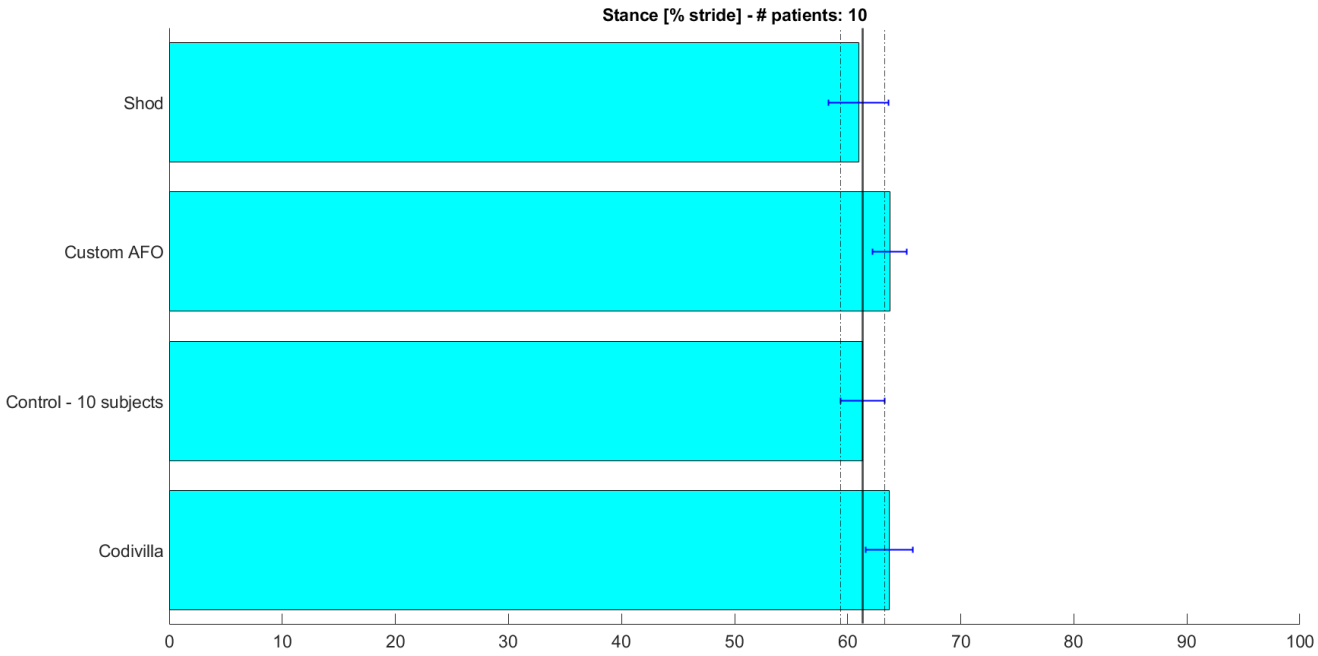

Figure 40: The mean percentage of the stance time on the stride time for each walking condition at the affected leg. Blue lines indicate the standard deviations. Black vertical lines represent the average value ± the standard deviation of the parameter for the control group composed by 10 healthy subjects.

Numerically, the mean values and standard deviations of **stance time** are the following:

- **Shod**: 61.0 ± 2.7 [% stride time]
- **Codivilla spring AFO**: 63.7 ± 2.1 [% stride time]
- **Custom AFO**: 63.7 ± 1.5 [% stride time]
- **Control**: 61.3 ± 1.9 [% stride time]

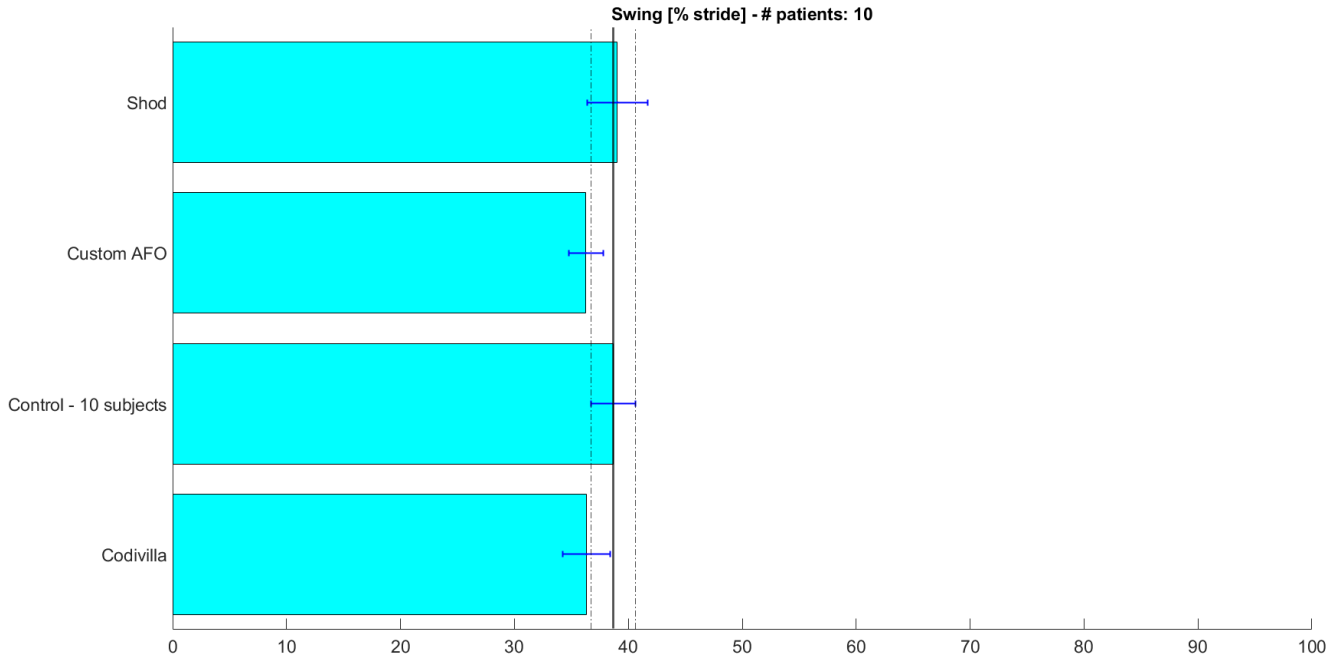

Figure 41: The mean percentage of the swing time on the stride time for each walking condition at the affected leg. Blue lines indicate the standard deviations. Black vertical lines represent the average value ± the standard deviation of the parameter for the control group composed by 10 healthy subjects.

The mean values and standard deviations of **swing time** are the following:

- **Shod**: 39.0 ± 2.7 [% stride time]
- **Codivilla spring AFO**: 36.3 ± 2.1 [% stride time]
- **Custom AFO**: 36.3 ± 1.5 [% stride time]
- **Control**: 38.7 ± 1.9 [% stride time]

Statistical analysis executed with Friedman test on all the patients of the study reports that both conditions wearing the Codivilla spring AFO and the custom AFO have a stance time – and consequently a swing time – significantly different from the same parameter but for the shod condition. Codivilla spring AFO allows patients to increase their stance time, thus decreasing their swing time, with a p-value of 0.002 while the custom AFO produces a higher stance time, and lower swing time, with a p-value of 0.002.

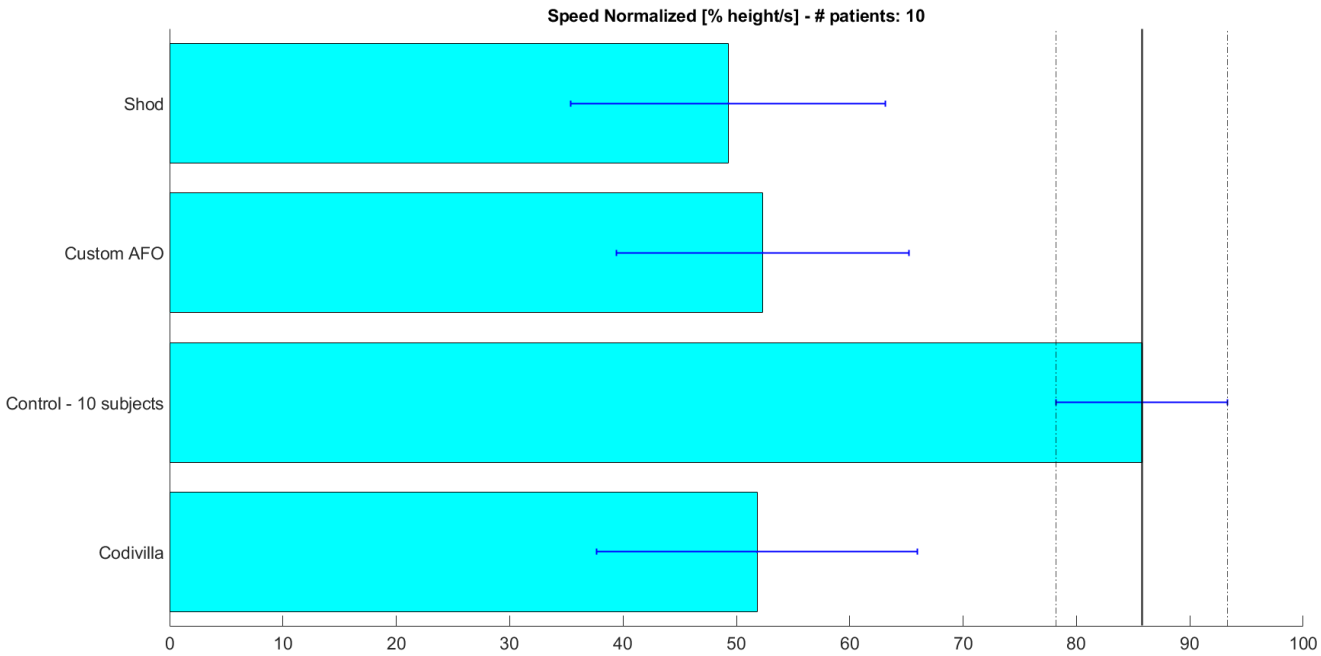

Figure 42: The mean speed of walking normalised on each patient height for each condition at the affected leg. Blue lines indicate the standard deviations. Black vertical lines represent the average value ± the standard deviation of the parameter for the control group composed by 10 healthy subjects.

The mean values and standard deviations of the **speed of walking** are the following:

- **Shod**: 49.3 ± 13.9 [% height/s]
- **Codivilla spring AFO**: 51.8 ± 14.1 [% height/s]
- **Custom AFO**: 52.3 ± 12.9 [% height/s]
- **Control**: 85.8 ± 7.6 [% height/s]

Statistical analysis executed with Friedman test on all the patients of the study reports that only the condition wearing the custom AFO allows patients to walk at a speed significantly higher than the one recorded when shod, with a p-value of 0.006. On the opposite, Codivilla spring AFO does not apport a significant difference in terms of walking speed with respect to the shod condition, with a p-value of 0.06.

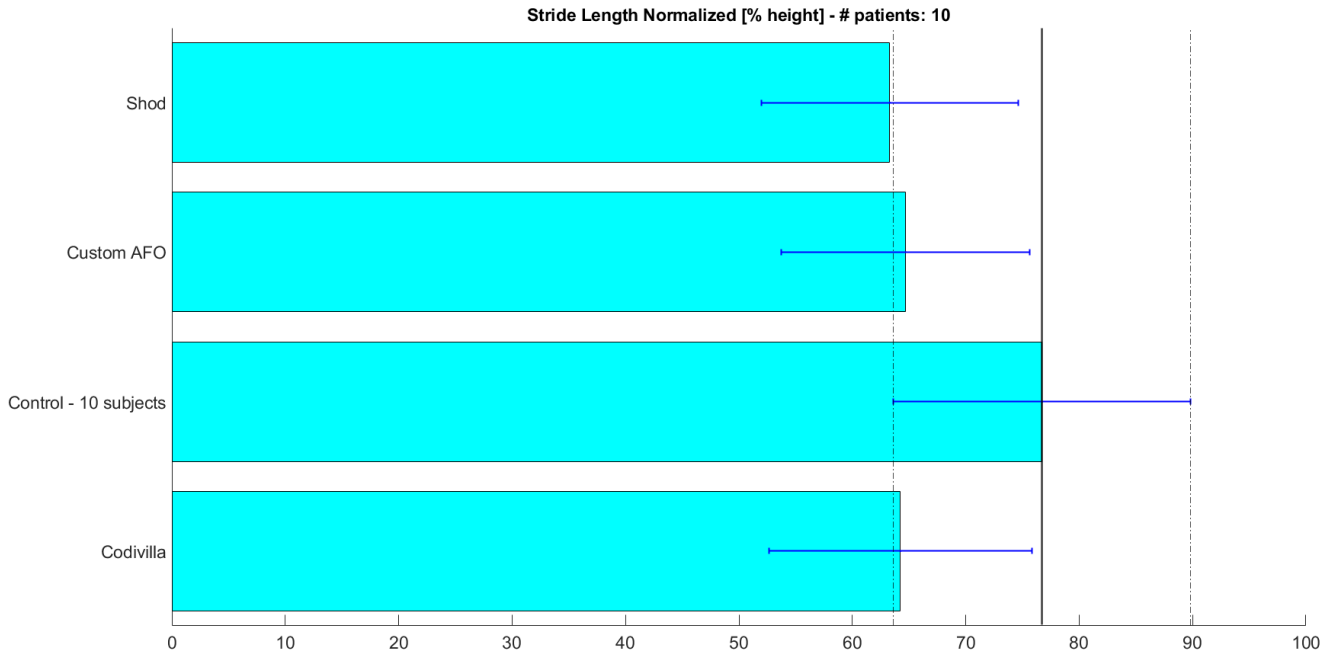

Figure 43: The mean stride length of walking normalised on each patient eight for each condition at the affected leg. Blue lines indicate the standard deviations. Black vertical lines represent the average value ± the standard deviation of the parameter for the control group composed by 10 healthy subjects.

The mean values and standard deviations of the s**tride length of walking** are the following:

- **Shod**: 63.3 ± 11.3 [% height]
- **Codivilla spring AFO**: 64.2 ± 11.6 [% height]
- **Custom AFO**: 64.7 ± 11.0 [% height]
- **Control**: 76.7 ± 13.1 [% height]

Statistical analysis executed with Friedman test on all the patients of the study reports that only the condition wearing the custom AFO allows patients to walk with a stride significantly longer than the one recorded when shod, with a p-value of 0.04. On the opposite, Codivilla spring AFO does not determine a significant difference in terms of stride length with respect to the shod condition, with a p-value of 0.09.

3.3 Kinematics and kinetics

The kinematics of ankle, knee and hip joints calculated for each patient are reported in the following paragraphs.

3.3.1 Ankle

In order to evaluate whether the custom AFO and the Codivilla spring AFO correctly support the foot during the swing phase of the gait cycle, Figures 44, 45 and 46 show the ankle kinematics of the affected leg for an exemplary patient in the sagittal, the frontal, and the transverse plane, respectively. The ankle kinematics in the sagittal plane for each patient is reported in the Appendix. Blue lines represent the mean angles recorded in the shod condition, the red ones represent the mean angles for the Codivilla spring and the green lines the mean angles while wearing the custom AFO. Angular data are reported as bands identified by the mean value ± 1 standard deviation. In addition, three vertical lines represent the stance phase duration for each of the three conditions.

Figures 47, 48 and 49 report the inter-patient average ankle joint angles in the affected leg in the sagittal, frontal and transverse plane, respectively. The violet curves represent the mean angles recorded in a 10-subject control group (average age = 28.2 ± 10.0 years).

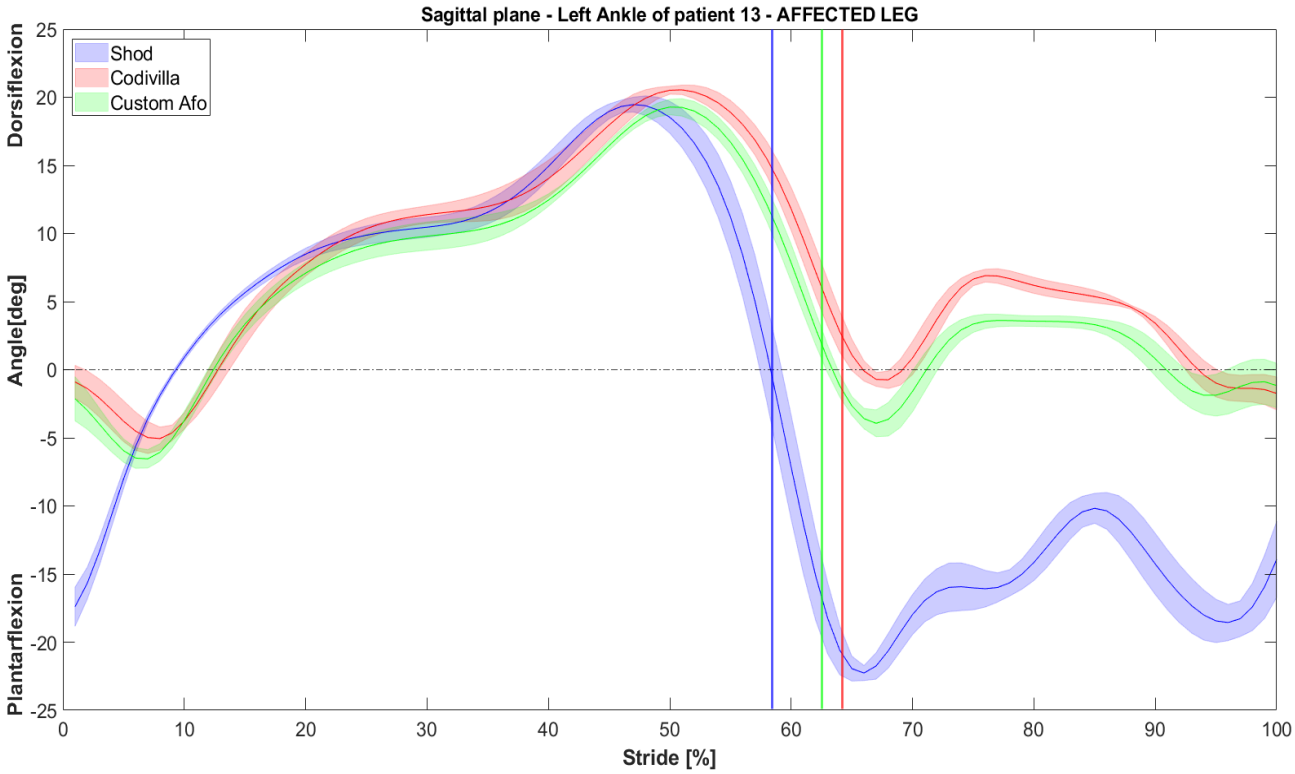

Figure 44: The ankle kinematics in the sagittal plane of the affected leg of an exemplary patient. The blue curve line represents the angles recorded during shod condition, the red one represent the ones recorded wearing the Codivilla spring and the green curve are the angles recorded wearing the custom AFO.

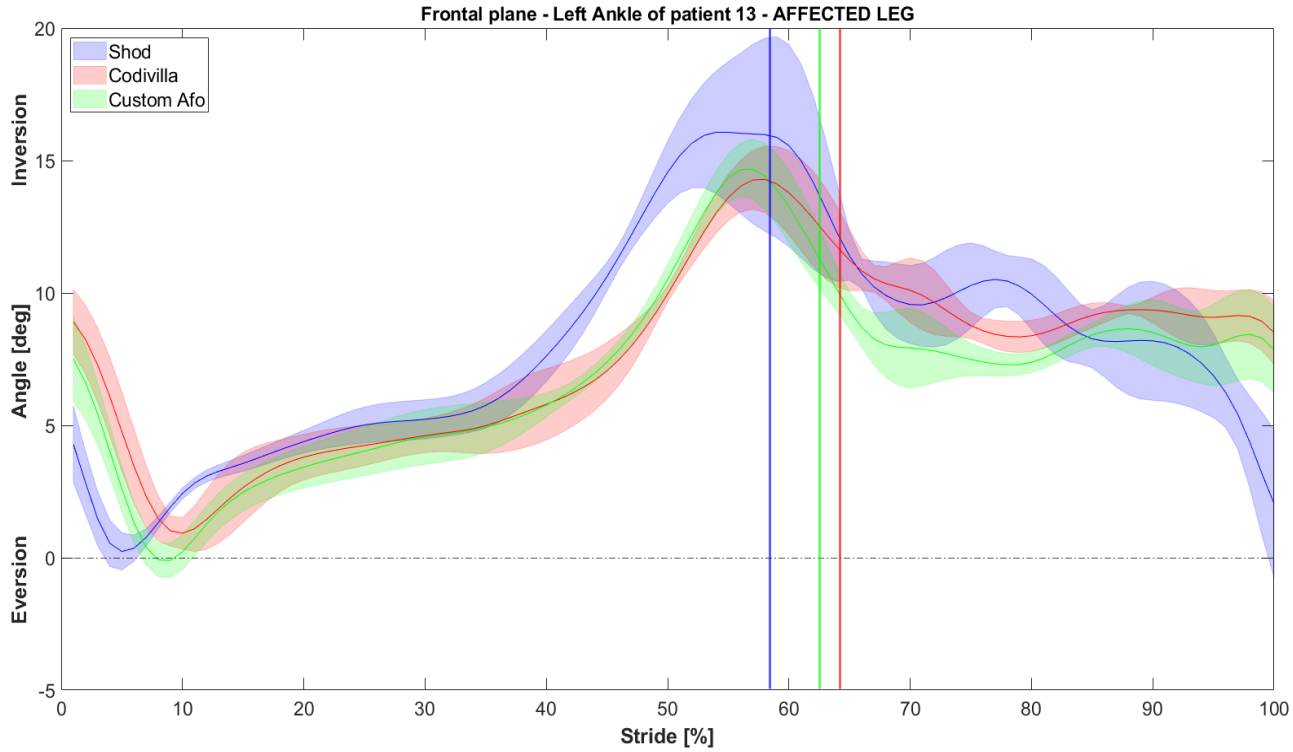

Figure 45: The ankle kinematics in the frontal plane of the affected leg of an exemplary patient.

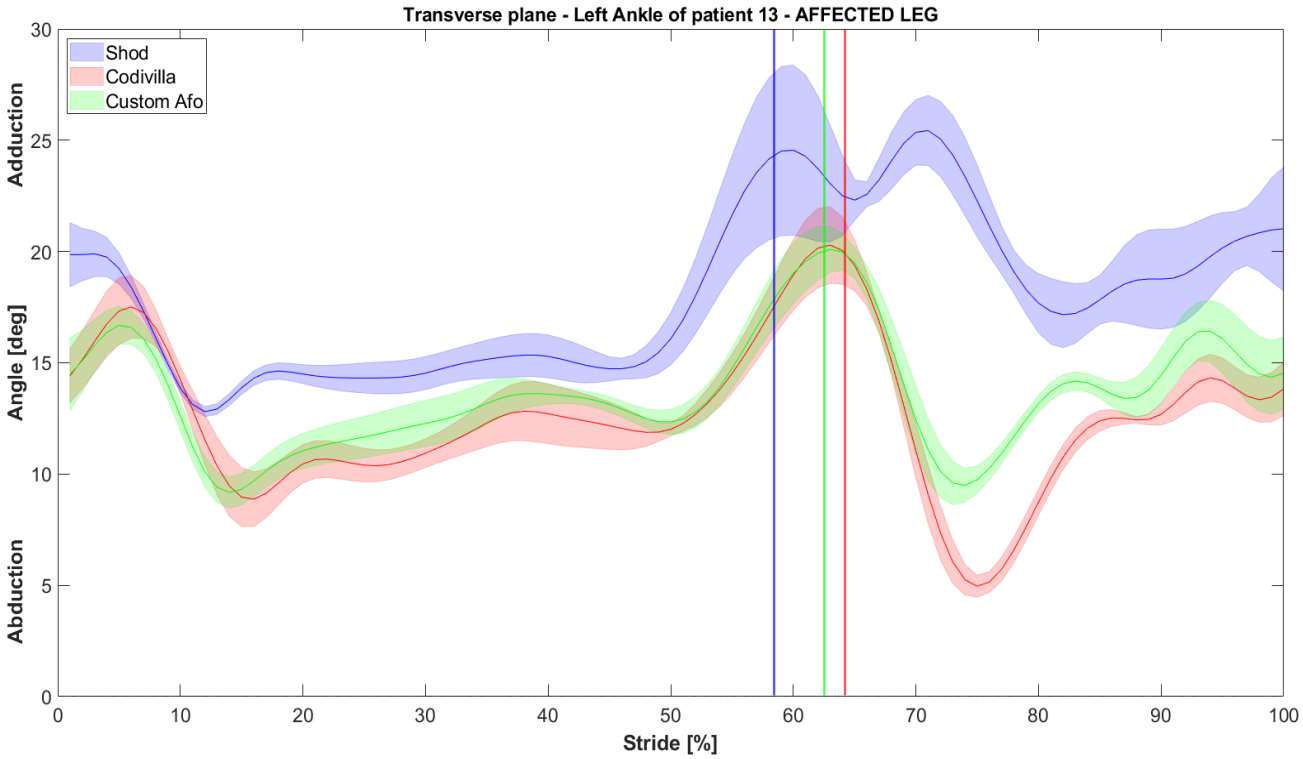

Figure 46: The ankle kinematics in the transverse plane of the affected leg of an exemplary patient.

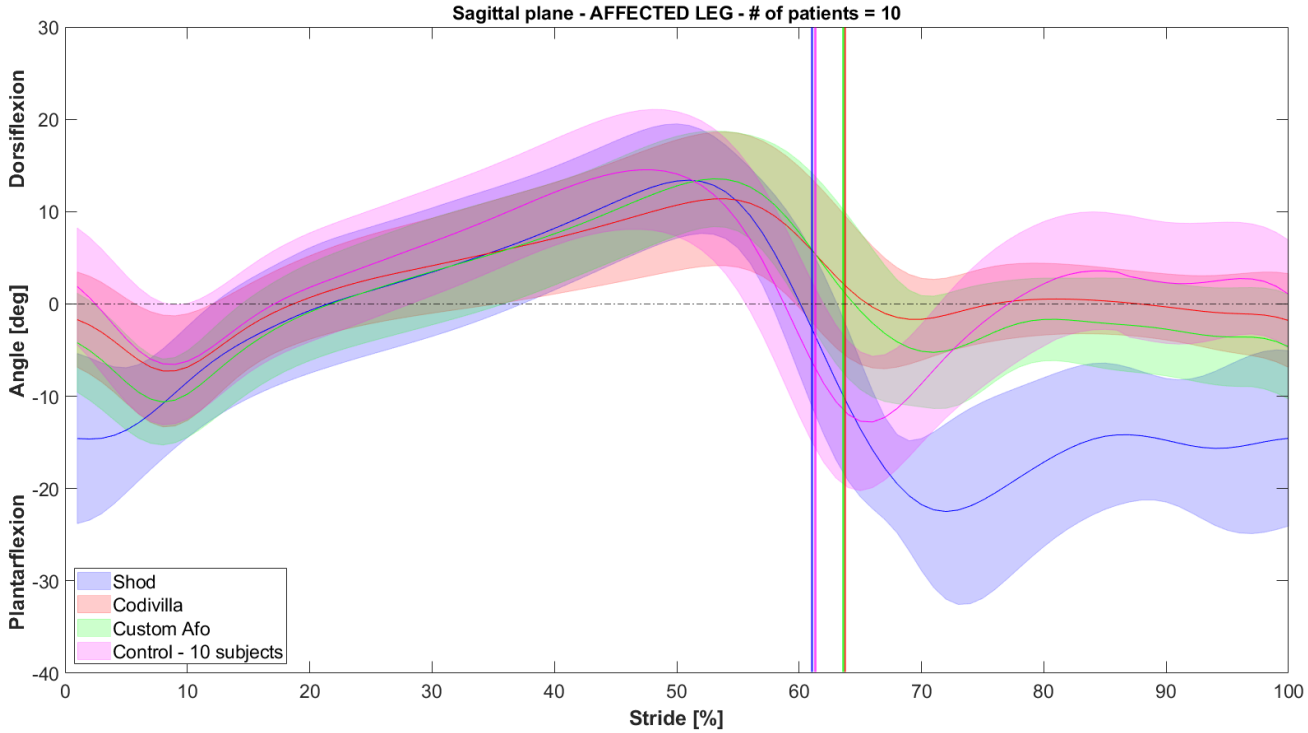

Figure 47: Ankle kinematics comparison of the affected leg in the sagittal plane between patients. The violet curve represents the mean angles of a control group composed by 10 healthy subjects.

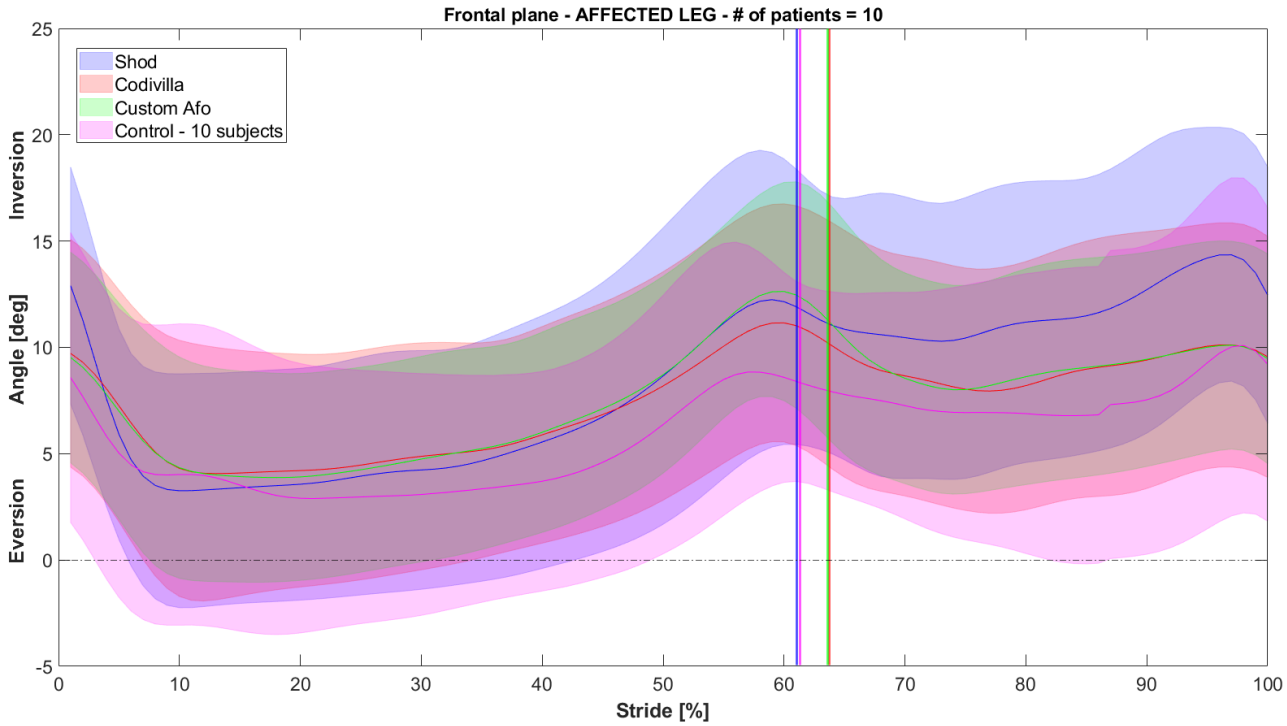

Figure 48: Ankle kinematics comparison of the affected leg in the frontal plane between the patients of the study and a control group composed by 10 healthy subjects (violet curve).

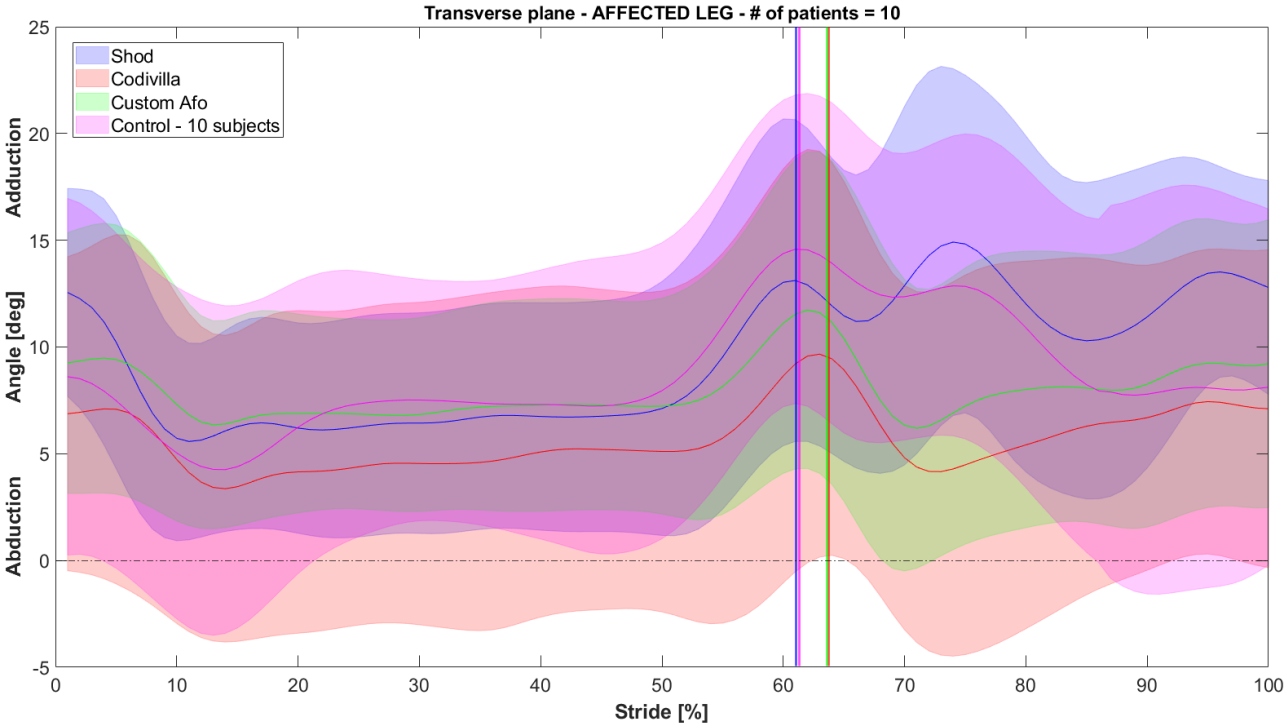

Figure 49: Ankle kinematics comparison of the affected leg in the transverse plane between the patients of the study and a control group composed by 10 healthy subjects (violet curve).

Lower limb joint angles have also been measured on the contralateral (healthy) leg of each patient in each walking condition. Figures 50, 51 and 52 report the mean values of the ankle angles in the sagittal, frontal and transverse plane respectively, measured on the healthy leg of the patients, and compared to the control group. The objective is to verify whether wearing an AFO affects the kinematics of the contralateral limb.

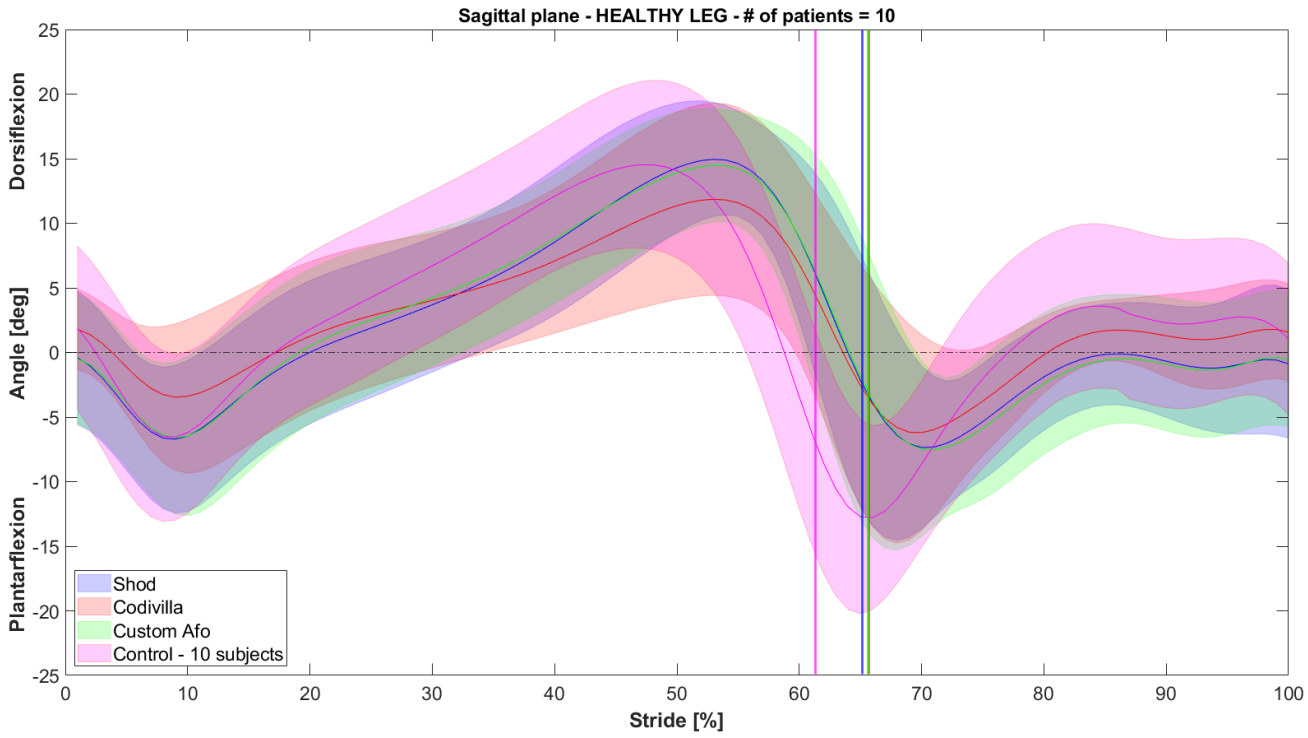

Figure 50: Ankle kinematics comparison of the healthy leg in the sagittal plane between the patients of the study. Violet curves represent mean sagittal angles of a control group composed by 10 healthy subjects.

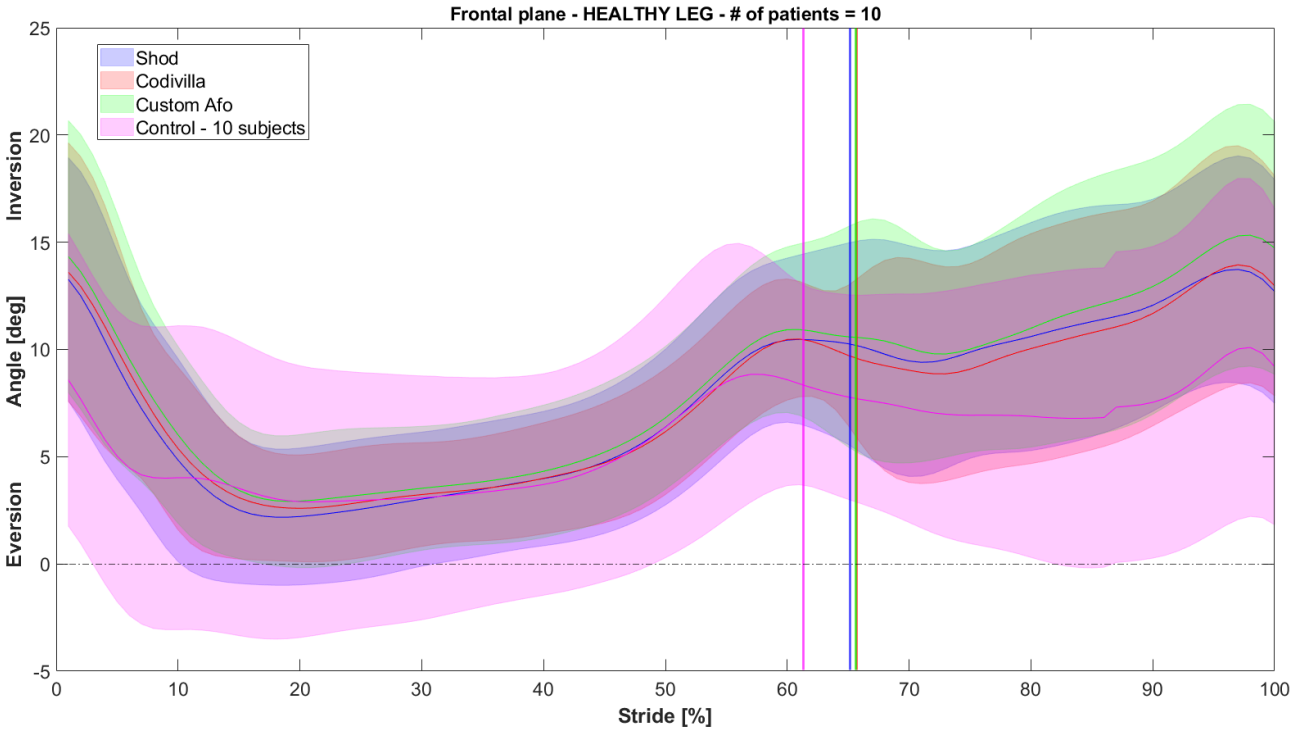

Figure 51: Ankle kinematics comparison of the healthy leg in the frontal plane between the patients of the study and a control group composed by 10 healthy subjects (violet curve).

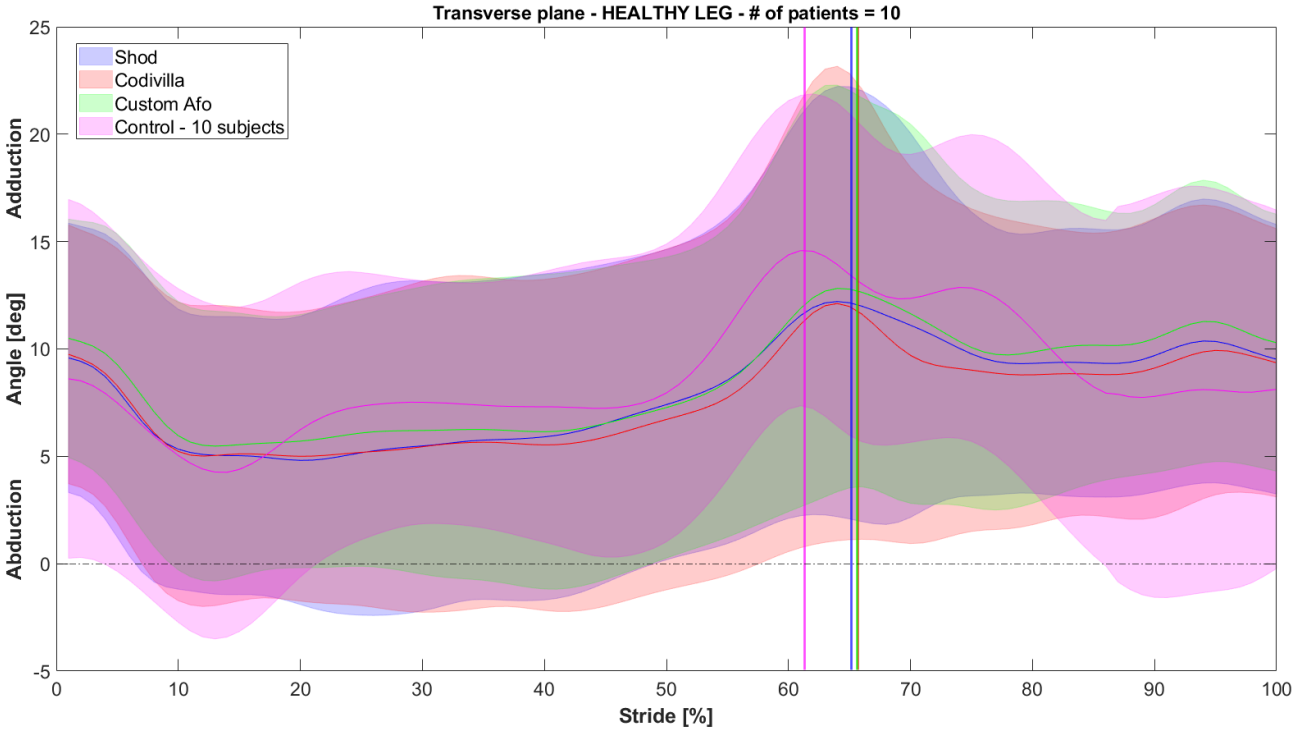

Figure 52: Ankle kinematics comparison of the healthy leg in the transverse plane between the patients of the study and a control group composed by 10 healthy subjects (violet curve).

3.3.2 Knee

Figures 53, 54 and 55 show the knee kinematics of the affected leg in an exemplary patient in the sagittal, frontal, and transverse plane respectively. Knee kinematics in the sagittal plane for each patient is reported in the Appendix. Blue lines represent the mean values of the angles for the shod condition, red ones for the Codivilla spring and green curve lines are for the custom AFO.

Figures 56, 57 and 58 report the inter-subject average knee kinematic angles in the affected leg in the sagittal, frontal and transverse plane respectively.

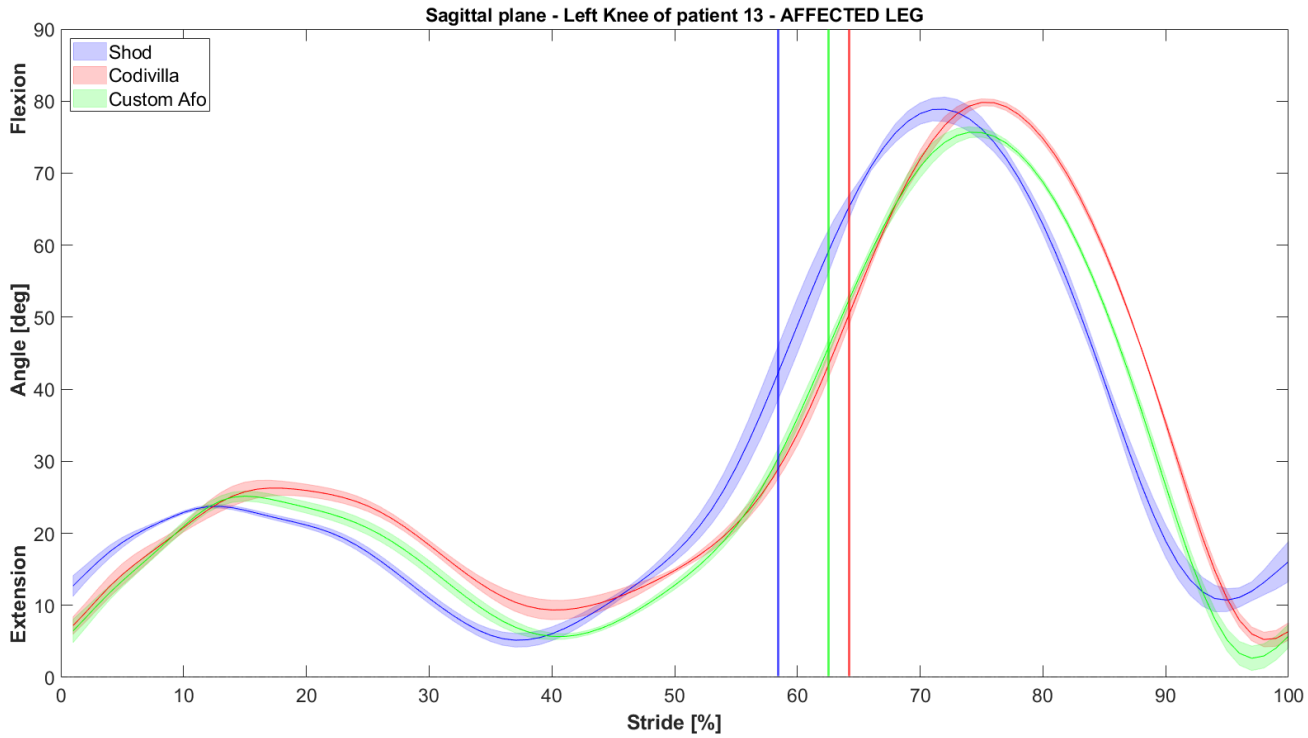

Figure 53: The knee kinematics in the sagittal plane of the affected leg of an exemplary patient.

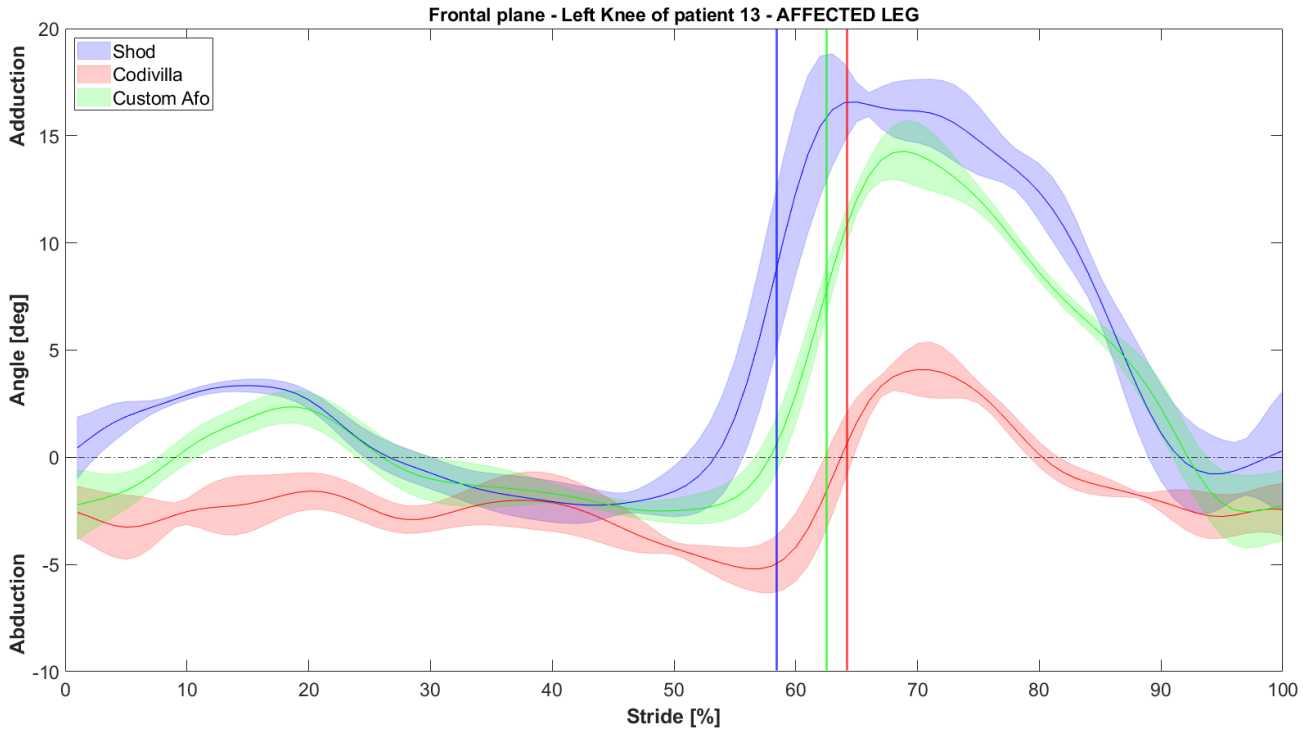

Figure 54: The knee kinematics in the frontal plane of the affected leg of an exemplary patient.

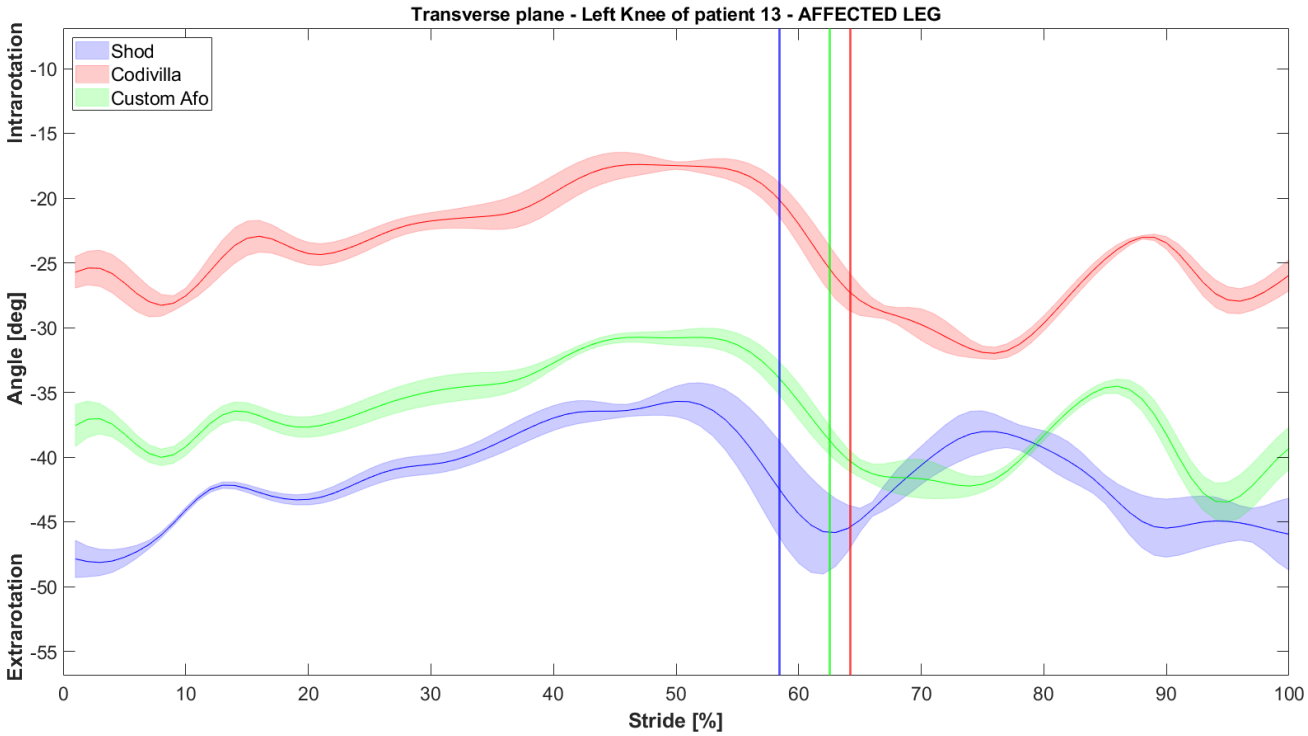

Figure 55: The knee kinematics in the transverse plane of the affected leg of an exemplary patient.

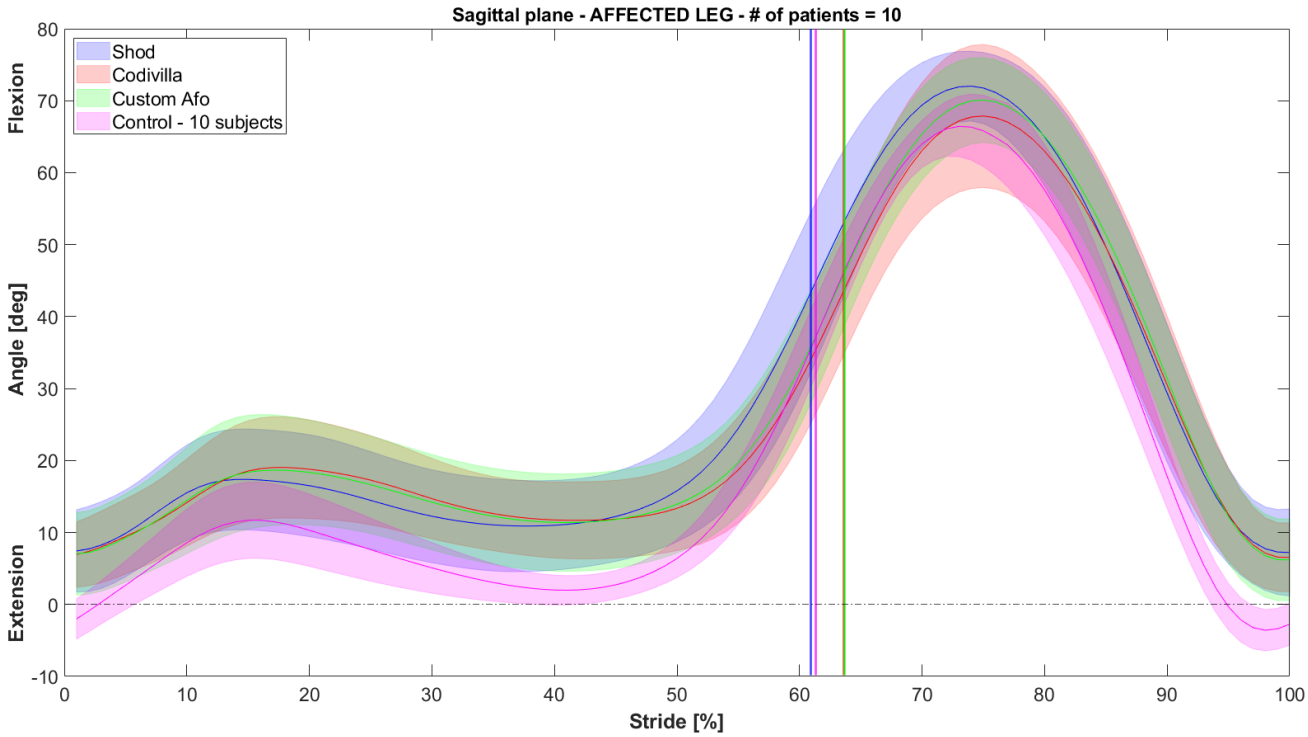

Figure 56: Knee kinematics comparison of the affected leg in the sagittal plane between the patients of the study and a control group composed by 10 healthy subjects (violet curve).

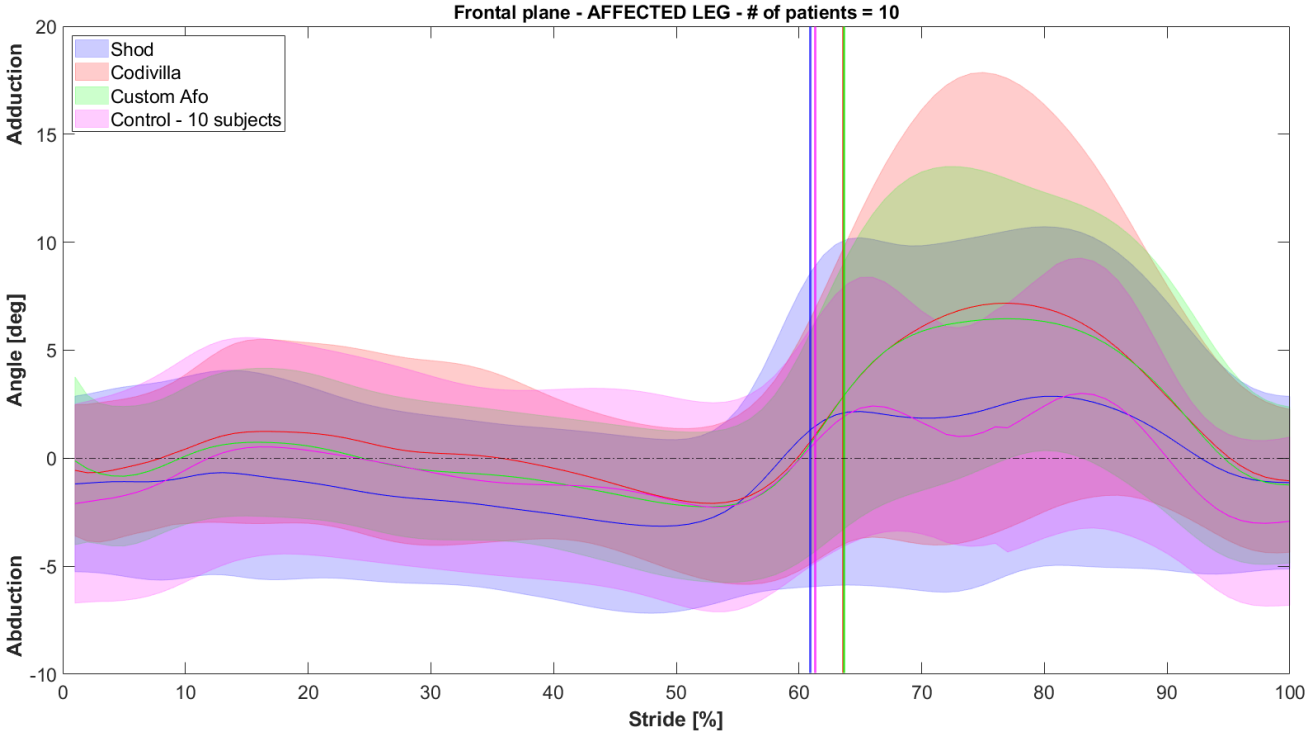

Figure 57: Knee kinematics comparison of the affected leg in the frontal plane between the patients of the study and a control group composed by 10 healthy subjects (violet curve).

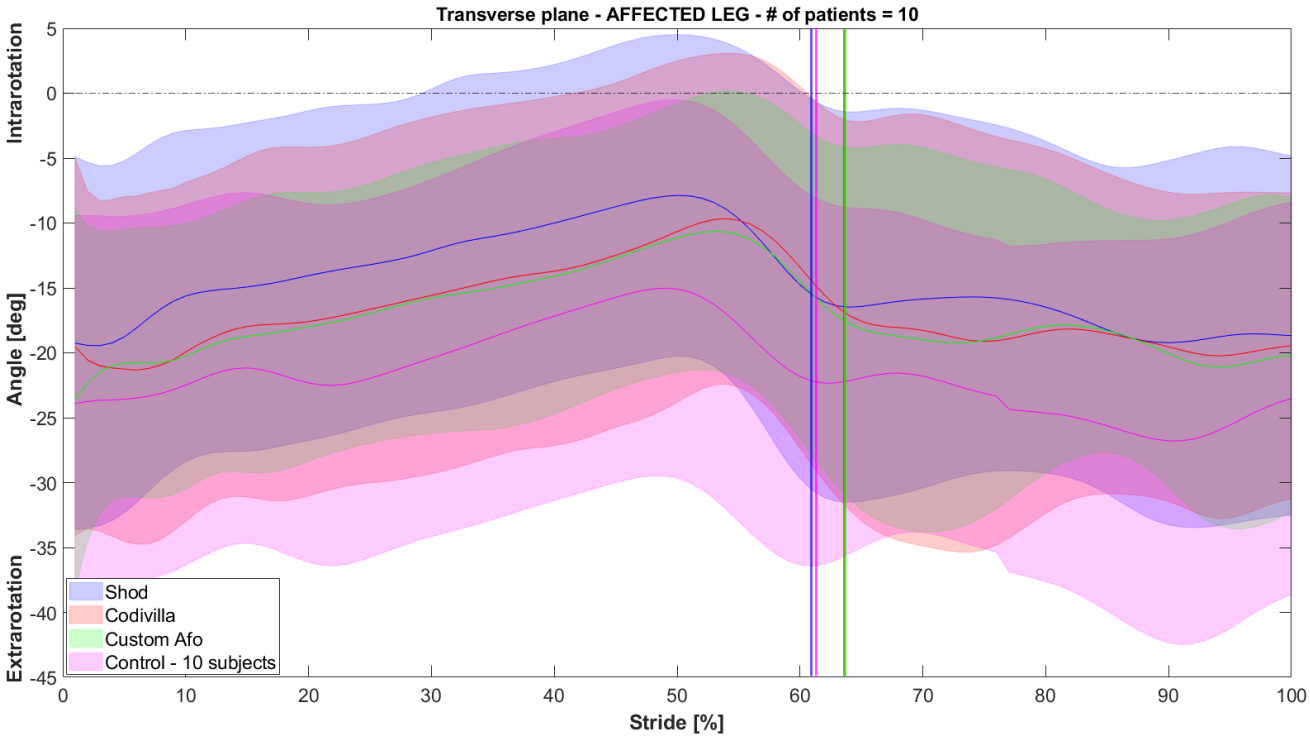

Figure 58: Knee kinematics comparison of the affected leg in the transverse plane between the patients of the study and a control group composed by 10 healthy subjects (violet curve).

Figures 59, 60 and 61 report the mean knee angles in the sagittal, frontal and transverse plane respectively, measured on the contralateral leg of the patients and compared to the 10-subject control group. The objective is to verify whether wearing an AFO affects the kinematics of the contralateral limb.

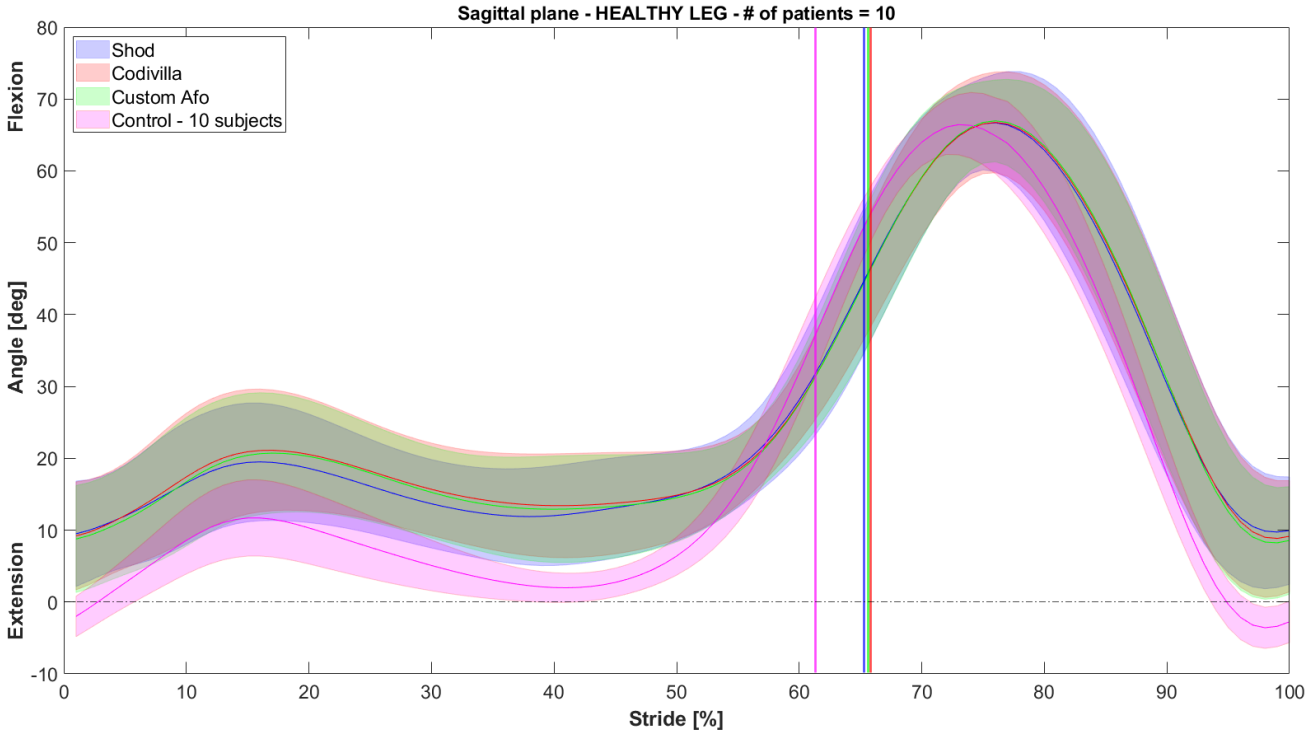

Figure 59: Knee kinematics comparison of the healthy leg in the sagittal plane between the patients of the study. Violet curves represent mean sagittal angles of a control group composed by 10 healthy subjects.

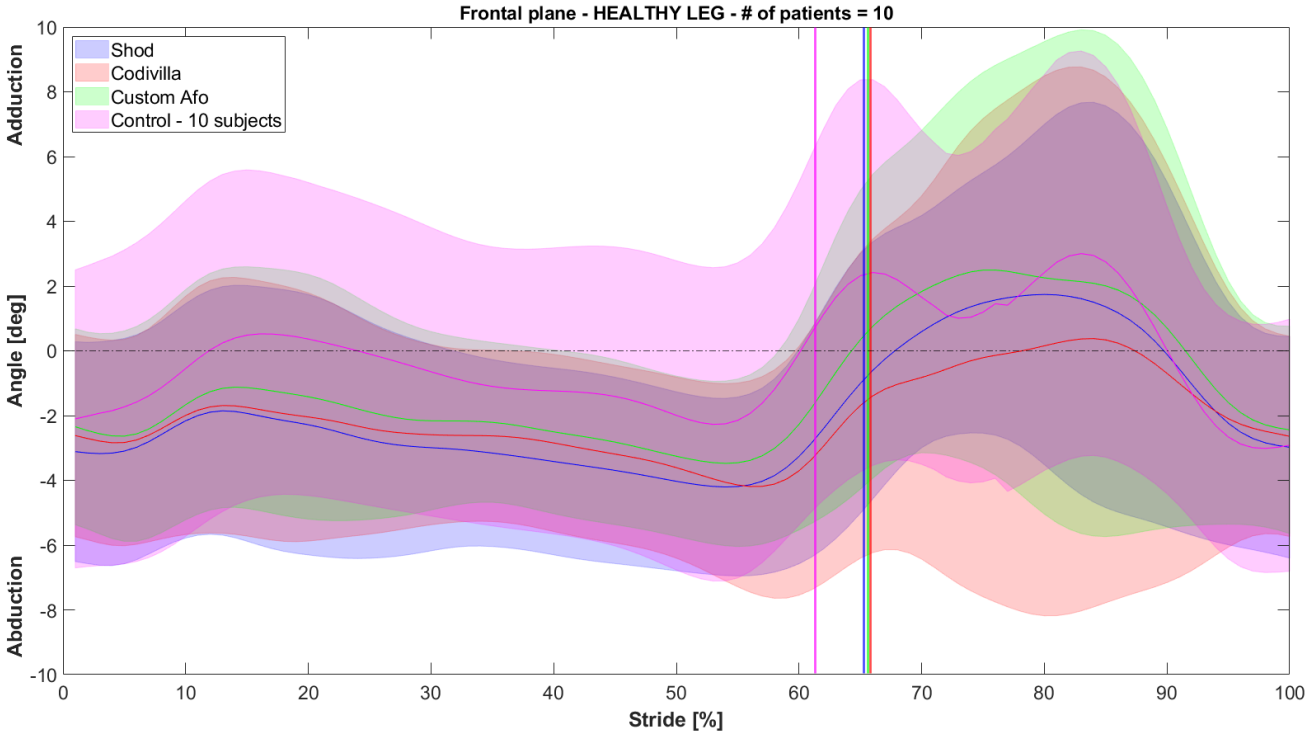

Figure 60: Knee kinematics comparison of the healthy leg in the frontal plane between the patients of the study. Violet curves represent mean sagittal angles of a control group composed by 10 healthy subjects.

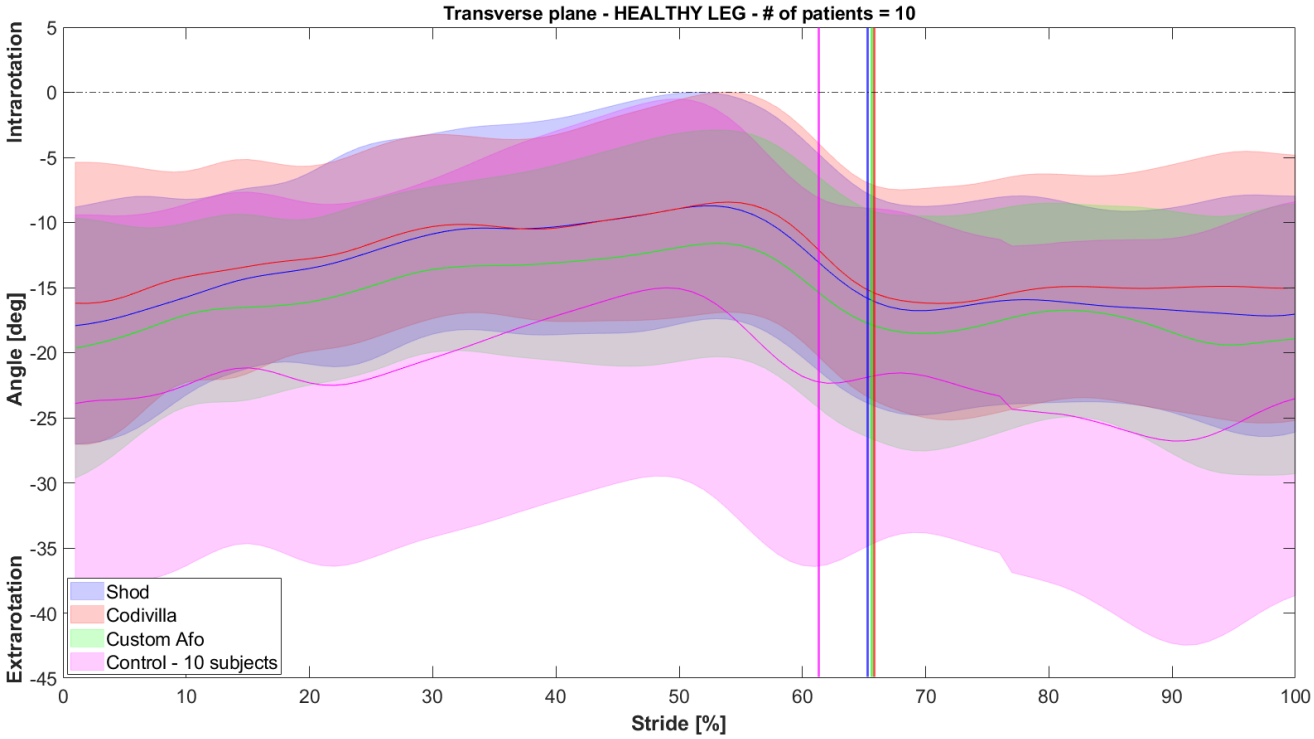

Figure 61: Knee kinematics comparison of the healthy leg in the transverse plane between the patients of the study. Violet curves represent mean sagittal angles of a control group composed by 10 healthy subjects.

3.3.3 Hip

Figures 62, 63 and 64 show the hip kinematics of the affected leg in an exemplary patient in the sagittal, frontal, and transverse plane respectively. Hip kinematics in the sagittal plane for each patient is reported in the Appendix. Blue lines represent the mean values of the angles for the shod condition, red ones for the Codivilla spring and green curve lines are for the custom AFO.

Figures 65, 66 and 67 report the inter-subject average hip kinematic angles in the affected leg in the sagittal, frontal and transverse plane respectively.

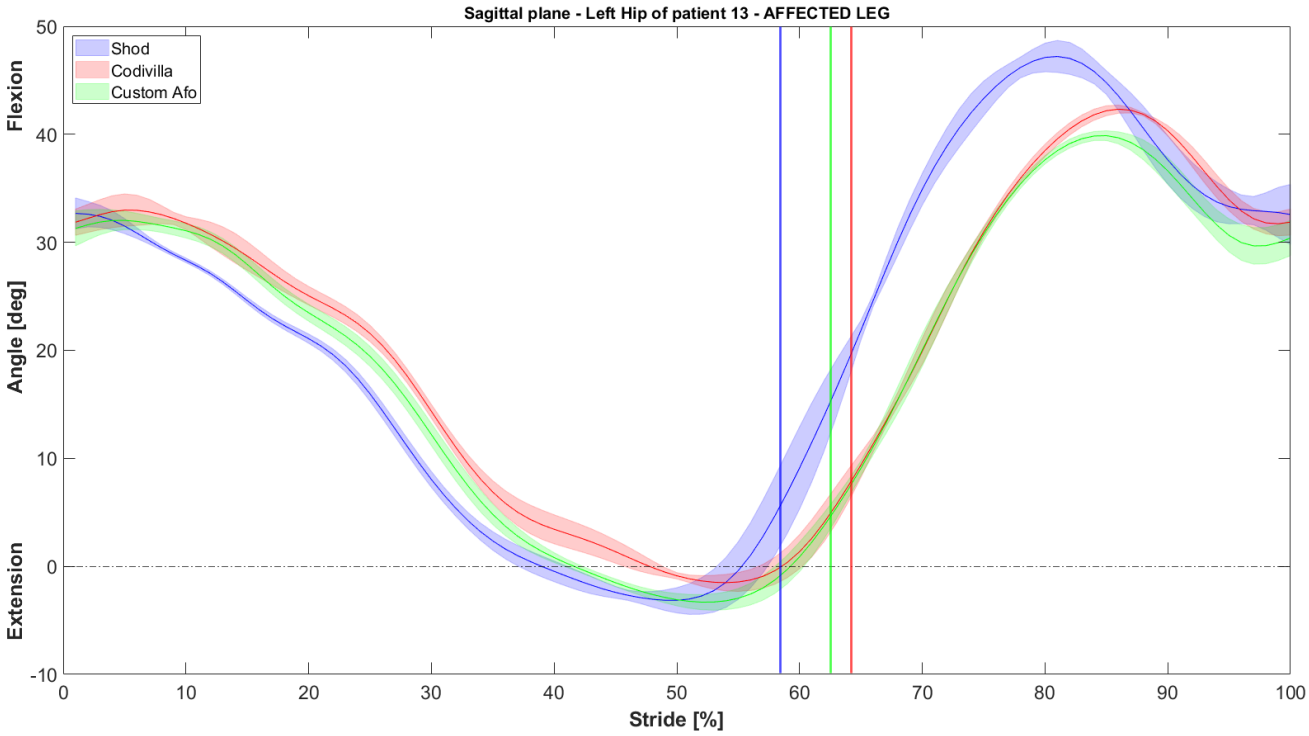

Figure 62: The hip kinematics in the sagittal plane of the affected leg of an exemplary patient.

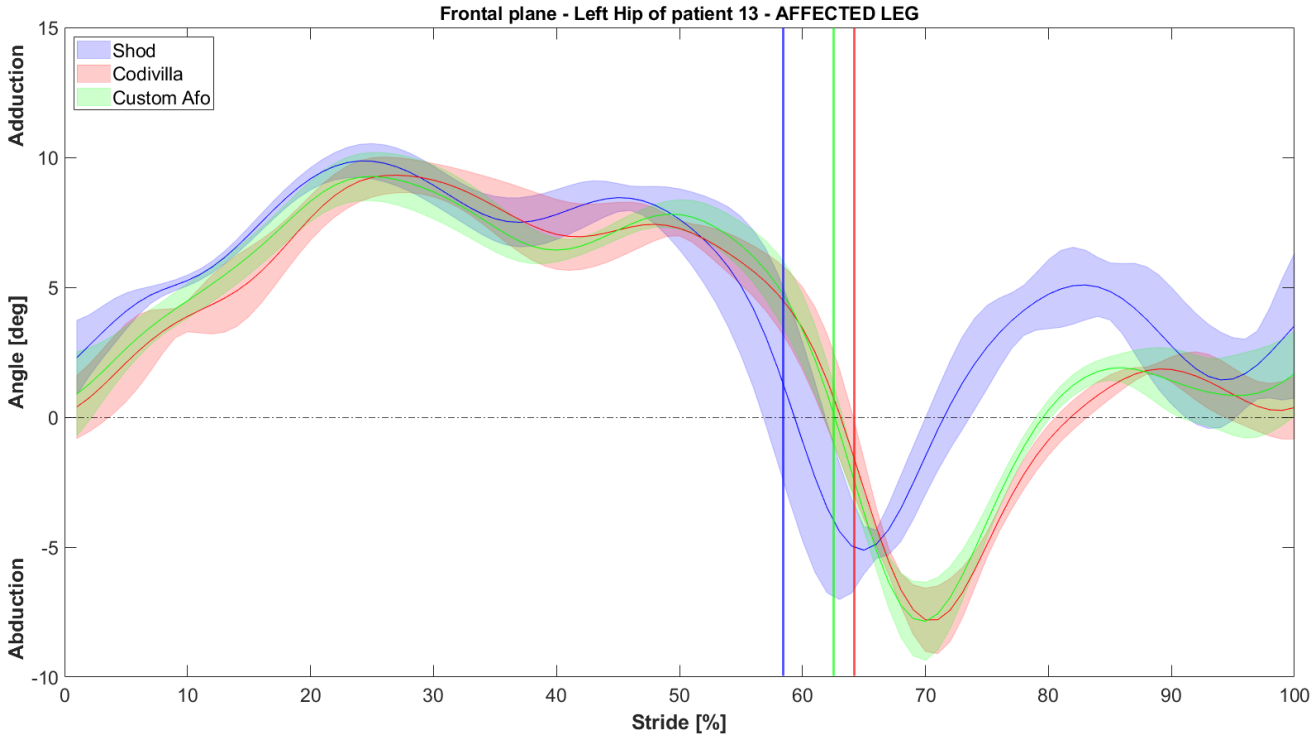

Figure 63: The hip kinematics in the frontal plane of the affected leg of an exemplary patient.

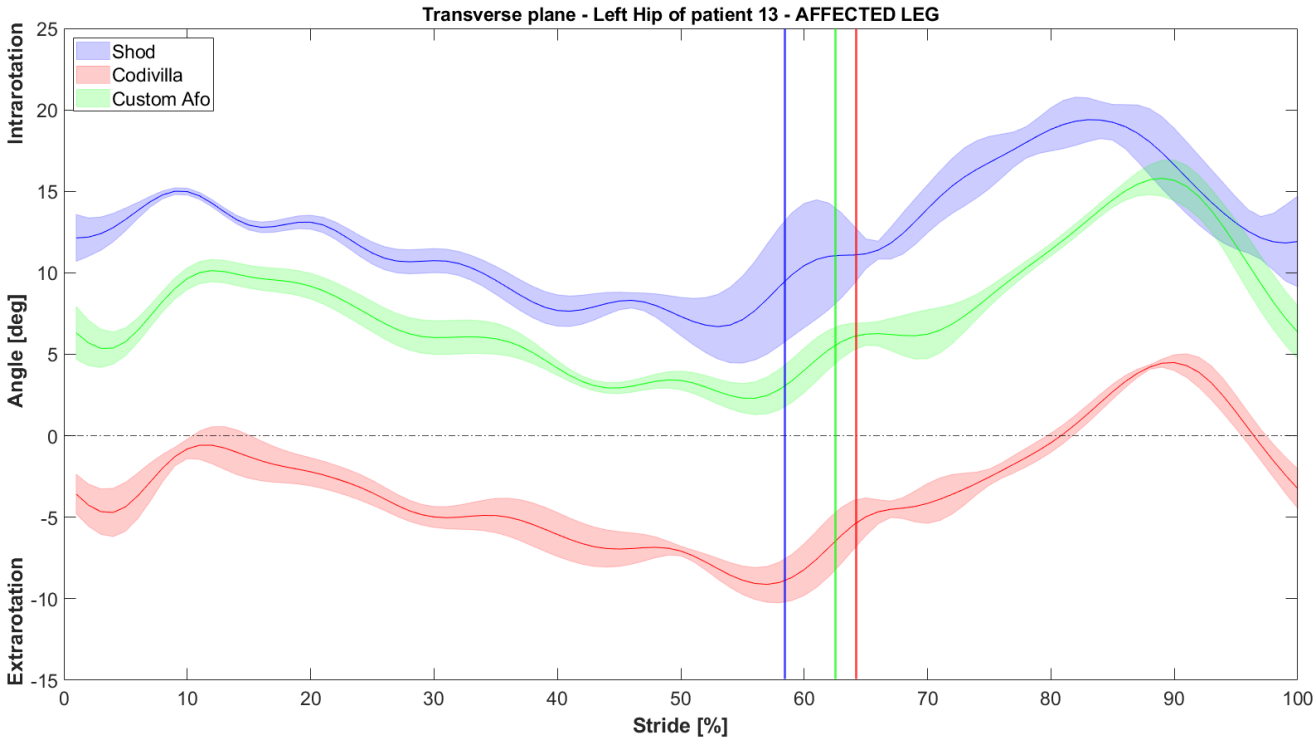

Figure 64: The hip kinematics in the transverse plane of the affected leg of an exemplary patient.

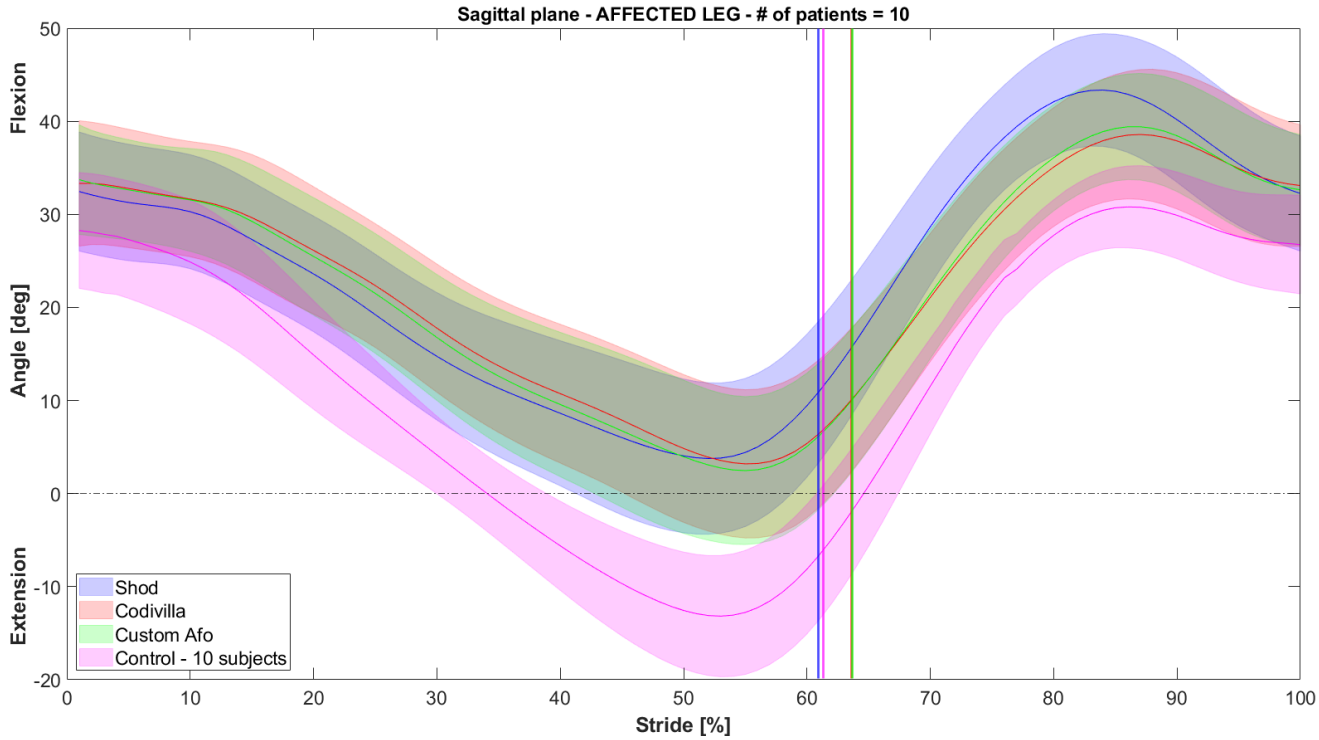

Figure 65: Hip kinematics comparison of the affected leg in the sagittal plane between the patients of the study and a control group composed by 10 healthy subjects (violet curve).

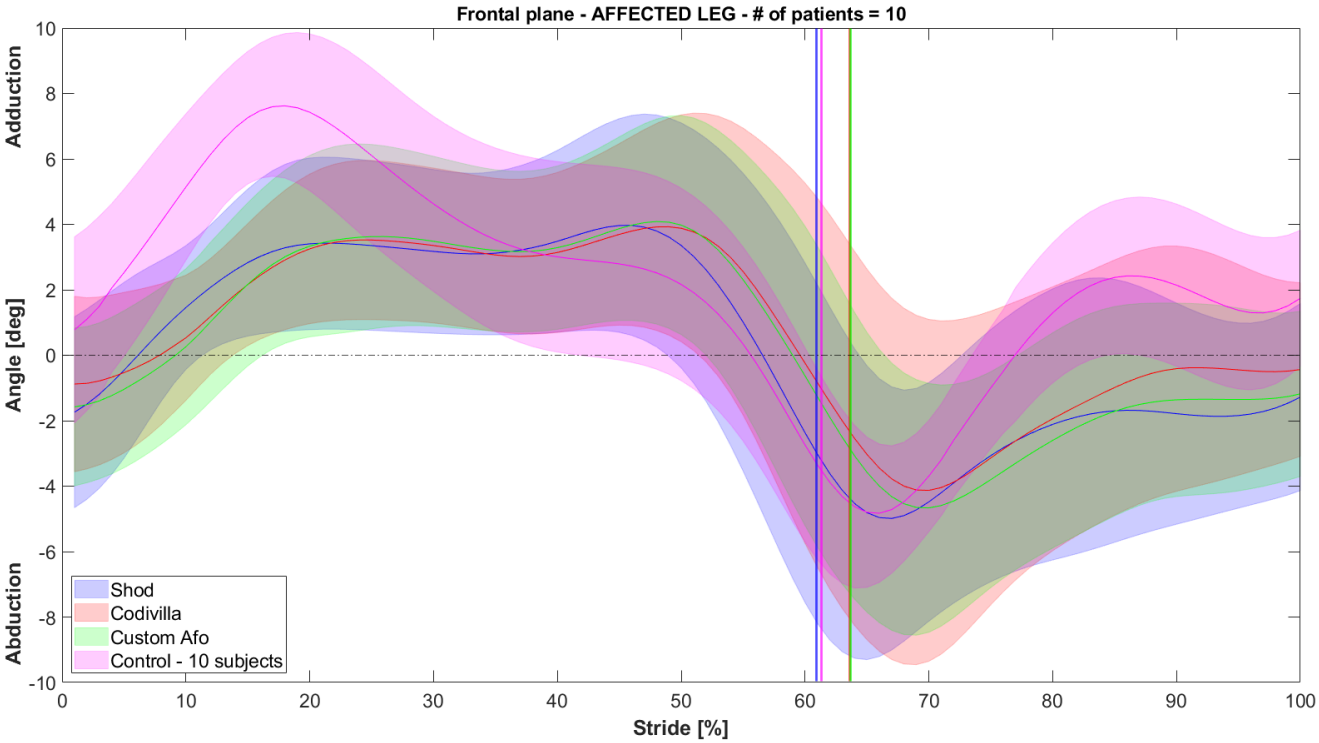

Figure 66: Hip kinematics comparison of the affected leg in the frontal plane between the patients of the study and a control group composed by 10 healthy subjects (violet curve).

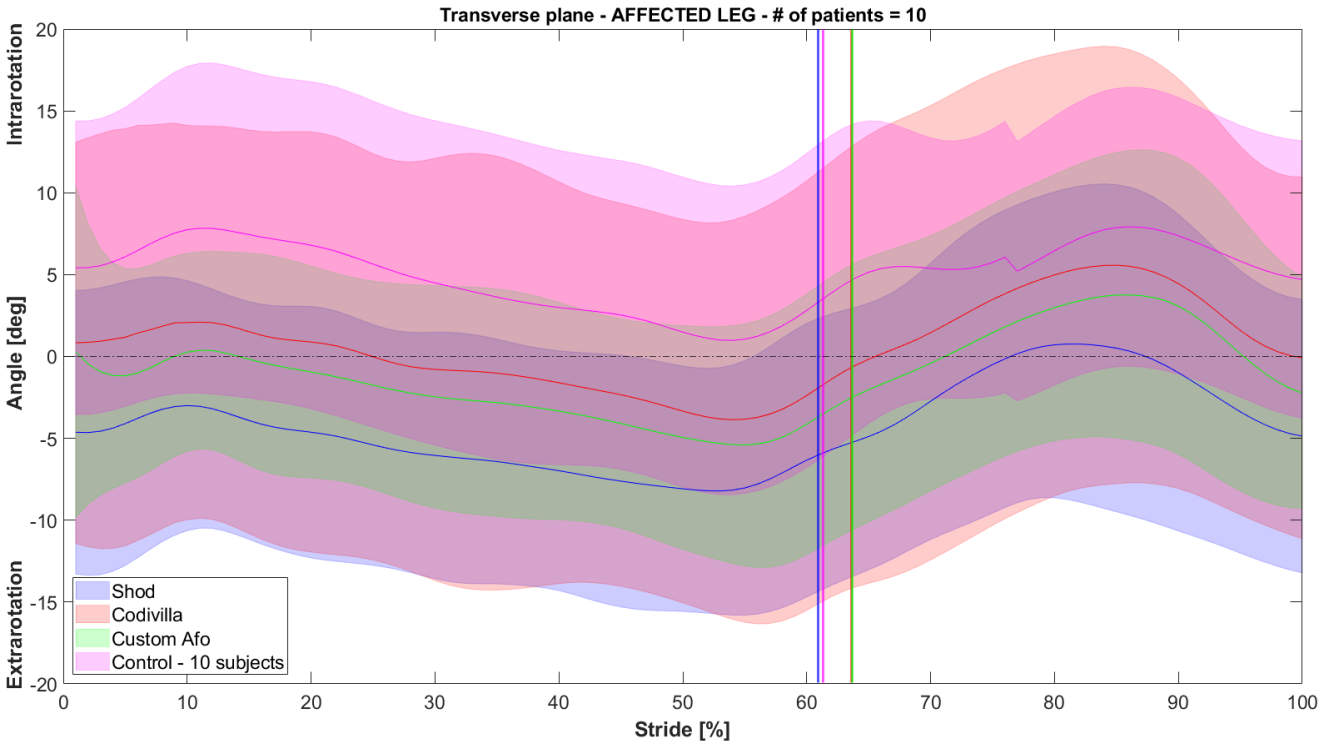

Figure 67: Hip kinematics comparison of the affected leg in the transverse plane between the patients of the study and a control group composed by 10 healthy subjects (violet curve).

In order to analyse the effects that an AFO can introduce in the healthy leg of a foot-drop patient, the kinematic angles have also been measured on the healthy leg of each patient during each walking condition. Figures 68, 69 and 70 report the mean values of the hip angles on the sagittal, the frontal and the transverse plane respectively, measured on the healthy leg of the patients, and compared to a control group of 10 subjects. The objective is to verify whether wearing an AFO affects the kinematics of the contralateral limb.

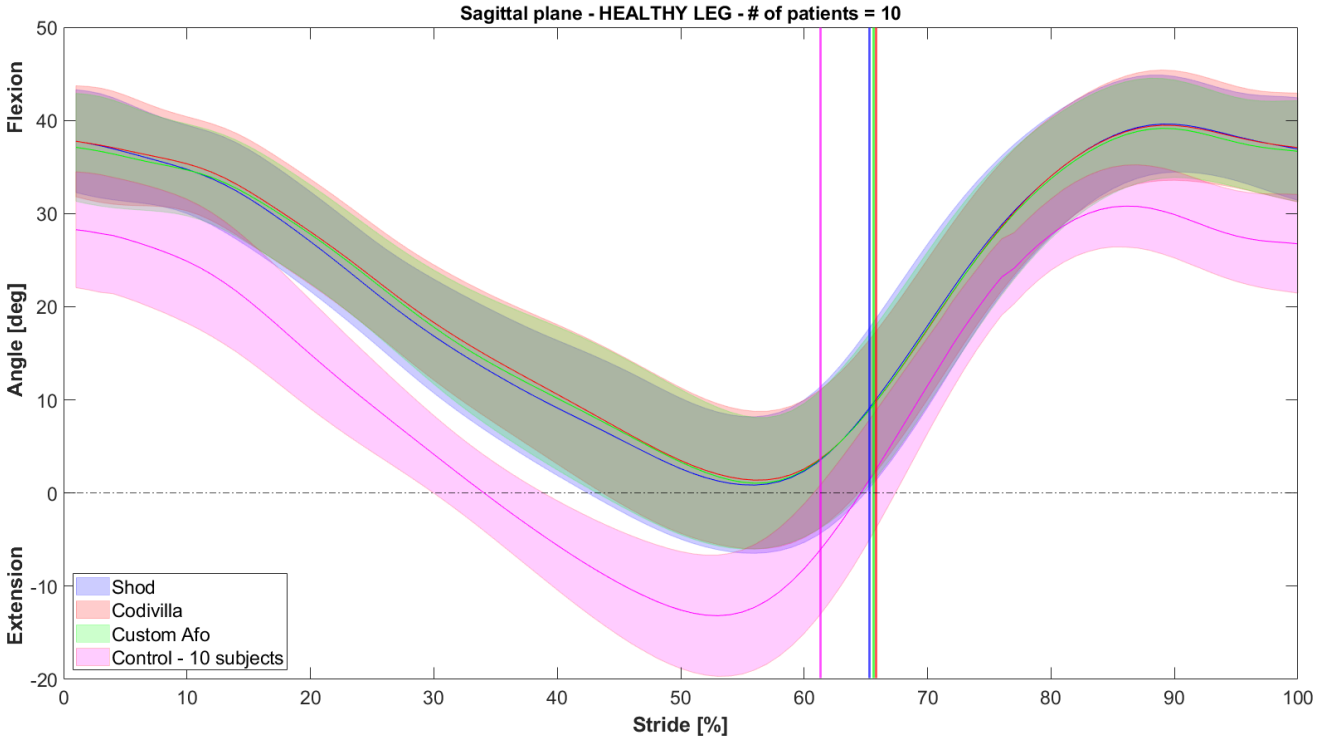

Figure 68: Hip kinematics comparison of the healthy leg in the sagittal plane between the patients of the study. Violet curves represent mean sagittal angles of a control group composed by 10 healthy subjects.

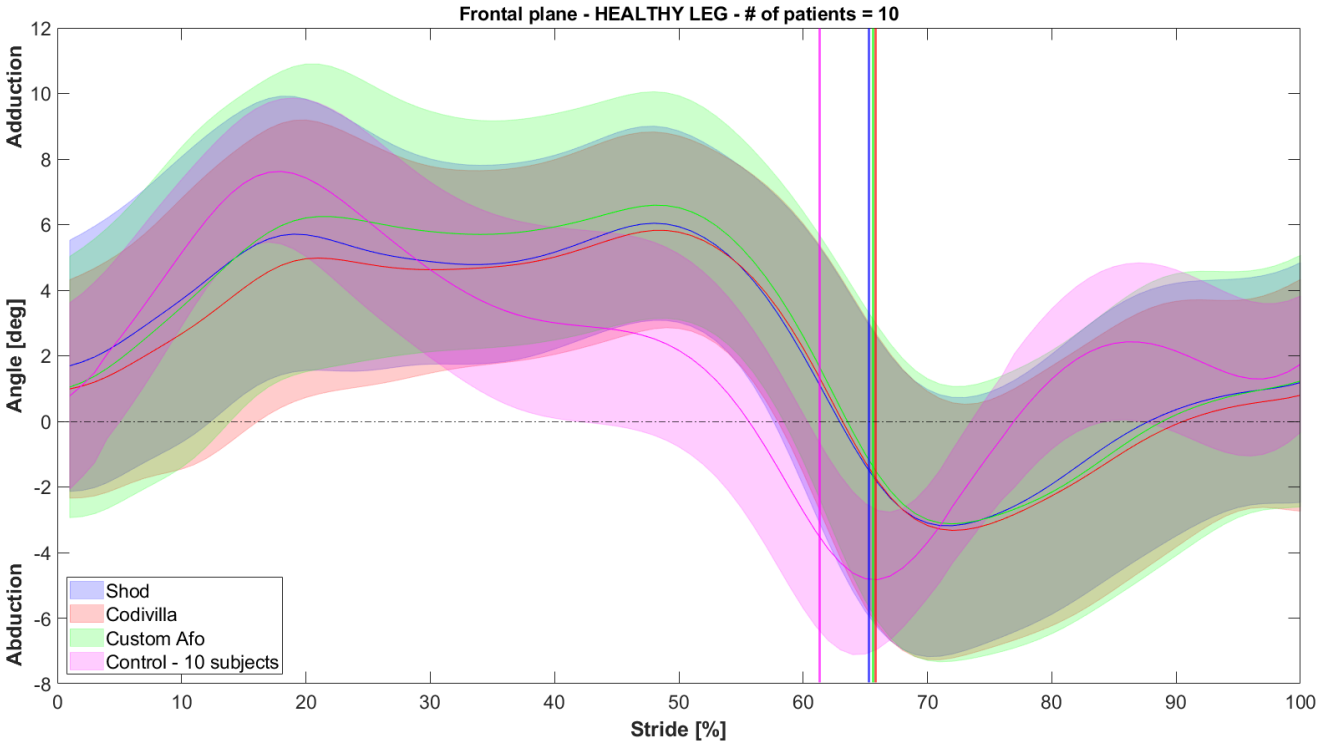

Figure 69: Hip kinematics comparison of the healthy leg in the frontal plane between the patients of the study. Violet curves represent mean sagittal angles of a control group composed by 10 healthy subjects.

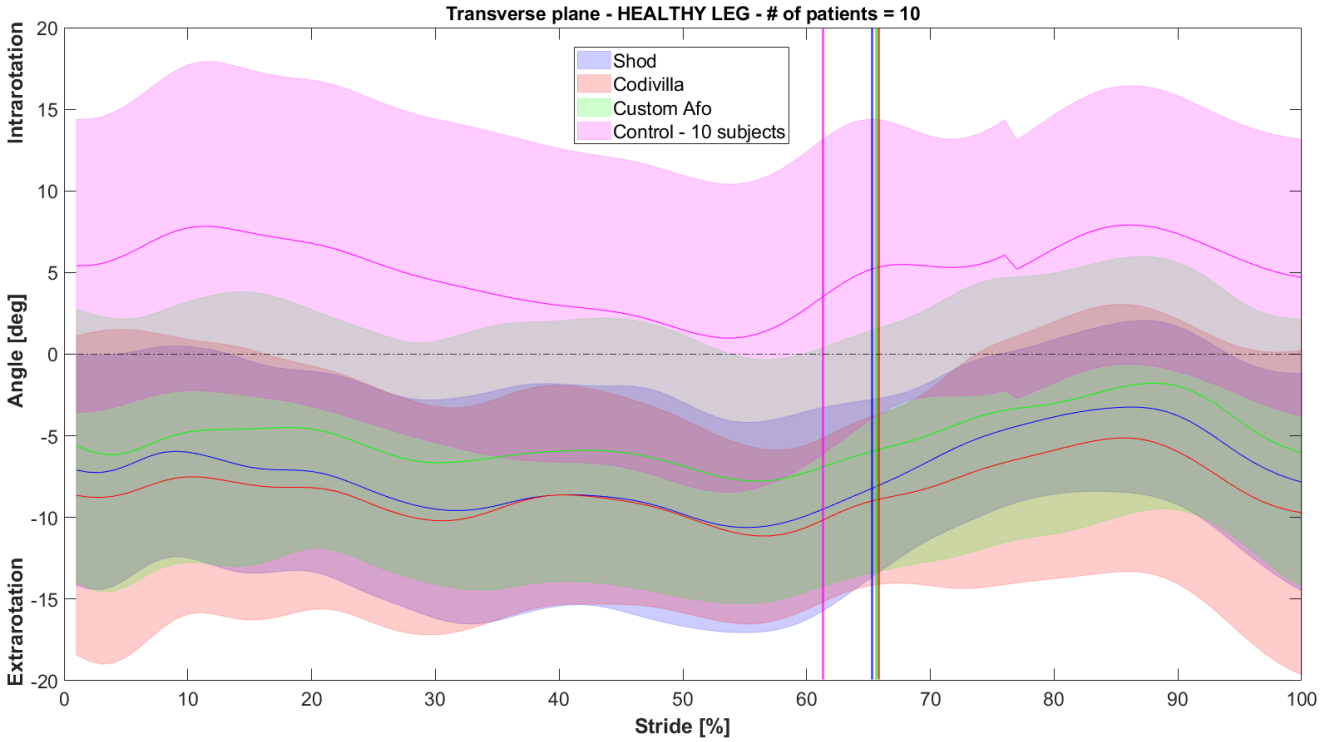

Figure 70: Hip kinematics comparison of the healthy leg in the transverse plane between the patients of the study. Violet curves represent mean sagittal angles of a control group composed by 10 healthy subjects.

3.3.4 Statistical analysis

The effects of the three walking conditions on the minimum, maximum and ROM of lower limb joint rotations in the affected leg are reported in Tables 3, 4 and 5. The kinematic parameters were calculated in each of the three anatomical planes, during the stance phase, swing phase, and in the full gait cycle. Control kinematic values are reported in the last column of each table.

The variables that, in accordance with the results of the Friedman test, resulted significantly different from the shod condition have been highlighted in red in the tables. P-values are reported for each parameter.

In order to evaluate whether wearing an AFO causes significantly differences in the kinematics of the healthy leg of foot-drop patients, Tables 6, 7 and 8 report the same kinematic data considering the not-affected leg in the sagittal, the frontal and the transverse plane respectively. P-values are reported for parameters significantly different ($p < 0.05$) with respect to shod condition.

AFFECTED LEG – SAGITTAL PLANE											CONTROL		
# PATIENTS: 10 MEAN AGE: 64.9 ± 11.4 YEARS		SHOD			CODIVILLA			CUSTOM-AFO			# SUBJECTS: 10 MEAN AGE: 28.2 ± 10.0 YEARS		
		STANCE	SWING	GAIT	STANCE	SWING	GAIT	STANCE	SWING	GAIT	STANCE	SWING	GAIT
HIP	EXT	-0.1 [-2.9; 6.7]	6.1 [3.8; 16.6]	-0.1 [-2.9; 6.7]	0.1 [-2.6; 5.3]	7.4 [3.8; 13.3]	0.1 [-2.6; 5.3]	-0.4 [-3.3; 5.4] p<0.05	6.7 [4.1; 14.2]	-0.4 [-3.3; 5.4] p<0.05	-12.2 [-17.0; -8.8]	/	/
50% [25% - 75%]	FLEX	32.4 [28.7; 36.0]	45.8 [40.4; 47.4]	45.8 [40.4; 47.4]	35.1 [29.0; 38.8]	39.0 [34.5; 43.9] p<0.05	39.0 [34.5; 43.9] p<0.05	33.7 [29.1; 37.5]	40.0 [36.3; 43.6] p<0.05	40.0 [36.8; 43.6] p<0.05	/	32.9 [30.8; 34.4]	/
	ROM	28.4 [24.1; 35.9]	33.6 [29.3; 41.4]	39.9 [39.2; 48.0]	31.7 [25.6; 34.6]	28.7 [24.1; 35.5] p<0.05	36.0 [29.9; 42.3] p<0.05	31.8 [27.1; 35.6] p<0.05	30.5 [26.7; 33.8] p<0.05	39.0 [35.4; 40.9]	/	/	46.5 [43.1; 48.7]
KNEE	EXT	5.3 [4.6; 8.1]	6.1 [4.7; 7.7]	5.1 [4.6; 6.9]	6.5 [5.4; 6.9]	6.2 [3.1; 6.9]	5.7 [3.1; 6.5]	5.0 [4.4; 7.9]	5.1 [2.4; 6.1]	4.6 [2.4; 5.7]	1.8 [-0.5; 2.5]	/	/
50% [25% - 75%]	FLEX	42.2 [37.9; 49.1]	71.7 [70.1; 79.1]	71.7 [70.1; 79.1]	44.3 [38.2; 46.7]	68.9 [64.1; 76.4]	68.9 [64.1; 76.4]	46.5 [42.0; 47.7]	70.5 [66.6; 75.8]	70.5 [66.6; 75.8]	/	68.2 [67.0; 69.1]	/
	ROM	38.6 [32.4; 41.8]	66.2 [63.2; 71.3]	68.6 [63.2; 73.0]	40.3 [31.7; 43.6]	63.9 [58.4; 71.6]	66.3 [58.4; 71.6] p<0.05	41.4 [37.2; 45.9]	64.8 [60.9; 71.5]	66.8 [62.6; 71.7]	/	/	71.3 [68.7; 73.7]
ANKLE	PLA	-15.3 [-17.9; -11.6]	-23.6 [-32.4; -21.3]	-23.6 [-32.4; -21.3]	-10.6 [-14.9; -7.5] p<0.05	-5.7 [-12.2; -2.6] p<0.05	-10.6 [-16.5; -8.3] p<0.05	-11.1 [-15.8; -7.6] p<0.05	-9.3 [-11.9; -4.4] p<0.05	-11.5 [-15.8; -7.6] p<0.05	/	-14.4 [-19.7; -10.2]	/
50% [25% - 75%]	DOR	12.9 [11.1; 19.1]	0.2 [-5.4; 5.7]	12.9 [11.1; 19.1]	14.9 [10.6; 17.1]	4.9 [0.8; 7.0] p<0.05	14.9 [10.6; 17.1]	13.9 [10.6; 19.3]	2.2 [-1.4; 5.6]	13.9 [10.6; 19.3]	14.9 [8.6; 21.7]	/	/
	ROM	31.0 [29.0; 37.0]	25.1 [16.8; 30.0]	40.9 [32.4; 47.5]	26.0 [25.5; 28.7] p<0.05	9.1 [7.7; 15.9] p<0.05	26.6 [25.5; 28.7] p<0.05	27.0 [23.0; 30.0]	11.5 [7.8; 16.0] p<0.05	27.0 [25.2; 30.0] p<0.05	/	/	28.1 [26.3; 32.4]

Table 3: The kinematics of the affected leg in the sagittal plane for hip, knee, and ankle joint. Each cell reports the median value, the 25th and the 75th percentile of the considered variable. Red cell indicates that the median value of the variable represented is significantly different with respect to the same variable in shod condition.

AFFECTED LEG – FRONTAL PLANE											CONTROL		
# PATIENTS: 10 MEAN AGE: 64.9 ± 11.4 YEARS		SHOD			CODIVILLA			CUSTOM-AFO			# SUBJECTS: 10 MEAN AGE: 28.2 ± 10.0 YEARS		
		STANCE	SWING	GAIT	STANCE	SWING	GAIT	STANCE	SWING	GAIT	STANCE	SWING	GAIT
HIP 50% [25% - 75%]	ABD	-3.3 [-7.4; -2.4]	-5.7 [-9.6; -3.5]	-5.7 [-9.6; -3.5]	-2.6 [-7.7; -1.8]	-5.8 [-9.3; -1.9]	-5.8 [-9.3; -2.5]	-3.2 [-7.5; -2.4]	-5.8 [-8.9; -2.8]	-5.8 [-8.9; -3.0]	/	-5.9 [-7.0; -4.9]	/
	ADD	5.0 [3.2; 5.5]	0.0 [-2.2; 2.8]	5.0 [3.2; 5.5]	4.9 [3.3; 6.3]	0.5 [-1.8; 3.5]	4.9 [3.3; 6.3]	4.7 [3.6; 6.4]	-0.9 [-2.5; 2.5]	4.7 [3.6; 6.4]	7.1 [6.0; 7.3]	/	/
	ROM	8.3 [7.5; 11.9]	6.4 [5.5; 7.9]	11.4 [9.9; 15.0]	9.2 [7.5; 11.1]	6.0 [4.2; 7.9]	10.2 [8.9; 14.2]	9.1 [7.7; 11.3]	5.3 [4.0; 7.1]	10.5 [9.5; 14.1]	/	/	12.6 [11.5; 14.2]
KNEE 50% [25% - 75%]	ABD	-4.6 [-5.6; -0.5]	-3.9 [-6.3; 0.9]	-4.9 [-6.3; -0.5]	-3.2 [-5.4; 0.1]	-2.7 [-5.1; -0.7]	-3.6 [-5.8; -1.1]	-3.8 [-5.3; 0.1]	-3.3 [-4.8; 0.5]	-3.8 [-3.8; -0.6]	/	-6.2 [-7.0; -1.8]	/
	ADD	2.6 [-2.0; 5.4]	5.3 [1.4; 9.9]	5.3 [1.4; 9.9]	4.0 [1.7; 6.8]	7.5 [3.5; 11.2]	7.8 [3.5; 11.2]	5.4 [0.9; 7.1]	8.5 [3.1; 11.1]	8.5 [3.1; 11.1]	1.8 [-0.1; 5.1]	/	/
	ROM	5.1 [2.6; 7.5]	9.2 [6.5; 11.9]	10.0 [6.5; 13.8]	5.7 [4.0; 7.1]	9.3 [6.5; 12.2]	10.5 [7.9; 12.9]	6.7 [4.1; 10.1]	11.0 [7.3; 14.9]	12.1 [7.6; 16.1]	/	/	9.7 [8.1; 11.6]
ANKLE 50% [25% - 75%]	EV	2.4 [0.2; 5.6]	10.2 [2.2; 12.6]	2.2 [0.2; 5.6]	2.7 [0.8; 6.2]	8.1 [3.3; 9.7]	2.7 [0.8; 6.2]	1.7 [-0.2; 5.3]	7.2 [5.4; 8.7]	1.7 [-0.2; 5.3]	1.8 [-0.7; 5.4]	/	/
	INV	14.5 [11.5; 16.9]	15.6 [12.5; 20.3]	15.6 [12.5; 20.3]	12.3 [10.6; 14.2] p<0.05	11.5 [8.8; 14.1] p<0.05	12.3 [10.6; 14.4] p<0.05	13.8 [10.7; 15.0]	11.3 [9.6; 14.0] p<0.05	14.0 [10.7; 15.0] p<0.05	/	11.6 [9.2; 15.5]	/
	ROM	13.9 [9.7; 15.0]	7.4 [4.8; 11.4]	14.3 [12.4; 16.1]	8.5 [7.7; 12.7] p<0.05	3.6 [3.6; 5.0] p<0.05	9.0 [7.7; 12.7] p<0.05	10.3 [8.7; 13.8]	4.1 [2.7; 5.6] p<0.05	10.3 [9.1; 13.8]	/	/	10.3 [7.4; 11.8]

Table 4: The kinematics of the affected leg in the frontal plane for hip, knee, and ankle joint. Each cell reports the median value, the 25th and the 75th percentile of the considered variable. Red cell indicates that the median value of the variable represented is significantly different with respect to the same variable in shod condition.

AFFECTED LEG – TRANSVERSE PLANE											CONTROL		
# PATIENTS: 10 MEAN AGE: 64.9 ± 11.4 YEARS		SHOD			CODIVILLA			CUSTOM-AFO			# SUBJECTS: 10 MEAN AGE: 28.2 ± 10.0 YEARS		
		STANCE	SWING	GAIT	STANCE	SWING	GAIT	STANCE	SWING	GAIT	STANCE	SWING	GAIT
HIP	EXT	**-12.5** *[-14.9; -6.1]*	**-10.3** *[-12.6; -3.9]*	**-13.1** *[-14.9; -6.1]*	**-8.9** *[-12.4; -3.6]*	**-6.4** *[-11.5; -0.9]*	**-8.9** *[-13.1; -3.6]*	**-6.5** *[-13.0; -0.4]*	**-4.9** *[-11.0; 2.4]*	**-6.5** *[-13.0; -0.8]*	/	**-0.1** *[-2.9; 8.0]*	/
50%	INT	**-2.6** *[-7.0; 2.1]*	**-0.1** *[-5.0; 5.7]*	**-0.1** *[-4.8; 5.7]*	**0.8** *[-4.3; 3.1]*	**4.9** *[-3.9; 8.7]*	**4.9** *[-3.8; 8.7]*	**1.4** *[-4.6; 5.4]*	**3.7** *[-4.6; 12.6]*	**3.7** *[-2.6; 12.6]*	**5.8** *[3.6; 12.6]*	/	/
[25% - 75%]	ROM	**7.8** *[6.9; 9.4]*	**9.9** *[7.2; 12.3]*	**12.1** *[9.9; 14.6]*	**9.1** *[6.5; 12.4]*	**10.5** *[7.0; 12.2]*	**13.0** *[9.4; 15.8]*	**8.0** *[6.0; 9.2]*	**10.0** *[7.2; 10.9]*	**12.3** *[9.1; 14.7]*	/	/	**10.9** *[7.8; 11.8]*
KNEE	EXT	**-21.6** *[-29.1; -16.9]*	**-25.6** *[-31.3; -15.7]*	**-25.6** *[-31.3; -16.9]*	**-21.8** *[-28.8; -17.7]*	**-22.0** *[-32.0; -18.0]*	**-22.6** *[-32.0; -18.0]*	**-26.0** *[-26.3; -17.3]*	**-26.3** *[-33.4; -17.3]*	**-26.4** *[-33.4; -17.3]*	/	/	/
50%	INT	**-5.6** *[-8.7; 2.8]*	**-11.1** *[-14.5; -1.9]*	**-5.6** *[-8.7; -2.8]*	**-6.6** *[-16.9; 1.5]*	**-13.9** *[-21.4; -3.2]*	**-6.6** *[-16.9; 1.5]*	**-10.7** *[-16.7; -2.8]*	**-16.7** *[-18.9; -3.3]* **p<0.05**	**-10.1** *[-16.7; -2.8]*	**-13.9** *[-19.2; 1.4]*	/	/
[25% - 75%]	ROM	**14.7** *[13.5; 19.1]*	**12.8** *[9.3; 16.8]*	**17.8** *[13.5; 22.6]*	**15.8** *[13.3; 16.9]*	**12.6** *[8.2; 14.9]*	**16.4** *[15.3; 18.1]*	**14.6** *[12.0; 16.8]*	**10.2** *[8.2; 14.2]*	**15.4** *[13.4; 16.8]*	/	/	**17.1** *[12.6; 18.9]*
ANKLE	ABD	**3.0** *[0.2; 6.2]*	**8.5** *[1.6; 12.0]*	**3.0** *[0.2; 6.2]*	**2.0** *[-3.6; 5.7]*	**2.2** *[-3.4; 6.2]* **p<0.05**	**0.8** *[-4.3; 4.8]*	**4.3** *[0.2; 7.1]*	**5.8** *[-3.1; 6.6]*	**4.3** *[-3.1; 5.6]*	**3.2** *[-0.5; 7.1]*	/	/
50%	ADD	**15.2** *[13.5; 18.6]*	**22.4** *[14.8; 24.4]*	**22.4** *[14.8; 24.4]*	**10.0** *[8.5; 15.5]* **p<0.05**	**9.5** *[8.1; 14.9]* **p<0.05**	**10.0** *[8.5; 15.5]* **p<0.05**	**12.6** *[11.0; 16.2]*	**12.5** *[10.4; 15.8]*	**12.6** *[11.0; 16.2]*	/	**17.3** *[14.3; 20.0]*	/
[25% - 75%]	ROM	**12.0** *[9.6; 13.7]*	**10.1** *[8.8; 16.6]*	**14.6** *[12.4; 20.9]*	**10.1** *[8.4; 11.8]*	**9.5** *[8.3; 12.0]*	**11.9** *[10.8; 12.7]*	**10.3** *[8.2; 11.3]*	**10.1** *[6.8; 11.5]*	**11.1** *[9.9; 12.4]* **p<0.05**	/	/	**12.9** *[11.6; 15.9]*

Table 5: The kinematics of the affected leg in the transverse plane for hip, knee, and ankle joint. Each cell reports the median value, the 25th and the 75th percentile of the considered variable. Red cell indicates that the median value of the variable represented is significantly different with respect to the same variable in shod condition.

HEALTHY LEG – SAGITTAL PLANE											CONTROL		
# PATIENTS: 10 MEAN AGE: 64.9 ± 11.4 YEARS		SHOD			CODIVILLA			CUSTOM-AFO			# SUBJECTS: 10 MEAN AGE: 28.2 ± 10.0 YEARS		
		STANCE	SWING	GAIT	STANCE	SWING	GAIT	STANCE	SWING	GAIT	STANCE	SWING	GAIT
HIP	EXT	**-1.8** *[-4.2; 7.7]*	**5.2** *[3.1; 14.4]*	**-1.8** *[-4.2; 7.7]*	**-1.9** *[-3.6; 8.9]*	**4.1** *[3.3; 15.8]*	**-1.9** *[-3.6; 8.9]*	**-1.0** *[-3.8; 7.7]*	**7.2** *[3.3; 14.1]*	**-1.0** *[-3.8; 7.7]*	**-12.2** *[-17.0; -8.8]*	/	/
50%	FLEX	**37.2** *[33.7; 42.9]*	**39.9** *[36.9; 45.4]*	**40.0** *[37.1; 45.4]*	**37.3** *[33.6; 43.9]*	**39.6** *[36.6; 45.8]*	**39.6** *[36.8; 45.8]*	**37.3** *[32.4; 42.7]*	**38.9** *[36.7; 44.5]*	**39.5** *[36.9; 44.5]*	/	**32.9** *[30.8; 34.4]*	/
[25% - 75%]	ROM	**36.6** *[33.5; 38.9]*	**32.1** *[28.8; 34.4]*	**40.6** *[35.7; 42.8]*	**35.3** *[32.5; 39.3]*	**32.2** *[26.9; 33.3]*	**39.5** *[35.3; 41.1]*	**34.9** *[33.6; 38.4]*	**29.8** *[27.7; 34.5]*	**38.8** *[36.0; 41.4]*	/	/	**46.5** *[43.1; 48.7]*
KNEE	EXT	**6.0** *[0.5; 12.8]*	**8.1** *[1.2; 12.1]*	**6.0** *[0.5; 12.1]*	**5.0** *[1.0; 12.7]*	**6.1** *[0.6; 12.7]*	**3.8** *[0.3; 12.5]*	**5.1** *[0.3; 12.3]*	**5.6** *[-0.2; 11.2]*	**5.0** *[-0.2; 11.2]*	**1.8** *[-0.5; 2.5]*	/	/
50%	FLEX	**43.4** *[41.2; 45.5]*	**69.5** *[63.7; 74.8]*	**69.5** *[63.7; 74.8]*	**44.7** *[40.5; 52.4]*	**69.1** *[63.3; 74.5]*	**69.1** *[63.3; 74.5]*	**44.5** *[40.5; 48.6]*	**69.2** *[63.5; 73.3]*	**69.2** *[63.5; 73.3]*	/	**68.2** *[67.0; 69.1]*	/
[25% - 75%]	ROM	**39.3** *[32.7; 41.9]*	**62.4** *[59.7; 64.5]*	**62.8** *[60.4; 64.9]*	**38.3** *[36.3; 43.4]*	**62.3** *[61.6; 66.1]*	**62.8** *[62.0; 66.1]*	**40.3** *[34.8; 42.1]*	**62.6** *[60.3; 66.5]*	**63.5** *[60.3; 66.6]*	/	/	**71.3** *[68.7; 73.7]*
ANKLE	PLA	**-8.6** *[-14.6; -6.8]*	**-11.8** *[-12.6; -6.5]*	**-12.6** *[-14.6; -9.9]*	**-9.4** *[-14.2; -7.1]*	**-9.9** *[-13.7; -7.1]*	**-13.4** *[-14.5; -9.8]*	**-10.9** *[-13.7; -7.5]*	**-12.9** *[-14.4; -6.0]*	**-13.7** *[-14.6; -12.1]*	/	**-14.4** *[-19.7; -10.2]*	/
50%	DOR	**16.1** *[13.5; 16.9]*	**4.7** *[1.2; 7.2]*	**16.1** *[13.5; 16.9]*	**15.9** *[11.9; 16.2]*	**4.6** *[1.1; 7.5]*	**15.9** *[11.9; 16.2]*	**15.5** *[12.6; 16.2]*	**4.0** *[0.4; 6.5]*	**15.5** *[12.6; 16.2]*	**14.9** *[8.6; 21.7]*	/	/
[25% - 75%]	ROM	**25.7** *[22.4; 27.8]*	**14.1** *[10.3; 15.6]*	**29.6** *[24.7; 30.6]*	**25.9** *[21.3; 28.8]*	**13.5** *[11.6; 15.5]*	**29.8** *[23.9; 30.8]*	**25.6** *[23.1; 27.4]*	**14.4** *[11.8; 15.1]*	**28.8** *[26.1; 30.0]*	/	/	**28.1** *[26.3; 32.4]*

Table 6: The kinematics of the unaffected leg in the sagittal plane for hip, knee, and ankle joint. Each cell reports the median value, the 25th and the 75th percentile of the considered variable. Red cell indicates that the median value of the variable represented is significantly different with respect to the same variable in shod condition.

HEALTHY LEG – FRONTAL PLANE											CONTROL		
# PATIENTS: 10 MEAN AGE: 64.9 ± 11.4 YEARS		SHOD			CODIVILLA			CUSTOM-AFO			# SUBJECTS: 10 MEAN AGE: 28.2 ± 10.0 YEARS		
		STANCE	SWING	GAIT	STANCE	SWING	GAIT	STANCE	SWING	GAIT	STANCE	SWING	GAIT
HIP 50% [25% - 75%]	ABD	-2.6 [-4.7; -1.3]	-3.8 [-7.4; -2.9]	-3.8 [-7.4; -2.9]	-2.2 [-5.4; -0.9]	-3.9 [-7.2; -1.5]	-3.9 [-7.2; -1.8]	-2.5 [-5.8; -1.6]	-4.4 [-7.7; -2.3]	-4.4 [-7.7; -2.8]	/	-5.9 [-7.0; -4.9]	/
	ADD	7.0 [4.3; 7.6]	1.4 [-1.7; 2.6]	7.0 [4.3; 7.6]	6.8 [4.3; 7.3]	2.1 [-2.4; 3.5]	6.8 [4.3; 7.3]	7.0 [5.0; 8.1]	1.9 [-1.4; 3.4]	7.0 [5.0; 8.1]	7.1 [6.0; 7.3]	/	/
	ROM	9.1 [7.5; 9.3]	5.9 [4.1; 6.8]	10.6 [8.9; 11.7]	8.7 [8.0; 10.0]	5.3 [3.6; 6.3]	11.1 [8.4; 11.8]	9.6 [7.8; 11.4]	5.8 [5.0; 6.4]	11.7 [9.2; 12.8]	/	/	12.6 [11.5; 14.2]
KNEE 50% [25% - 75%]	ABD	-4.8 [-6.1; -1.9]	-2.9 [-6.3; -0.4]	-4.8 [-6.1; -1.9]	-6.3 [-7.1; -1.4]	-2.7 [-7.4; -1.2]	-6.3 [-7.2; -1.9]	-4.8 [-5.8; -1.4]	-2.7 [-6.1; -0.7]	-4.8 [-5.8; -1.6]	/	-6.2 [-7.0; -1.8]	/
	ADD	0.8 [-2.3; 2.6]	2.7 [1.8; 8.5]	2.7 [1.8; 8.5]	0.1 [-3.6; 3.2]	1.4 [-1.3; 7.8]	1.9 [-1.3; 7.8]	1.4 [-2.2; 3.8]	2.3 [1.3; 9.2]	2.3 [1.3; 9.2]	1.8 [-0.1; 5.1]	/	/
	ROM	4.7 [3.2; 6.6]	7.3 [4.7; 8.8]	9.3 [5.3; 11.3]	4.7 [3.8; 7.4]	7.2 [3.9; 9.0]	10.2 [5.1; 11.6]	5.4 [3.3; 7.0] p<0.05	8.9 [4.3; 9.3]	9.5 [4.7; 12.1]	/	/	9.7 [8.1; 11.6]
ANKLE 50% [25% - 75%]	EV	1.1 [0.0; 4.5]	6.9 [5.0; 10.4]	1.1 [0.0; 4.5]	1.2 [0.0; 3.7]	6.7 [3.8; 9.2]	1.2 [0.0; 3.7]	1.4 [0.0; 4.5]	6.5 [4.3; 11.5]	1.4 [0.0; 4.5]	1.8 [-0.7; 5.4]	/	/
	INV	14.7 [11.4; 18.6]	12.9 [10.9; 19.1]	14.8 [11.6; 19.4]	14.1 [11.6; 17.4]	13.1 [11.4; 18.0]	15.0 [12.1; 18.0]	15.0 [11.3; 22.1]	14.5 [11.7; 21.0]	15.8 [11.9; 22.6]	/	11.6 [9.2; 15.5]	/
	ROM	12.4 [9.4; 14.1]	6.0 [4.9; 11.7]	13.0 [10.1; 15.0]	12.5 [8.9; 15.7]	6.3 [5.1; 12.0]	12.6 [9.8; 15.8]	12.6 [9.2; 16.3]	6.8 [5.2; 12.6]	12.9 [10.2; 16.9]	/	/	10.3 [7.4; 11.8]

Table 7: The kinematics of the unaffected leg in the frontal plane for hip, knee, and ankle joint. Each cell reports the median value, the 25th and the 75th percentile of the considered variable. Red cell indicates that the median value of the variable represented is significantly different with respect to the same variable in shod condition.

HEALTHY LEG – TRANSVERSE PLANE											CONTROL		
# PATIENTS: 10 MEAN AGE: 64.9 ± 11.4 YEARS		SHOD			CODIVILLA			CUSTOM-AFO			# SUBJECTS: 10 MEAN AGE: 28.2 ± 10.0 YEARS		
		STANCE	SWING	GAIT	STANCE	SWING	GAIT	STANCE	SWING	GAIT	STANCE	SWING	GAIT
HIP 50% [25% - 75%]	EXT	-14.4 [-16.1; -7.0]	-9.0 [-14.5; -6.8]	-14.4 [-16.1; -7.1]	-15.2 [-18.5; -10.6]	-11.5 [-18.4; -8.8]	-15.2 [-18.9; -10.6]	-13.5 [-15.8; -8.5]	-10.4 [-14.5; -7.2]	-13.5 [-15.8; -8.6]	/	-0.1 [-2.9; 8.0]	/
	INT	-1.4 [-8.5; 2.3]	-0.4 [-8.0; 1.9]	0.2 [-7.6; 3.9]	-6.4 [-10.2; 0.9]	-4.8 [-8.7; 1.7]	-4.8 [-8.3; 2.3]	-0.6 [-7.9; 3.5]	-0.0 [-7.2; 2.8]	0.2 [-7.2; 4.0]	5.8 [3.6; 12.6]	/	/
	ROM	9.2 [7.3; 10.1]	8.3 [6.2; 9.7]	12.5 [8.1; 15.0]	9.1 [7.9; 10.8]	7.6 [5.7; 10.9]	12.1 [7.9; 14.2]	8.2 [7.2; 10.7]	7.8 [5.4; 9.1]	10.0 [8.3; 12.6]	/	/	10.9 [7.8; 11.8]
KNEE 50% [25% - 75%]	EXT	-23.6 [-26.3; -17.6]	-22.9 [-27.9; -16.8]	-24.7 [-28.1; -18.0]	-21.3 [-26.6; -13.1]	-20.6 [-28.3; -17.1]	-21.9 [-28.7; -17.1]	-26.1 [-28.4; -14.5]	-29.0 [-30.3; -16.3]	-29.0 [-30.3; -16.9]	/	/	/
	INT	-6.5 [-14.1; -2.5]	-11.2 [-18.6; -6.6]	-6.5 [-14.1; -2.5]	-4.5 [-12.5; -2.4]	-10.1 [-14.1; -4.9]	-4.5 [-11.2; -2.4]	-10.3 [-12.3; -4.6]	-10.8 [-16.0; -7.6]	-9.5 [-12.0; -4.6]	-13.9 [-19.2; 1.4]	/	/
	ROM	17.8 [11.1; 19.0]	10.6 [8.0; 12.9]	17.8 [13.3; 19.1]	15.0 [10.7; 17.1]	10.6 [8.8; 12.9]	17.7 [14.6; 18.1]	15.0 [9.6; 17.7]	11.2 [8.5; 15.3]	15.8 [14.0; 20.1]	/	/	17.1 [12.6; 18.9]
ANKLE 50% [25% - 75%]	ABD	4.4 [-2.2; 7.4]	5.8 [1.4; 12.4]	4.4 [-2.2; 7.4]	1.8 [-3.0; 9.0]	4.9 [-1.9; 12.2]	1.8 [-4.5; 9.0]	4.3 [-1.6; 7.9]	8.5 [-2.2; 13.3]	4.3 [-2.3; 7.9]	3.2 [-0.5; 7.1]	/	/
	ADD	14.8 [11.0; 20.6]	14.7 [10.9; 20.5]	15.1 [11.2; 20.7]	14.6 [8.9; 19.5]	14.7 [8.1; 19.1]	15.0 [9.1; 19.5]	15.5 [7.8; 22.3]	15.9 [9.6; 22.5]	16.1 [9.7; 22.5]	/	17.3 [14.3; 20.0]	/
	ROM	13.0 [10.1; 13.3]	10.2 [8.2; 10.8]	13.3 [11.0; 14.4]	12.1 [10.3; 13.9]	9.8 [6.9; 11.4]	13.9 [10.4; 15.5]	11.4 [9.4; 13.5]	9.8 [7.4; 12.6]	14.1 [9.4; 14.7]	/	/	12.9 [11.6; 15.9]

Table 8: The kinematics of the unaffected leg in the transverse plane for hip, knee, and ankle joint. Each cell reports the median value, the 25th and the 75th percentile of the considered variable. Red cell indicates that the median value of the variable represented is significantly different with respect to the same variable in shod condition.

3.4 sEMG data

As stated in Section 1, the activation of the tibialis anterior in the affected limb of a foot-drop patient is usually lower than that in a healthy subject. Beyond that, it is useful to analyse the muscular activation of the main lower limb muscles. The electromyographic evaluations of the rectus femoris, biceps femoris, tibialis anterior and gastrocnemius across all patients are reported in this paragraph. Figures 71, 72, 73 and 74 show the enveloped EMG surface signals of these muscles, for the affected leg of an exemplary patient of the study. EMG signals for each patient are reported in the Appendix. Each figure shows the average value – in μV – and the standard deviations of the muscular activation across the walking trials, for each walking condition. Vertical lines, coloured as the curve ones, represent the mean percentage of stride time in which the stance phase ends and the swing phase begins, across the walking trials for each condition.

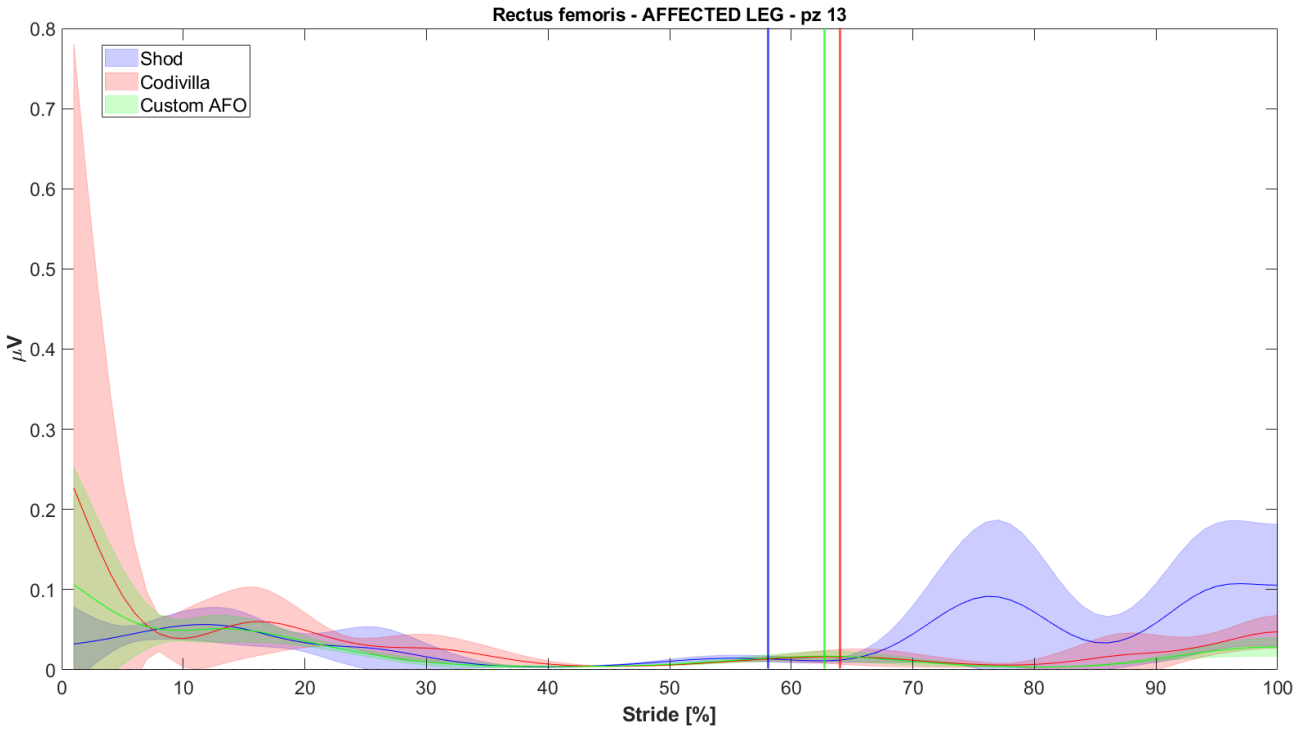

Figure 71: The rectus femoris muscular activation in the affected leg of an exemplary patient. Mean values ± SD of the muscular activation across the walking trials are shown for the shod (blue), Codivilla spring (red) and the custom AFO (green) conditions.

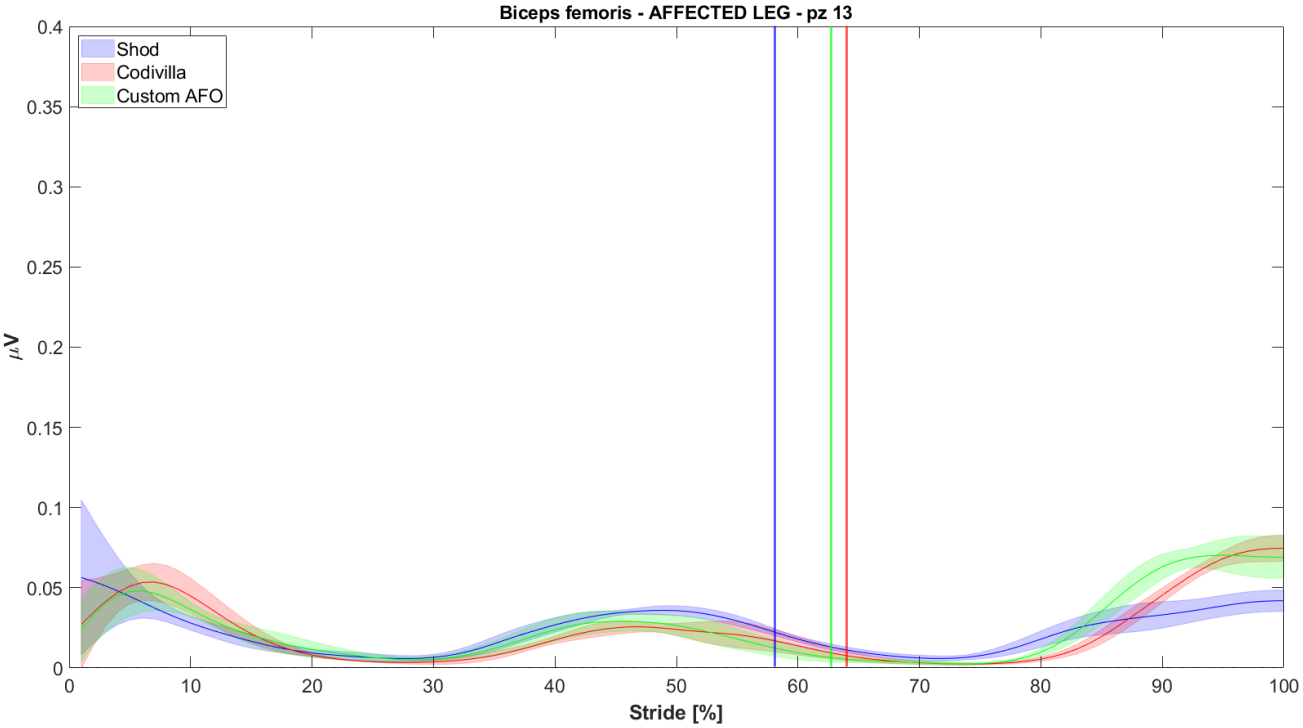

Figure 72: The biceps femoris muscular activation in the affected leg of an exemplary patient. Mean values ± SD of the muscular activation across the walking trials are shown for the shod (blue), Codivilla spring (red) and the custom AFO (green) conditions.

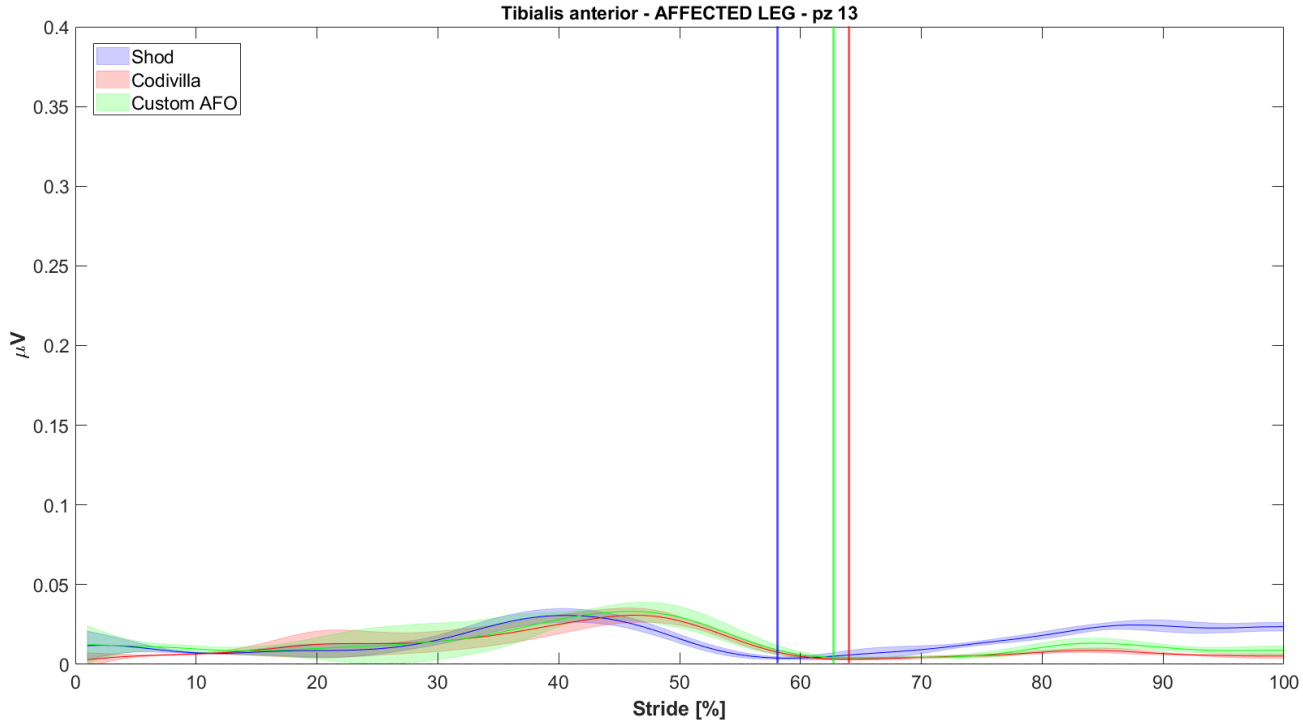

Figure 73: The tibialis anterior muscular activation in the affected leg of an exemplary patient. Mean values ± SD of the muscular activation across the walking trials are shown for the shod (blue), Codivilla spring (red) and the custom AFO (green) conditions.

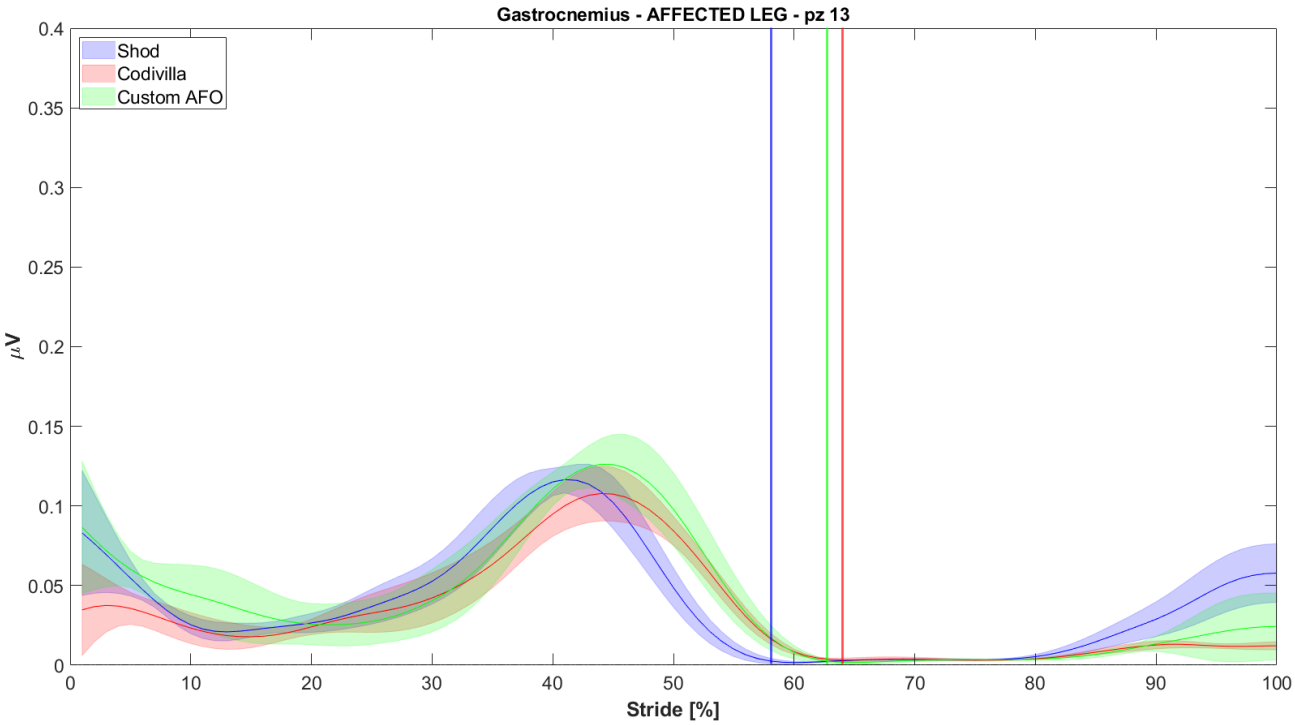

Figure 74: The gastrocnemius muscular activation in the affected leg of an exemplary patient. Mean values ± SD of the muscular activation across the walking trials are shown for the shod (blue), Codivilla spring (red) and the custom AFO (green) conditions.

In order to evaluate the degree of impairment, the muscular activation of the affected leg was compared to that of the healthy leg in each walking condition. Figures 75, 76, 77 and 78 show the comparison between the average inter-subject muscular activation in the affected leg (green curve) and the contralateral (violet curve), of the rectus femoris, the biceps femoris, the tibialis anterior and the gastrocnemius, respectively. The enveloped EMG signals are expressed as a percentage of the maximum muscular contraction recorded between corresponding muscles in the affected and healthy leg of each patient during the gait session and for each walking condition. Vertical lines represent the mean percentage of stride time in which the foot-off takes place, across the walking trials, during the shod condition for the affected leg and the healthy one.

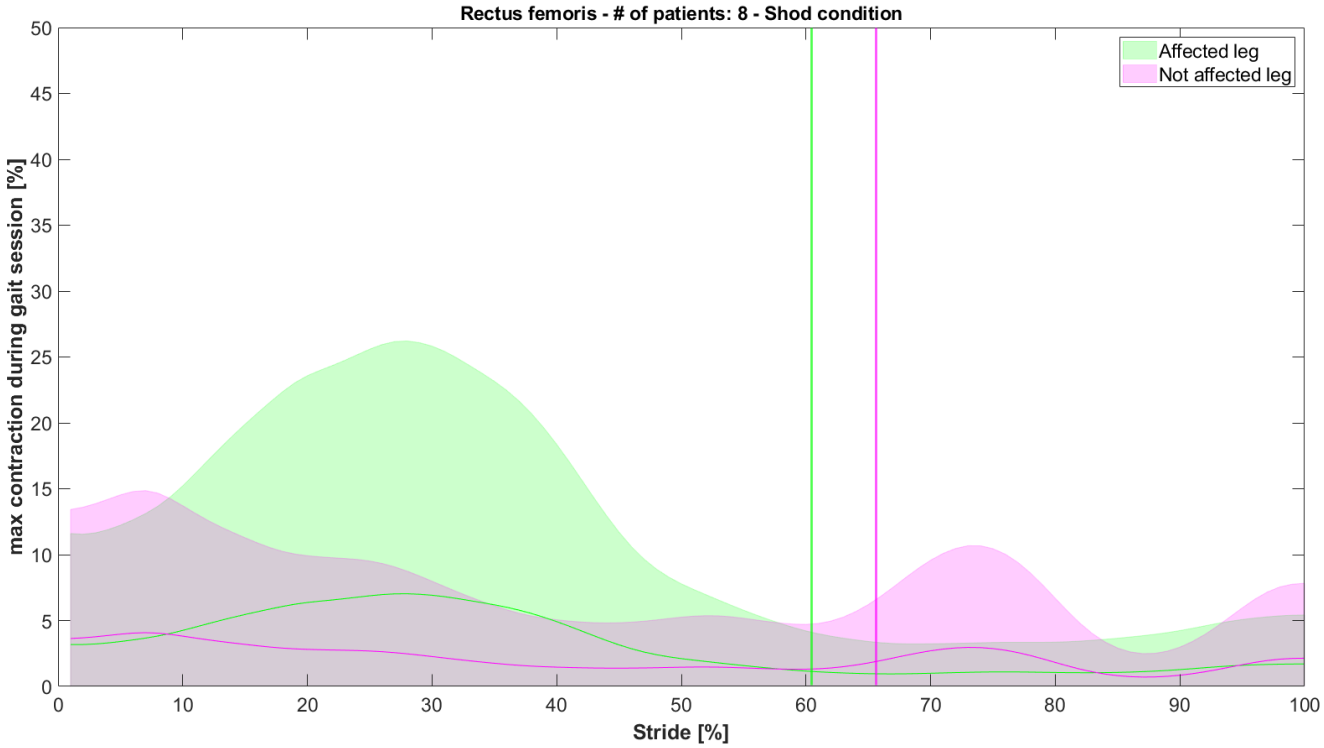

Figure 75: Rectus femoris muscular activation - Comparison between the average signals measured across the patients of the study, for the affected leg (green curve) and the healthy one (violet curve).

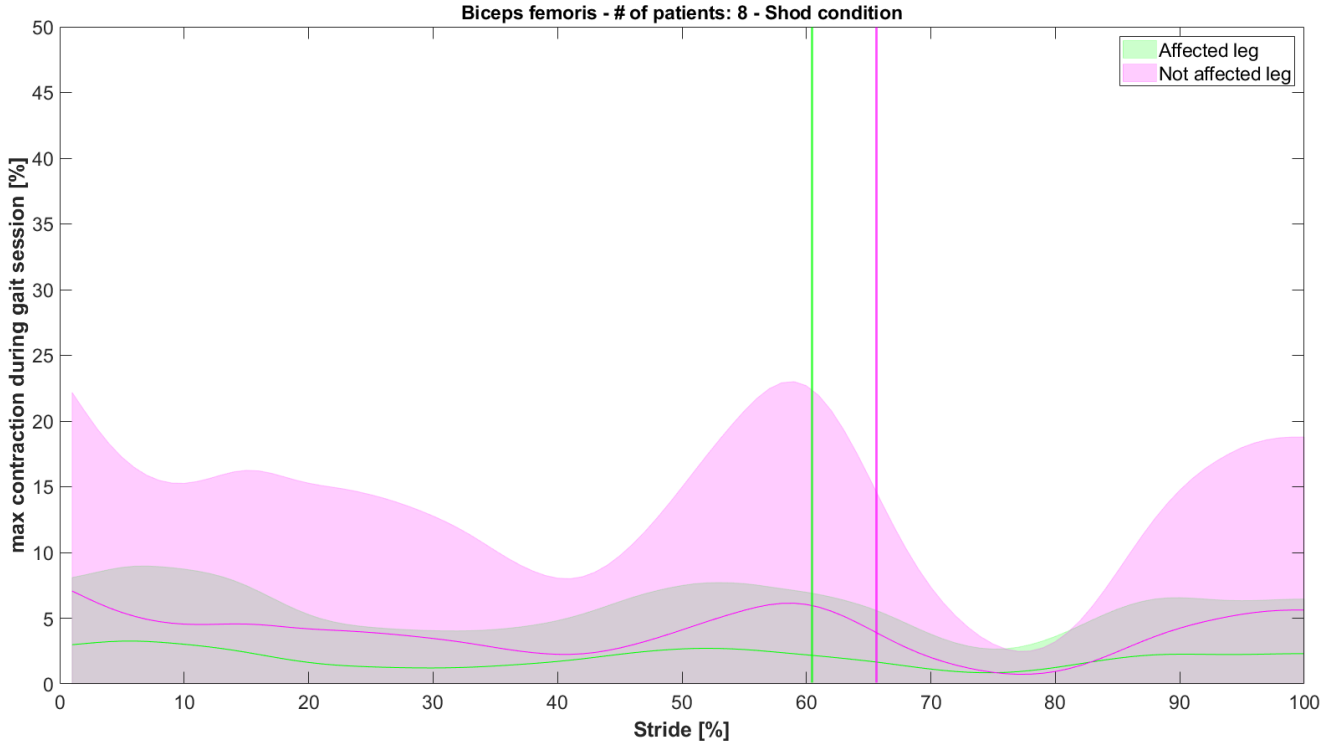

Figure 76: Biceps femoris muscular activation - Comparison between the average signals measured across the patients of the study, for the affected leg (green curve) and the healthy one (violet curve).

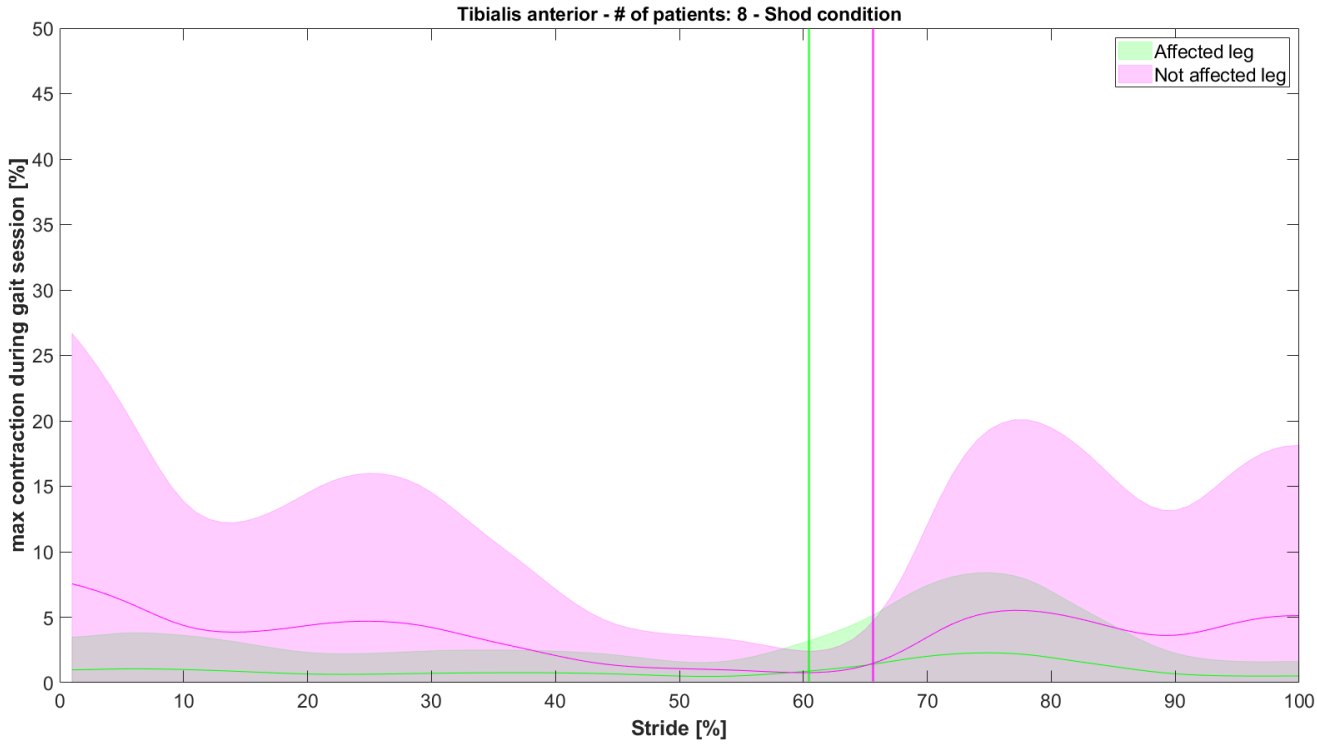

Figure 77: Tibialis anterior muscular activation - Comparison between the average signals measured across the patients of the study, for the affected leg (green curve) and the healthy one (violet curve).

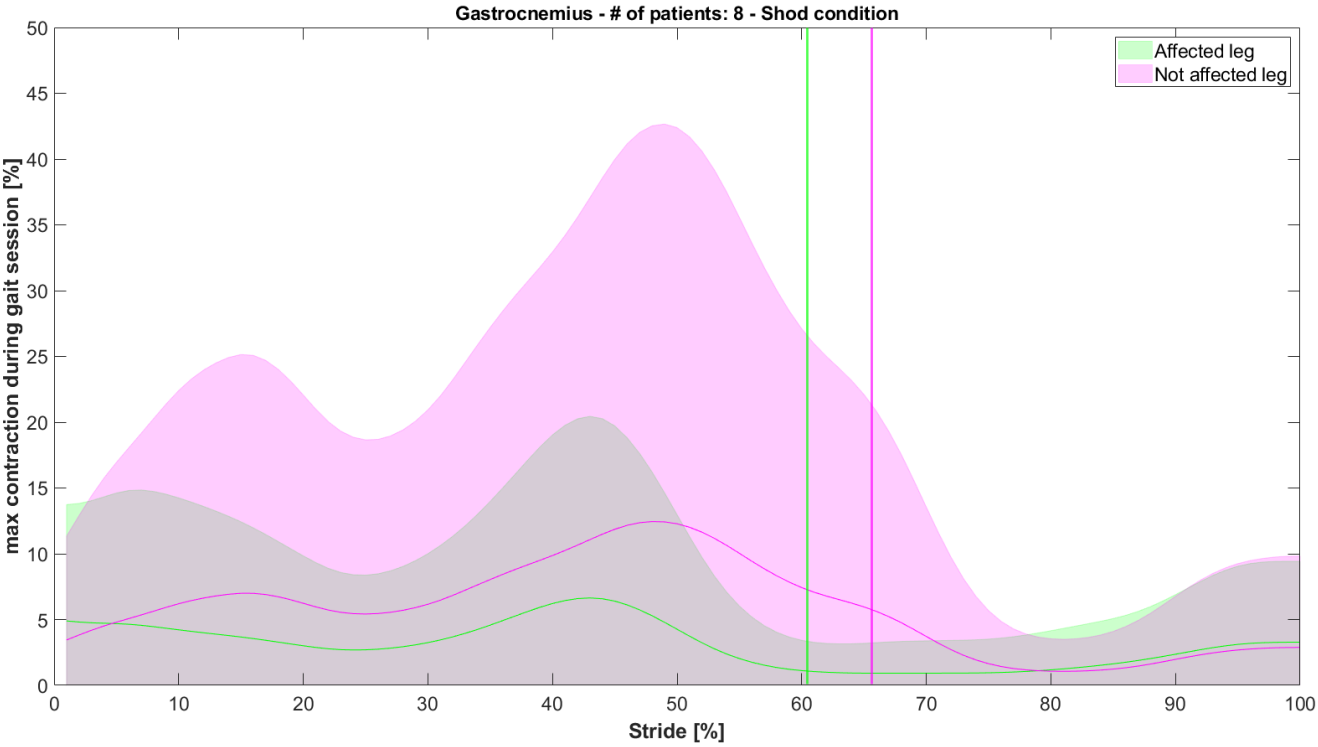

Figure 78: Gastrocnemius muscular activation - Comparison between the average signals measured across the patients of the study, for the affected leg (green curve) and the healthy one (violet curve).

Figures 79, 80, 81 and 82 report the enveloped EMG signals of the affected leg averaged across patients for the rectus femoris, the biceps femoris, the tibialis anterior and the gastrocnemius, respectively. Average EMG data has been reported as a blue line for shod, red line for the Codivilla spring, and green line for the custom AFO condition. The enveloped EMG signals are expressed as a percentage of the maximum contraction recorded on the gait session for each patient, considering each walking trial, each walking condition, and both legs (affected and contralateral). Vertical lines represent the mean percentage of stride time in which the foot-off takes place for the affected leg, across the walking trials, for each walking condition.

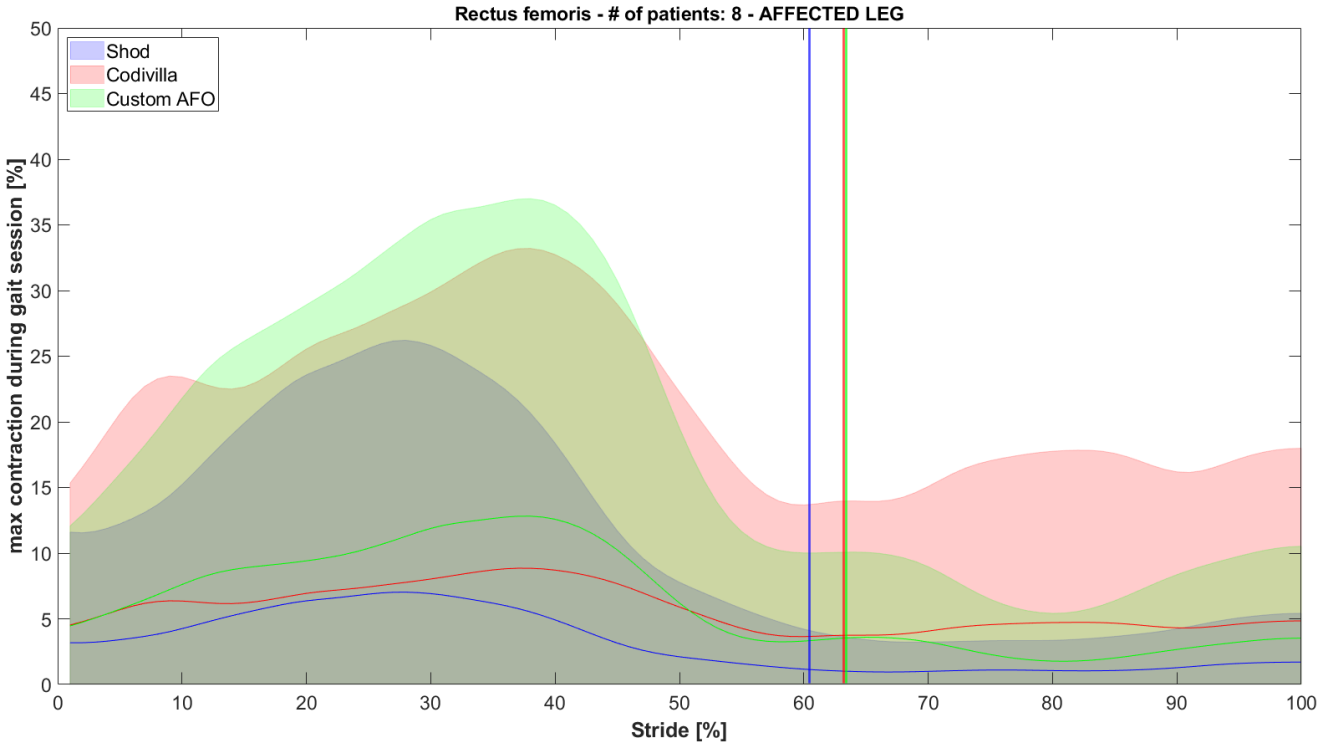

Figure 79: Average rectus femoris muscular activation across foot-drop patients – Curves represent the normalisation of the raw signal on the maximum contraction of rectus femoris recorded during the gait session for each patient, considering each walking trial, each walking condition, both legs.

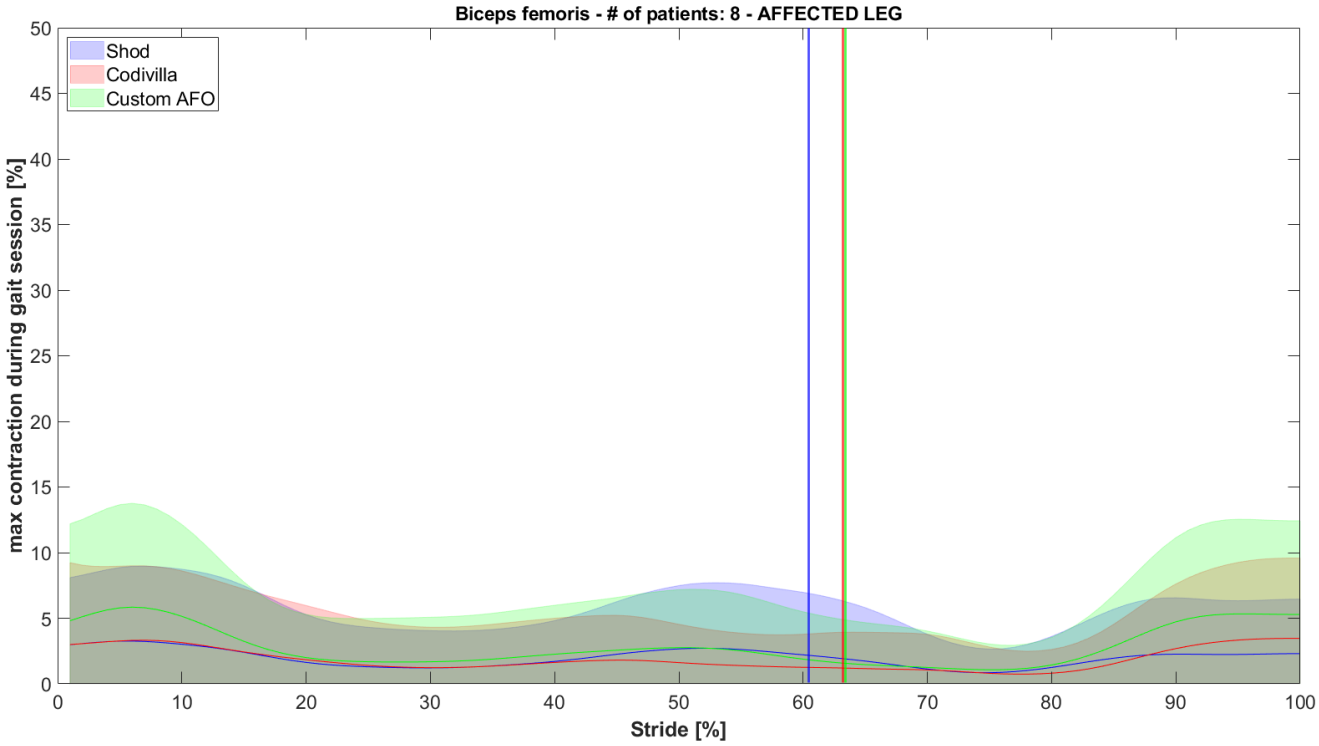

Figure 80: Average biceps femoris muscular activation across foot-drop patients – Curves represent the normalisation of the raw signal on the maximum contraction of biceps femoris recorded during the gait session for each patient, considering each walking trial, each walking condition, both legs.

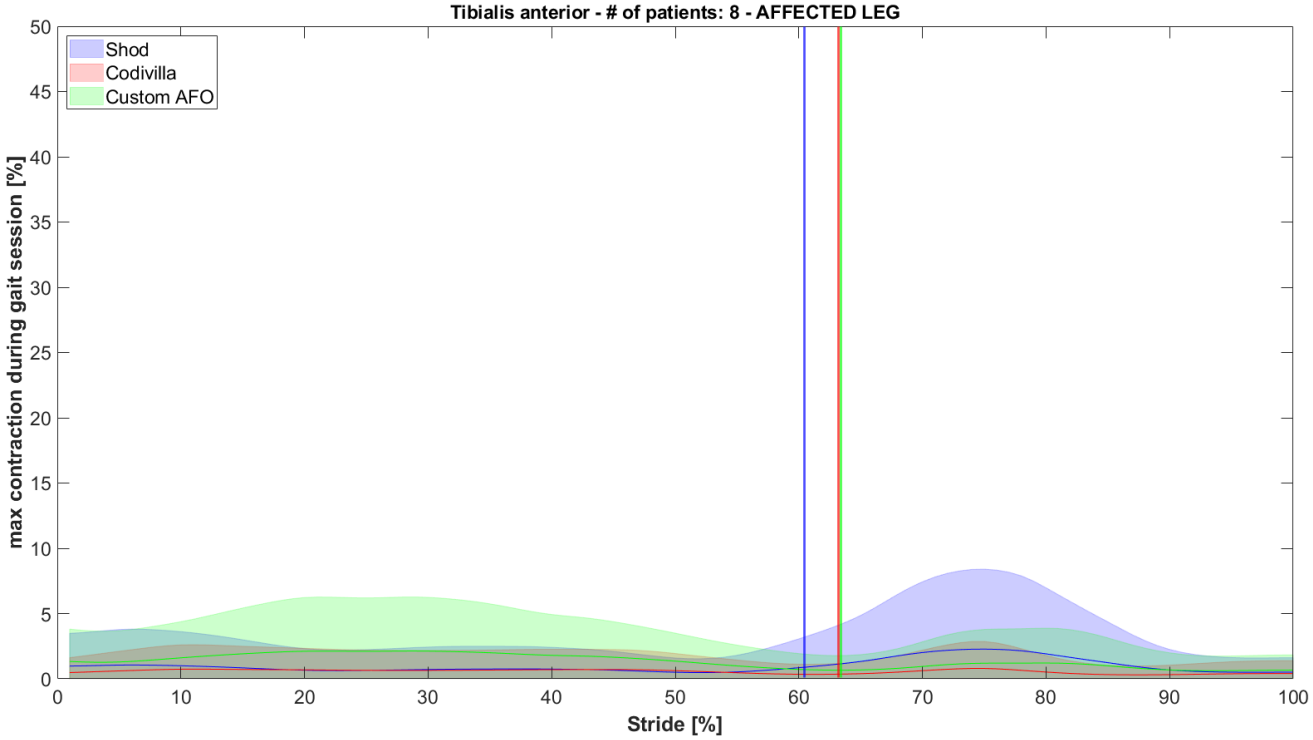

Figure 81: Average tibialis anterior muscular activation across foot-drop patients – Curves represent the normalisation of the raw signal on the maximum contraction of tibialis anterior recorded during the gait session for each patient, considering each walking trial, each walking condition, both legs.

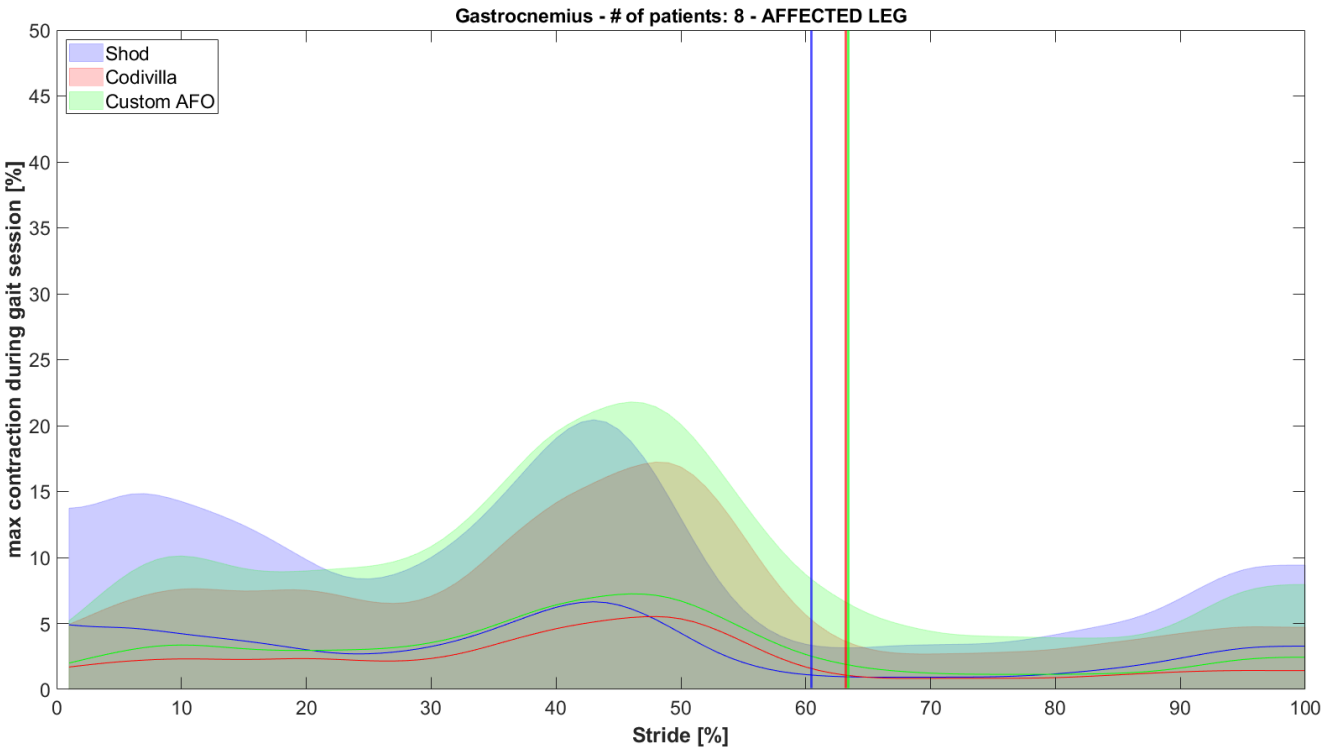

Figure 82: Average gastrocnemius muscular activation across foot-drop patients – Curves represent the normalisation of the raw signal on the maximum contraction of gastrocnemius recorded during the gait session for each patient, considering each walking trial, each walking condition, both legs.

In order to have normal reference values for the EMG signal of muscles involved in the ankle plantar/dorsiflexion during gait, Figures 83 and 84 show the muscular activation – of the tibialis anterior and the gastrocnemius respectively – recorded in a 25-subject control group walking barefoot following the RFM Protocol (average age = 53.1 ± 8.7 years). These data have been normalised to the maximum voluntary contraction of the same muscle. The vertical line represents the mean percentage of stride time in which the foot-off takes place.

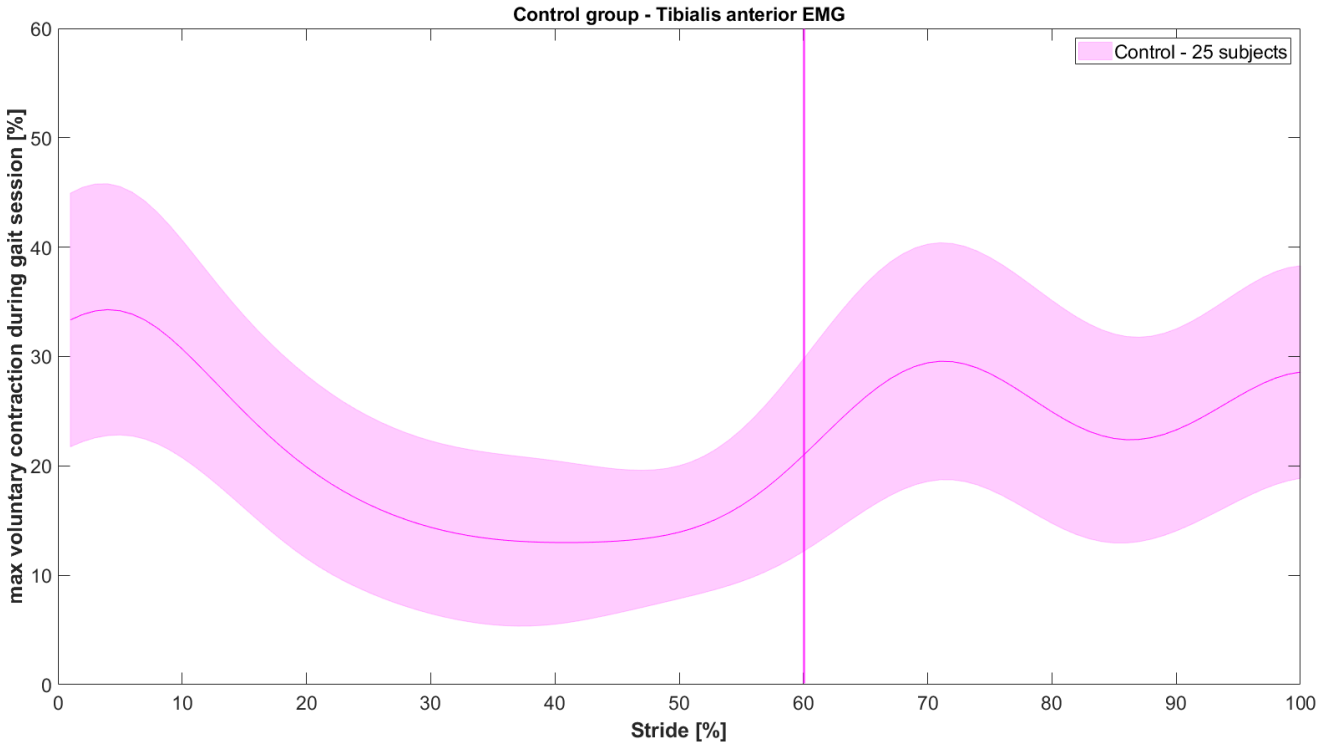

Figure 83: Average tibialis anterior muscular activation across a control group (mean age = 53.1 ± 8.7 years). Each subject muscular contraction has been normalised on the maximum voluntary contraction of the tibialis anterior.

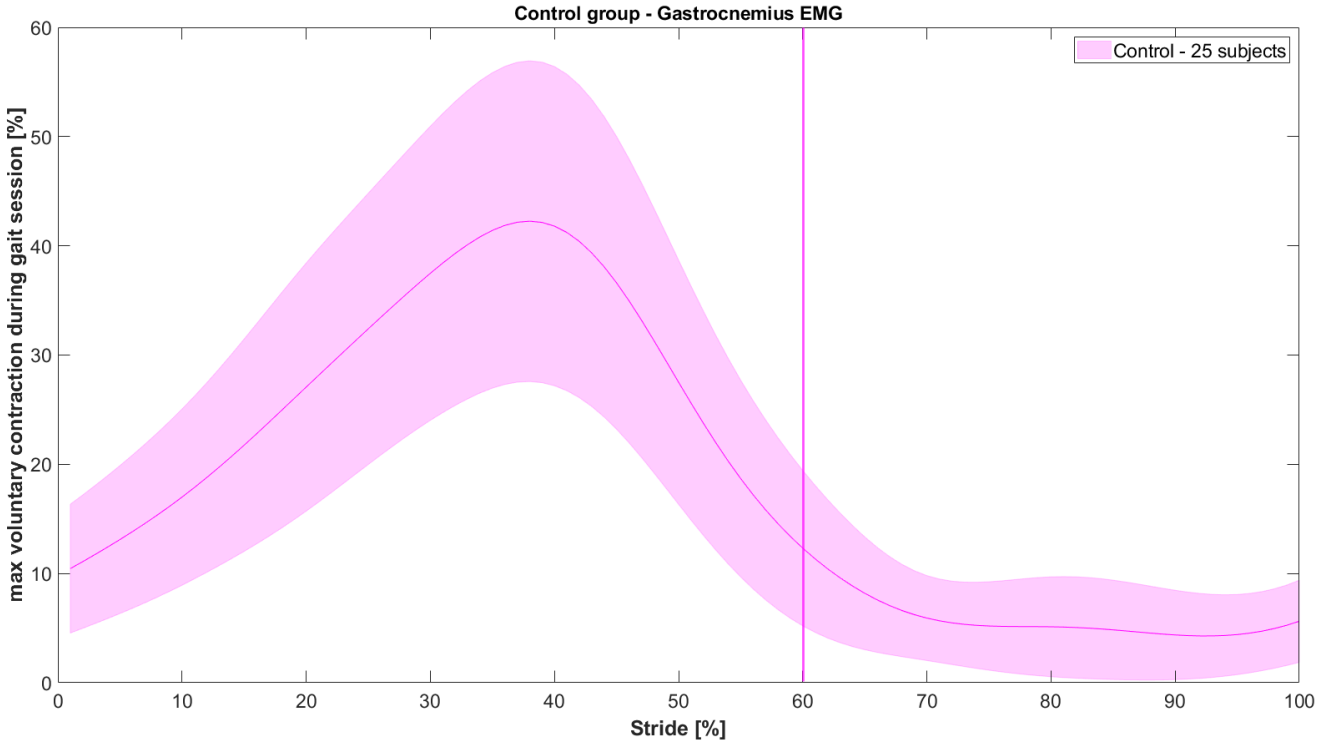

Figure 84: Average gastrocnemius muscular activation across a control group (mean age = 53.1 ± 8.7 years). Each subject muscular contraction has been normalised on the maximum voluntary contraction of the gastrocnemius.

3.5 Energy contribution

In accordance with the procedure described in Paragraph 2.5.3.4, the present section is reporting the estimated energy balance in the custom AFO due to its flexion/extension motion in the stance phase of gait. The energy has been estimated using the resisting torque/angle relationship measured in the mechanical tests (see Paragraph 2.4). Figure 85 reports the average torque and flexion angle of the AFO in the sagittal plane for an exemplary patient. The work done/absorbed by the AFO has been calculated as the dot product of the AFO calf-shell flexion/extension angle at any instant of the stance phase – as estimated via gait analysis in stance - and the corresponding sagittal-plane resisting moment as from relationship obtained in the mechanical tests. The resisting moment produced by each custom AFO, and the corresponding flexion/extension angle, are reported in the Appendix.

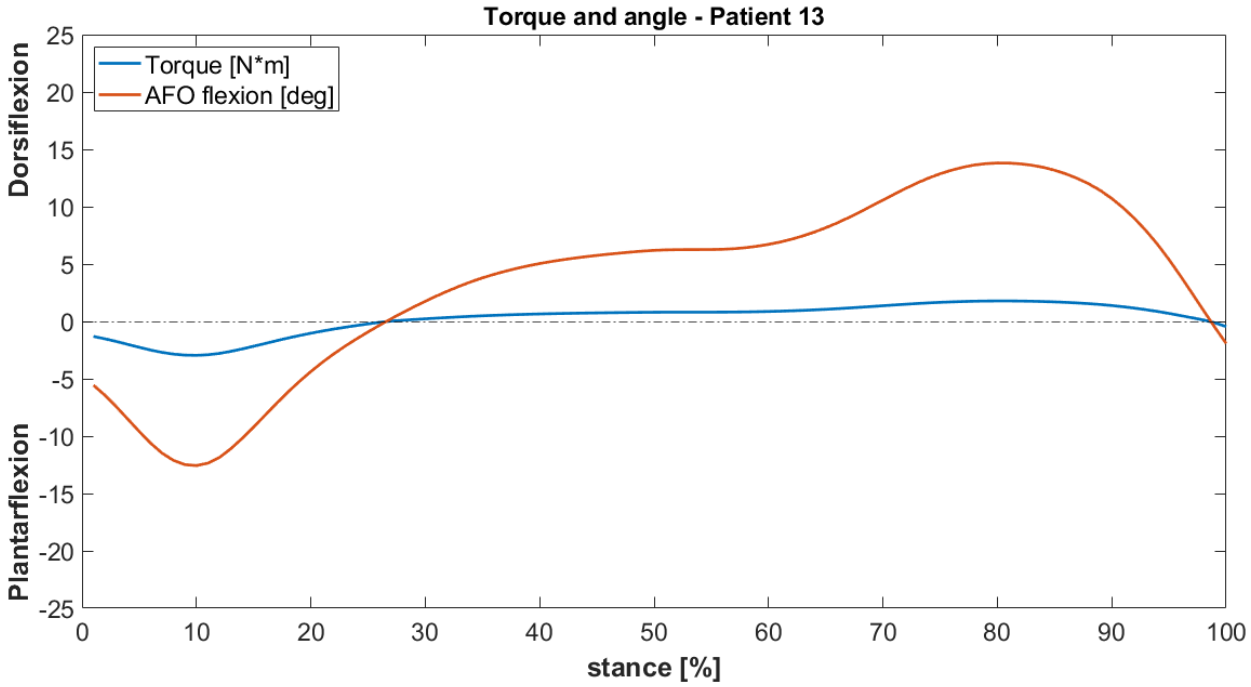

Figure 85: The mean torque moment (blue curve) produced by the custom AFO of an exemplary patient during the stance phase of the gait. It is proportional to the mean flexion/extension angle of the AFO in the sagittal plane (red curve) across the walking trials. The proportionality variable is the average dorsiflexion/extension stiffness measured across the mechanical testing trials.

The energy is considered absorbed by the AFO whenever the torque and the angle first derivative have the same sign, while it is considered as energy released by the AFO to the

patient when the torque and the angle first derivative have opposite signs. Figure 86 shows the mean work produced by the AFO of an exemplary patient, while the work done/absorbed by each AFO in the study is reported in the Appendix.

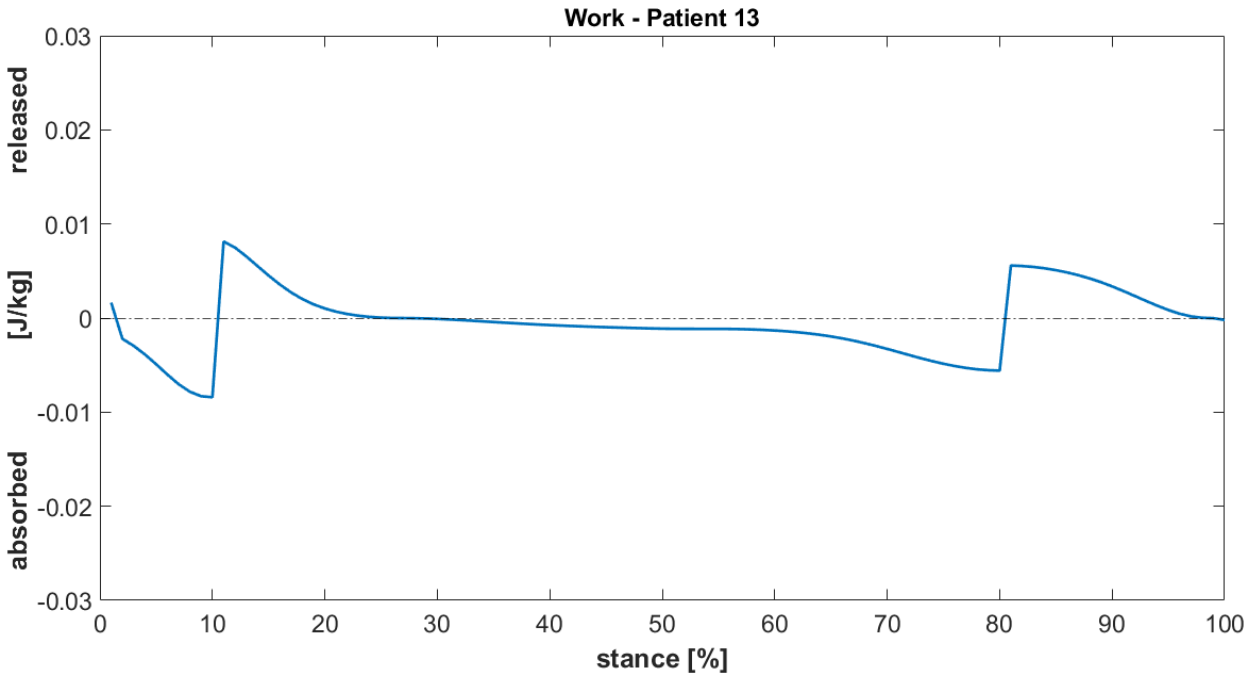

Figure 86: The average energy absorbed or released by the custom AFO of an exemplary patient during the stance phase of the gait cycle, due to the dynamic behaviour of the device. Each value is normalized on the patient's weight.

It is possible to quantify the power produced by the AFO at any instant of the stance phase from the energy absorbed/released by it. The power has been calculated as the time derivative of the work and follows the sign convention chosen for the work. Figure 87 shows the mean power produced by the AFO of an exemplary patient during the stance phase; the power of all the AFOs evaluated in this study are reported in the Appendix.

Figures 88 and 89 report the intra-subject average work and power for each AFO of the study.

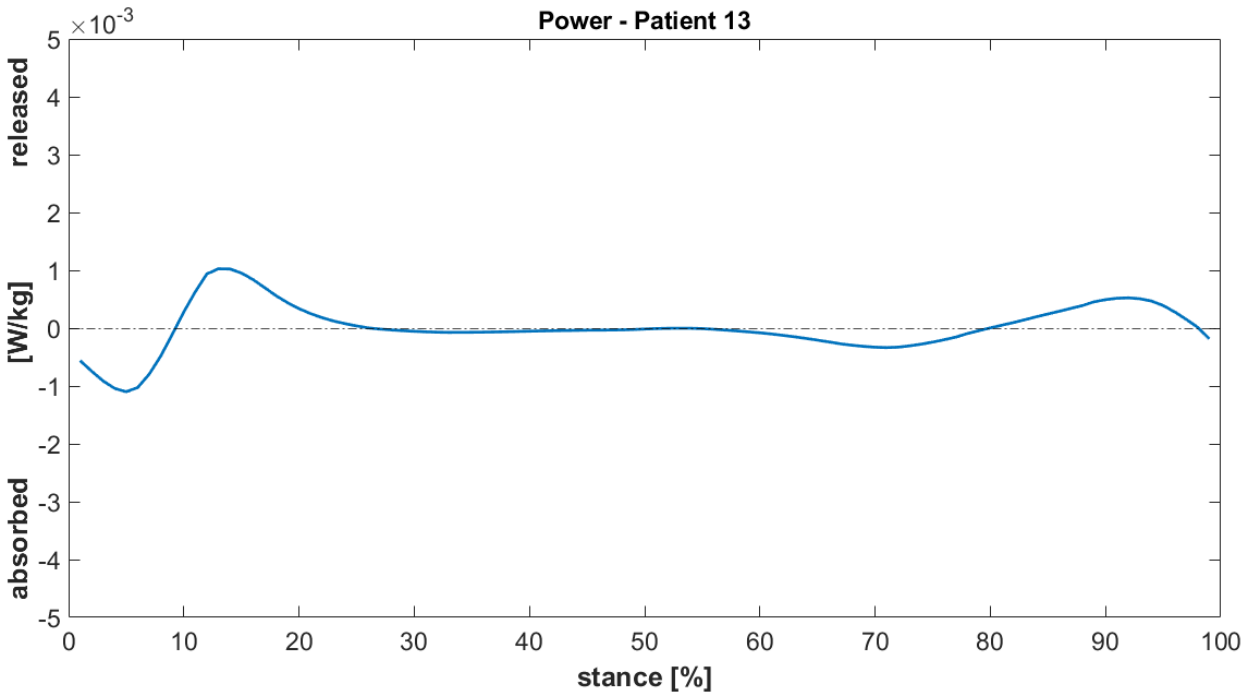

Figure 87: The average power produced by the custom AFO of an exemplary patient at any instant of the stance phase of the gait cycle, due to the dynamic behaviour of the device.

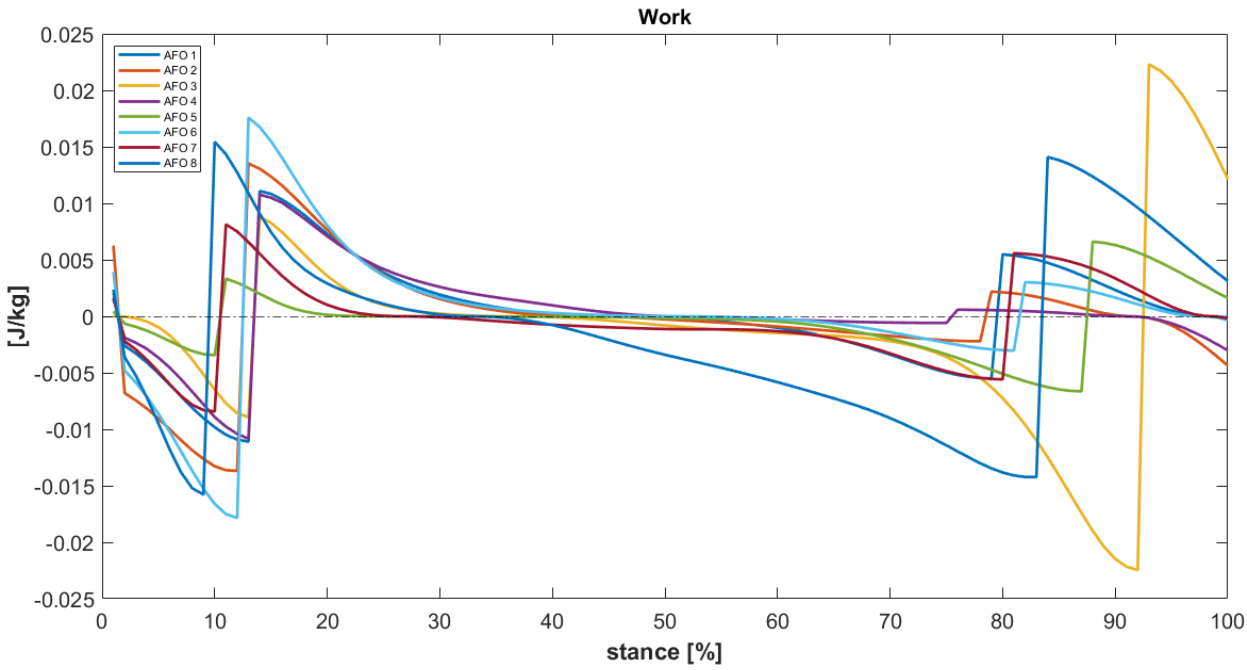

Figure 88: Comparison between the average energy absorbed or released by the custom AFO of the study's patients during the stance phase of the gait cycle, due to the dynamic behaviour of the device. Each curve is normalised based on the patient's weight.

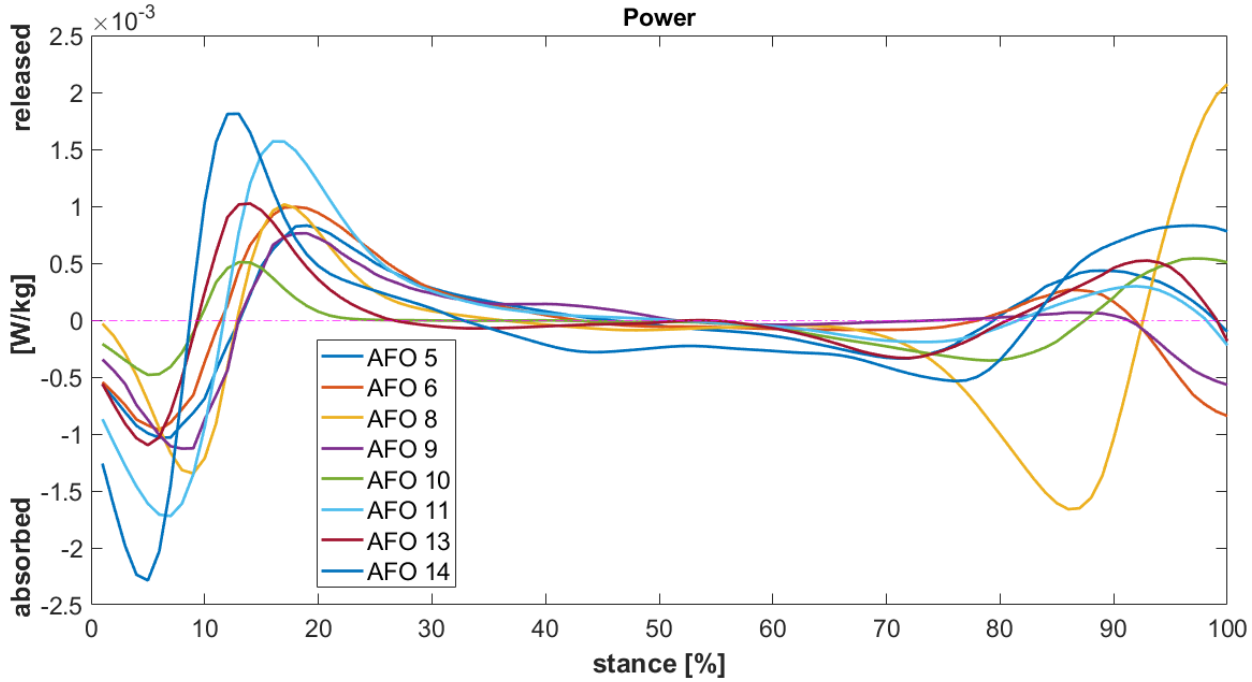

Figure 89: Comparison between the average power produced by the custom AFO of the study's patients.

Figures 90, 91 and 92 report, respectively, the average torque and angle, work and power produced/absorbed by the custom AFO across all patients.

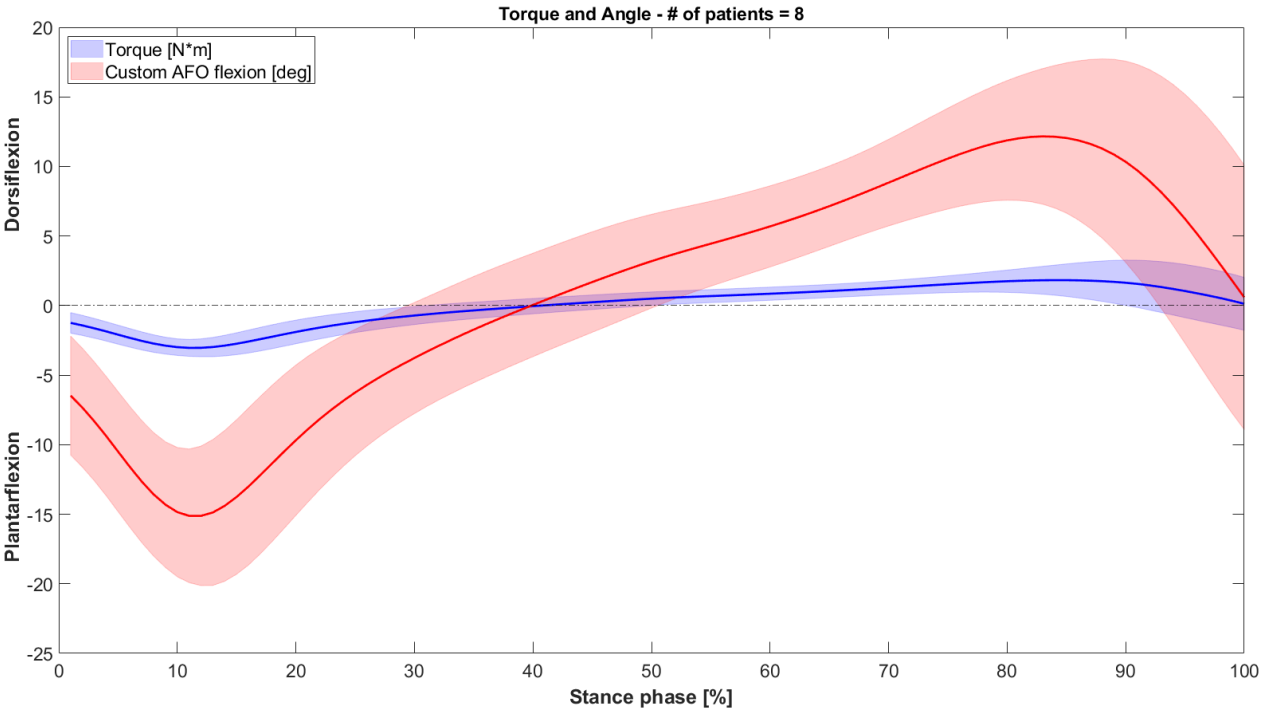

Figure 90: The mean torque moment and flexion/extension angle of the custom AFO in the sagittal plane measured across the study's patients.

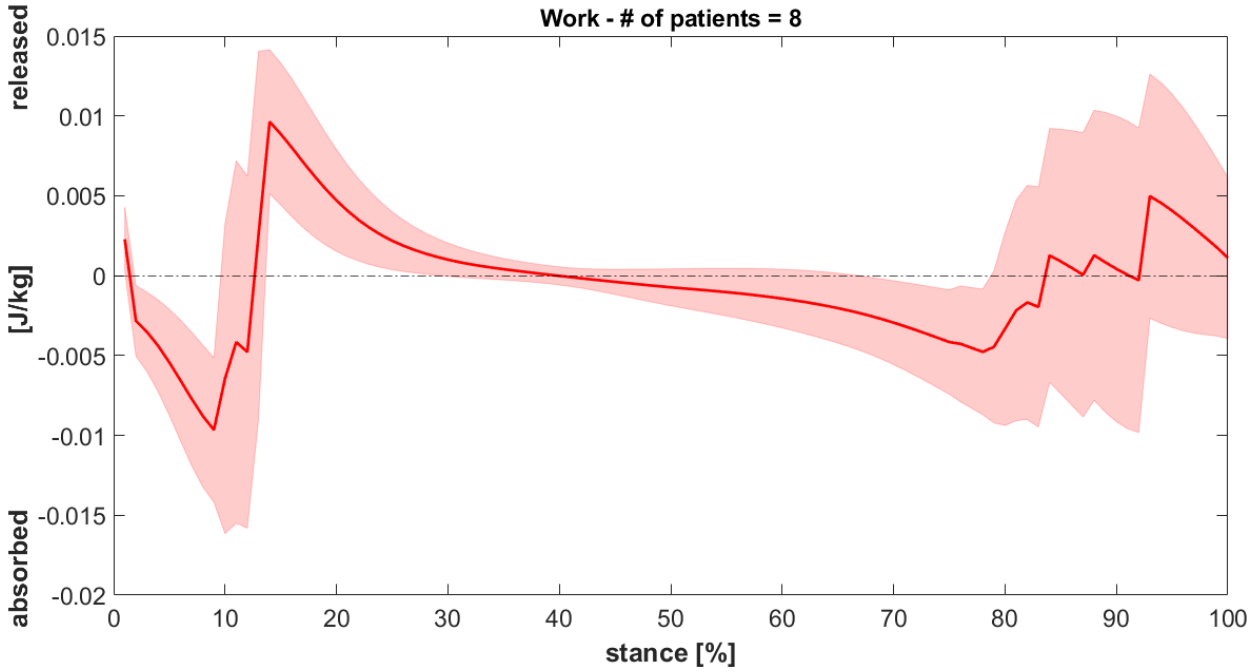

Figure 91: The mean work produced by the custom AFO in the sagittal plane measured across the study's patients.

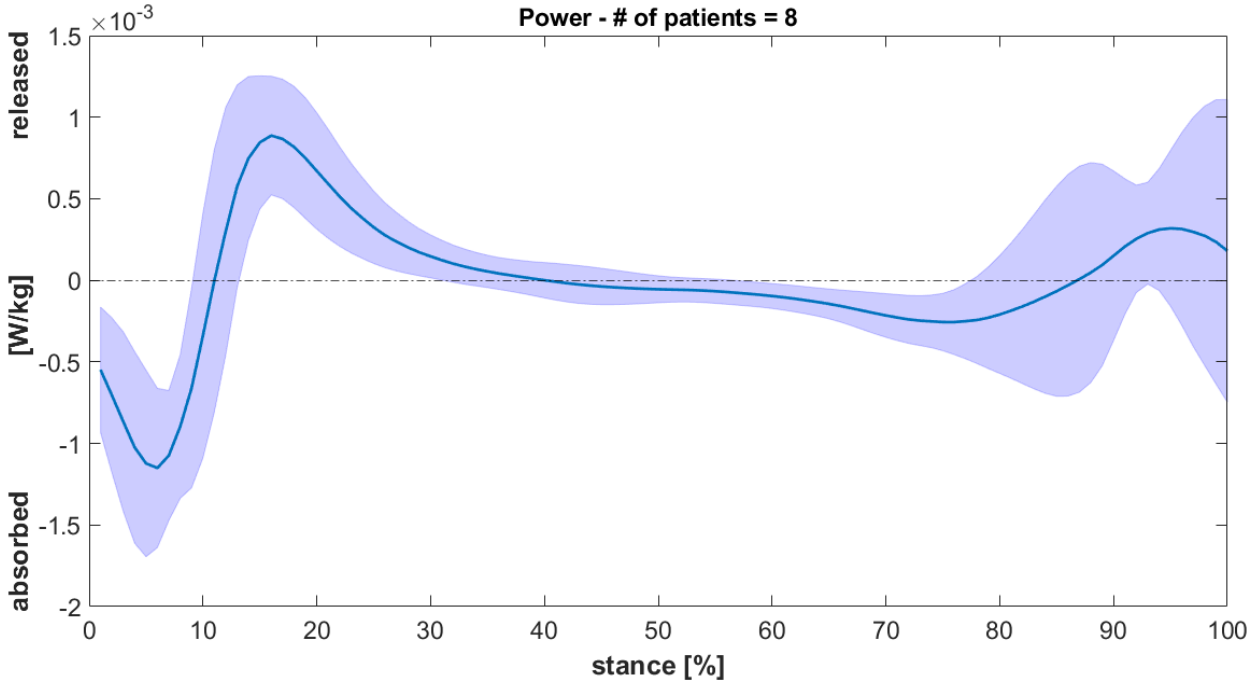

Figure 92: The mean power produced by the custom AFO in the sagittal plane measured across the study's patients.

3.6 Comfort evaluation

The comfort perceived by each patient wearing the AFOs during the gait session has been assessed via a 0 - 10 VAS right after the walking trials. For both AFOs – the Codivilla spring and the custom AFO – patients filled the questionnaire which scored the following four domains: the comfort at the foot-plate, the comfort at the calf shell, the overall comfort, and the perceived push at the foot-off. Table 9 reports the collected VAS scores for each of the 10 patients.

Patient ID	Comfort at the foot-plate		Comfort at the calf shell		Perceived push at the foot-off		Overall comfort	
	Codivilla spring	Custom AFO	Codivilla spring	Custom AFO	Codivilla spring	Custom AFO	Codivilla spring	Custom AFO
2	2.9	10.0	5.2	9.9	1.3	10.0	5.0	10.0
3	9.5	9.7	4.7	9.7	6.3	9.6	6.4	9.7
4	6.8	8.2	6.8	7.2	7.4	5.9	7.0	7.5
6	9.1	9.4	2.8	8.6	4.4	4.5	4.7	6.9
8	1.3	3.9	3.7	6.3	7.1	8.3	3.3	7.3
9	5.9	6.2	6.7	7.8	6.1	7.8	6.1	7.0
10	8.3	9.6	0.9	9.2	8.5	9.5	6.3	9.7
11	5.5	7.0	4.7	8.0	6.5	7.5	5.2	8.5
13	1.1	9.0	6.4	8.8	0.6	9.7	6.3	9.0
14	1.4	10.0	5.5	8.0	0.4	5.4	2.8	10.0
Average ± std	**5.2 ± 3.1**	**8.3 ± 1.9**	**4.7 ± 1.8**	**8.4 ± 1.1**	**4.9 ± 2.9**	**7.8 ± 1.9**	**5.3 ± 1.3**	**8.6 ± 1.2**

Table 9: The evaluation of the comfort perceived by each patient wearing both AFOs, on a VAS from 0 to 10.

4. Discussion

This thesis aimed at reporting the design principles, the manufacturing procedures, and the main outcomes of the functional and comfort evaluation of a novel fibreglass-reinforced polyamide custom PD-AFO manufactured via SLS for a cohort of 10 mild foot-drop patients. Functional evaluation was performed via gait analysis in controlled laboratory conditions using a validated and widely used skin-marker-based lower limb protocol. Each patient was asked to walk at comfortable speed along a 10 m pathway in three conditions: wearing his/her footwears (without AFO), wearing a standard off-the-shelf AFO (Codivilla spring), and wearing the custom AFO. Large variability in lower limb morphology, degree of impairment at the ankle deficit, foot postural alterations and functional demands were present in the foot-drop population: the functional evaluation allowed us to objectively measure the walking improvements that each patient reached wearing the custom AFO. Since AFOs are worn several hours per day, another important parameter to consider was the comfort perceived by the foot-drop patients during walking, as well as the perceived push at the foot-off. An original procedure to measure the work done/absorbed by the custom AFO during the stance phase of walking due to its mechanical properties and deformation has been proposed.

The current section is organised as follows: discussion of the results reported in Section 3, limits of the study and future developments.

4.1 Discussion of the results

Spatiotemporal parameters

In terms of spatiotemporal parameters, according with the results showed in Paragraph 3.3, both AFOs appear to improve walking stability by resulting in larger stance time and thus lower swing time. Stance time (heel-strike to toe-off) increased from 61.0 ± 2.7 % (shod) to 63.7 ± 2.1 % (Codivilla spring) and 63.7 ± 1.5 % (custom AFO). This improved stability provided patients more confidence and resulted in faster walking speed and longer stride length with respect to the shod condition. Wearing the custom AFO has been shown to significantly improve the normalised walking speed (52.3 ± 12.9 % height/s) and the walking stride length (64.7 ± 11.0 % height) with respect to the shod condition (49.3 ± 13.9 % height/s; 63.3 ± 11.3 % height). The Codivilla spring, despite showing improved walking speed (51.8 ± 14.1 % height/s) and stride length (64.2 ± 11.6 % height), did not show any statistically significant difference with respect to the shod condition.

Kinematics and kinetics

The primary function of an AFO is to support the foot during the swing phase of the gait cycle, thus to prevent the foot from dropping loose which could increase the risk of falling. Secondarily, wearing an AFO can be useful to avoid those compensations at the other lower limb joints, which are necessary to restore enough clearance between foot and ground.

By the analysis of the results in Paragraph 3.2, it is notable that both the Codivilla spring and the custom AFO corrected the ankle kinematics of the affected leg during the swing phase of the gait cycle, reducing the plantarflexion angle and the ROM in the sagittal plane with respect to the shod condition. While the latter showed a mean maximum plantarflexion angle of 22.5 ± 9.5 deg, with a mean ROM of 25.1 deg in the swing phase, Codivilla spring resulted in 1.8 ± 5.1 deg in plantarflexion, ROM of 3.8 deg, and the custom AFO resulted in 5.2 ± 6.1 deg in plantarflexion with a mean swing ROM of 6.6 deg. Furthermore, the knee and hip kinematics of the affected leg in the sagittal plane also improved wearing the AFOs. The maximum knee flexion decreased from 72.0 ± 4.9 deg (shod) to 67.9 ± 2.8 deg (Codivilla spring) and 70.1 ± 5.9 deg (custom AFO) and the maximum hip flexion decreased from 43.4 ± 6.0 deg (shod) to 38.6 ± 7.0 deg (Codivilla spring) and 39.4 ± 5.7 deg (custom AFO). The hip ROM in the sagittal plane significantly

decreased from 32.5 deg (shod) to 28.5 deg (Codivilla spring) and 29.4 deg (custom AFO). The comparison of these results with the control kinematic data showed that patients' kinematics were more similar to the reference values in the AFO condition. Focusing on the kinematics in the frontal and transverse planes, the greatest evidence is that, during the swing phase, the ankle inversion and adduction decreased while wearing an AFO with respect to the shod condition. The consequence is a reduction of the ankle ROM in the frontal plane, from 4.1 deg (shod) to 2.2 deg (Codivilla spring) and 3.3 deg (custom AFO).

At last, it is clear that both the Codivilla spring and the custom AFO have not significantly altered – or apported any significant difference to – the biomechanics of the healthy limb in any of the three anatomical planes.

Therefore, it is possible to state that wearing the custom AFO allows foot-drop patients to reduce the risk for stumbling, with a remarkable support to the foot during the swing phase of walking and a highest medio-lateral stability during the stance phase.

Electromyography

The analysis of the EMG signals showed in Paragraph 3.4, revealed that, as predictable, there was no or little activation of the tibialis anterior m. - which is the main ankle dorsiflexor muscle - in the affected leg – during the swing phase of the gait cycle. In fact, the maximum normalised activation during the swing phase was 2.3 ± 6.1 % in the affected leg and 5.5 ± 14.6 % in the contralateral leg, used as control. Focusing on other lower limb muscles – such as the rectus femoris, biceps femoris and the gastrocnemius – it is notable that the rectus femoris of the affected leg has a maximum activation during the midstance phase (7.0 ± 19.2 %) greater than the same parameter in the contralateral leg (2.5 ± 6.2 %). This result could be explained by the slightly higher knee extension, during the midstance phase of walking in the affected limb, with respect to the contralateral one (Figures 56 and 59). The rectus femoris is in fact the main responsible for knee extension, as well as for hip flexion. On the other hand, gastrocnemius showed a greater activation, during late stance and late swing phases, for the healthy leg with respect to the affected one, while biceps femoris was slightly higher, during the foot-off phase, in the unaffected leg with respect to the affected one.

With regard to the AFO conditions, the only significant evidence was for the muscular activation of the rectus femoris in the affected leg during the midstance, which had a mean

maximum value of 12.8 ± 24.2 % and 8.9 ± 24.3 % wearing the custom AFO and the Codivilla spring, respectively; for the shod condition it was 7.0 ± 19.2 %. This result, (Figure 79) can be considered as the consequence of a moderate greater hip flexion during midstance wearing the AFOs (Figure 65).

Conversely, the tibialis anterior, the gastrocnemius and the biceps femoris of the affected leg did not present any significant difference in muscular activation by wearing the AFOs with respect to the shod condition.

Energetic contribution

Due to the good flexibility of the custom AFO in the sagittal plane, it was possible to assume that some energy could be absorbed and released by the AFO during the stance phase of walking. Considering the data processed and showed in Paragraph 3.5, the custom AFO showed to release a moderate amount of energy at the foot-off ($1.5 \times 10^{-3} \pm 5 \times 10^{-3}$ $\frac{J}{kg}$). This energy appears to be correlated to the degree of ankle dorsiflexion at toe-off. In fact, as shown in Figure 88, the more the patient dorsiflexes the ankle during stance, such as patients #8, #10 and #14 who reached almost 20 deg of ankle dorsiflexion in the late stance, the more resisting torque is produced at the AFO calf shell, resulting in a relevant absorption of energy during midstance, which is then released at the foot-off. The maximum work input gained as energy push, helpful for the swing phase, was 1.3×10^{-2} $\frac{J}{kg}$ for patient #8.

Therefore, the energetic contribution of the custom AFO to the push-off phase depends on the walking biomechanics and on the amount of ankle dorsiflexion during the stance phase: patients who have the ankle plantarflexed at foot-off will spend energy to produce a force capable to extend the AFO calf shell, while those who start the swing phase with the ankle still dorsiflexed will have an energy return from the AFO, contributing to the push-off.

Comfort evaluation

As reported in Table 9 at Paragraph 3.6, the custom AFO resulted to be more comfortable than the off-the-shelf Codivilla spring (8.6 ± 1.2 vs 5.3 ± 1.3). All patients gave a significantly higher score to the comfort perceived at the calf shell wearing the custom AFO rather than the Codivilla spring (8.4 ± 1.1 vs 4.7 ± 1.8), due to the softer shell

of the AFO, which is more compliant with the patients' leg morphology. Moreover, the custom AFO resulted to be more comfortable at the foot-plate (8.3 ± 1.9 vs 5.2 ± 3.1). At last, with regard to the perceived push at foot-off, almost all patients felt a higher contribution from the custom AFO than from the Codivilla spring (7.8 ± 1.9 vs 4.9 ± 2.9).

It is important to highlight that the custom AFO, which aims to fit the patient morphology perfectly, can be designed to correct possible foot postural alterations, such as hyper-pronation, by manually correcting patient's foot posture during the scanning phase, avoiding the use of additional and expensive orthotic insoles. Furthermore, hyper-supinated patients may benefit from the use of the custom AFO due to a better weight and pressure distribution to the AFO foot-plate, thus relieving excessive loads on hindfoot and forefoot.

Another important aspect to consider is the lower stiffness of the custom AFO compared to the Codivilla spring. The greater flexibility of the custom AFO allows for some degree of plantarflexion, which is beneficial and comfortable for patients who have a good plantarflexion residual force.

4.2 Limits of the study

The present study and its outcome should be considered in light of some limitations.

The soft tissue artefact (STA), which is due to the soft tissue movement between passive reflective skin markers and underlying bone during motion, is the main source of errors in human motion analysis using stereophotogrammetry: the kinematics results of the present study may have been affected by it.

The energetic contribution of the AFO to the push-off phase was estimated without considering the possible contribution of the footplate. Only the flexion between the AFO calf-shell and the AFO footplate has been considered for the energy calculation, while the footplate flexion about the metatarsal phalangeal joint axis was not considered in the energetic analysis.

Another limit of the present study is the fact that patients had only a few minutes to familiarise themselves with the AFOs before starting the gait session, and this may have affected the perceived comfort.

At last, since the present fibreglass-reinforced polyamide was for the first time used here for a dynamic orthosis, and its mechanical properties may change over time in relation to its use and wear, the AFO stiffness and the functional outcome should be reassessed at longer follow-ups (e.g. 12 months).

4.3 Future developments

Since the main objective of this study was to evaluate the biomechanics and the comfort of the custom PD-AFO for foot-drop patients, a cohort of patients with wider deficits, such as bilateral patients, should be investigated. Moreover, while walking is the most common daily motor task, other motor tasks such as slow running and stair ascending/descending should be tested in future endeavours.

For the energetic contribution measurement, a future development could be to consider the AFO flexion due to the flexion between phalanges and metatarsals, which could be significant for the AFO energy storage/release.

At last, it would be interesting to develop a procedure capable of measuring the optimal minimum stiffness that allows the patient to walk correctly, without losing stability.

4.4 Conclusions

The current study has allowed us to evaluate the effects of a novel custom AFO on gait and energy exchange in a cohort of 10 mild foot-drop patients. For the foot-drop patients recruited here, the custom AFO resulted more comfortable than a standard orthosis, supported the foot in the swing phase of gait by preventing passive ankle plantarflexion and reducing the sagittal-plane ROM, and allowed for significant faster walking speed and longer stride length with respect to the no-AFO condition. The present custom AFO is effectively a two-devices-in-one, since it can also replace a standard plantar orthosis in case of severely pronated or supinated feet. It has been shown that due to its dynamic behaviour, the custom AFO can return some of the energy stored at midstance to the ankle in the foot-off phase. While the results of this study should be confirmed in a larger cohort of foot-drop patients with different degrees of impairment and at longer follow-ups, the present custom AFO appears to be a suitable and reliable alternative for those patients who are not fully satisfied with standard off-the-shelf solutions.

Appendix

The sagittal kinematics, electromyographic, and energetic data for each patient of the study.

Patient 2

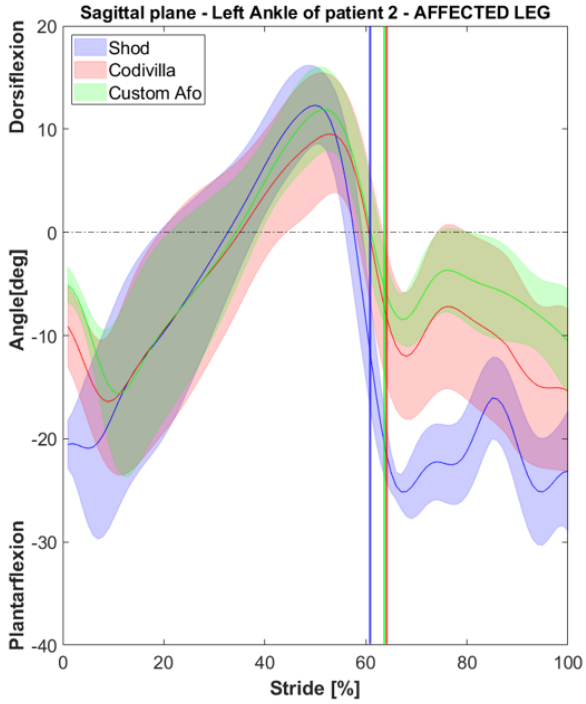

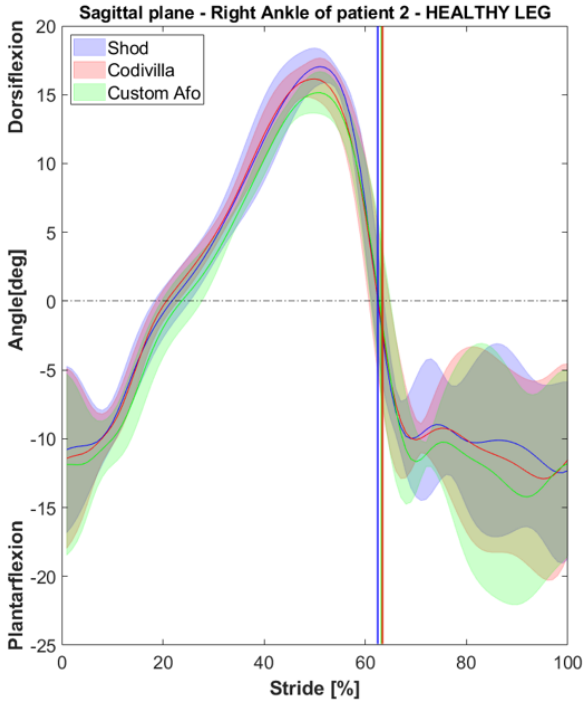

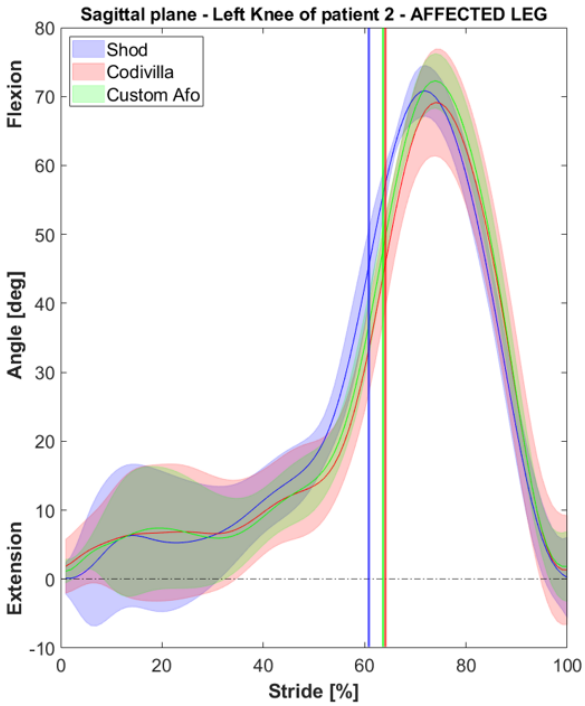

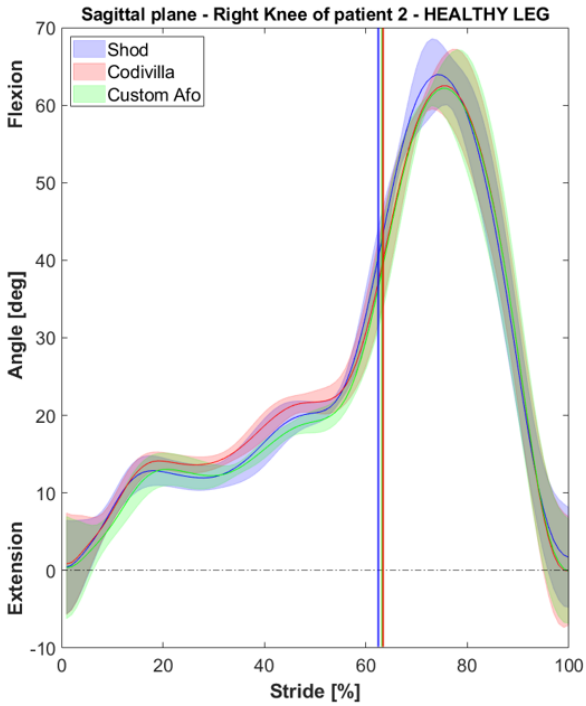

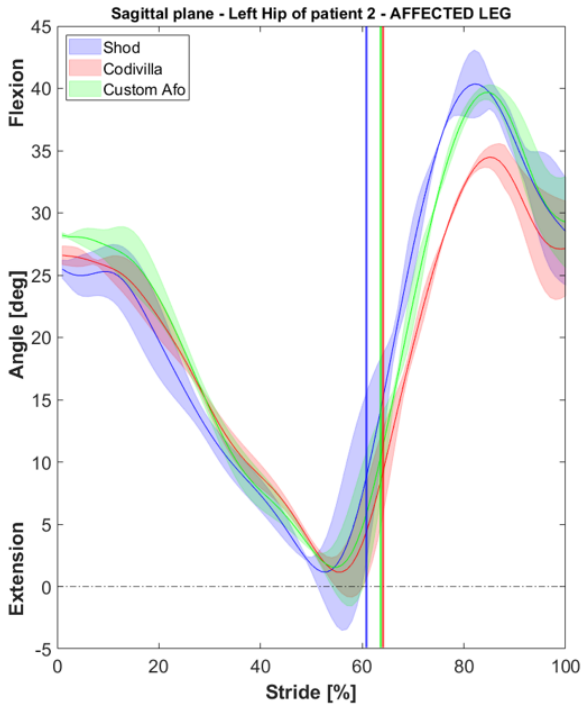
Sagittal plane - Left Hip of patient 2 - AFFECTED LEG
Shod
Codivilla
Custom Afo
Flexion
Extension
Angle [deg]
Stride [%]

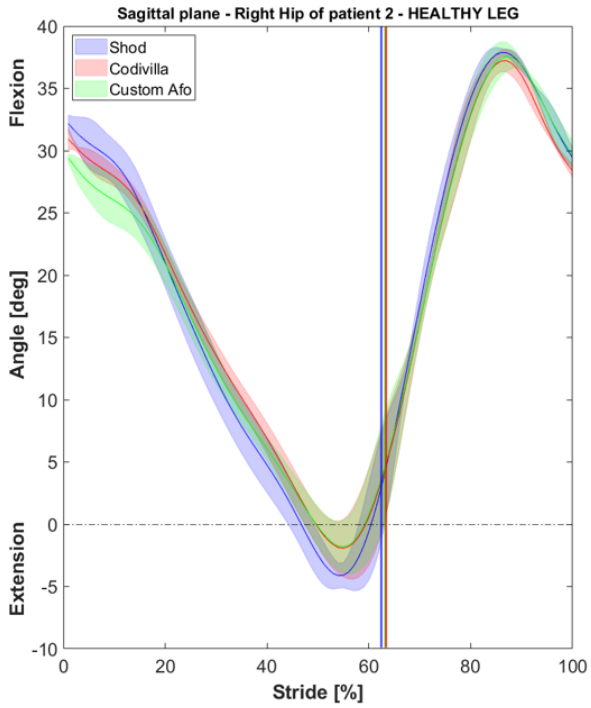
Sagittal plane - Right Hip of patient 2 - HEALTHY LEG
Shod
Codivilla
Custom Afo
Flexion
Extension
Angle [deg]
Stride [%]

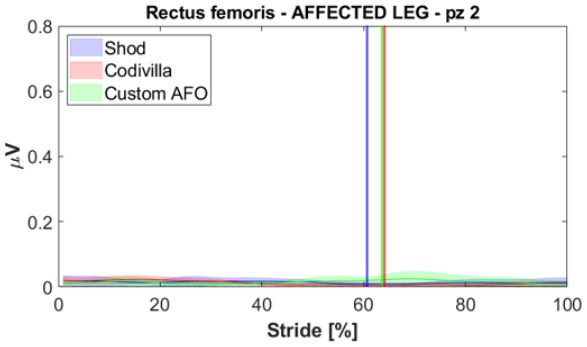
Rectus femoris - AFFECTED LEG - pz 2
Shod
Codivilla
Custom AFO
μV
Stride [%]

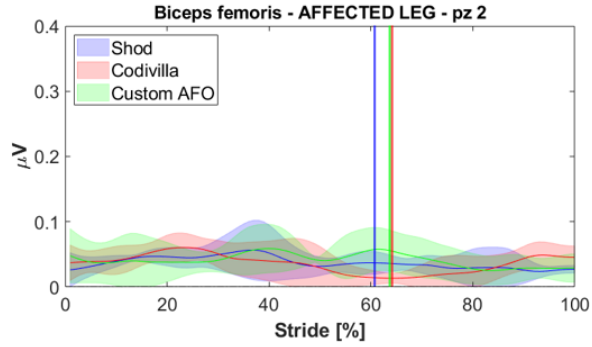
Biceps femoris - AFFECTED LEG - pz 2
Shod
Codivilla
Custom AFO
μV
Stride [%]

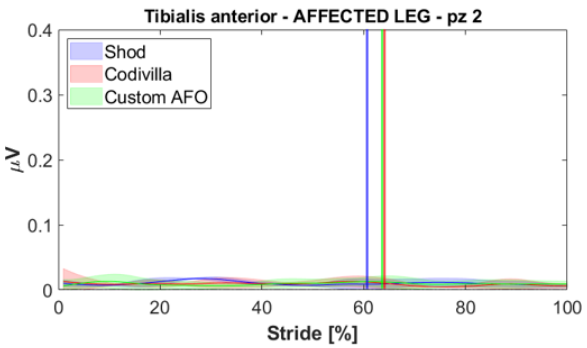
Tibialis anterior - AFFECTED LEG - pz 2
Shod
Codivilla
Custom AFO
μV
Stride [%]

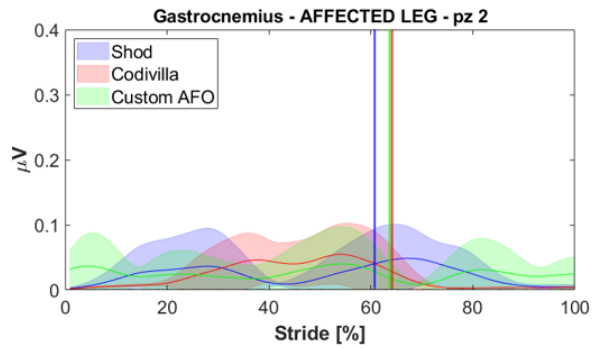
Gastrocnemius - AFFECTED LEG - pz 2
Shod
Codivilla
Custom AFO
μV
Stride [%]

Patient 3

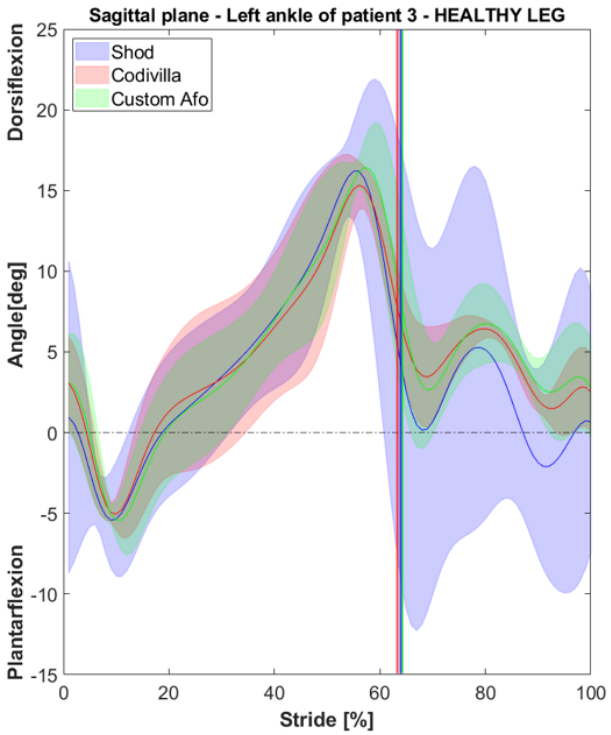
Sagittal plane - Left ankle of patient 3 - HEALTHY LEG
Shod
Codivilla
Custom Afo
Dorsiflexion
Plantarflexion
Angle[deg]
Stride [%]

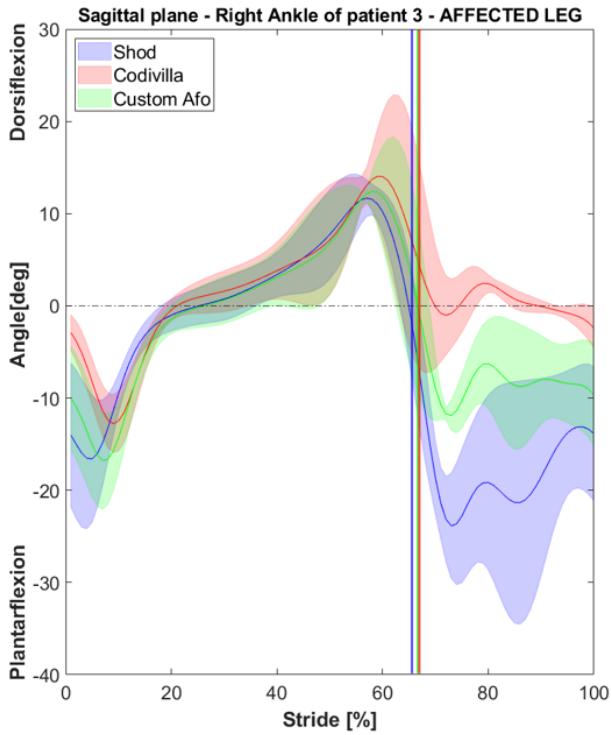
Sagittal plane - Right Ankle of patient 3 - AFFECTED LEG
Shod
Codivilla
Custom Afo
Dorsiflexion
Plantarflexion
Angle[deg]
Stride [%]

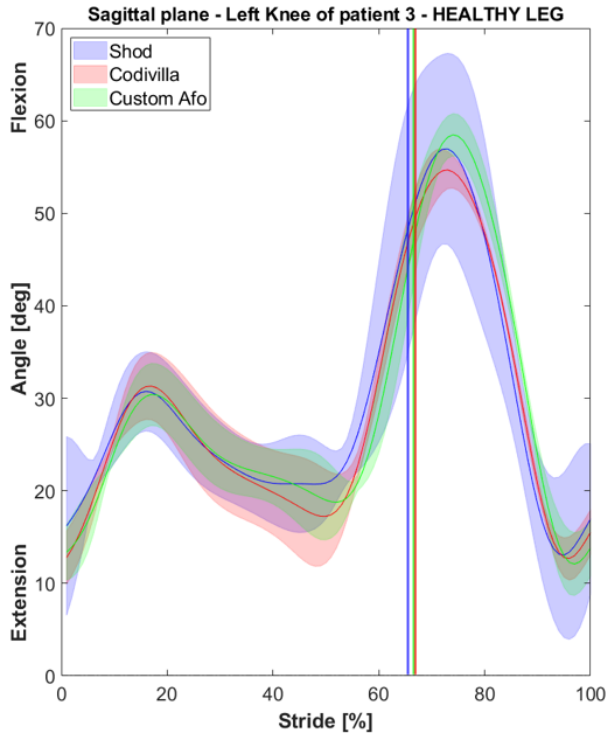
Sagittal plane - Left Knee of patient 3 - HEALTHY LEG
Shod
Codivilla
Custom Afo
Flexion
Extension
Angle [deg]
Stride [%]

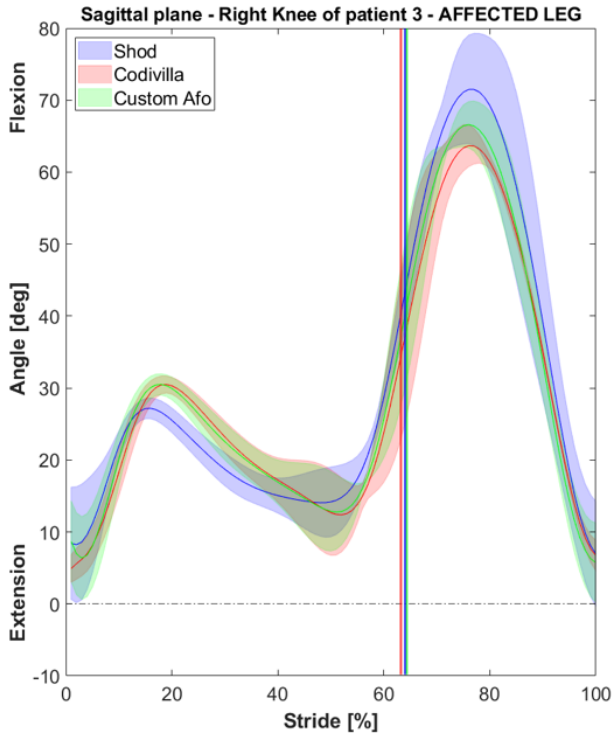
Sagittal plane - Right Knee of patient 3 - AFFECTED LEG
Shod
Codivilla
Custom Afo
Flexion
Extension
Angle [deg]
Stride [%]

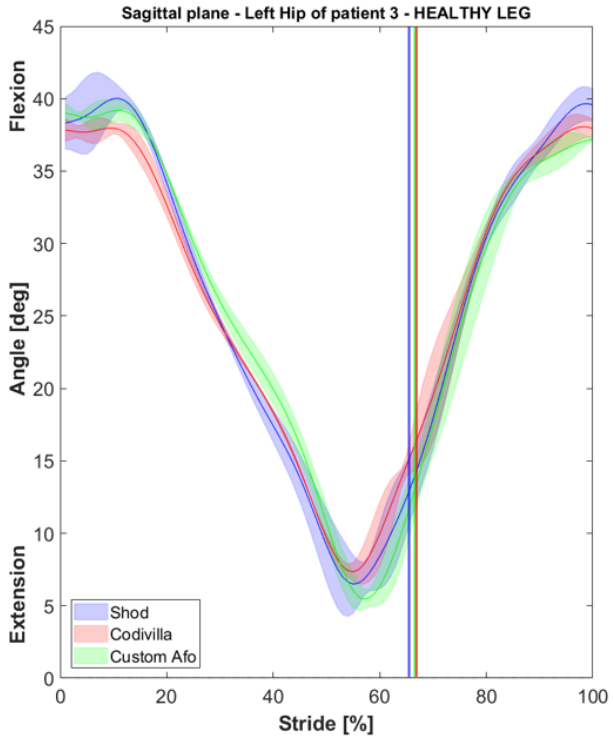
Sagittal plane - Left Hip of patient 3 - HEALTHY LEG
Flexion
Extension
Angle [deg]
Stride [%]
Shod
Codivilla
Custom Afo

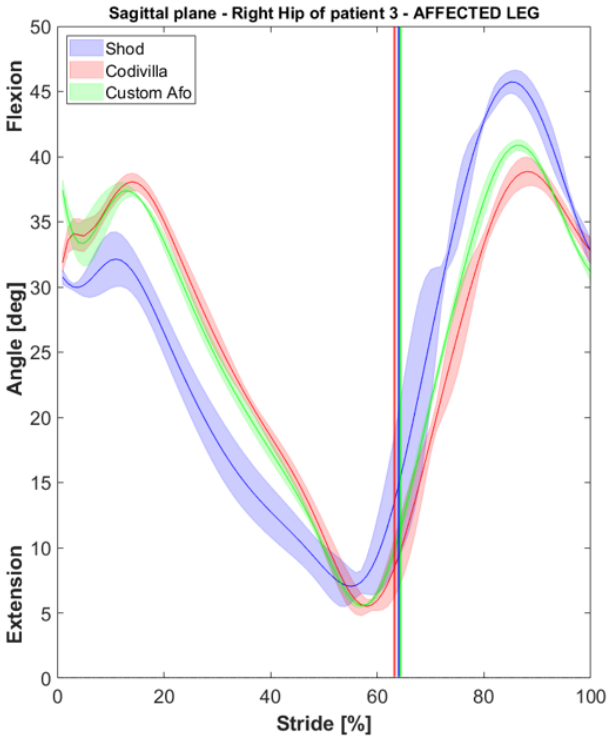
Sagittal plane - Right Hip of patient 3 - AFFECTED LEG
Flexion
Extension
Angle [deg]
Stride [%]
Shod
Codivilla
Custom Afo

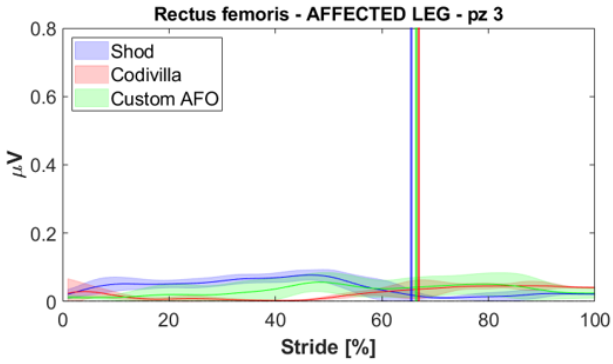
Rectus femoris - AFFECTED LEG - pz 3
μV
Stride [%]
Shod
Codivilla
Custom AFO

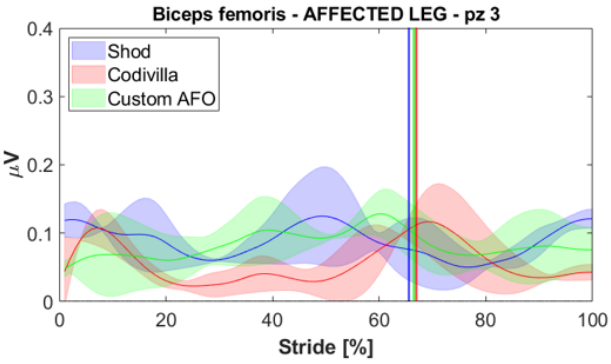
Biceps femoris - AFFECTED LEG - pz 3
μV
Stride [%]
Shod
Codivilla
Custom AFO

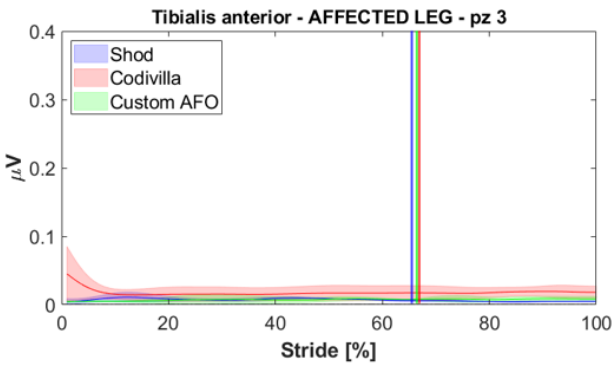
Tibialis anterior - AFFECTED LEG - pz 3
μV
Stride [%]
Shod
Codivilla
Custom AFO

Patient 4

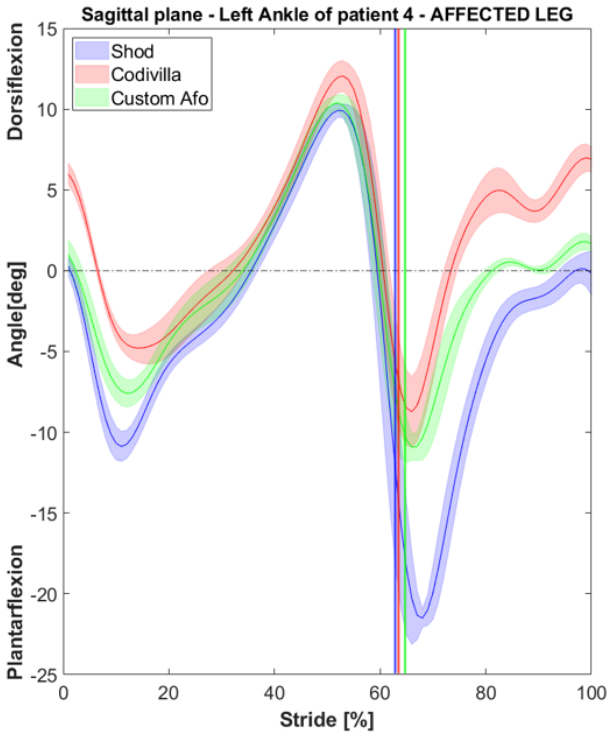
Sagittal plane - Left Ankle of patient 4 - AFFECTED LEG
Shod
Codivilla
Custom Afo
Dorsiflexion
Plantarflexion
Angle[deg]
Stride [%]

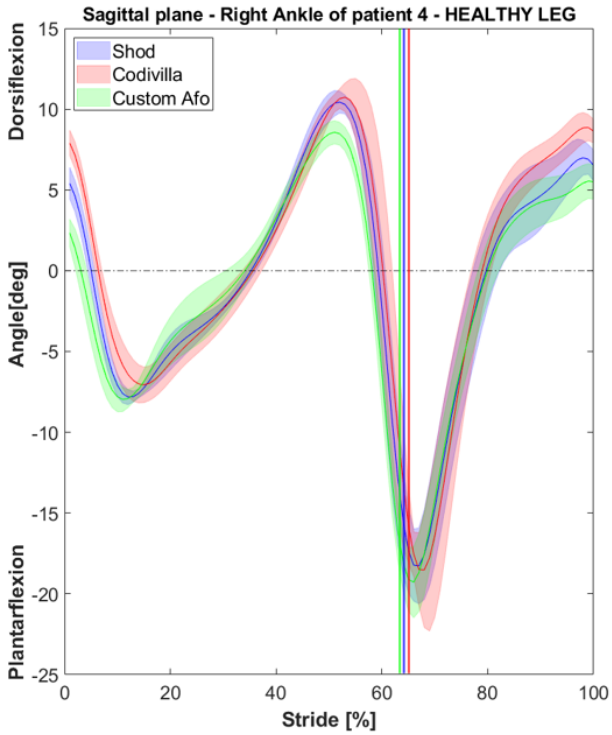
Sagittal plane - Right Ankle of patient 4 - HEALTHY LEG
Shod
Codivilla
Custom Afo
Dorsiflexion
Plantarflexion
Angle[deg]
Stride [%]

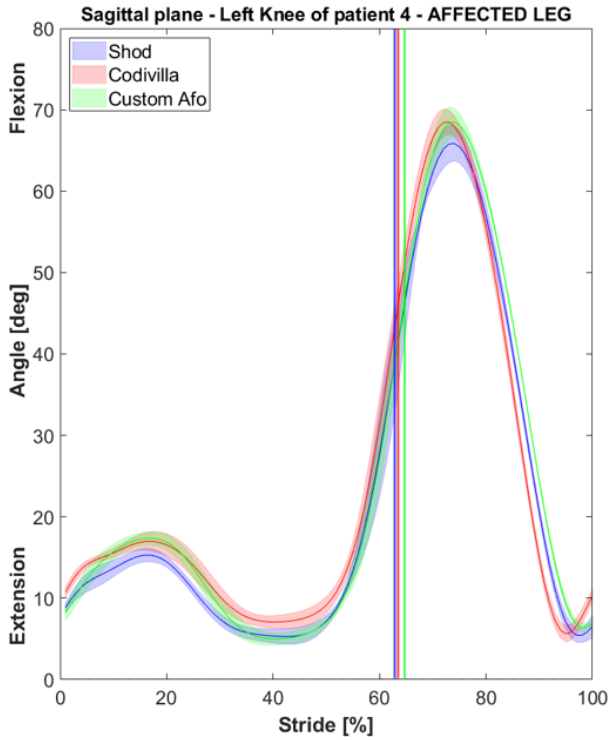
Sagittal plane - Left Knee of patient 4 - AFFECTED LEG
Shod
Codivilla
Custom Afo
Flexion
Extension
Angle [deg]
Stride [%]

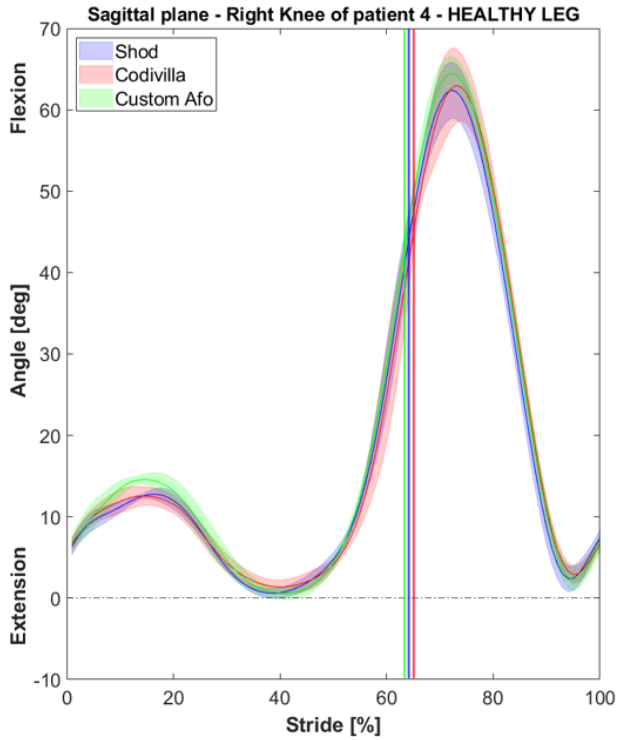
Sagittal plane - Right Knee of patient 4 - HEALTHY LEG
Shod
Codivilla
Custom Afo
Flexion
Extension
Angle [deg]
Stride [%]

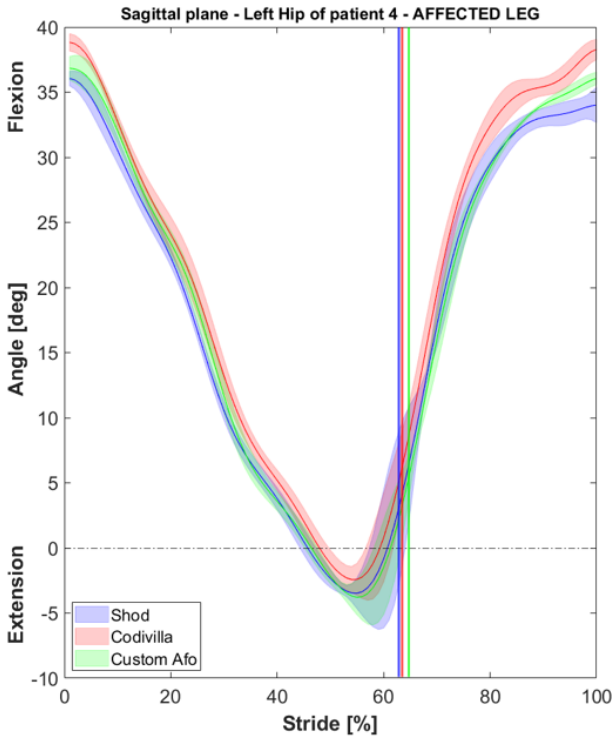
Sagittal plane - Left Hip of patient 4 - AFFECTED LEG
Flexion
Extension
Angle [deg]
Stride [%]
Shod
Codivilla
Custom Afo

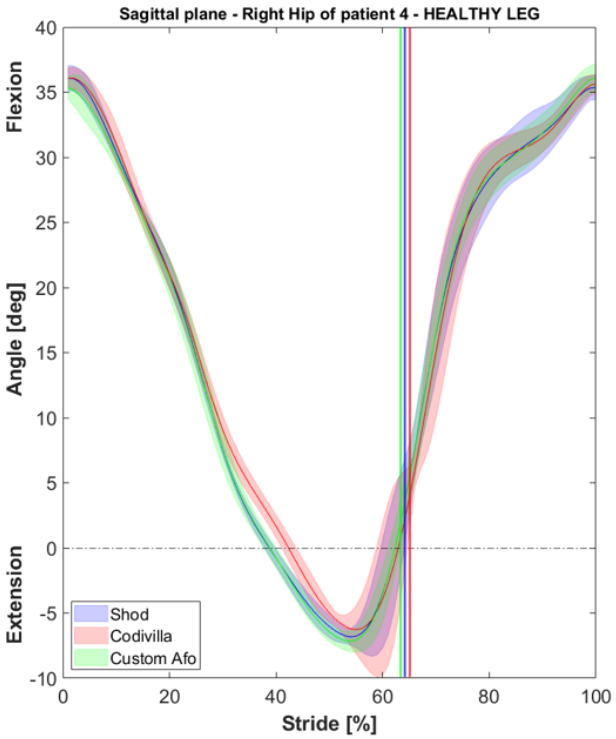
Sagittal plane - Right Hip of patient 4 - HEALTHY LEG
Flexion
Extension
Angle [deg]
Stride [%]
Shod
Codivilla
Custom Afo

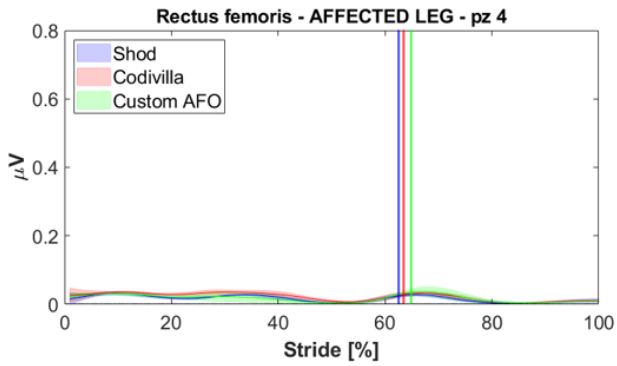
Rectus femoris - AFFECTED LEG - pz 4
μV
Stride [%]
Shod
Codivilla
Custom AFO

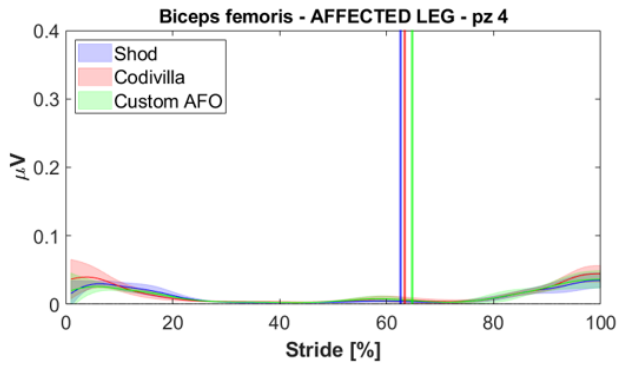
Biceps femoris - AFFECTED LEG - pz 4
μV
Stride [%]
Shod
Codivilla
Custom AFO

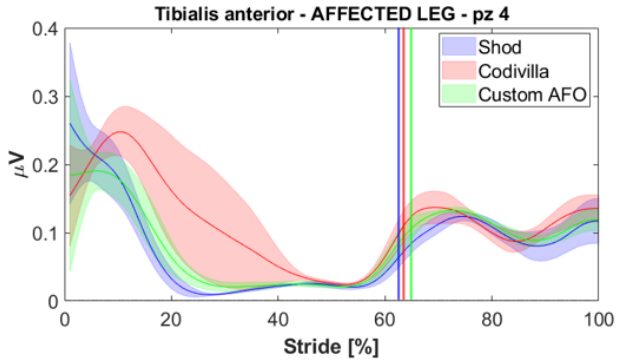
Tibialis anterior - AFFECTED LEG - pz 4
μV
Stride [%]
Shod
Codivilla
Custom AFO

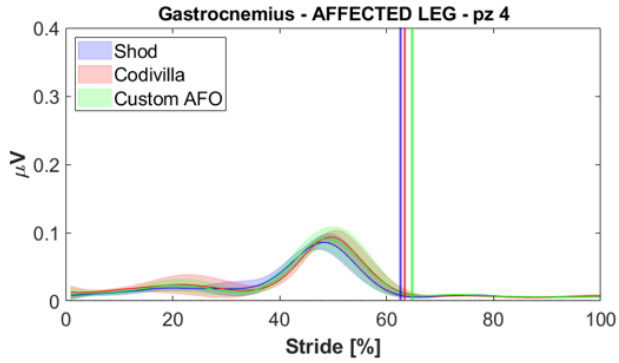
Gastrocnemius - AFFECTED LEG - pz 4
μV
Stride [%]
Shod
Codivilla
Custom AFO

Patient 5

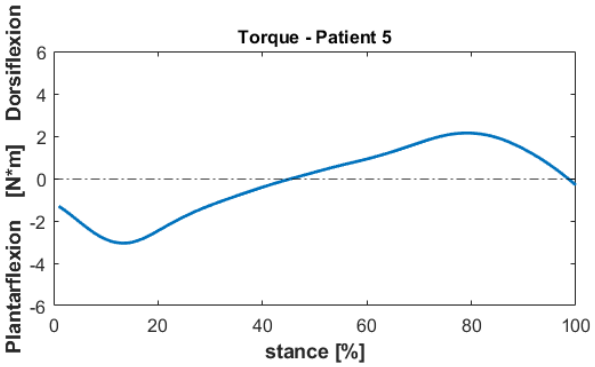

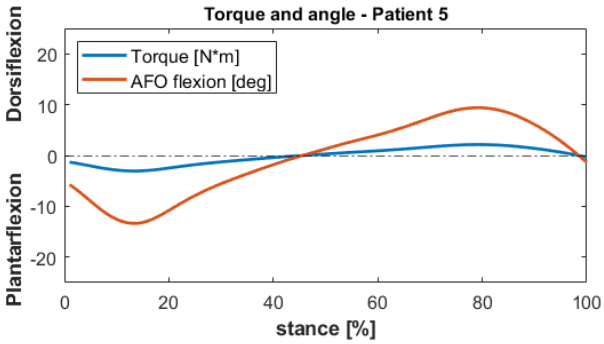

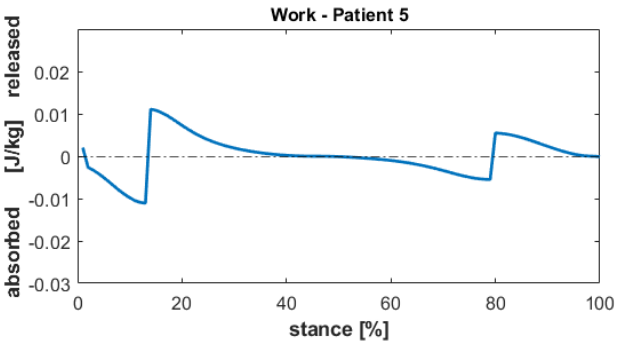

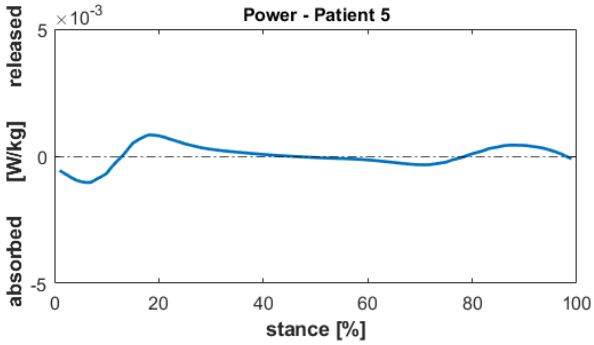

Patient 6

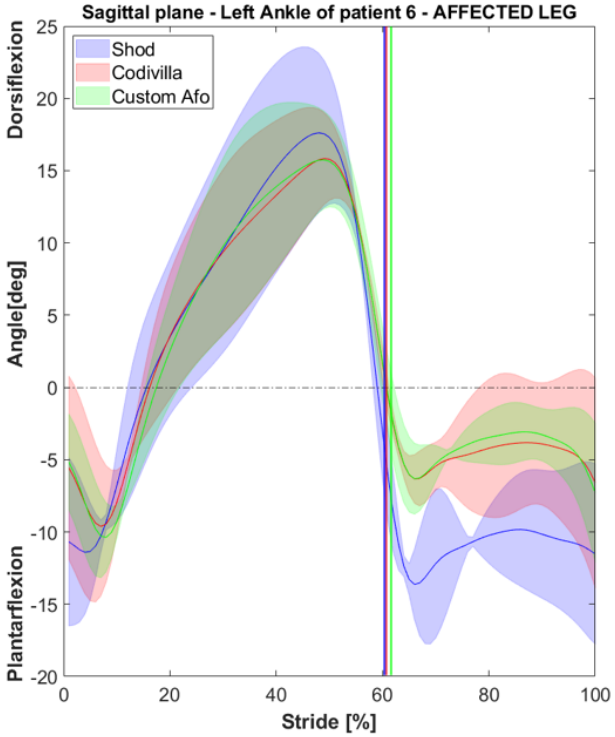

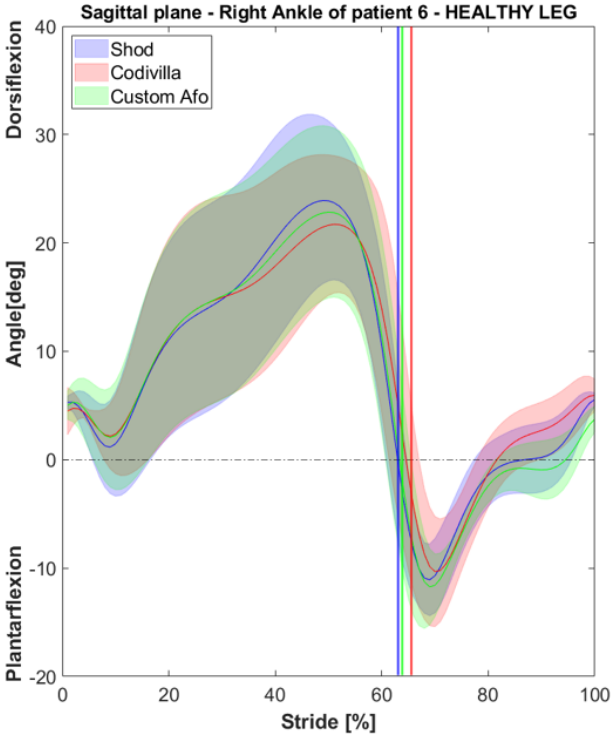

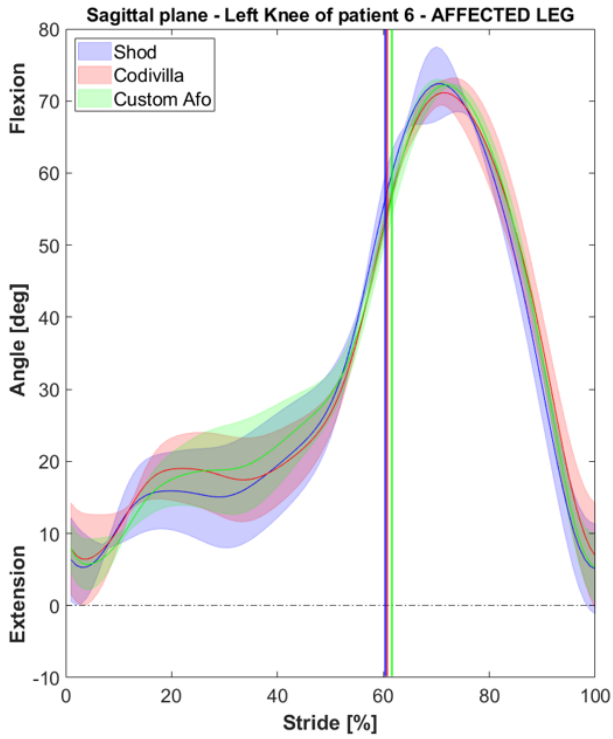
Sagittal plane - Left Knee of patient 6 - AFFECTED LEG
Shod
Codivilla
Custom Afo
Flexion
Extension
Angle [deg]
Stride [%]

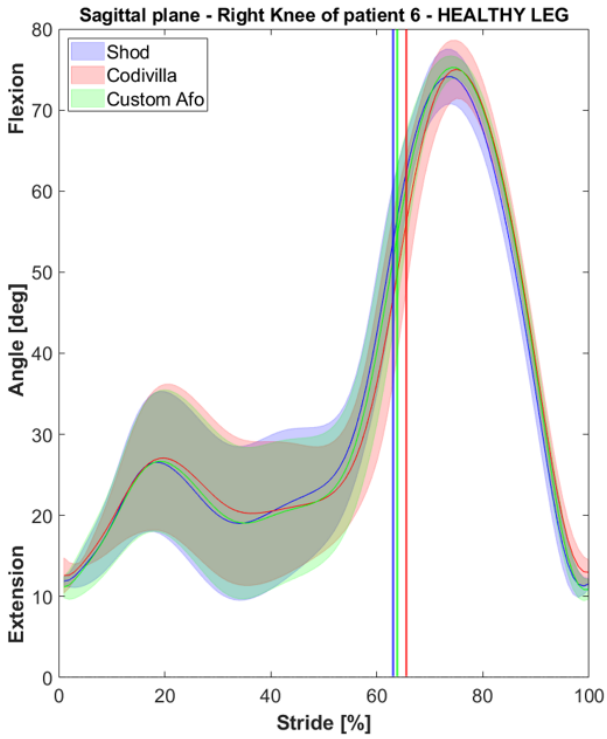
Sagittal plane - Right Knee of patient 6 - HEALTHY LEG
Shod
Codivilla
Custom Afo
Flexion
Extension
Angle [deg]
Stride [%]

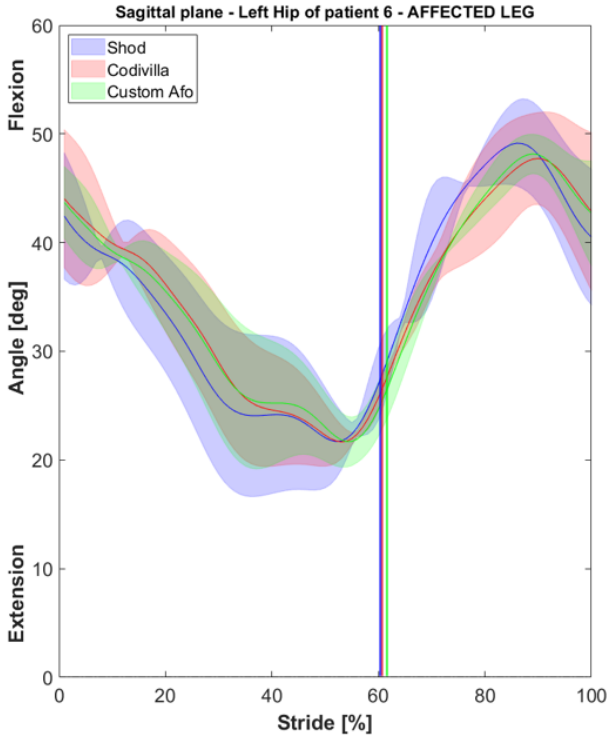
Sagittal plane - Left Hip of patient 6 - AFFECTED LEG
Shod
Codivilla
Custom Afo
Flexion
Extension
Angle [deg]
Stride [%]

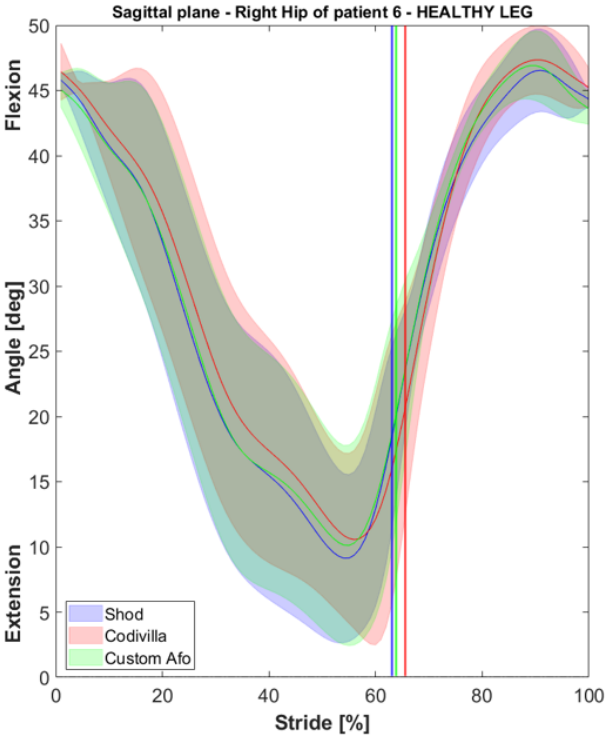
Sagittal plane - Right Hip of patient 6 - HEALTHY LEG
Shod
Codivilla
Custom Afo
Flexion
Extension
Angle [deg]
Stride [%]

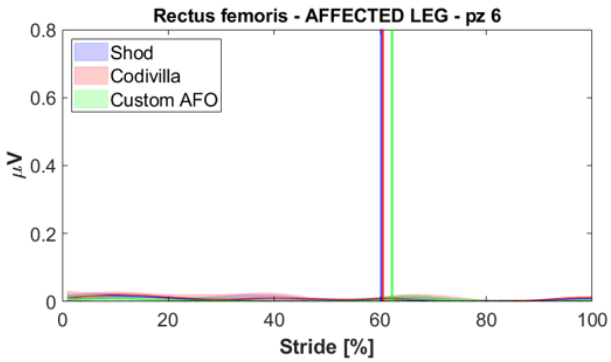
Rectus femoris - AFFECTED LEG - pz 6
Shod
Codivilla
Custom AFO
μV
Stride [%]

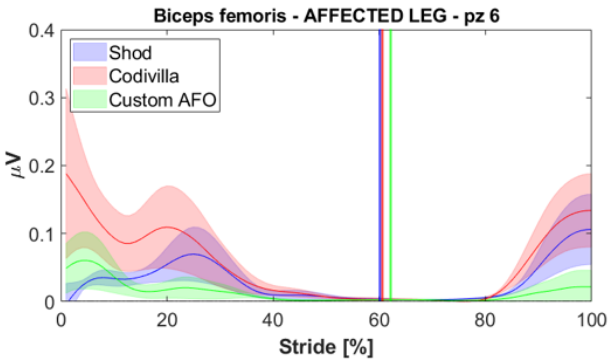
Biceps femoris - AFFECTED LEG - pz 6
Shod
Codivilla
Custom AFO
μV
Stride [%]

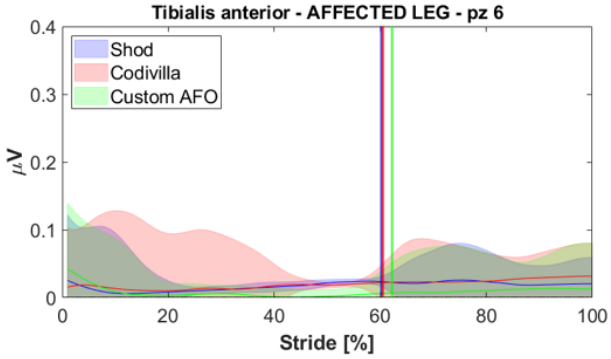
Tibialis anterior - AFFECTED LEG - pz 6
Shod
Codivilla
Custom AFO
μV
Stride [%]

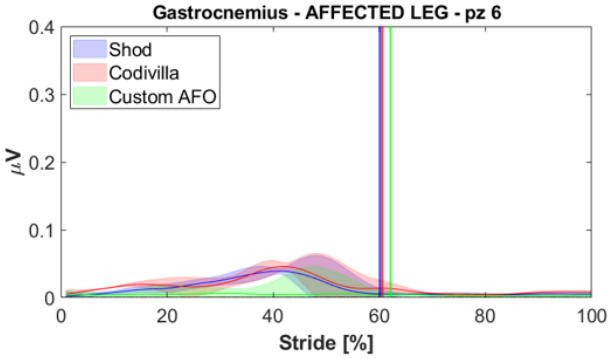
Gastrocnemius - AFFECTED LEG - pz 6
Shod
Codivilla
Custom AFO
μV
Stride [%]

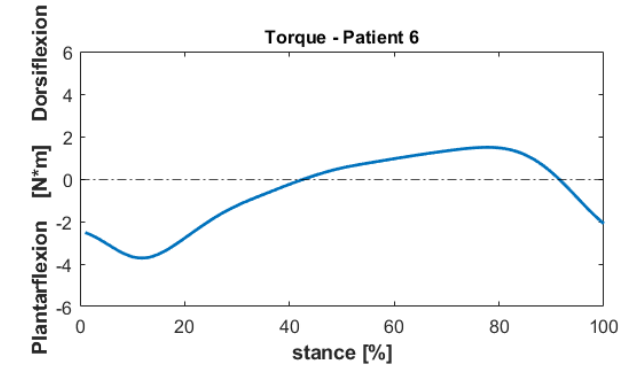
Torque - Patient 6
Dorsiflexion
[N*m]
Plantarflexion
stance [%]

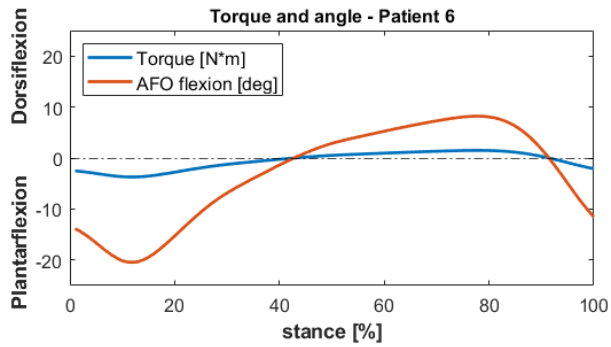
Torque and angle - Patient 6
Torque [N*m]
AFO flexion [deg]
Dorsiflexion
Plantarflexion
stance [%]

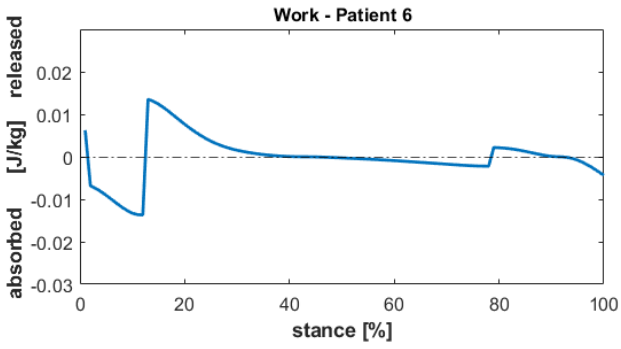
Work - Patient 6
released
[J/kg]
absorbed
stance [%]

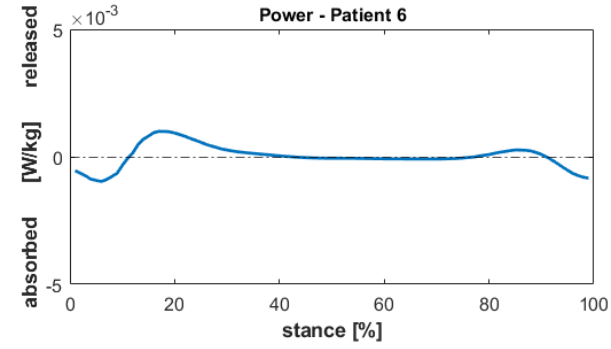
Power - Patient 6
released
[W/kg]
absorbed
stance [%]

Patient 8

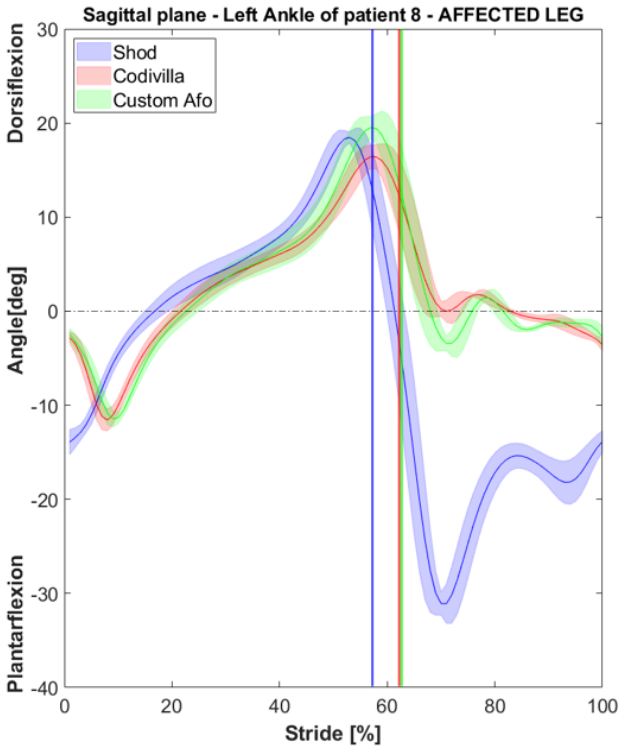
Sagittal plane - Left Ankle of patient 8 - AFFECTED LEG
Shod
Codivilla
Custom Afo
Dorsiflexion
Plantarflexion
Angle[deg]
Stride [%]

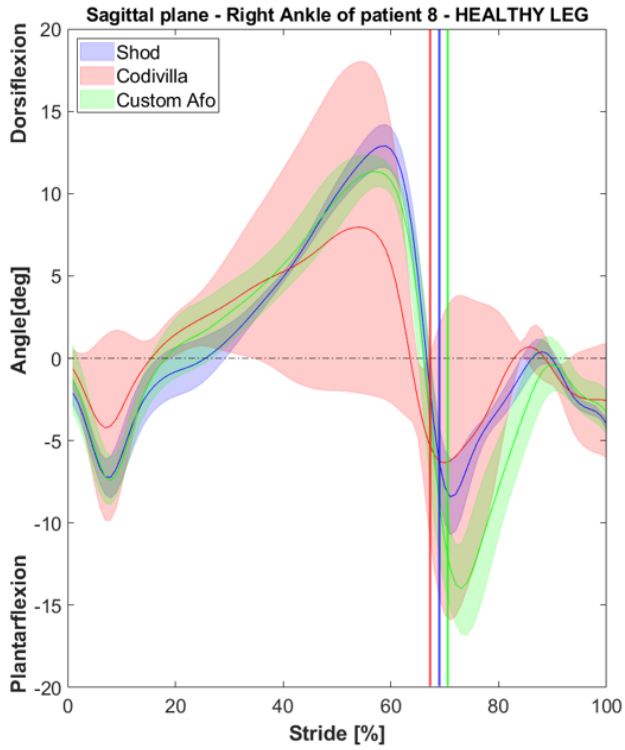
Sagittal plane - Right Ankle of patient 8 - HEALTHY LEG
Shod
Codivilla
Custom Afo
Dorsiflexion
Plantarflexion
Angle[deg]
Stride [%]

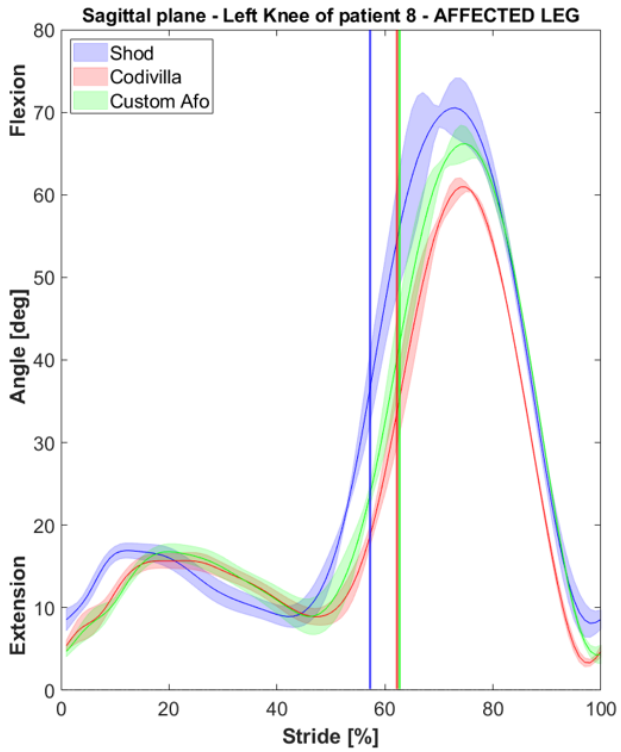
Sagittal plane - Left Knee of patient 8 - AFFECTED LEG
Shod
Codivilla
Custom Afo
Flexion
Extension
Angle [deg]
Stride [%]

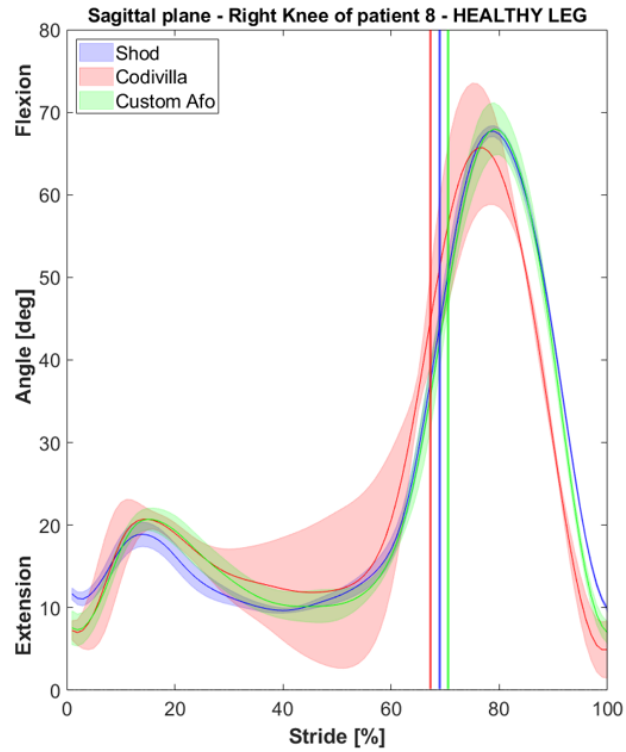
Sagittal plane - Right Knee of patient 8 - HEALTHY LEG
Shod
Codivilla
Custom Afo
Flexion
Extension
Angle [deg]
Stride [%]

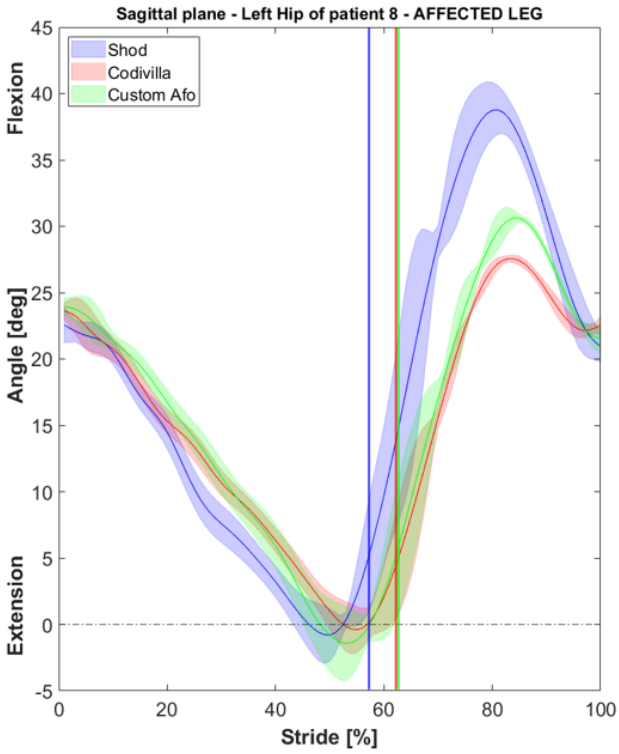
Sagittal plane - Left Hip of patient 8 - AFFECTED LEG
Shod
Codivilla
Custom Afo
Flexion
Extension
Angle [deg]
Stride [%]

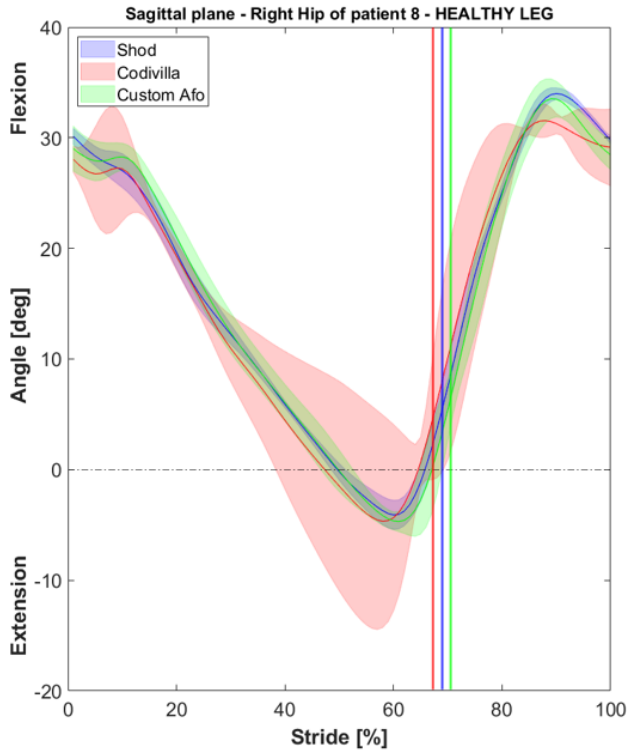
Sagittal plane - Right Hip of patient 8 - HEALTHY LEG
Shod
Codivilla
Custom Afo
Flexion
Extension
Angle [deg]
Stride [%]

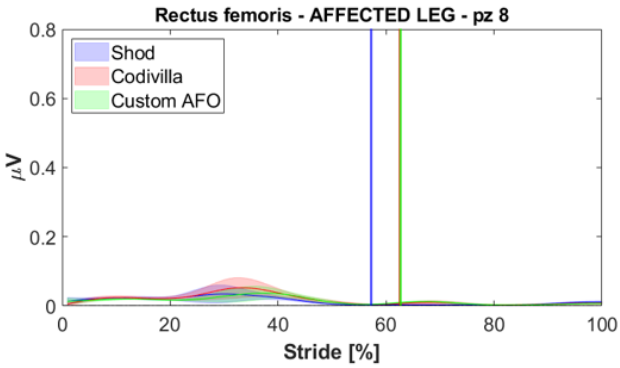
Rectus femoris - AFFECTED LEG - pz 8
Shod
Codivilla
Custom AFO
μV
Stride [%]

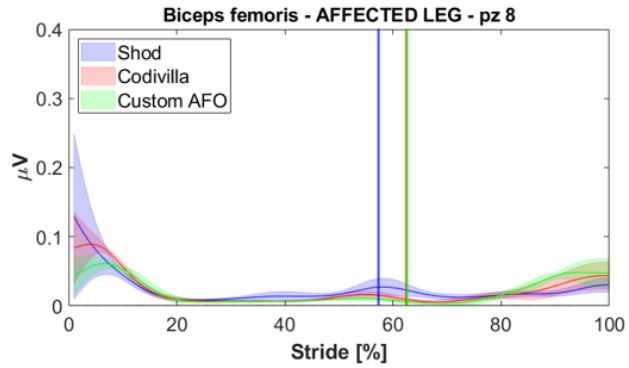
Biceps femoris - AFFECTED LEG - pz 8
Shod
Codivilla
Custom AFO
μV
Stride [%]

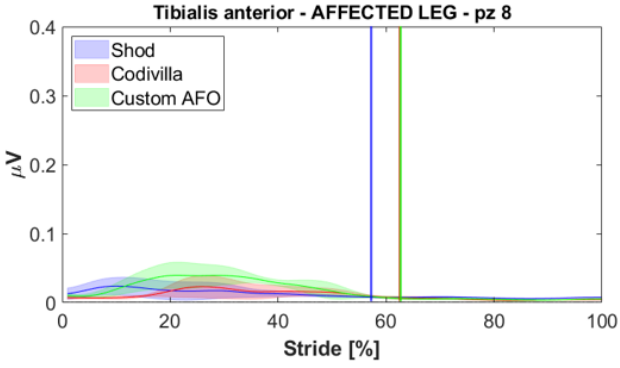
Tibialis anterior - AFFECTED LEG - pz 8
Shod
Codivilla
Custom AFO
μV
Stride [%]

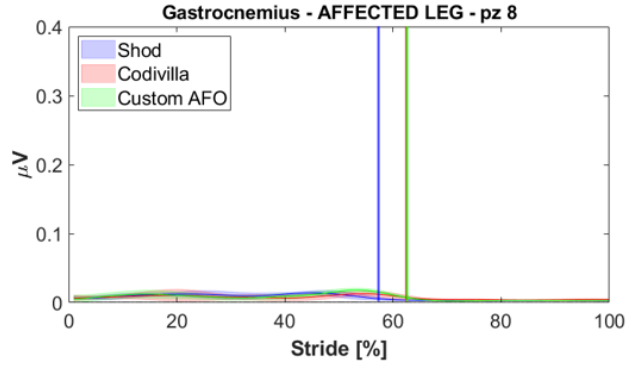
Gastrocnemius - AFFECTED LEG - pz 8
Shod
Codivilla
Custom AFO
μV
Stride [%]

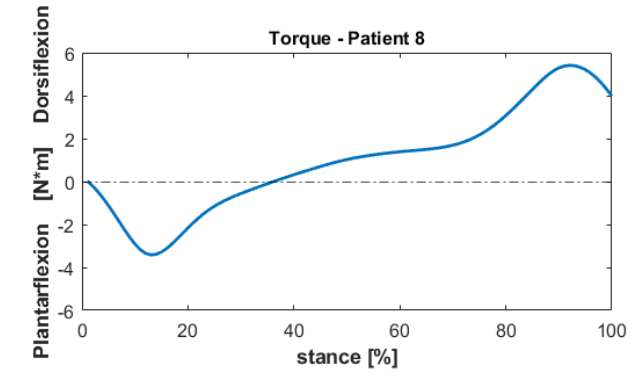
Torque - Patient 8
Dorsiflexion
Plantarflexion
[N*m]
stance [%]

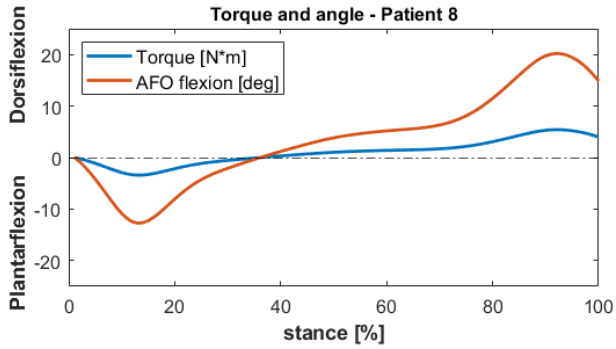
Torque and angle - Patient 8
Torque [N*m]
AFO flexion [deg]
Dorsiflexion
Plantarflexion
stance [%]

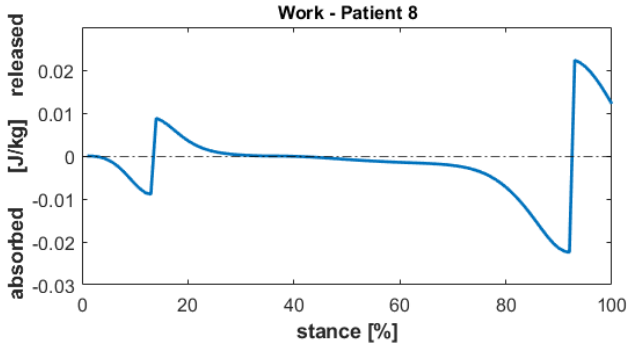
Work - Patient 8
released
absorbed
[J/kg]
stance [%]

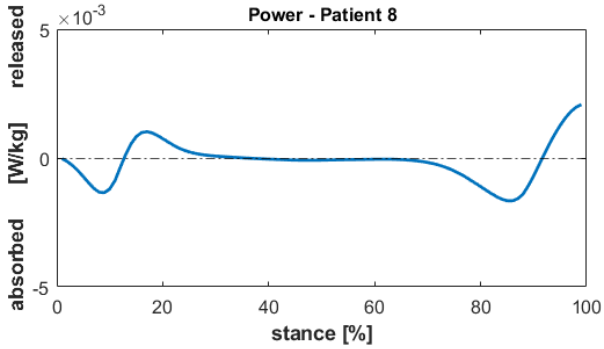
Power - Patient 8
released
absorbed
[W/kg]
stance [%]

Patient 9

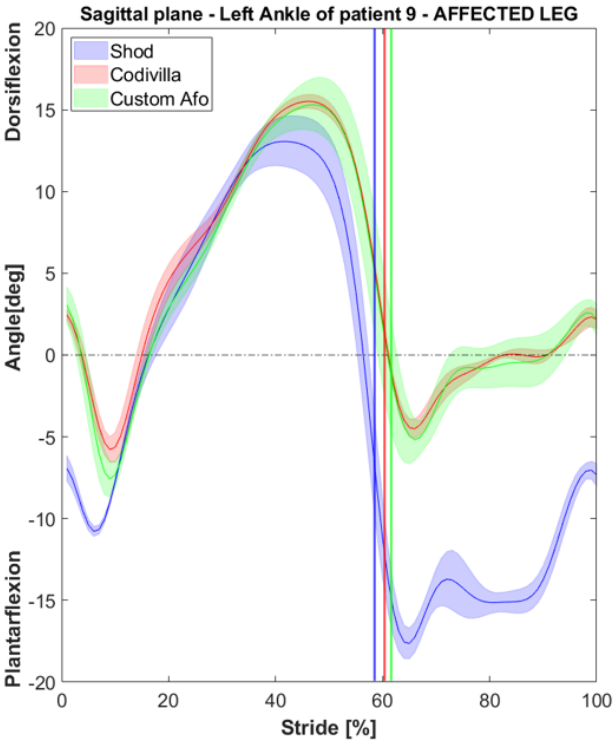
Sagittal plane - Left Ankle of patient 9 - AFFECTED LEG
Shod
Codivilla
Custom Afo
Dorsiflexion
Plantarflexion
Angle[deg]
Stride [%]

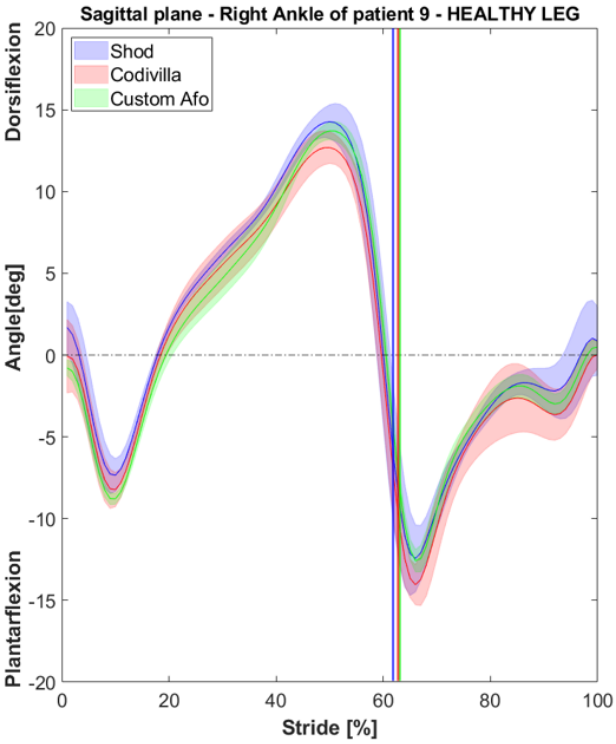
Sagittal plane - Right Ankle of patient 9 - HEALTHY LEG
Shod
Codivilla
Custom Afo
Dorsiflexion
Plantarflexion
Angle[deg]
Stride [%]

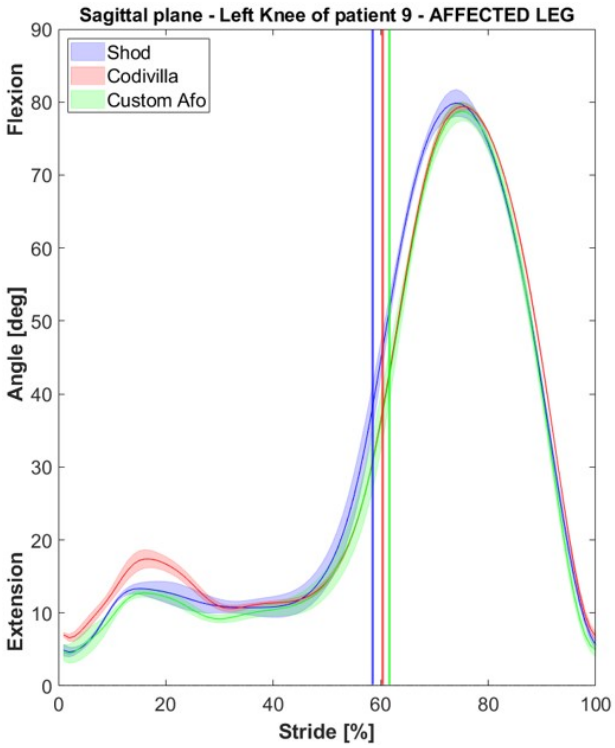
Sagittal plane - Left Knee of patient 9 - AFFECTED LEG
Shod
Codivilla
Custom Afo
Flexion
Extension
Angle [deg]
Stride [%]

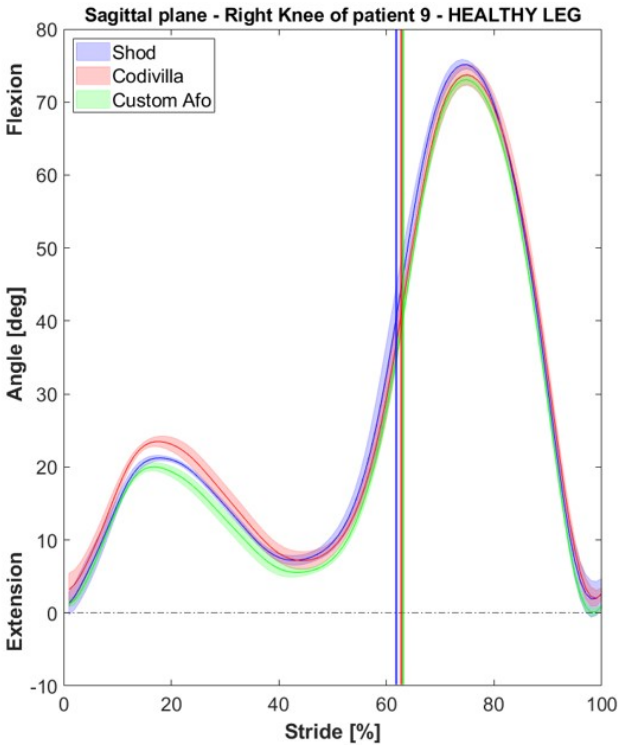
Sagittal plane - Right Knee of patient 9 - HEALTHY LEG
Shod
Codivilla
Custom Afo
Flexion
Extension
Angle [deg]
Stride [%]

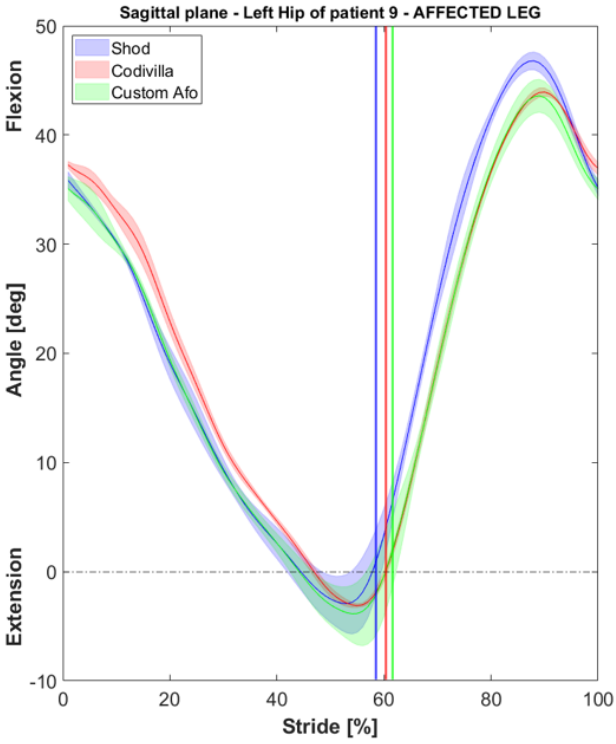
Sagittal plane - Left Hip of patient 9 - AFFECTED LEG
Shod
Codivilla
Custom Afo
Flexion
Extension
Angle [deg]
Stride [%]

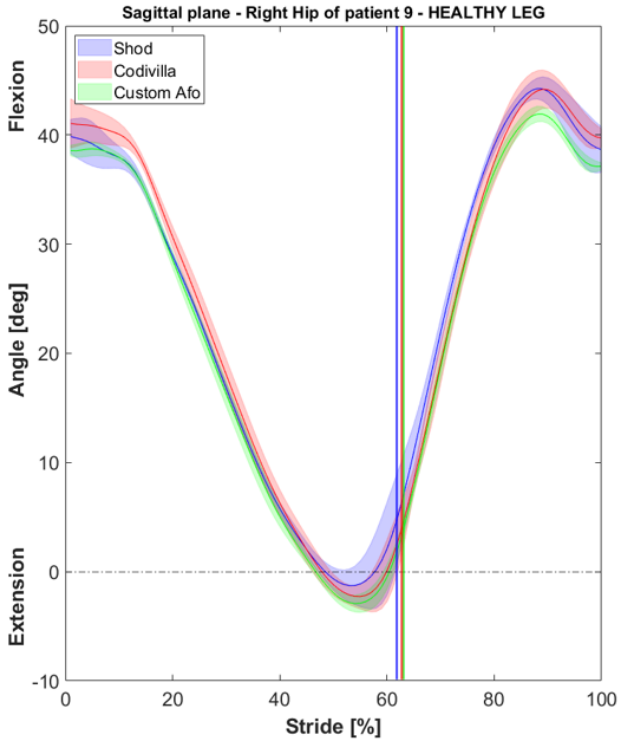
Sagittal plane - Right Hip of patient 9 - HEALTHY LEG
Shod
Codivilla
Custom Afo
Flexion
Extension
Angle [deg]
Stride [%]

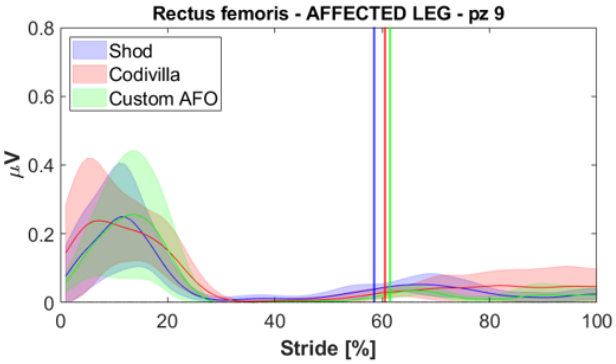
Rectus femoris - AFFECTED LEG - pz 9
Shod
Codivilla
Custom AFO
μV
Stride [%]

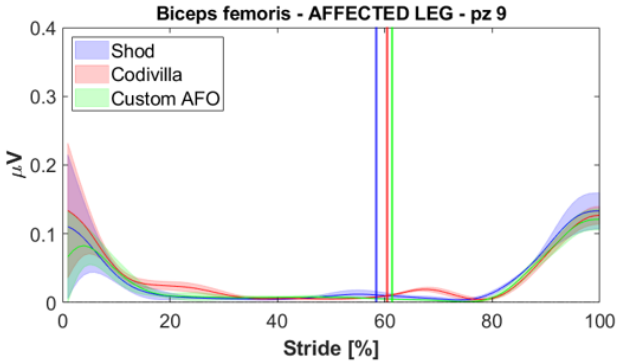
Biceps femoris - AFFECTED LEG - pz 9
Shod
Codivilla
Custom AFO
μV
Stride [%]

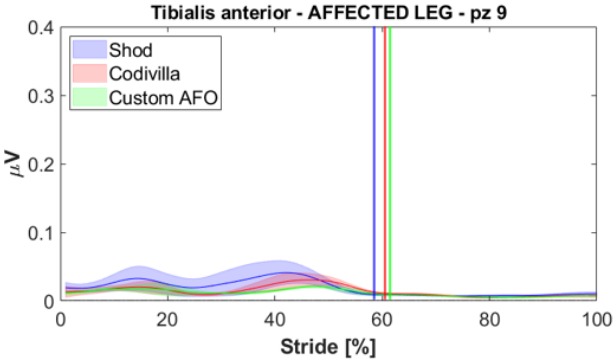
Tibialis anterior - AFFECTED LEG - pz 9
Shod
Codivilla
Custom AFO
μV
Stride [%]

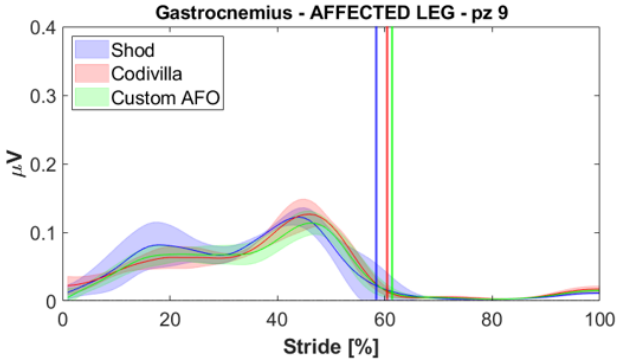
Gastrocnemius - AFFECTED LEG - pz 9
Shod
Codivilla
Custom AFO
μV
Stride [%]

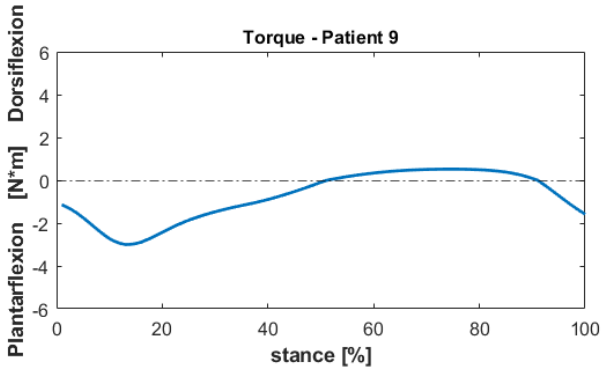
Torque - Patient 9
Dorsiflexion
Plantarflexion
[N*m]
stance [%]

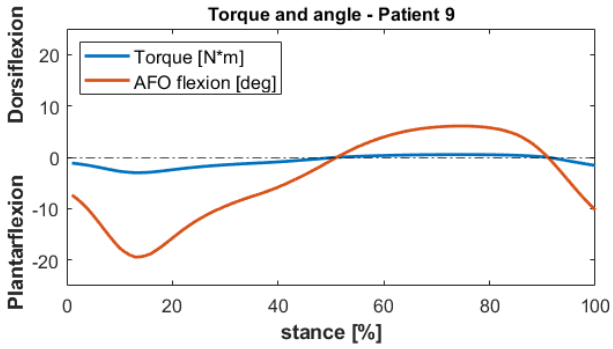
Torque and angle - Patient 9
Torque [N*m]
AFO flexion [deg]
Dorsiflexion
Plantarflexion
stance [%]

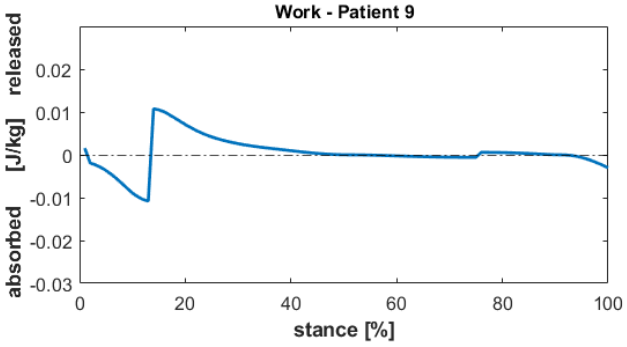
Work - Patient 9
released
absorbed
[J/kg]
stance [%]

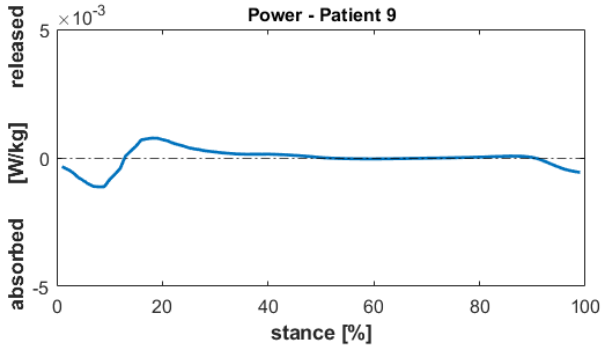
Power - Patient 9
released
absorbed
[W/kg]
stance [%]

Patient 10

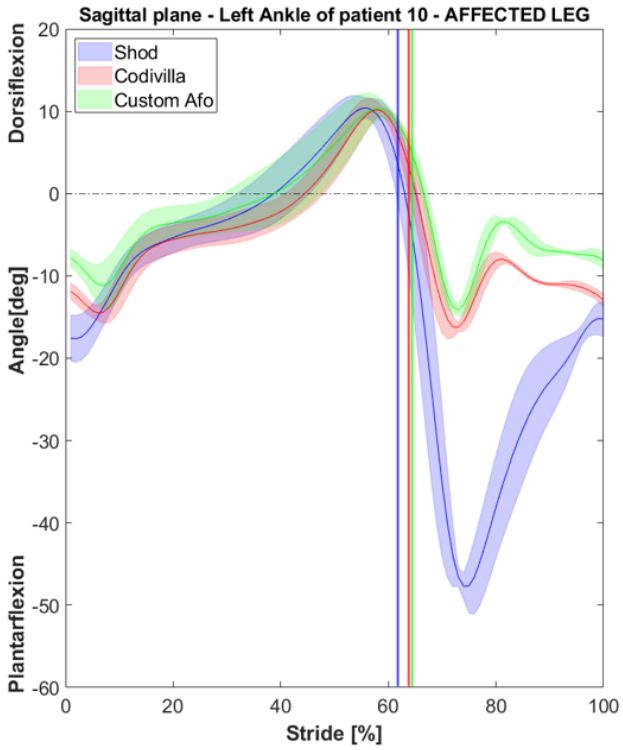
Sagittal plane - Left Ankle of patient 10 - AFFECTED LEG
Shod
Codivilla
Custom Afo
Dorsiflexion
Plantarflexion
Angle[deg]
Stride [%]

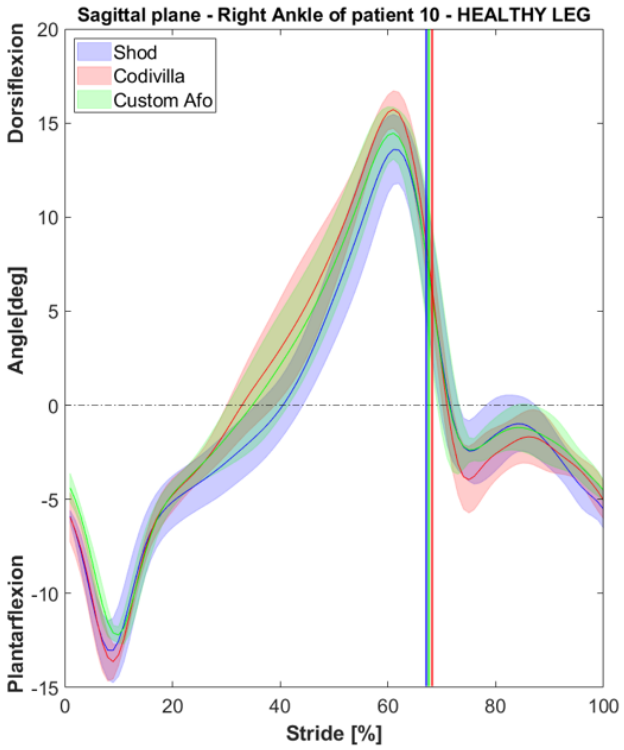
Sagittal plane - Right Ankle of patient 10 - HEALTHY LEG
Shod
Codivilla
Custom Afo
Dorsiflexion
Plantarflexion
Angle[deg]
Stride [%]

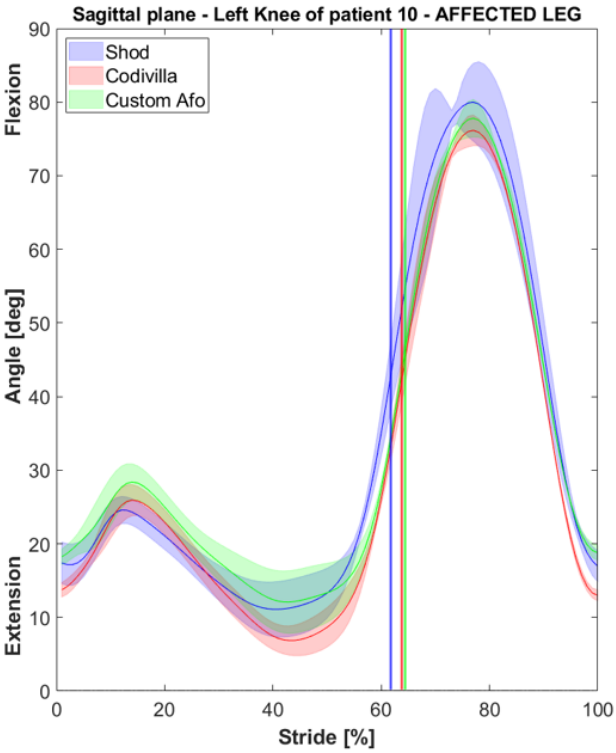
Sagittal plane - Left Knee of patient 10 - AFFECTED LEG
Shod
Codivilla
Custom Afo
Flexion
Extension
Angle [deg]
Stride [%]

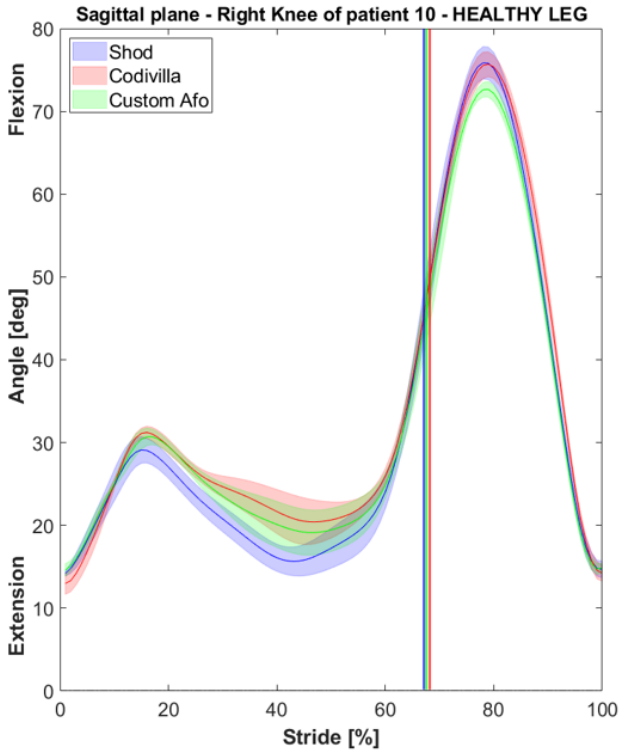
Sagittal plane - Right Knee of patient 10 - HEALTHY LEG
Shod
Codivilla
Custom Afo
Flexion
Extension
Angle [deg]
Stride [%]

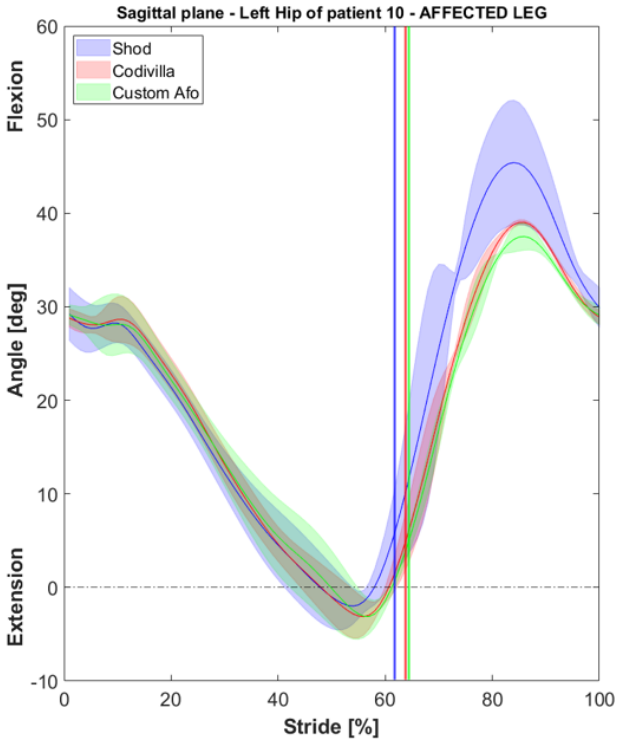
Sagittal plane - Left Hip of patient 10 - AFFECTED LEG
Shod
Codivilla
Custom Afo
Flexion
Extension
Angle [deg]
Stride [%]

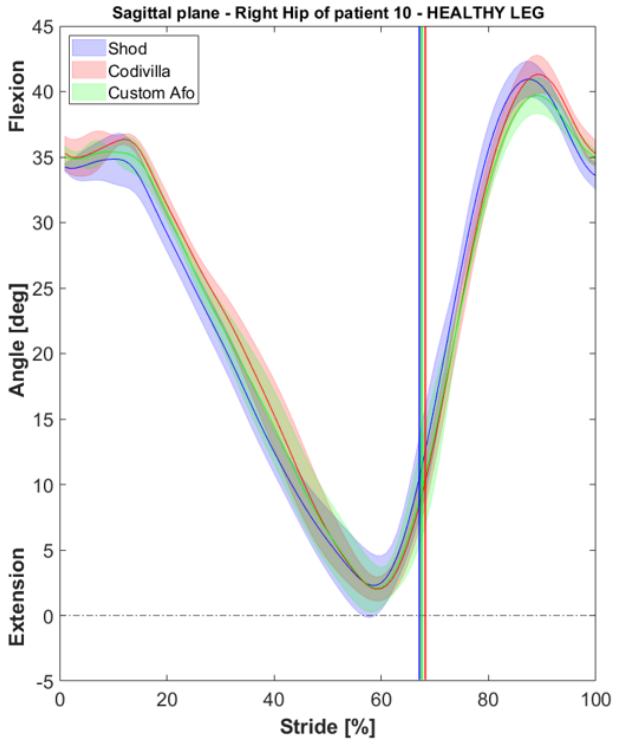
Sagittal plane - Right Hip of patient 10 - HEALTHY LEG
Shod
Codivilla
Custom Afo
Flexion
Extension
Angle [deg]
Stride [%]

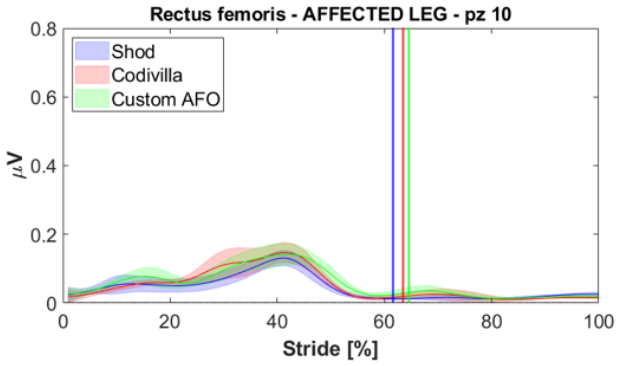
Rectus femoris - AFFECTED LEG - pz 10
Shod
Codivilla
Custom AFO
μV
Stride [%]

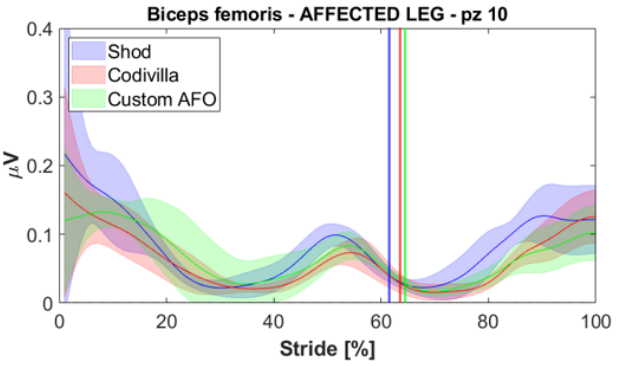
Biceps femoris - AFFECTED LEG - pz 10
Shod
Codivilla
Custom AFO
μV
Stride [%]

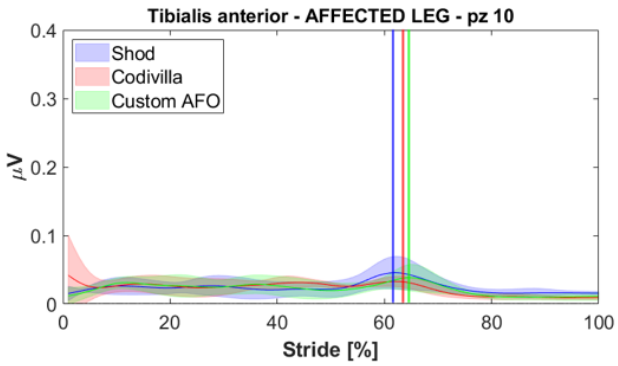
Tibialis anterior - AFFECTED LEG - pz 10
Shod
Codivilla
Custom AFO
μV
Stride [%]

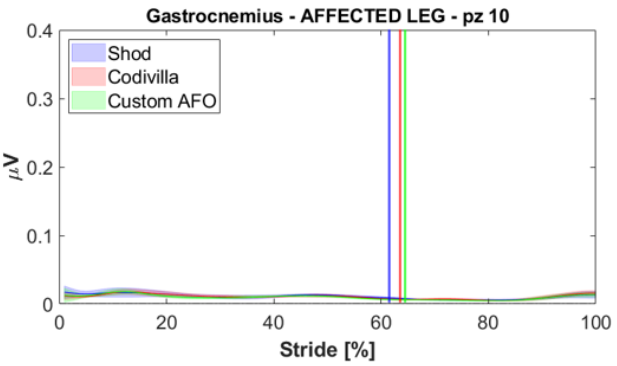
Gastrocnemius - AFFECTED LEG - pz 10
Shod
Codivilla
Custom AFO
μV
Stride [%]

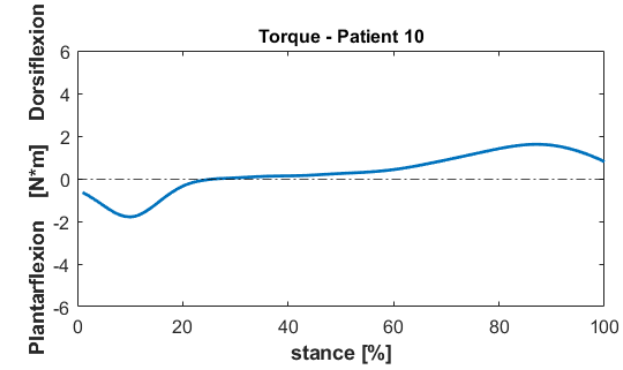
Torque - Patient 10
Dorsiflexion
Plantarflexion
[N*m]
stance [%]

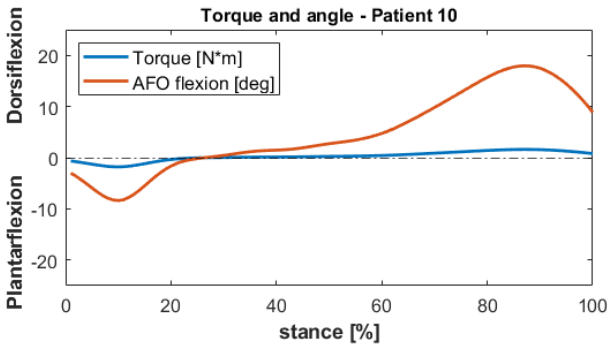
Torque and angle - Patient 10
Torque [N*m]
AFO flexion [deg]
Dorsiflexion
Plantarflexion
stance [%]

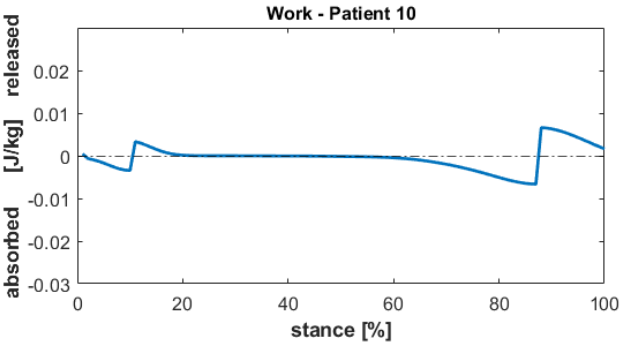
Work - Patient 10
released
absorbed
[J/kg]
stance [%]

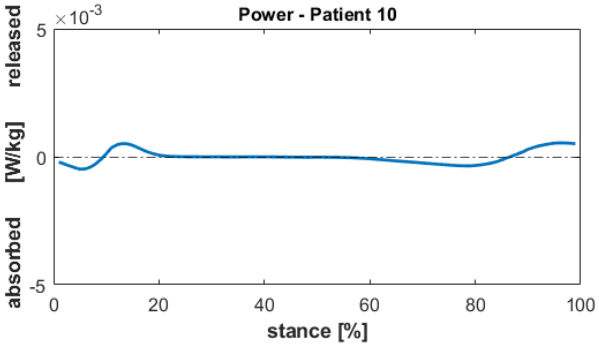
Power - Patient 10
released
absorbed
[W/kg]
stance [%]

Patient 11

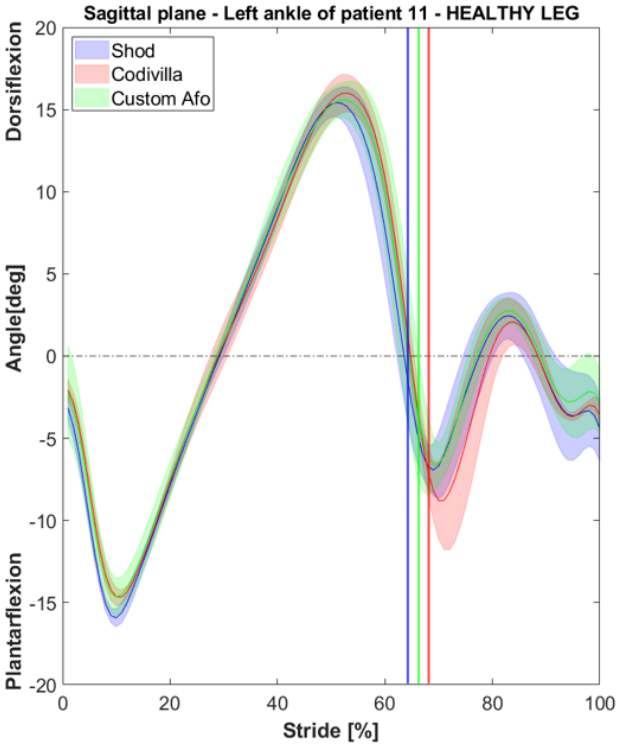
Sagittal plane - Left ankle of patient 11 - HEALTHY LEG
Shod
Codivilla
Custom Afo
Dorsiflexion
Plantarflexion
Angle[deg]
Stride [%]

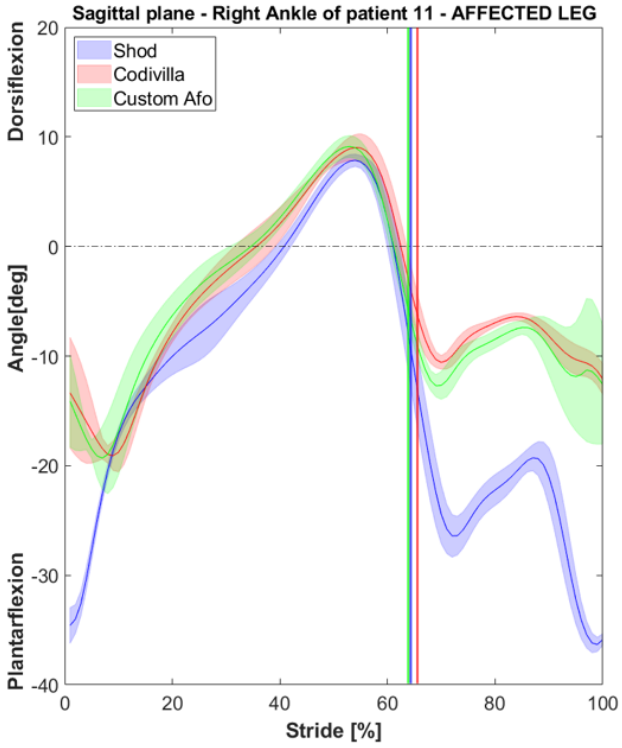
Sagittal plane - Right Ankle of patient 11 - AFFECTED LEG
Shod
Codivilla
Custom Afo
Dorsiflexion
Plantarflexion
Angle[deg]
Stride [%]

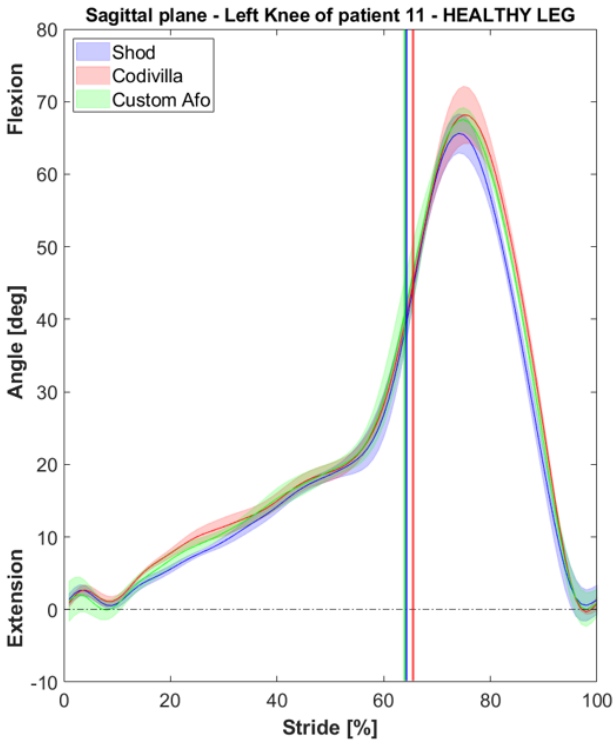
Sagittal plane - Left Knee of patient 11 - HEALTHY LEG
Shod
Codivilla
Custom Afo
Flexion
Extension
Angle [deg]
Stride [%]

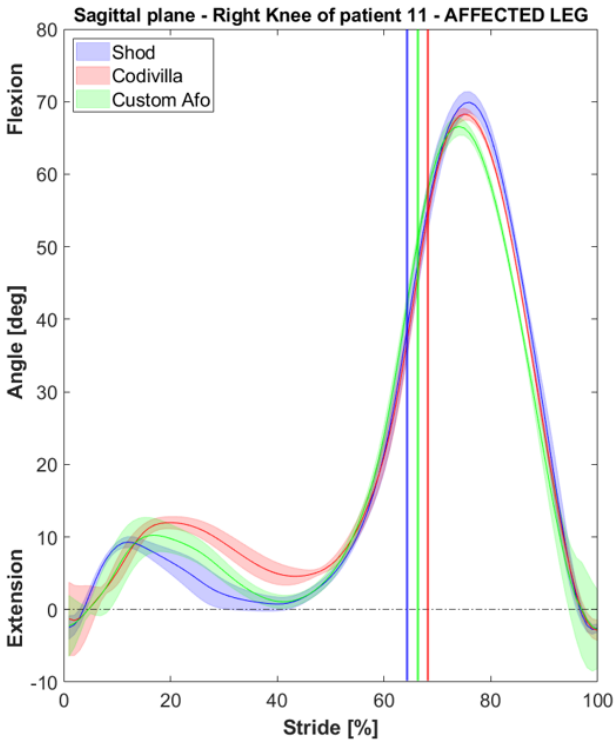
Sagittal plane - Right Knee of patient 11 - AFFECTED LEG
Shod
Codivilla
Custom Afo
Flexion
Extension
Angle [deg]
Stride [%]

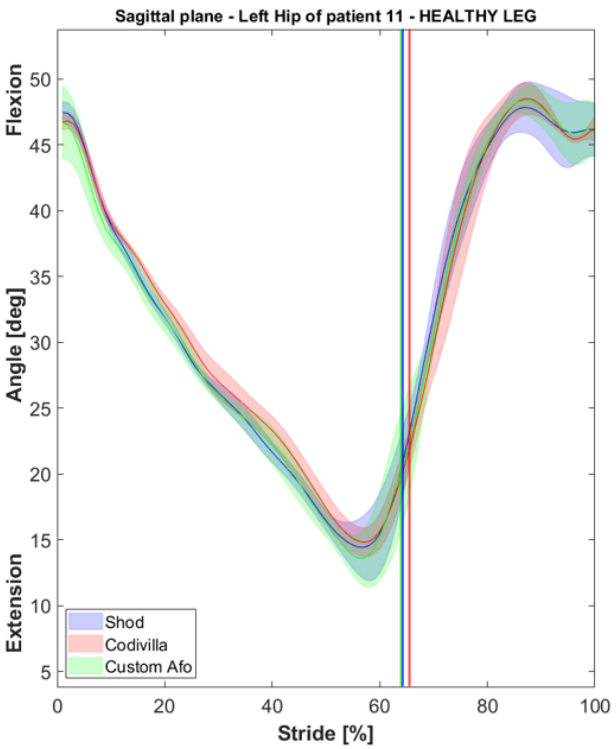
Sagittal plane - Left Hip of patient 11 - HEALTHY LEG
Shod
Codivilla
Custom Afo
Flexion
Extension
Angle [deg]
Stride [%]

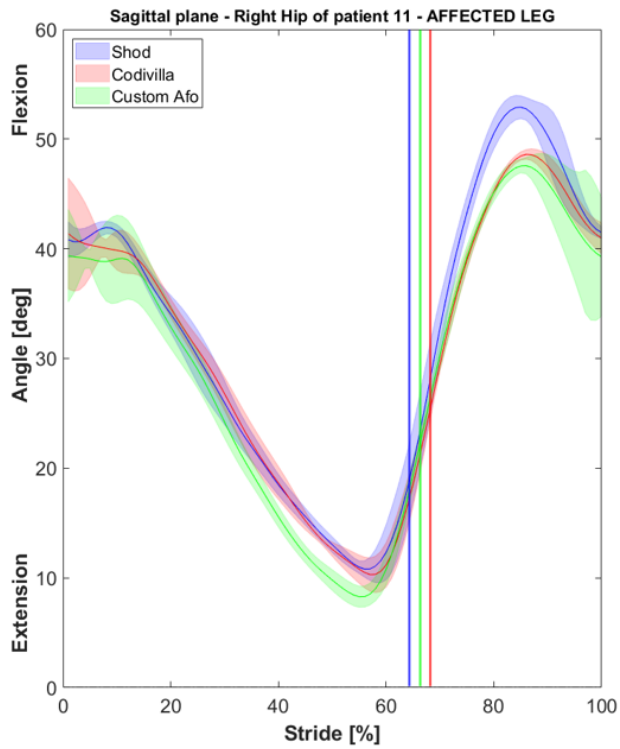
Sagittal plane - Right Hip of patient 11 - AFFECTED LEG
Shod
Codivilla
Custom Afo
Flexion
Extension
Angle [deg]
Stride [%]

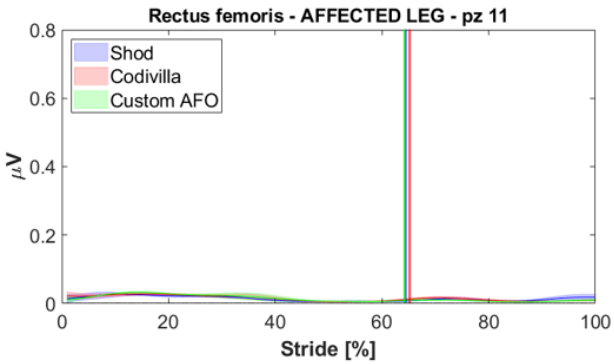
Rectus femoris - AFFECTED LEG - pz 11
Shod
Codivilla
Custom AFO
μV
Stride [%]

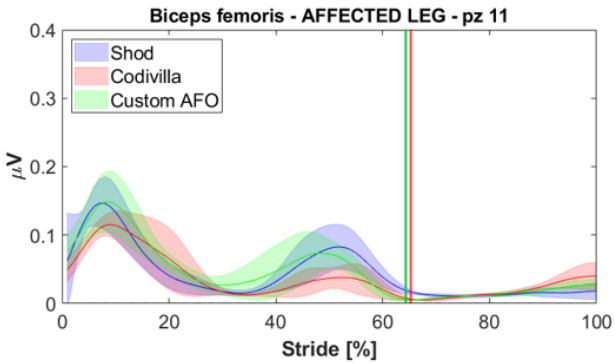
Biceps femoris - AFFECTED LEG - pz 11
Shod
Codivilla
Custom AFO
μV
Stride [%]

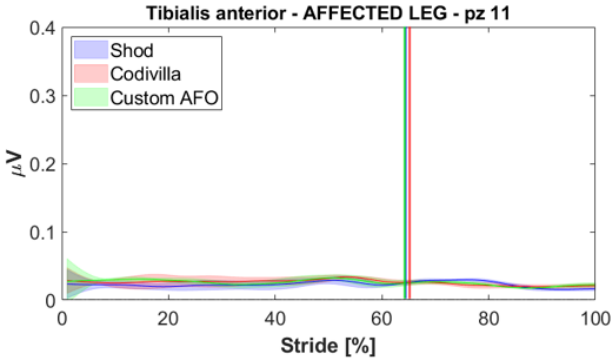
Tibialis anterior - AFFECTED LEG - pz 11
Shod
Codivilla
Custom AFO
μV
Stride [%]

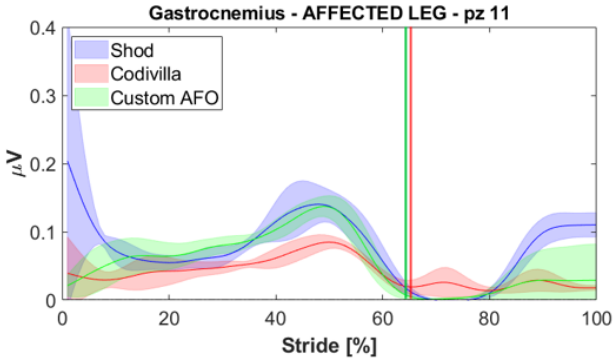
Gastrocnemius - AFFECTED LEG - pz 11
Shod
Codivilla
Custom AFO
μV
Stride [%]

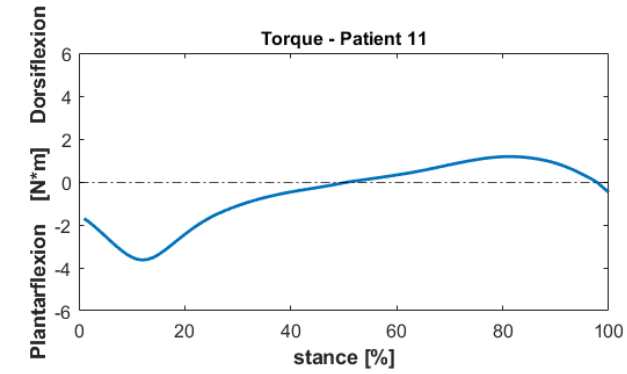
Torque - Patient 11
Dorsiflexion
[N*m]
Plantarflexion
stance [%]

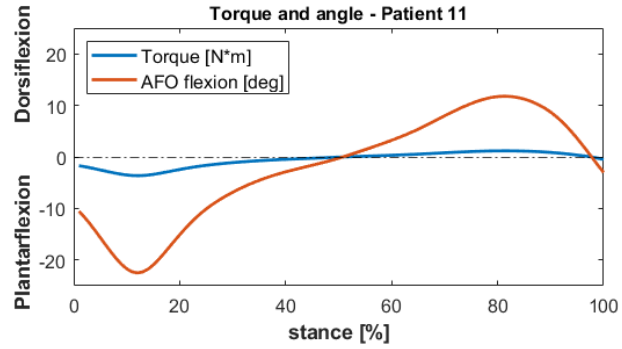
Torque and angle - Patient 11
Torque [N*m]
AFO flexion [deg]
Dorsiflexion
Plantarflexion
stance [%]

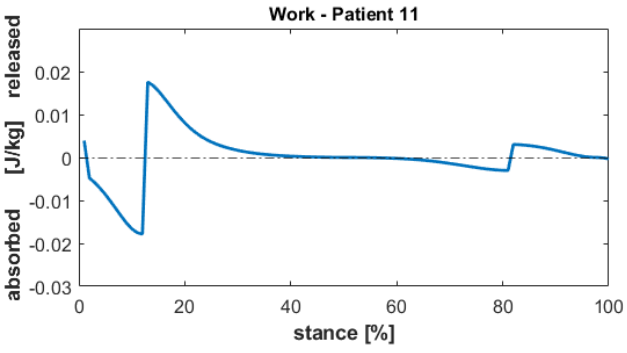
Work - Patient 11
released
[J/kg]
absorbed
stance [%]

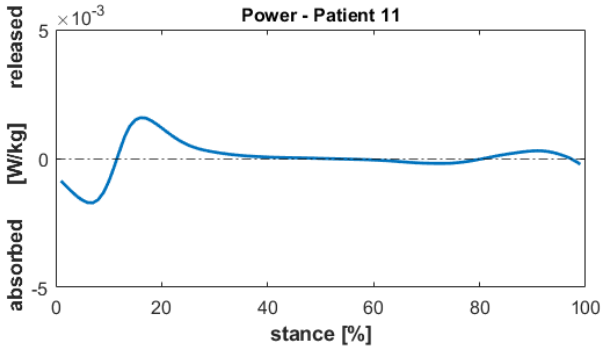
Power - Patient 11
released
[W/kg]
absorbed
stance [%]

Patient 14

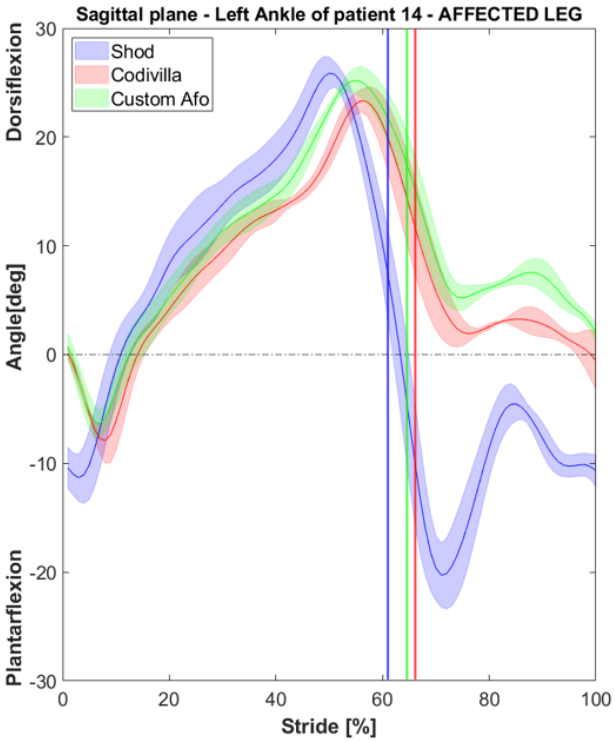
Sagittal plane - Left Ankle of patient 14 - AFFECTED LEG
Shod
Codivilla
Custom Afo
Dorsiflexion
Plantarflexion
Angle[deg]
Stride [%]

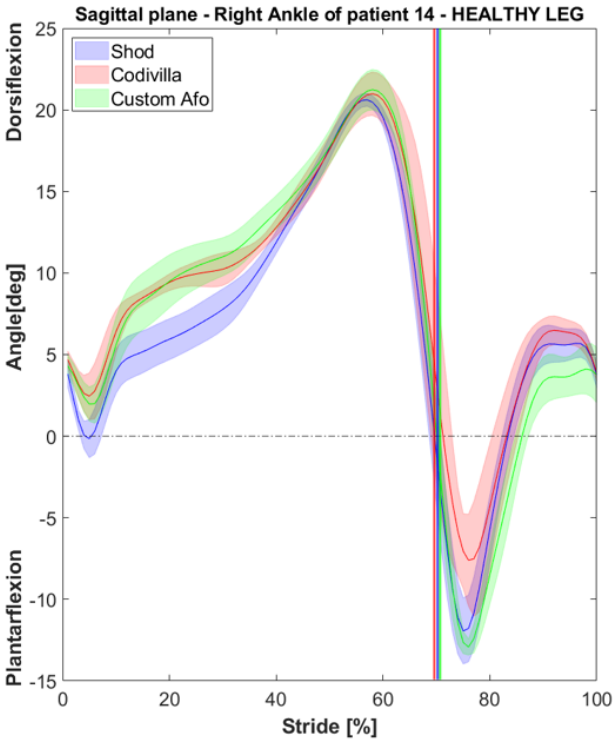
Sagittal plane - Right Ankle of patient 14 - HEALTHY LEG
Shod
Codivilla
Custom Afo
Dorsiflexion
Plantarflexion
Angle[deg]
Stride [%]

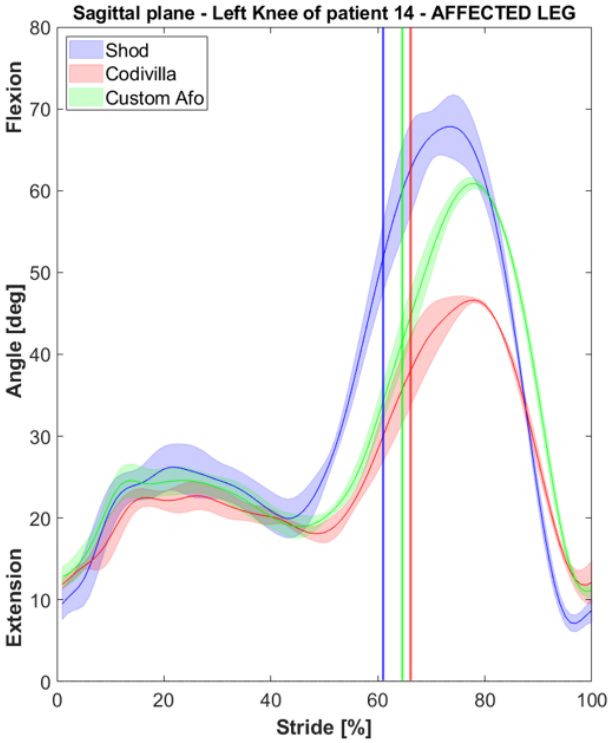
Sagittal plane - Left Knee of patient 14 - AFFECTED LEG
Shod
Codivilla
Custom Afo
Flexion
Extension
Angle [deg]
Stride [%]

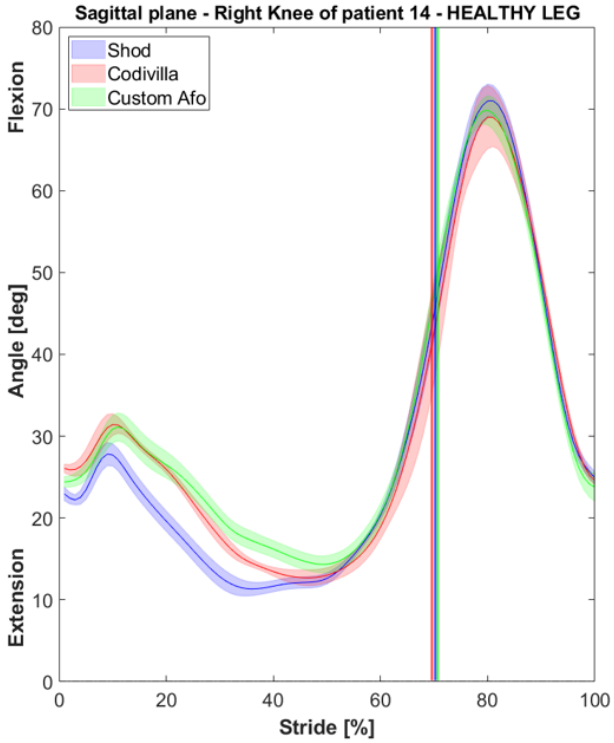
Sagittal plane - Right Knee of patient 14 - HEALTHY LEG
Shod
Codivilla
Custom Afo
Flexion
Extension
Angle [deg]
Stride [%]

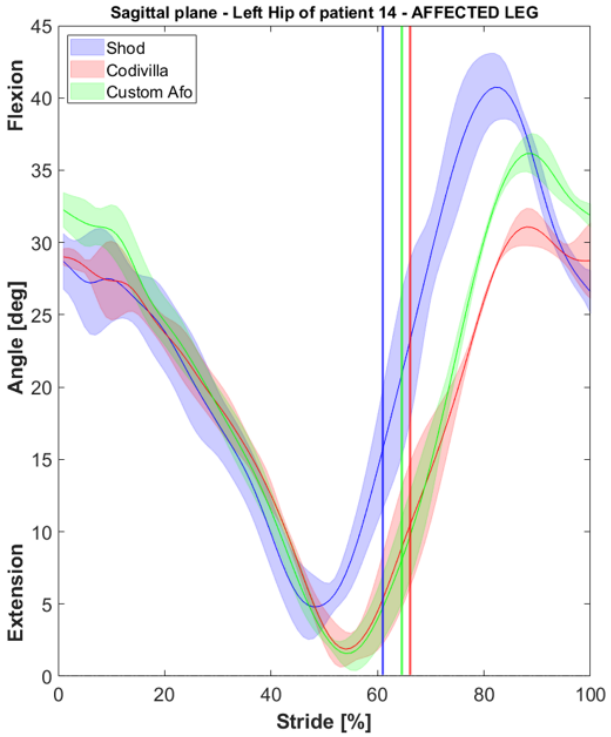
Sagittal plane - Left Hip of patient 14 - AFFECTED LEG
Shod
Codivilla
Custom Afo
Flexion
Extension
Angle [deg]
Stride [%]

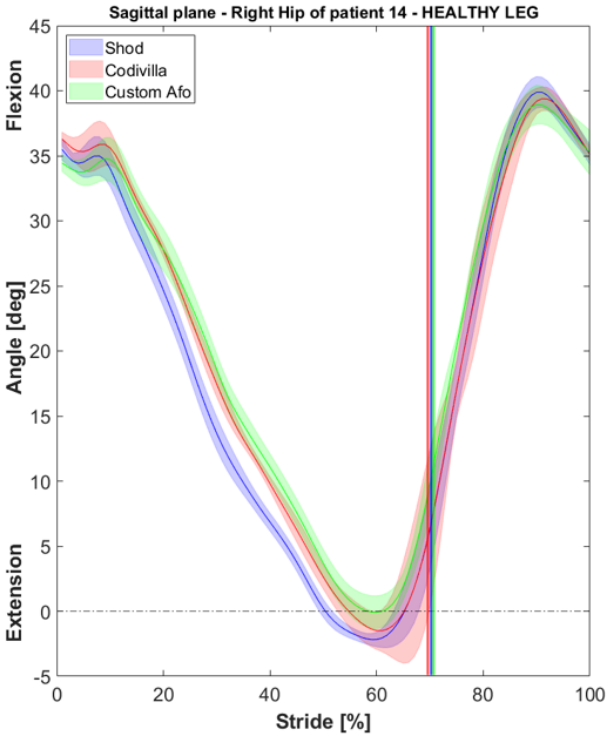
Sagittal plane - Right Hip of patient 14 - HEALTHY LEG
Shod
Codivilla
Custom Afo
Flexion
Extension
Angle [deg]
Stride [%]

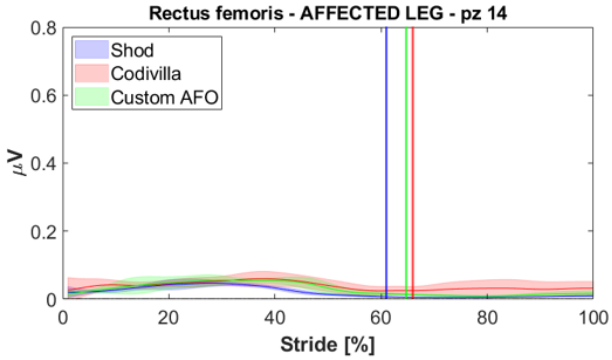
Rectus femoris - AFFECTED LEG - pz 14
Shod
Codivilla
Custom AFO
μV
Stride [%]

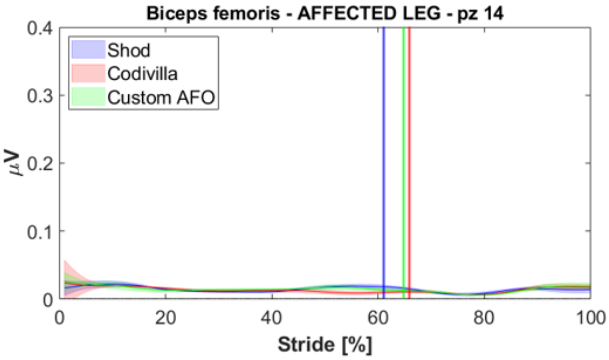
Biceps femoris - AFFECTED LEG - pz 14
Shod
Codivilla
Custom AFO
μV
Stride [%]

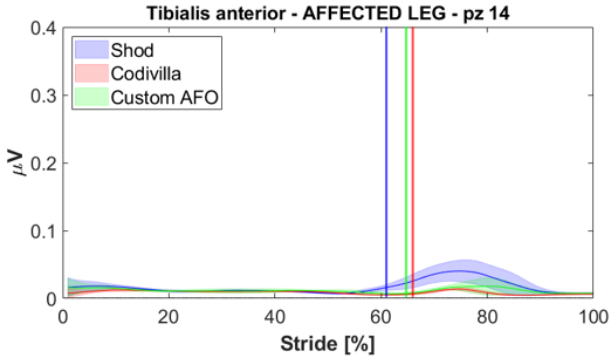
Tibialis anterior - AFFECTED LEG - pz 14
Shod
Codivilla
Custom AFO
μV
Stride [%]

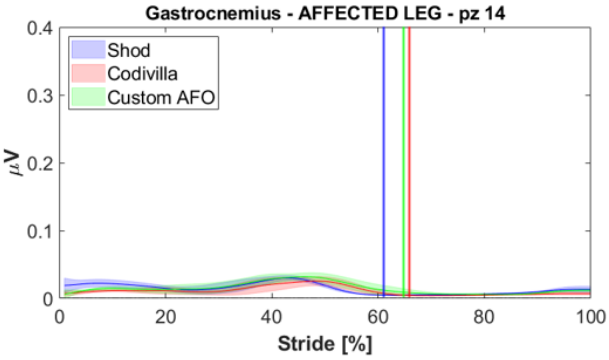
Gastrocnemius - AFFECTED LEG - pz 14
Shod
Codivilla
Custom AFO
μV
Stride [%]

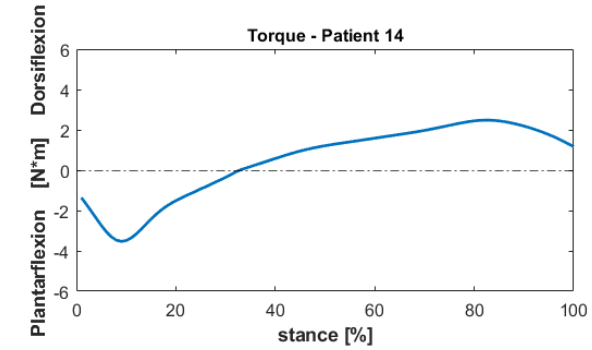
Torque - Patient 14
Dorsiflexion
[N*m]
Plantarflexion
stance [%]

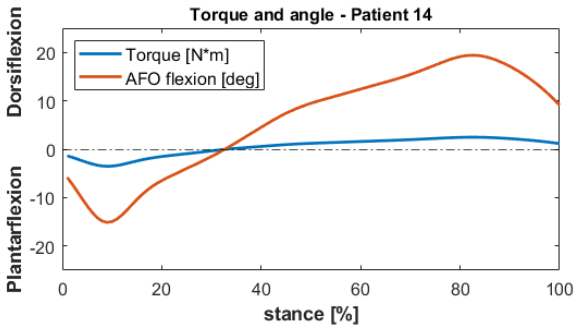
Torque and angle - Patient 14
Torque [N*m]
AFO flexion [deg]
Dorsiflexion
Plantarflexion
stance [%]

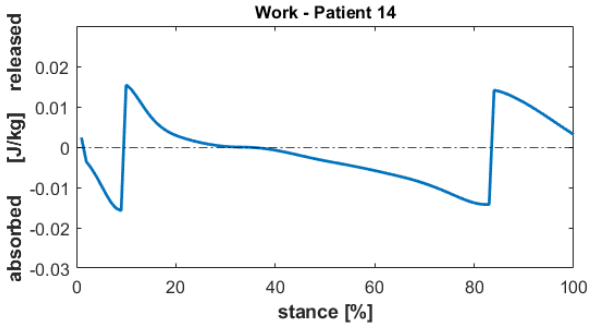
Work - Patient 14
released
[J/kg]
absorbed
stance [%]

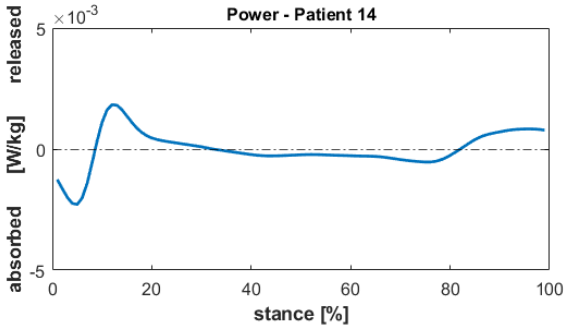
Power - Patient 14
released
[W/kg]
absorbed
stance [%]

List of figures

List of tables

References

[1] "Hip Anatomy - Physiopedia." https://www.physiopedia.com/Hip_Anatomy?utm_source=physiopedia&utm_medium=search&utm_campaign=ongoing_internal (accessed Sep. 19, 2022).

[2] Uchechukwu Chukwuemeka, "Rectus Femoris - Physiopedia." https://www.physiopedia.com/Rectus_Femoris?utm_source=physiopedia&utm_medium=search&utm_campaign=ongoing_internal (accessed Sep. 19, 2022).

[3] "Biceps Femoris - Physiopedia." https://www.physiopedia.com/index.php?title=Biceps_Femoris&oldid=298630 (accessed Sep. 20, 2022).

[4] "Knee Anatomy." https://www.arthritis-health.com/types/joint-anatomy/knee-anatomy (accessed Sep. 20, 2022).

[5] "Knee Biomechanics - Recon - Orthobullets." https://www.orthobullets.com/recon/9065/knee-biomechanics (accessed Sep. 20, 2022).

[6] "Ankle Joint - Physiopedia." https://www.physiopedia.com/index.php?title=Ankle_Joint&oldid=312966 (accessed Sep. 20, 2022).

[7] "Ankle and Foot - Physiopedia." https://www.physiopedia.com/index.php?title=Ankle_and_Foot&oldid=308226 (accessed Sep. 20, 2022).

[8] "Plantar Aponeurosis - Physiopedia." https://www.physiopedia.com/index.php?title=Plantar_Aponeurosis&oldid=289145. (accessed Sep. 20, 2022).

[9] "Leg muscles: Anatomy and function of the leg compartments | Kenhub." https://www.kenhub.com/en/library/anatomy/leg-muscles (accessed Sep. 20, 2022).

[10] "Muscles of the Foot - Dorsal - Plantar - TeachMeAnatomy." https://teachmeanatomy.info/lower-limb/muscles/foot/ (accessed Sep. 20, 2022).

[11] "Biomechanics of the ankle - ScienceDirect." https://www.sciencedirect.com/science/article/pii/S1877132716300483 (accessed Sep. 20, 2022).

[12] "Foot Drop - StatPearls - NCBI Bookshelf." https://www.ncbi.nlm.nih.gov/books/NBK554393/ (accessed Sep. 20, 2022).

[13] M. Á. García-Martínez, J. C. Montejo González, A. García-de-Lorenzo y Mateos, and S. Teijeira, "Muscle weakness: Understanding the principles of myopathy and neuropathy in the critically ill patient and the management options," *Clin Nutr*, vol. 39, no. 5, pp. 1331–1344, May 2020, doi: 10.1016/J.CLNU.2019.05.027.

[14] G. Rogati, P. Caravaggi, and A. Leardini, "Design principles, manufacturing and evaluation techniques of custom dynamic ankle-foot orthoses: a review study," *J Foot Ankle Res*, vol. 15, no. 1, pp. 1–12, Dec. 2022, doi: 10.1186/S13047-022-00547-2/TABLES/1.

[15] "Foot Drop Symptoms, Steppage Gait & Other Warning Signs." https://www.spine-health.com/conditions/leg-pain/foot-drop-symptoms-steppage-gait-other-warning-signs (accessed Sep. 20, 2022).

[16] "Surgery of the peripheral nerves - PubMed." https://pubmed.ncbi.nlm.nih.gov/16796131/ (accessed Sep. 21, 2022).

[17] P. Caravaggi *et al.*, "Development of a Novel Passive-Dynamic Custom AFO for Drop-Foot Patients: Design Principles, Manufacturing Technique, Mechanical Properties

Characterization and Functional Evaluation," *Applied Sciences 2022, Vol. 12, Page 4721*, vol. 12, no. 9, p. 4721, May 2022, doi: 10.3390/APP12094721.

[18] "Experimental comparisons of passive and powered ankle-foot orthoses in individuals with limb reconstruction | Journal of NeuroEngineering and Rehabilitation | Full Text." https://jneuroengrehab.biomedcentral.com/articles/10.1186/s12984-018-0455-y (accessed Sep. 22, 2022).

[19] D. P. Ferris, J. M. Czerniecki, and B. Hannaford, "An Ankle-Foot Orthosis Powered by Artificial Pneumatic Muscles," *J Appl Biomech*, vol. 21, no. 2, pp. 189–197, May 2005, doi: 10.1123/JAB.21.2.189.

[20] "Un'analisi comparativa tra produzione convenzionale e produzione additiva di ortesi caviglia-piede – Stampare in 3D." https://stamparein3d.it/unanalisi-comparativa-tra-produzione-convenzionale-e-produzione-additiva-di-ortesi-caviglia-piede/ (accessed Sep. 23, 2022).

[21] "Modellazione a deposizione fusa - Wikipedia." https://it.wikipedia.org/wiki/Modellazione_a_deposizione_fusa (accessed Sep. 25, 2022).

[22] "Stereolitografia - Wikipedia." https://it.wikipedia.org/wiki/Stereolitografia (accessed Sep. 25, 2022).

[23] "Aids to the examination of the peripheral nervous system LONDON: HER MAJESTY'S STATIONERY OFFICE," 1976.

[24] D. Morley *et al.*, "The Manchester–Oxford Foot Questionnaire (MOXFQ): Development and validation of a summary index score," *Bone Joint Res*, vol. 2, no. 4, p. 66, Apr. 2013, doi: 10.1302/2046-3758.24.2000147.

[25] G. Rogati *et al.*, "A novel apparatus to assess the mechanical properties of Ankle-Foot Orthoses: Stiffness analysis of the Codivilla spring," *J Biomech*, vol. 142, p. 111239, Sep. 2022, doi: 10.1016/J.JBIOMECH.2022.111239.

[26] G. Rogati, A. Leardini, M. Ortolani, and P. Caravaggi, "Validation of a novel Kinect-based device for 3D scanning of the foot plantar surface in weight-bearing," *J Foot Ankle Res*, vol. 12, no. 1, Sep. 2019, doi: 10.1186/S13047-019-0357-7.

[27] B. Scholarsarchive, D. A. Bruening, and J. G. Richards, "Optimal Ankle Axis Position for Articulated Footwear," 2005, Accessed: Oct. 05, 2022. [Online]. Available: https://scholarsarchive.byu.edu/facpub.1628.https://scholarsarchive.byu.edu/facpub/1628

[28] T. Kobayashi, A. K. L. Leung, and S. W. Hutchins, "Techniques to measure rigidity of ankle-foot orthosis: A review," *J Rehabil Res Dev*, vol. 48, no. 5, pp. 565–576, 2011, doi: 10.1682/JRRD.2010.10.0193.

[29] A. Leardini, Z. Sawacha, G. Paolini, S. Ingrosso, R. Nativo, and M. G. Benedetti, "A new anatomically based protocol for gait analysis in children," *Gait Posture*, vol. 26, no. 4, pp. 560–571, Oct. 2007, doi: 10.1016/J.GAITPOST.2006.12.018.

[30] T. Paternostro-Sluga *et al.*, "Reliability and validity of the Medical Research Council (MRC) scale and a modified scale for testing muscle strength in patients with radial palsy," *J Rehabil Med*, vol. 40, no. 8, pp. 665–671, Sep. 2008, doi: 10.2340/16501977-0235.

[31] R. C. Browning, E. A. Baker, J. A. Herron, and R. Kram, "Effects of obesity and sex on the energetic cost and preferred speed of walking," *J Appl Physiol*, vol. 100, no. 2, pp. 390–398, Feb. 2006, doi: 10.1152/JAPPLPHYSIOL.00767.2005/ASSET/IMAGES/LARGE/ZDG0020664070007.JPEG.

[32] A. Cappozzo, F. Catani, U. della Croce, and A. Leardini, "Position and orientation in space of bones during movement: anatomical frame definition and determination," *Clinical Biomechanics*, vol. 10, no. 4, pp. 171–178, Jun. 1995, doi: 10.1016/0268-0033(95)91394-T.

[33] E. S. Grood and W. J. Suntay, "A Joint Coordinate System for the Clinical Description of Three-Dimensional Motions: Application to the Knee," *J Biomech Eng*, vol. 105, no. 2, pp. 136–144, May 1983, doi: 10.1115/1.3138397.

[34] *Post hoc analysis for Friedman's Test (R code)*. 2010. Accessed: Oct. 31, 2022. [Online]. Available: https://www.r-statistics.com/2010/02/post-hoc-analysis-for-friedmans-test-r-code/